Evolution structurale et métamorphique de la croûte continentale archéenne (craton de Dherwar, Inde du Sud)

Hughes Bouhallier

H. BOUHALLIER

ISSN 1240-1498
ISBN 2-905532-59-9

évolution structurale et métamorphique de la croûte continentale archéenne

(CRATON DE DHARWAR, INDE DU SUD)

MÉMOIRES

1995

Géosciences Rennes

n° 60

MEMOIRES DE GEOSCIENCES - RENNES

n° 60

Hugues BOUHALLIER

EVOLUTION STRUCTURALE ET METAMORPHIQUE DE LA CROUTE CONTINENTALE ARCHEENNE (CRATON DE DHARWAR, INDE DU SUD)

Thèse de Doctorat de l'Université de Rennes I
soutenue le 25 Mars 1994

Géosciences - Rennes
UPR-CNRS n°4661
Université de Rennes I
Campus de Beaulieu
F - 35042 - RENNES Cédex
(France)

1995

ISSN : 1240-1498

ISBN : 2-905532-59-9

1995

GEOSCIENCES-RENNES
UPR-CNRS n°4661
Université de Rennes I - Campus de Beaulieu
F-35042-RENNES Cédex (France)

Hugues BOUHALLIER

Evolution structurale et métamorphique de la croûte continentale archéenne (Craton de Dharwar, Inde du Sud).

Mémoires de Géosciences Rennes, n° 60, 277p.

La publication du travail d'Hugues Bouhallier intervient quelques mois après sa disparition.

L'année 1994 l'a vu mener trois combats : voir son fils naître, finir sa thèse et vaincre sa maladie.

Il a perdu le dernier malgré le courage et la volonté qui le caractérisaient.

L'injustice de cette défaite nous a profondément atteints : l'arrivée de Gaspard et la bonne fin de son travail intelligent étaient pour nous preuve d'invincibilité.

Je voudrais simplement répéter le dernier mot que j'ai prononcé en tant que directeur de thèse le jour de sa soutenance le 25 mars 1994 : Merci Hugues.

A Rennes le 13 Avril 1995

P. Choukroune

Remerciements

Nombreuses sont les personnes qui, par leur gentillesse et leur compétence, m'ont aidé et encouragé dans ce travail. J'aimerais de ce fait, remercier la totalité des personnes de l'Institut des Sciences de la Terre de Rennes et plus particulièrement, l'ensemble du personnel enseignant.

Merci à N. Arndt, B. Auvray, M. Ballèvre, M. Jayananda, A. S. Janardhan, B. Mahabaleswar, H. Martin, J.J. Peucat, dont j'ai pu apprécier sur le terrain, la gentillesse et la compétence.

Merci à S. Fourcade, R. Capdevila, O. Merle, D. Gapais et J. Ludden pour leurs conseils, aides et encouragements, aux gens du Muséum d'Histoires Naturelles de Paris et plus spécialement M. Guiraud, et à certains responsables du BRGM dont Messieurs Chantraine, Duermael, Milési, Le Blanc, Valla, et Villey, qui par leur tact et leur compréhension ont en fait, très largement contribué à la réalisation de ce travail.

Un grand Merci à Gérard Gruau et Pierre Choukroune.

ABSTRACT

The aim of this thesis is to characterize the tectonic and metamorphic evolution of an Archaean continental segment (>2.5 Ga). The studied area is the Dharwar craton (South India) where deeper and deeper structural levels outcrop from North to South. This area has not been affected by post-Archaean deformation.

We show that the disclosed strain field is the result of interfering gravitational diapiric bodies and regional shortening. At crustal scale, structures (diapirs and transcurrent shear zones) were developed within a single event that can be dated at around 2.5 Ga. They are synchronous with (i) an episode of juvenile continental crust formation (Closepet batholith) and (ii) regional metamorphism (migmatisation, granulitisation). Strain fields are not consistent with thrusts and stacking structures as usually observed in modern collision belts.

The petrographic study reveals that some specific diapiric zones, which underwent fast burial, have recorded a metamorphic prograde history associated with a pressure increase (from 3 to 7-8 kbar). Furthermore, these areas display some differences in the fluid phase that seem to be linked with the variations of permeability resulting from the type and the geometry of the metamorphic fabrics.

In summary, the Archaean continental crust of Dharwar craton does not display any structure that could be responsible for the thickening of the crust. The regional strain results from body forces (diapirism) associated with boundary forces (transcurrent shear zones). The gravitational diapiric instabilities which concern large volumes of crust cannot be the result of crustal thickening and constitute a distinctive feature of Archaean tectonics.

Key-words: Archaean, tectonic, strain fields, diapirism, fluid channeling, South India.

SOMMAIRE

PARTIE A

INTRODUCTION

1. POURQUOI ÉTUDIER L'ARCHÉEN ?

L'Archéen est une période géologique qui représente à elle seule près du tiers de l'histoire de notre planète. Elle débute vers 3.9 Ga, ce qui est l'âge des plus anciennes reliques de roches crustales trouvées à la surface de la Terre, et s'achève vers 2.5 Ga. Paradoxalement, cette période de l'histoire de la Terre est relativement peu connue. En particulier, les mécanismes responsables de la formation et de la croissance de la croûte continentale archéenne restent pour l'essentiel à découvrir. Il y a deux raisons fondamentales à cela : (i) les endroits où la croûte continentale archéenne a conservé ses caractères primaires sont, en définitive, relativement rares ; dans nombre de cas, les terrains archéens à l'affleurement ont été affectés par des événements tectono-métamorphiques et/ou magmatiques plus récents ce qui a eu comme conséquences d'effacer leurs caractères tectoniques et magmatiques originels ; (ii) plusieurs méthodes d'étude sont, dans le cas de l'Archéen, totalement inopérantes ; c'est le cas par exemple de la paléontologie et du paléomagnétisme. Ces deux "inconvénients" majeurs ont eu comme résultat que nombre de géologues, et plus particulièrement les tectoniciens, ont dirigé l'essentiel de leurs efforts vers la connaissance des 500 derniers millions d'années de l'évolution de la Terre, négligeant ainsi près des neuf-dixièmes de son histoire.

Cette disparité des efforts a eu dans le passé récent des conséquences excessivement dommageables pour la connaissance de la dynamique de la croûte archéenne. Beaucoup d'auteurs, imprégnés qu'ils étaient des résultats acquis sur la croûte actuelle ou récente, ont voulu transposer ces résultats et les mécanismes que l'on en déduit, à la croûte archéenne. A force de souligner les ressemblances qui existent entre la croûte continentale archéenne et la croûte continentale moderne et d'en oublier les différences, une partie de la communauté scientifique s'est vue convaincre de l'uniformitarisme de la dynamique de la croûte continentale. Ainsi, à partir de scénarios actualistes, on a tenté d'extrapoler à l'Archéen les principes de la tectonique des plaques sans trop se soucier de savoir si les modèles ainsi proposés étaient compatibles avec les observations structurales.

Pourtant, des différences géologiques fondamentales existent entre les périodes modernes et archéennes.

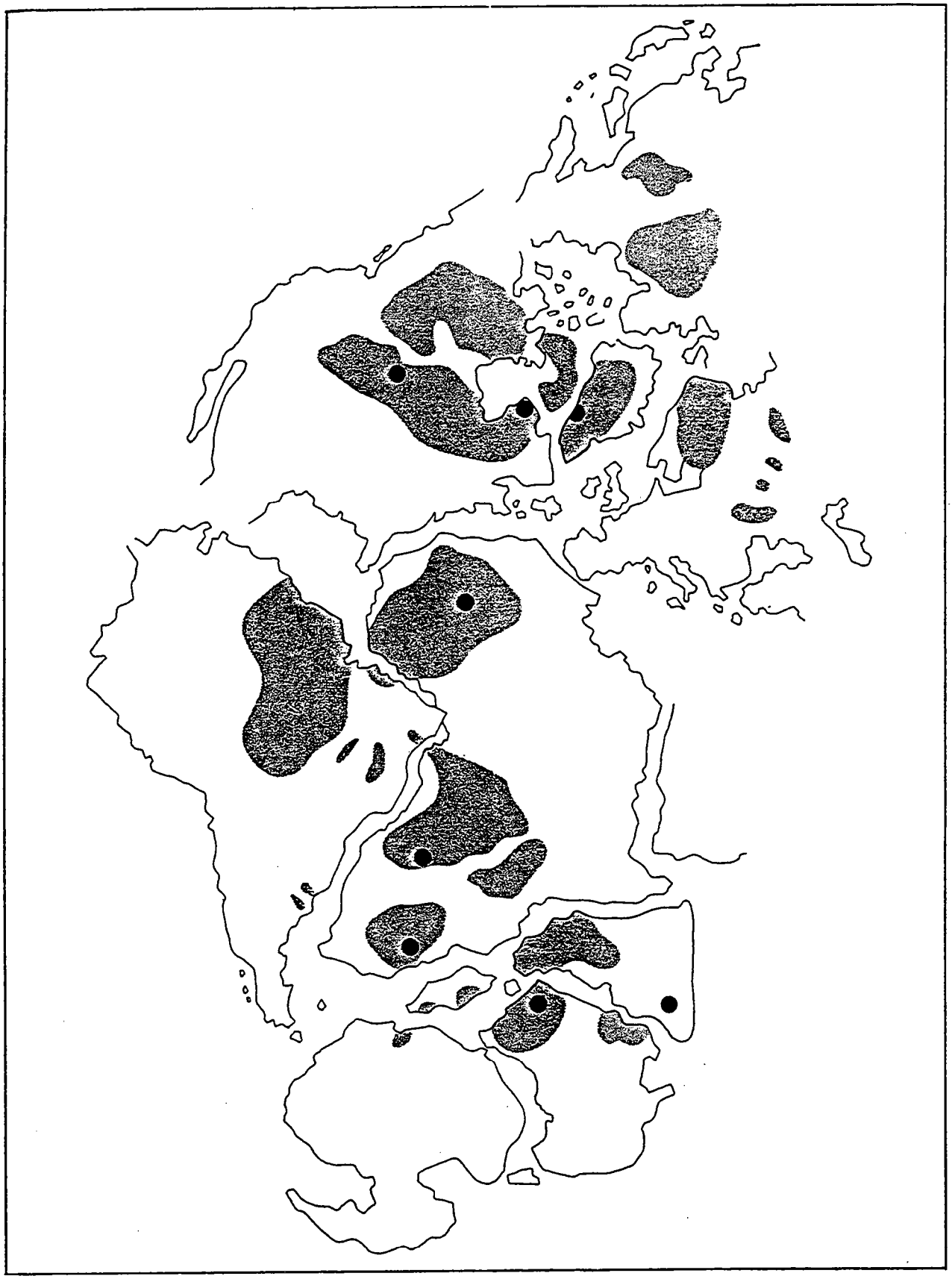

Fig. A . 1. Répartition terrestre des cratons archéens. Les zones en grisé indiquent les régions géologiques dont l'âge est supérieur à 2.7 Ga ; les disques indiquent les lieux où il existe des roches de 3.5 Ga ou plus, d'après Moorbath, (1979).

2. LES SPÉCIFICITÉS DE L'ARCHÉEN

Dans cette partie, nous énumérons les grands traits spécifiques de l'Archéen. Il ne s'agit évidemment pas de détailler chacun d'entre eux (le lecteur pourra se référer aux travaux cités) mais plutôt de remarquer que l'Archéen est une période de l'histoire de notre planète où ont existé et perduré des phénomènes géologiques majeurs dont on ne retrouve actuellement peu ou plus les équivalents.

2. 1. La première croûte continentale

Indépendamment du fait de savoir comment la croûte archéenne se formait (Arth & Hanson 1975 ; Moorbath, 1975 ; Arth, 1979 ; Barker, 1979 ; Condie, 1981, 1993 ; Dewey & Windley, 1981 ; Jahn et al., 1981 ; Martin, 1986 ; Arculus & Ruff, 1990 ; Rapp et al., 1991 ; Winther & Newton, 1991 ; Martin, 1993), il est bien clair que ce qui caractérise la période archéenne est qu'elle correspond au moment où apparaissent et se stabilisent les grandes masses continentales que nous connaissons aujourd'hui. Il est à peu près établi qu'avant 4.2 Ga, il n'y avait pas ou très peu de croûte continentale sialique alors qu'à 2.5 Ga, de nombreuses masses de croûte continentale sont déjà présentes (Fig. A . 1). L'Archéen demeure donc, avant toute chose, la période de l'histoire de notre planète où apparaissent et se conservent les continents (Fig. A . 2 et A . 3). Plusieurs études montrent qu'aux environs de 3.9 Ga, les premiers continents apparaissent (Hurley, 1968 ; Hurley & Rand, 1969 ; Veizer & Jansen, 1979 ; McLennan & Taylor, 1982). La période de croissance rapide se situerait entre 3.8 et 1.7 Ga, c'est à dire au cours de l'Archéen et du Protérozoïque inférieur (Veizer and Jansen, 1979 ; McLennan & Taylor, 1982 ; Allègre, 1985 ; Taylor & McLennan, 1985). En effet, dans cet intervalle de temps, ce sont constitués les fondements des continents actuels. Ainsi, à la fin de l'Archéen à 2.5 Ga, 70 à 80% de la croûte continentale étaient déjà formés (Taylor & McLennan, 1985).

Ceci est d'une importance capitale pour tout tectonicien qui pour l'Archéen doit raisonner à volume de croûte continentale non-constant, c'est à dire, qu'il doit intégrer à tout moment dans sa réflexion, le fait que le volume de la croûte continentale croît, et ce, de façon extrêmement rapide pour la période que nous considérons ici.

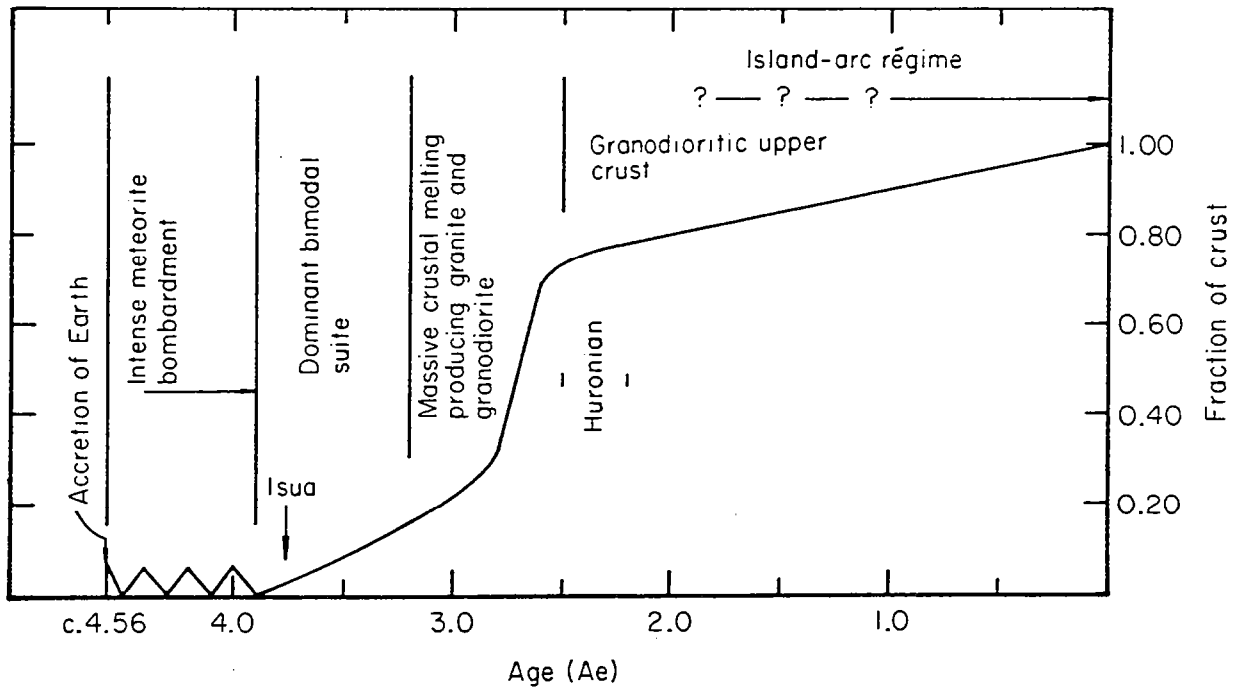

Fig. A. 2. Generalized model for the growth of the continental crust throughout geologic time, from Taylor & McLennan, (1985).

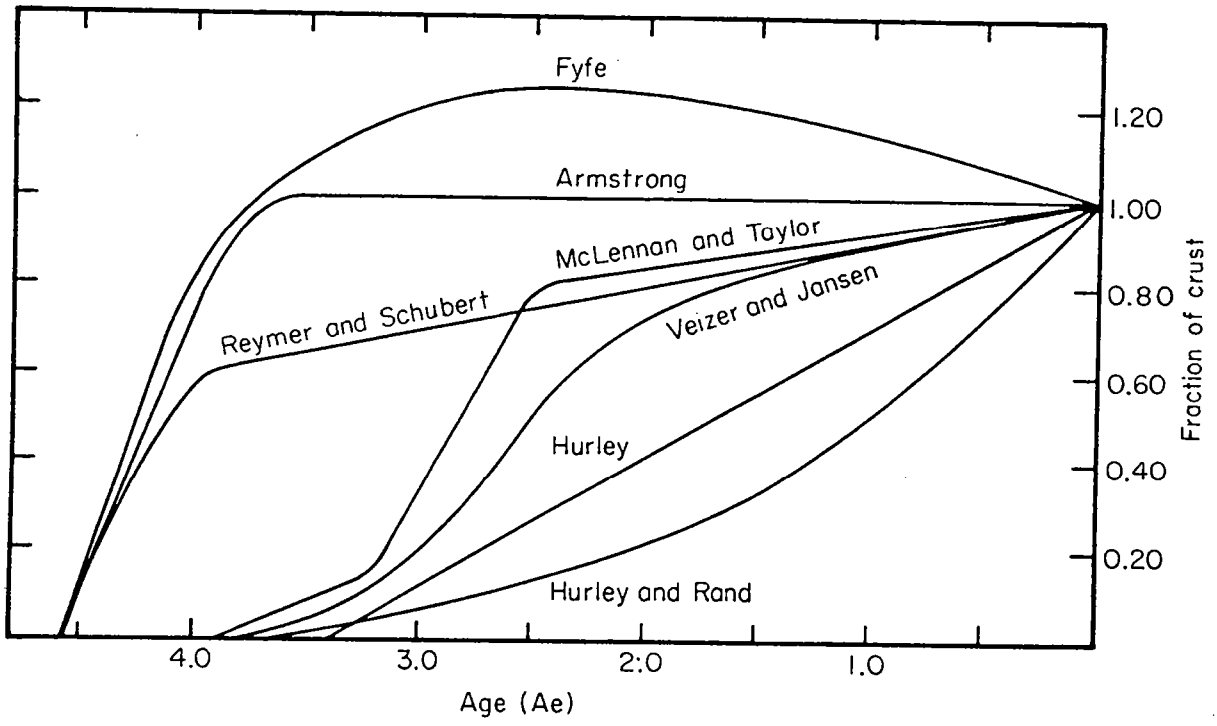

Fig. A. 3. A selection of crustal growth models. Models shown include those of Reymer & Schubert, 1984 ; Armstrong, 1981 ; Fyfe, 1978 ; Hurley, 1968 ; Hurley & Rand, 1969 ; Veizer & Jansen, 1979 ; and McLennan & Taylor, 1982 ; from Taylor & McLennan, 1985.

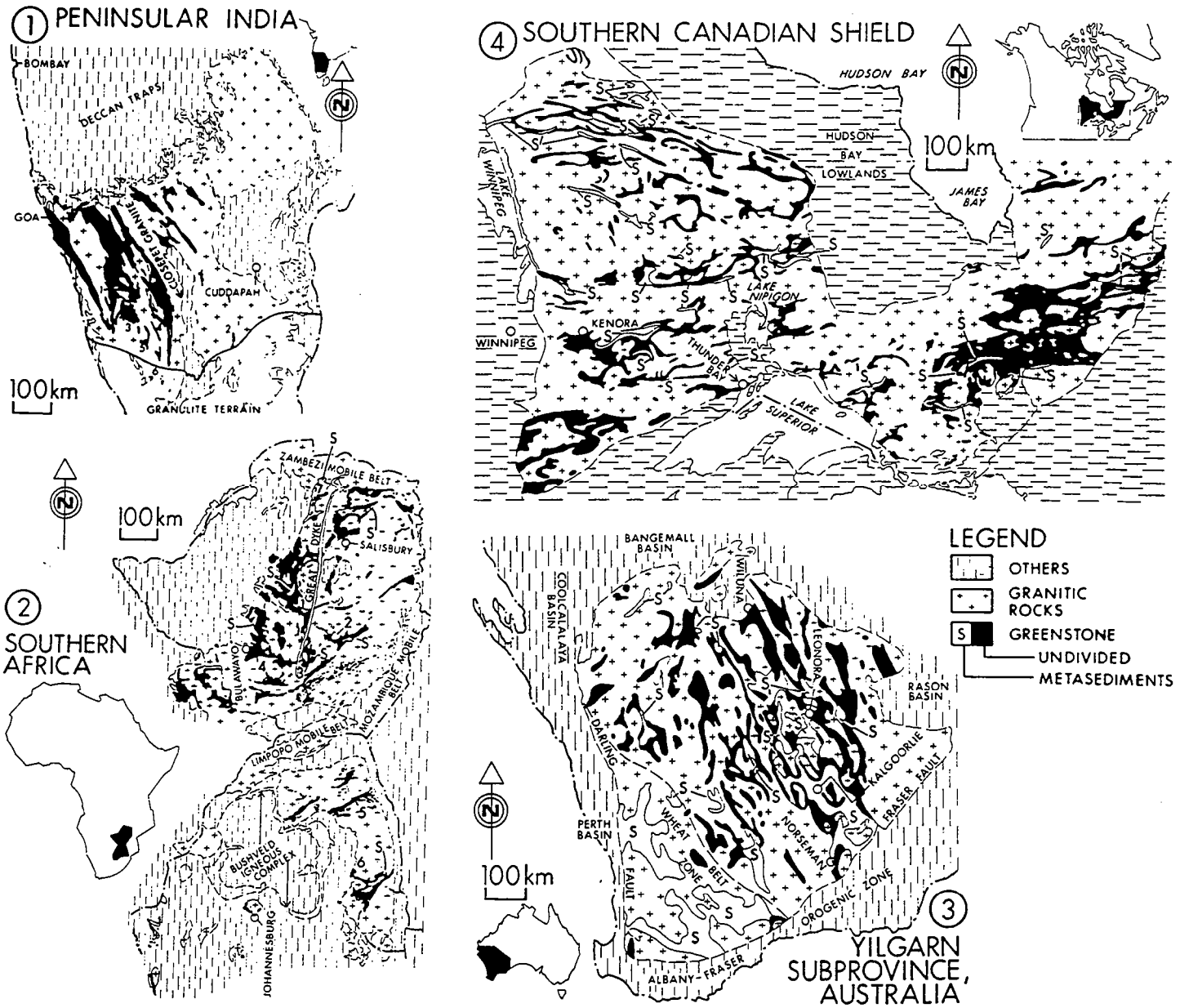

Fig. A. 4. Granite-greenstone terrains of (1) Peninsular India, (2) Southern Africa, (3) Yilgarn subprovince, Western Australia and (4) Southern Superior Province, Canadian shield. All are drawn to the same scale as are the inset maps for purposes of comparison. The greenstone belts are predominantly volcanic ; some sediment-rich parts, especially in the Yilgarn subprovince, are shown separately. Data sources : (1) Peninsular India (Naqvi et al., 1978) ; (2) Southern Africa (Anhaeusser, 1976) ; (3) Yilgarn subprovince (tectonic map of Australia and New Guinea, scale 1 / 50000000, Geological Society of Australia, Sydney ; and (4) Geological map of Canada, 1968, map N° 1250 A, scale 1 / 5000000, geological Survey of Canada with modifications and additions, from Goodwin, (1984).

2. 2. Une association lithologique bimodale

Pas moins de 25 cratons archéens ont été répertorié à la surface de la Terre (Fig. A. 1). Ces cratons ont tous en commun le fait d'être constitué de la juxtaposition de deux types d'unités lithologiques, à savoir (i) des ensembles granito-gneissique (TTG) et (ii) des ensembles volcaniques et sédimentaires (ceintures de roches vertes).

Sur la figure A. 4, nous présentons les cartes géologiques de quatre cratons archéens parmi les plus typiques. Un rapide examen de ces cartes (de même échelle) y révèle la présence de ceintures de roches vertes dont la répartition spatiale et la géométrie sont quasi identiques d'un craton à l'autre. Cette figure permet également de visualiser l'étendue de l'association lithologique bimodale "TTG-roches vertes" qui compose la totalité de la croûte continentale de ces différentes régions archéennes. La répartition de cette dernière est d'échelle continentale (1000 km), et l'on peut, par conséquent, raisonnablement penser qu'elle est l'expression de processus géodynamiques majeurs.

Lignée TTG

Cette suite magmatique constituée en proportions variables de tonalites trondhjémites et de granodiorites représente le constituant majeur de la croûte continentale archéenne. La composition des TTG a la particularité d'être constante de 3.9 à 2.5 Ga. Ce sont le plus souvent des roches quartzo-feldspathiques gneissiques, riches en plagioclase, contenant de la biotite et de la hornblende. Les plus anciens de ces témoins de la croûte continentale présentent des âges variables: 3.9 Ga au Groenland (Kinny, 1986), 3.9 Ga en Antartique (Black et al., 1986), 3.65 Ga en Afrique du Sud (Compston et Kröner, 1988), 3.45 Ga en Afrique de l'Ouest (Potrel, 1984), 3.6 Ga dans l'ex. URSS (Bibikova, 1984), 3.36 Ga en Inde (Beckinsale et al., 1980). Ces granitoïdes archéens sont supposés dériver par fusion partielle soit du manteau (Evans & Hanson, 1992) soit de protolithes basiques (Arth & Hanson, 1975 ; Glikson, 1979 ; Jahn et al., 1981, Jahn & Zhang, 1984, Martin, 1986, 1993). D'autres auteurs ont proposé qu'ils pourraient dériver de la cristallisation fractionnée d'un liquide basaltique hydraté (Barker, 1979 ; Arth et al., 1978 ; Kramers, 1988). Une fois encore, quels que soient le ou les modes de formation des TTG, ils impliquent tous "anormalement" fortes et les régimes thermiques élevés.

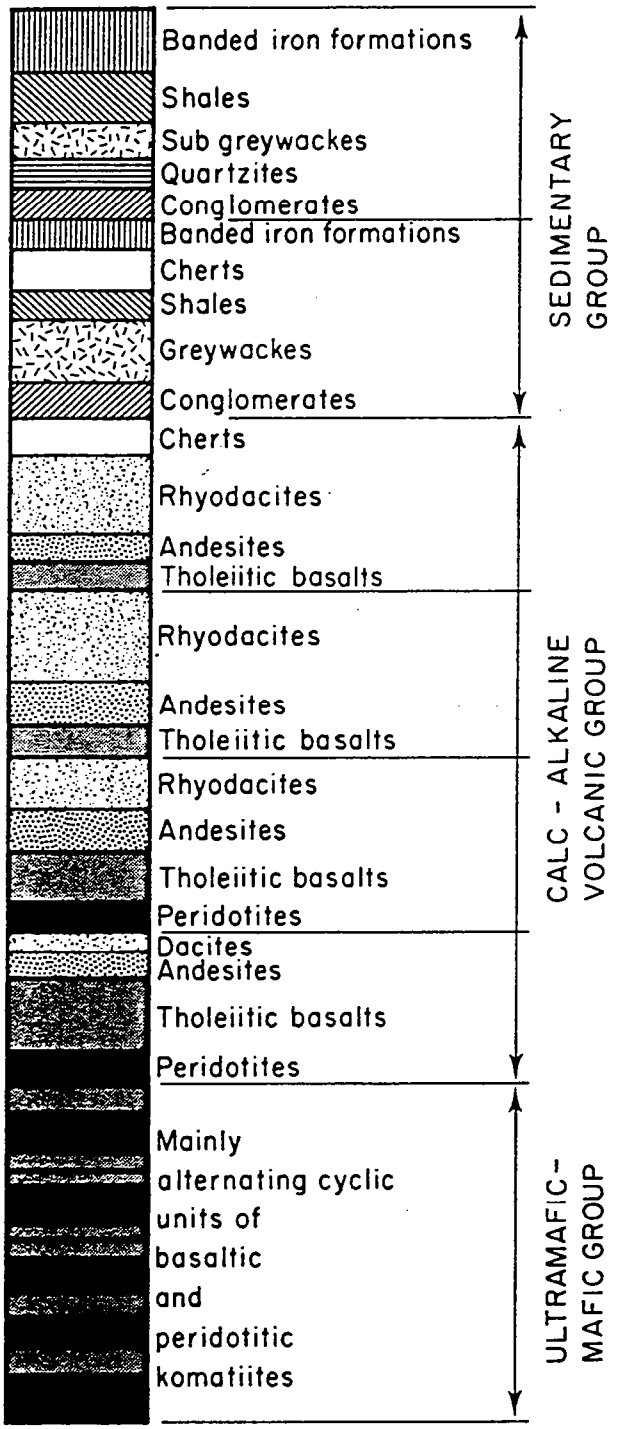

Fig. A . 5. Hypothetical stratigraphic succession for an Archaean greenstone belt based on the Barberton model, modified after Anhaeusser, (1971), from Windley, (1984).

Les ceintures de roches vertes

Les roches supracrustales des domaines archéens ont été abondamment étudiées et sont connues sous le terme de ceintures de roches vertes (greenstone belts). Elles sont assimilées à des bassins volcano-sédimentaires, dont la stratigraphie, les textures sédimentaires, la géochimie des roches volcaniques et sédimentaires sont remarquablement similaires d'un craton archéen à l'autre (Condie, 1981). On les retrouve sur tous les cratons archéens, et ont un âge variable globalement compris entre 3.5 Ga et 2.5 Ga (Condie, 1981). Leur évolution stratigraphique présente, d'une façon quasi systématique, une base de séquence essentiellement volcanique évoluant progressivement vers un sommet où prédominent les roches sédimentaires. Généralement, la base du groupe volcanique a une nature ultrabasique (péridotites et komatiites) tandis que le sommet présente davantage de roches calco-alcalines de nature basique et acide (Fig. A . 5).

2. 3. Une activité thermo-mécanique intense

La très grande majorité des spécificités relatives à cette période n'est en fait que la traduction plus ou moins directe des effets d'un seul paramètre : la température.

Deux principaux types de sources calorifiques doivent être pris en compte dans le bilan thermique terrestre. Le premier correspond à une quantité de chaleur héritée et par conséquent non renouvelable : il s'agit de la chaleur d'accrétion acquise lors des premiers stades de la formation de la Terre à laquelle s'ajoutent les chaleurs latentes de cristallisation du noyau et du manteau et celle dégagée par les isotopes radioactifs à courte période (I^{129}, Al^{26}) (Basaltic Volcanism Study Project, 1981). Cette énergie "fossile", qui se dissipe depuis 4.5 Ga était encore importante à l'Archéen. Le second type de source de chaleur correspond cette fois-ci à une production interne et continue provenant essentiellement de la désintégration des éléments radioactifs de longue période comme le K^{40}, l'U^{235} ou l'U^{238} et le Th^{232} (Wasserburg et al., 1964 ; McKenzie & Weiss, 1975, Lambert, 1976). Là aussi, le "stock" est limité, et la désintégration des éléments radioactifs décroissant

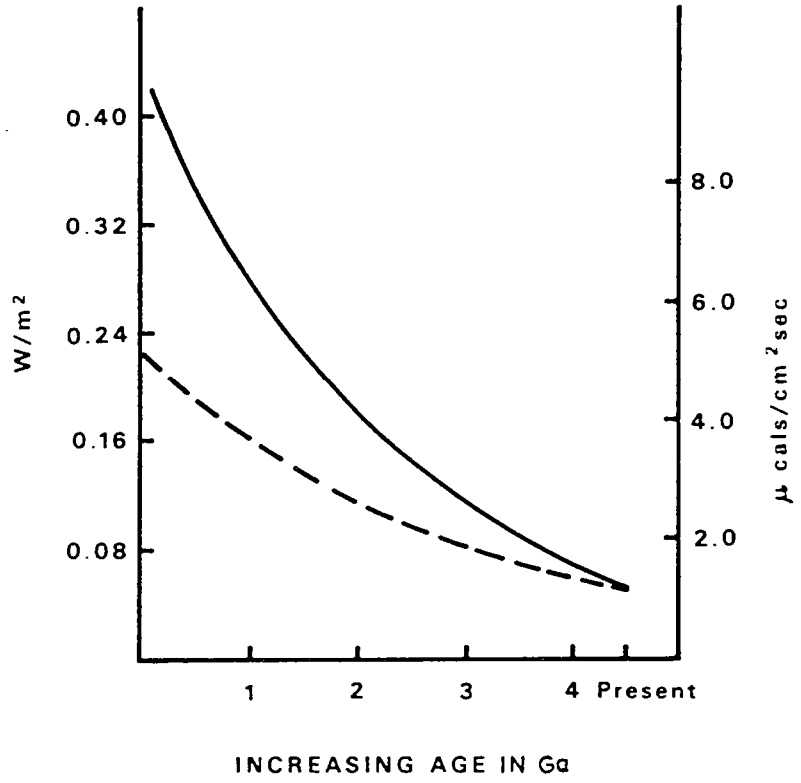

Fig. A . 6. Variation of average terrestrial heat flow (assumed to be 1.4 HFU) with time in a model of the Earth with a initial temperature sufficently great to permit convection throughout the mantle. The solid curve is for a model with chondritic abundances of radioactive elements ; the broken curve is for one with heat-flux equivalent to present values, but with a K/U ratio derived from measurements of crustal rocks - the model of Wasserburg et al. (1964), from Hargraves, (1984).

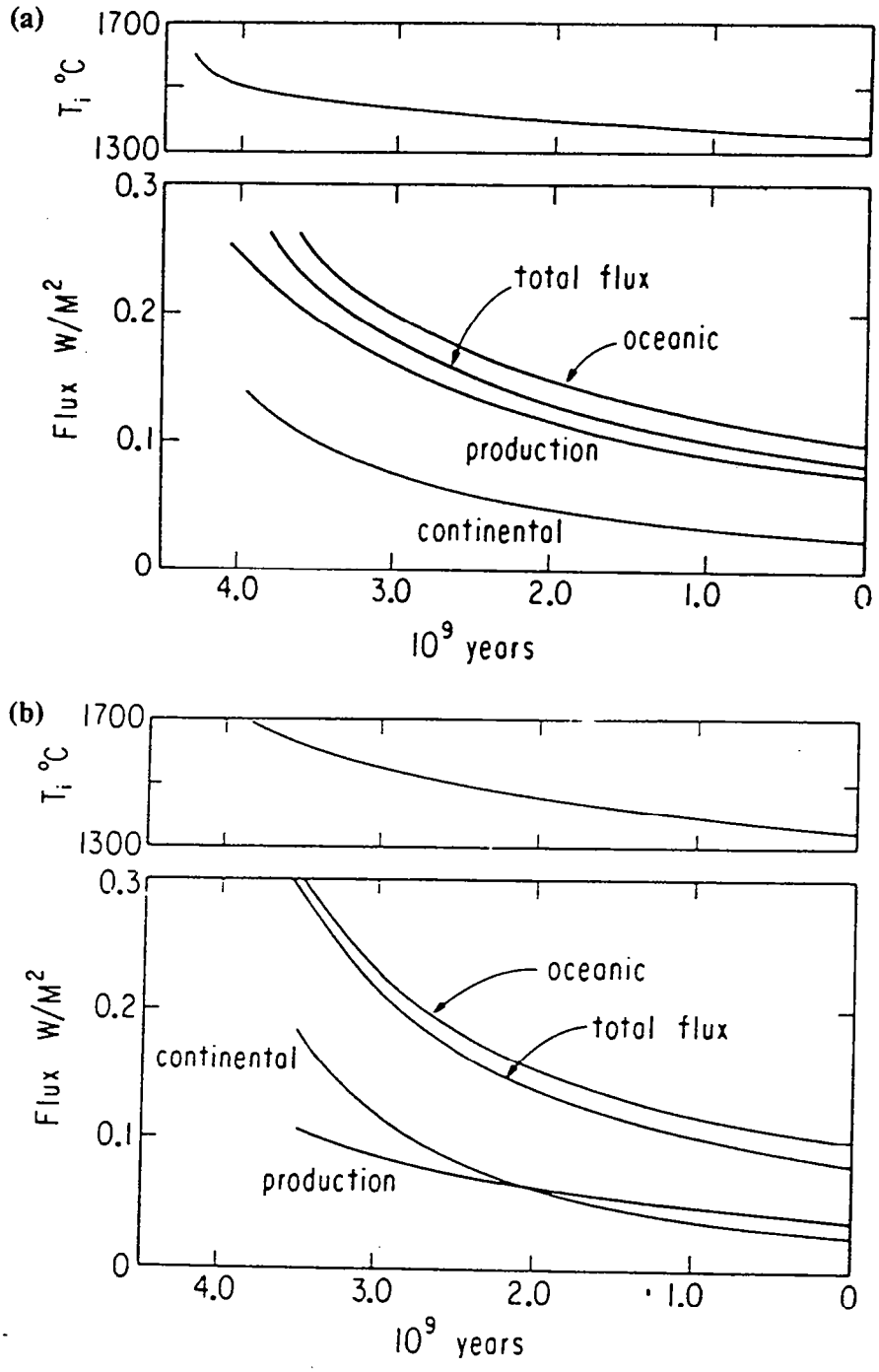

Fig. A . 7. (a) Interior temperature of the mantle (top diagram), radiogenic heat production per unit surface area, and regionalised heat flux as a function of time, assuming mantle-wide convection in the Earth, with a viscosity exponent, m=30, (b) Same as Figure (a) but with a layered mantle, and m=15, from Richter, (1984).

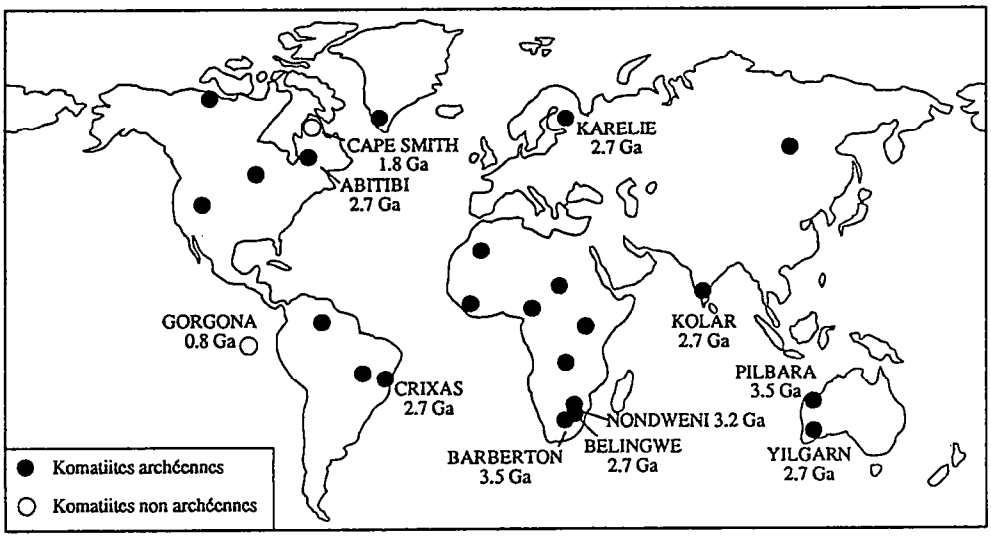

Fig. A . 8. Distribution spatiale et temporelle des principales komatiites (Tourpin, 1991).

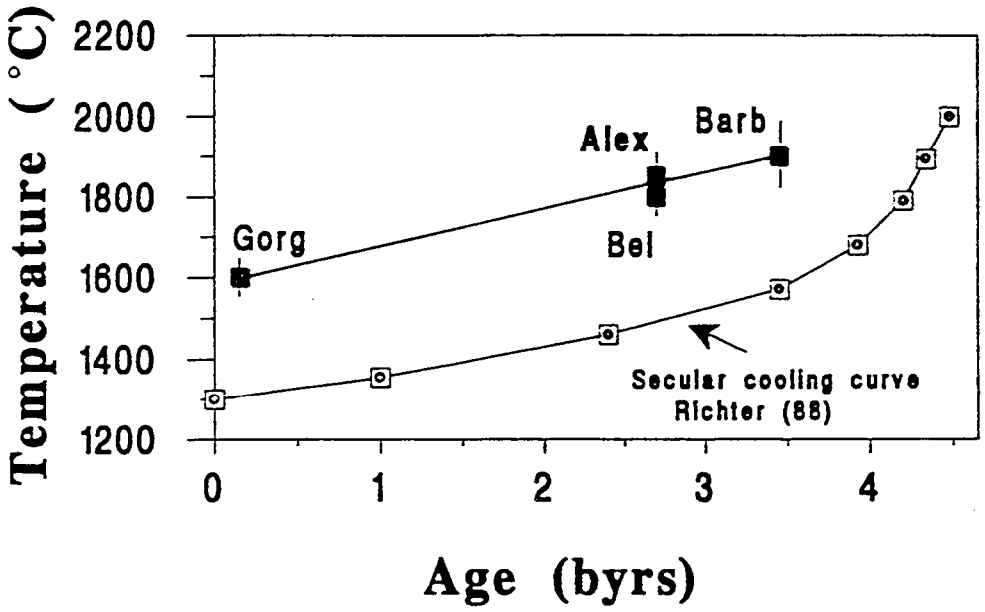

Fig. A . 9. Secular cooling curve for the Earth's mantle as given by Richter (1988). Also shown are the mantle potential temperature derived from komatiites. Uncertainties in the temperatures are indicated by error bars. It is suggested that the temperature derived from komatiites are maximum mantle plume temperatures. Alex=Alexo, Barb=Barberton, Bel=Belingwe, Gor=Gorgona, from Nisbet et al., 1993.

de façon exponentielle avec le temps, la quantité d'énergie libérée par ce phénomène se ralentit avec le temps. Ainsi, plus on remonte dans le temps, plus la quantité de chaleur produite était importante (Fig. A . 6)..

Pour faire face à cet excès énergétique, la Terre, à moins qu'elle ne surchauffe doit rapidement et efficacement consommer et/ou dissiper cette chaleur. La convection apparait comme le meilleur processus physique pour participer de façon efficace à la transformation d'énergie thermique en énergie cinétique. Différents modèles convectifs ont été imaginés pour l'Archéen (Fig. A . 7, ex : Richter, 1984, 1985). Ils reposent tous sur la même idée : dissiper ou consommer une plus forte quantité de chaleur.

Les komatiites

Il s'agit de roches volcaniques ultrabasiques très répandues à l'Archéen mais dont l'occurrence devient accidentelle ensuite (Fig. A . 8). Elles sont présentes dans pratiquement toutes les ceintures de roches vertes archéennes (Afrique du Sud, Canada, Australie, Finlande, Inde, Brésil...) et forment un des constituants majeurs du volcanisme archéen (Viljoen & Viljoen, 1969 ; Nesbitt et al., 1982 ; Goodwin, 1991). Composées principalement d'olivine, de pyroxènes et de verre, elles se caractérisent surtout par une teneur en MgO très élevée, d'au moins 18% (Arndt & Nisbet, 1982). Du fait de leur composition très magnésienne, de leur très faible teneur en REE et de leur température d'éruption élevée (1600-1700°C environ), il a été suggéré que ces roches étaient engendrées par un fort taux de fusion (50 à 60% au minimum) d'un manteau pyrolitique (50% olivine, 25% orthopyroxène, 15% clinopyroxène, 10 % grenat). Ainsi, l'étude de ces roches constitue l'une des plus puissantes sources d'informations permettant de contraindre la composition et surtout la température du manteau archéen. En effet, en considérant une remontée quasi adiabatique (1°C/km, Nisbet, 1982), leur présence implique des températures du manteau supérieures à 1700°C à 50km de profondeur (une remontée non-adiabatique impliquant des températures encore plus importantes). Ces roches se forment à partir de liquides qui de plus, excèdent de près de 300 °C les températures prédites par les modèles de refroidissement séculaires (Richter, 1988). Dans l'état actuel des connaissances, seule une dynamique impliquant des liquides convectifs de type "plumes" peut rendre compte de ces observations (Fig. A . 9, Nisbet et al., 1993).

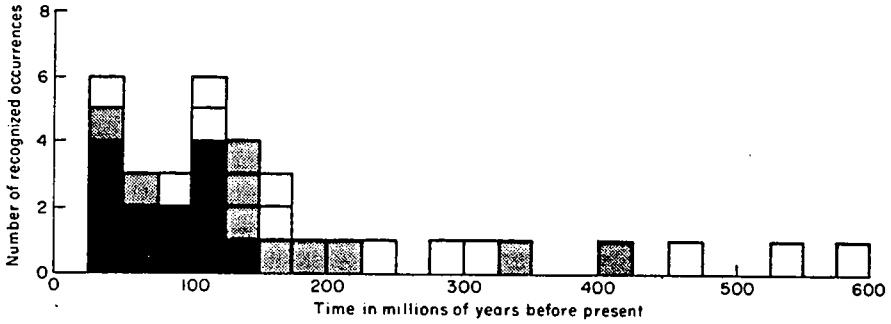

Fig. A . 10. Histogram showing incidence of blueschists of contrasting mineralogies with time. Open boxes represent epidote-bearing glaucophane schists, stippled pattern lawsonite (+/- epidote), and black boxes aragonite and/or jadeitic pyroxene and quartz (generally also lawsonite) from Ernst, (1972).

Les modifications des paramètres de la convection mantélique

Depuis longtemps, la convection mantélique a été proposée comme agent fondamental de la dynamique interne de la Terre (Holmes, 1928 ; Pekeris, 1935). Même si les modalités exactes des mouvements convectifs du manteau sont encore imparfaitement établies, leurs effets sur l'ensemble des processus géodynamiques ont été définitivement admis par l'ensemble de la communauté scientifique. Les caractéristiques qualitatives et quantitatives des mouvements convectifs se résument aux relations de deux nombres sans dimension : (i) le nombre de Reynolds, qui caractérise le rapport des forces motrices qui tendent à accélérer le fluide, aux forces de frottements qui tendent à le freiner et, (ii) le nombre de Raleigh, qui exprime le rapport entre le temps nécessaire pour dissiper une perturbation thermique locale par conduction thermique et le temps mis par un élément du fluide pour effectuer un tour complet dans une cellule de convection. Il indique en définitive, l'efficacité relative du transfert convectif et du transfert conductif. Or, ces deux nombres, d'une importance capitale dans les problèmes de convection, sont dépendants de la température. Il devient donc immédiat que les modalités de la convection mantélique devaient être significativement différentes à l'Archéen comparées aux périodes protérozoïque, phanérozoïques et actuelles.

2. 4. Absence de métamorphisme HP-BT dans la croûte continentale

L'une des caractéristiques essentielles des domaines archéens est l'absence de paragenèse index de haute pression (Windley & Bridgwater, 1971 ; Saggerson & Owen, 1971 ; Saggerson & Turner, 1972). Lambert (1976), discutant la nature des régimes thermiques archéens et remarquant l'absence des faciès métamorphiques "schistes bleus" et "éclogites" conclue à l'absence des environnements géodynamiques modernes qui les produisent actuellement. En effet, les profondeurs maximales enregistrées dans les terrains archéens n'excèdent pas 30-40 km pour des températures généralement comprises entre 650-900°C (Schreyer, 1967, Chinner & Sweatman, 1968). L'absence de paragenèses métamorphiques HP-BT est illustrée, (par exemple, mais pas seulement), par l'occurrence minéralogique de la glaucophane en fonction du temps (Fig. A . 10, Ernst, 1972). Ce minéral de métamorphisme, index des hautes pressions et des

basses températures apparait surtout cantonné au 600 derniers millions d'années avec une nette augmentation à partir du Mésozoïque. A notre connaissance, le plus ancien assemblage du faciès schistes bleus a été identifié en Chine et serait âgé de près de 1.8 Ga (Liou et al., 1988). Sa rareté dans les roches plus anciennes que 1.0 Ga a été discutée et a été utilisée comme une évidence marquant la spécificité des environnements géodynamiques anciens (Kröner, 1981 a, b).

Ainsi, l'Archéen, époque la plus longue de l'histoire géologique de la Terre, présente des caractéristiques thermiques et géologiques sensiblement différentes des périodes modernes. Ce sont principalement :

- *la formation et la préservation d'une grande quantité de masses continentales,*
- *un excès énergétique lié à de nombreux éléments radiogéniques,*
- *la présence de roches particulières (komatiites, TTG),*
- *l'absence d'indice de paragenèses HP-BT dans la croûte continentale*
- *une activité volcanique intense (ceintures de roches vertes).*

Un très large débat anime la communauté des Sciences de la Terre sur la signification de ces différences. Sont-elles le reflet et/ou la conséquence de processus géodynamiques (i) inconnus pour les périodes modernes, (ii) existant actuellement mais dont la représentativité actuelle n'est sans aucune commune mesure avec celle de l'Archéen, (iii) équivalents à ceux de l'actuel et sans véritable différence majeure.

Aussi, la géologie structurale peut et doit amener à cette discussion, un certain nombre de contraintes indépendantes des autres disciplines des Sciences de la Terre.

Partie B

FORMATION ET ÉVOLUTION DES PREMIERS CONTINENTS :

SYNTHÈSE DES TRAVAUX ANTÉRIEURS

1. LA FORMATION DE LA CROÛTE CONTINENTALE ARCHÉENNE

Aujourd'hui, il existe deux types d'environnements où l'on peut observer de la croûte continentale en formation : (i) les zones de subduction (ex : arcs insulaires, Andes), (ii) les zones intra-océaniques localisées à l'aplomb de plumes mantéliques (ex : Islande).

Ces deux environnements géodynamiques, même s'ils ne génèrent actuellement que très peu de croûte continentale juvénile, n'en demeurent pas moins les deux principaux candidats à l'origine de la formation des premiers continents archéens. Si les deux sont susceptibles de rendre compte à la fois des caractéristiques géochimiques et pétrologiques des séries TTG archéennes (Kröner, 1991), leurs implications sur la cinétique lithosphérique sont fondamentalement différentes. Le premier nécessite une tectonique globale impliquant le déplacement relatif d'entités lithosphériques dont la destruction dans les zones de convergence permet la production de croûte continentale. Le second ne nécessite pas de déplacements lithosphériques.

1. 2. Modèle de type "convergence lithosphérique"

Depuis l'avènement de la tectonique des plaques, les zones dites de subduction ou marges actives ont été reconnues comme étant le siège principal de la formation de croûte continentale actuelle (Dewey & Horsfield, 1970 ; Oxburgh & Turcotte, 1970). La déshydratation de la plaque océanique subductante provoque la fusion d'une partie du "coin de manteau" qui la recouvre, à laquelle succèdent des processus divers de type cristallisation fractionnée ou de type mélange magmatique à l'origine de la production massive de roches plutoniques et volcaniques (Ringwood, 1974). Ces régions sont linéaires, relativement étroites et parallèles aux zones de subduction.

Cet environnement est devenu un modèle classiquement invoqué pour expliquer la formation de la croûte continentale archéenne (Talbot, 1973). L'argument principal est le suivant. En supposant que la dissipation thermique s'effectue essentiellement par la production de croûte océanique dans des environnements de type rides médio-océaniques, de nombreux auteurs supposent qu'à l'Archéen, les rides étaient respectivement plus longues (Burke & Kidd, 1978 ; Hargraves, 1986) et plus rapides (Bickle, 1978 ;

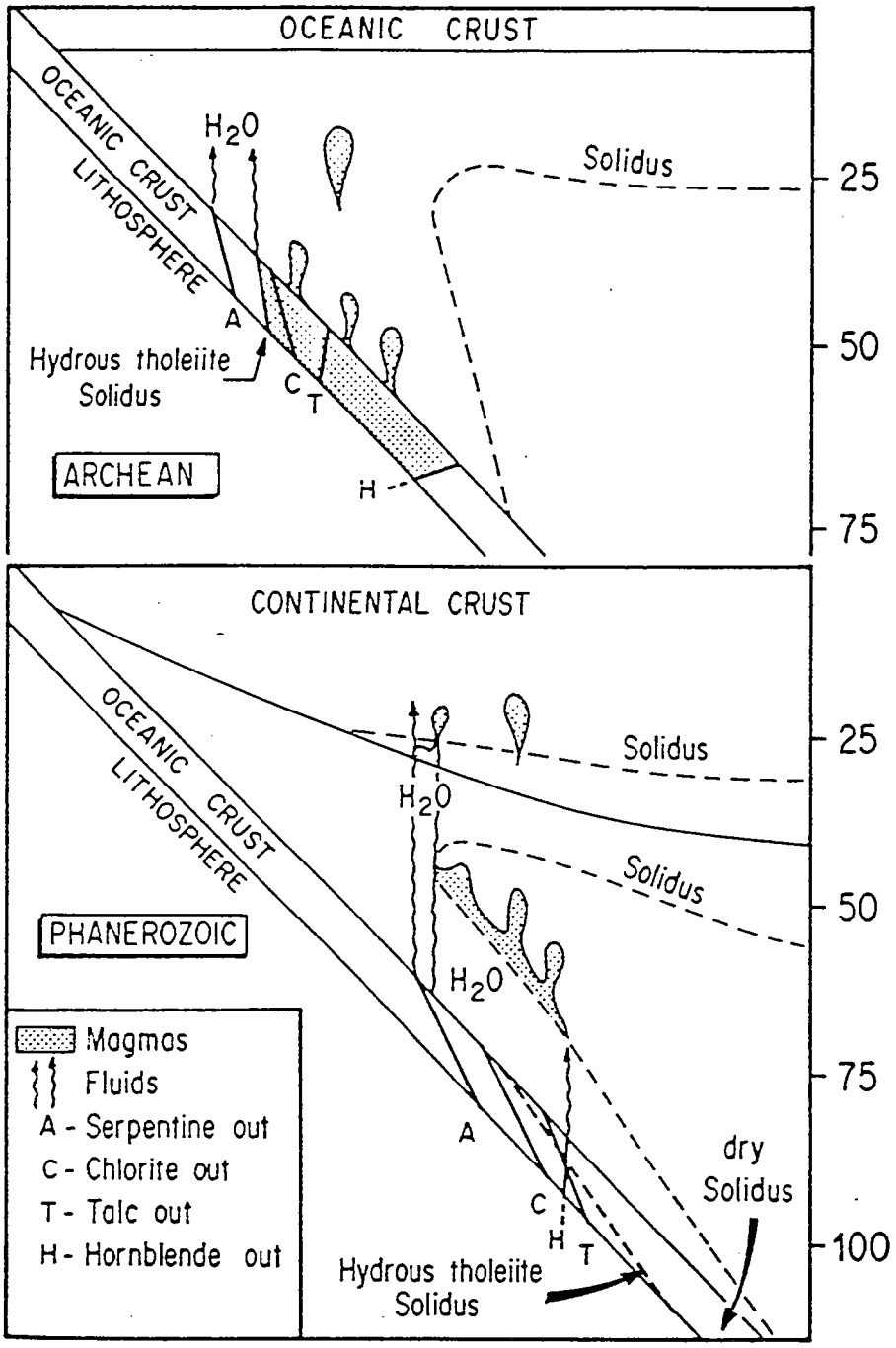

Fig. B. 1. Schematic cross sections of modern and Archaean subduction zones. Some dehydration reactions are showed : (A)=Anthophyllite-out ; (C)=Chlorite-out ; (T)=Talc-out ; (H)=Hornblende-out. Dotted lines (S) represent solidus curves for continental and oceanic crusts and mantle wedge ; the grey area shows the place where calc-alkaline magmas are generated and the arrows are the place where fluids go through. During the Archaean, high geothermal gradients along the Benioff plane initiated melting of the subducted slab, before it could dehydrated. Today, because of lower geothermal gradients, dehydration generally occurs before melting can begin, such as the source of calc-alkaline magmas is typically the mantle wedge metasomatized by slab dehydration fluids, from Martin, (1986).

Dewey & Windley, 1981 ; Windley, 1984) favorisant ainsi une destruction importante de lithosphère océanique dans les zones de subduction. Ces dernières, plus actives devaient donc être le siège d'une production massive et rapide de croûte continentale juvénile.

Un certain nombre d'auteurs suggèrent que les séries TTG archéennes résultent de la fusion partielle d'une source basaltique hydratée. Afin d'expliquer leur nature particulière et parce que leurs caractéristiques géochimiques nécessitent la présence de grenat au résidu, les conditions de fusion devaient être P> 12 kbar et T=1000-1100°C (Rapp et al., 1991). D'après Martin (1986), une zone de subduction dans un contexte thermique chaud peut rendre compte de telles observations (Fig. B . 1). En effet, l'association de géothermes élevés avec une croûte océanique jeune et chaude dans un environnement de type marge active (comme actuellement, dans la région des Rocas Verdes au Chili) facilite la fusion de la croûte océanique subductée avant sa déshydratation complète. Ainsi, la fusion de la croûte océanique serait à l'origine de la formation des lignées TTG.

Les conséquences de ce modèle sur la tectonique globale archéenne sont très importantes. En effet, ce type d'environnement nécessite une organisation cinématique de plaques lithosphériques analogue à celle de la tectonique des plaques actuelle.

1. 3. Modèle de type "plume intra-lithosphérique"

Si l'on suppose que le régime convectif du manteau était chaotique à l'Archéen (Campbell & Jarvis, 1984) et que cet état chaotique empêchait le déplacement de plaques océaniques épaisses et rigides, il est nécessaire de trouver une alternative au modèle précédent. Certains auteurs suggèrent que l'Archéen était marqué par l'activité de nombreux plumes mantéliques (Lambert, 1981 ; Reymer & Schubert, 1987 ; Campbell et al., 1989), plumes qui pouvaient être à l'origine de la formation de la croûte continentale juvénile (Schubert, 1988). En particulier, Kroner (1985, 1991) et Malloe (1982) présentent l'Islande comme un analogue actuel de ce qui aurait pu être un site de production de croûte continentale juvénile à l'Archéen. En effet, l'Islande, qui se situe aujourd'hui à l'aplomb d'un plume mantélique, présente des suites magmatiques de nature TTG tout à fait comparables à celles que l'on trouve dans les cratons archéens. Ainsi, l'arrivée massive de

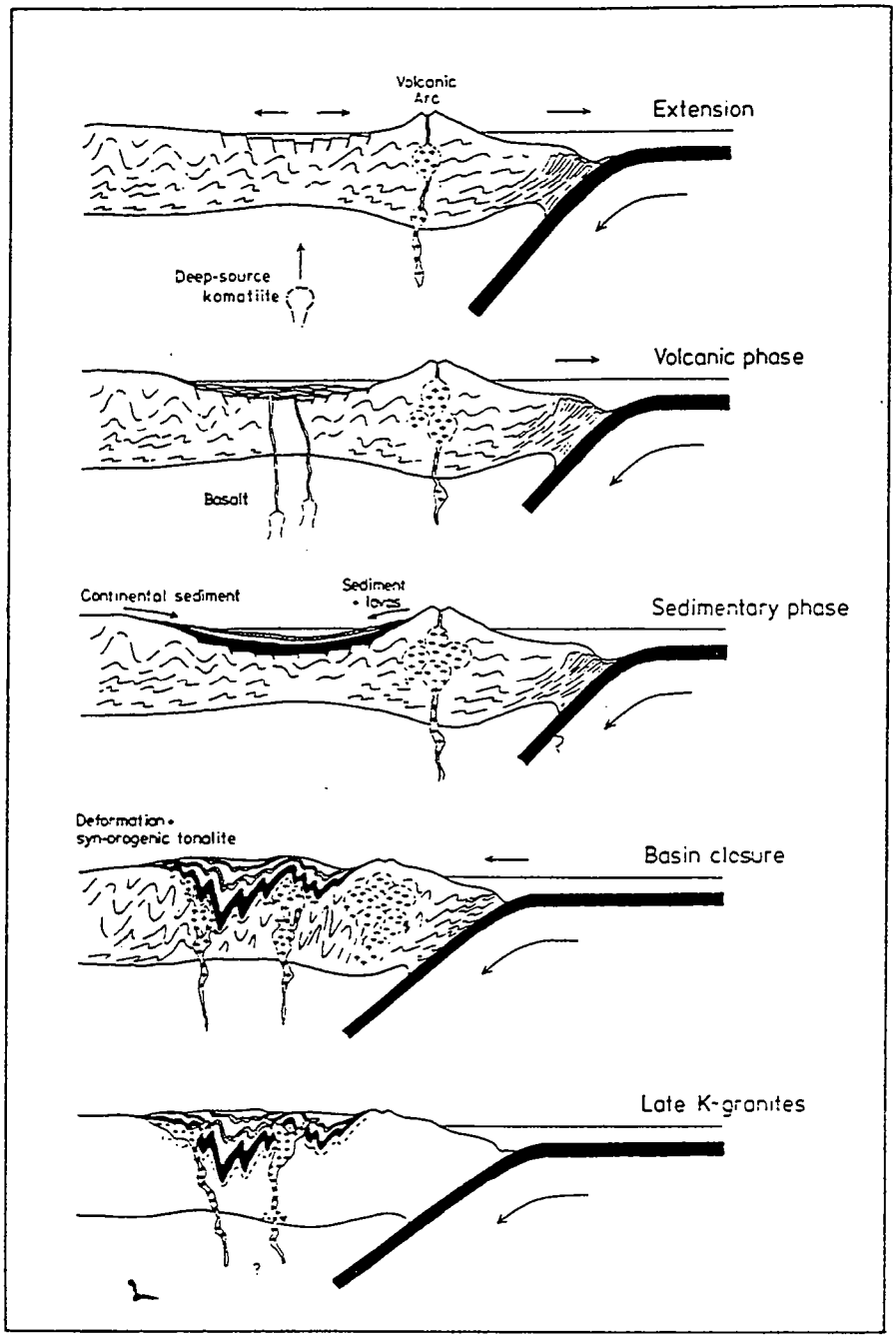

Fig. B. 2. Suggested development of an Archaean greenstone belt according to the "rocas verdes" model, with back-arc extension producing a greater component of crustal thinning rather than crustal rifting. Magma production exceeds that required for simple extension. Sediment source is mixed volcanigenic / continental and sequence may include calc-alkaline andesitic and salic lavas from the adjacent volcanic arc. Later movement of arc towards continent produces deformation and synclinal form of greenstone belt. Andean-type tonalitic to granitic plutons (derived from mantle by two- or three-stage process ; cf. Ringwood, 1974) may be syn to post-tectonic, with compositions dependent upon depth of melting of subducted oceanic crust, from Tarney et al., (1976).

magmas mantéliques à la base d'une croûte de nature basaltique peut induire la fusion partielle de cette dernière, laquelle fusion peut être à l'origine de la production de magmas de type TTG (Kröner & Layer, 1992).

Ce modèle a des conséquences très différentes du précédent sur la tectonique globale archéenne. En effet, il ne nécessite pas de déplacement de grandes entités lithosphériques. Il requiert uniquement une dynamique mantélique très active, marquée par la présence de nombreux panaches de type Islande.

2. LES CEINTURES DE ROCHES VERTES

Malgré de nombreuses études, la signification géodynamique des ceintures de roches vertes (l'autre constituant majeur de la croûte archéenne avec les séries TTG) demeure encore aujourd'hui très controversée. Pour un premier groupe d'auteurs, ces ceintures représenteraient les résidus d'une croûte océanique ayant recouvert la totalité du globe terrestre (ex : Fryer et al., 1979). Pour un deuxième groupe, elles résulteraient de l'évolution de zones de rifts développés entre deux plaques continentales sialiques divergentes (ex : Windley, 1973). Enfin, pour un dernier groupe, les ceintures de roches vertes représenteraient des bassins marginaux associés au développement de zones de subduction (ex : Tarney & Windley, 1981 ; Drury, 1983a). Ce modèle repose sur le fait que différents types de roches que l'on trouve dans les ceintures de roches vertes archéennes sont aussi présents dans les bassins marginaux actuels comme celui des "Rocas verdes" dans les Andes. Aussi, les environnements géodynamiques caractéristiques des zones de convergence lithosphérique sont considérés, par certains auteurs, comme des environnements susceptibles de rendre compte à la fois des caractéristiques pétrologiques, géochimiques et structurales des ceintures de roches vertes (Taira et al., 1992, Windley, 1993).

A ce dernier modèle, basé sur la convergence lithosphérique (Fig. B. 2), s'est ajoutée tout récemment une vision radicalement différente. En effet, Arndt et Albarède ont montré que les caractéristiques géologiques et géochimiques des tholéites archéennes (roche la plus abondante dans les ceintures de roches vertes), ne pouvaient, en fait, trouver d'analogue avec des basaltes modernes (Arndt & Albarède, 1992). Les basaltes archéens sont relativement pauvres en Al, présentent des

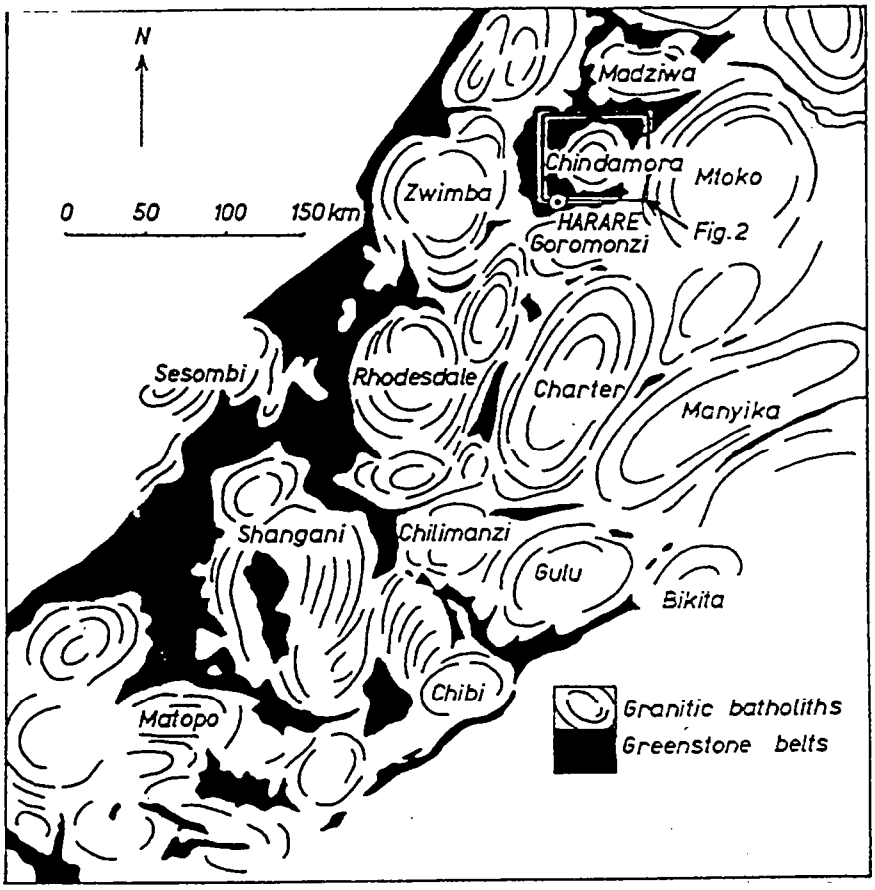

Fig. B . 3. General map of the Archaean craton of Zimbabwe showing the distribution of granitic batholiths and greenstone belts, after McGregor (1951), from Ramsay (1989).

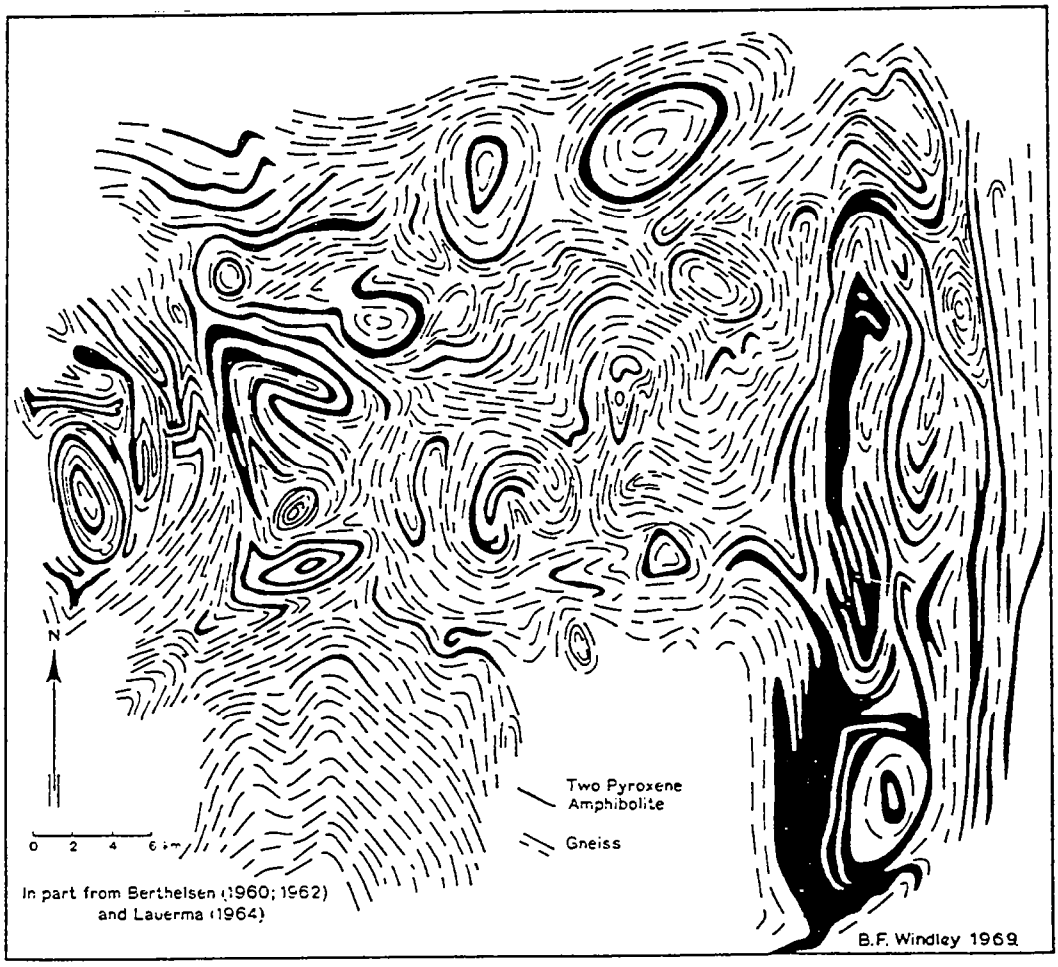

Fig. B. 4. The catazonal structural style of the High-grade basement terrain of the Fiskefjord region, W. Greenland, from Windley & Bridgewater (1971).

spectres de terres rares plats, voire enrichis en LREE. De plus, ils sont pauvres en éléments incompatibles mais riches en Fe, Ni et en Cr. De telles caractéristiques géochimiques suggèrent que les basaltes archéens se formaient par un fort taux de fusion partielle du manteau profond, ce qui, d'un point de vue du mode de genèse, pourrait correspondre à un environnement de type point chaud. Ainsi, les tholéites archéennes ne seraient ni les équivalents de rides médio-océaniques, ni d'éventuels reliques de bassins marginaux, mais représenteraient des sortes de plateaux volcaniques épais, témoins directs de la manifestation à la surface de la Terre de panaches issus du manteau profond.

On retrouve donc, au niveau de l'origine et de la signification des ceintures de roches vertes, la même opposition que pour les séries TTG entre les tenants d'une géodynamique basée sur des mouvements lithosphériques horizontaux et les tenants d'une géodynamique accordant une part plus importante aux mouvements verticaux de type "plume".

3. TECTONIQUE ARCHÉENNE

L'une des manifestations essentielles de la convergence lithosphérique est la collision continentale. Au cours des dernières années, différents auteurs ont suggéré que l'évolution structurale de certains cratons archéens témoignait de la convergence puis de la collision de domaines continentaux (ex : Burke et al., 1976 ; Light, 1982 ; Shackleton, 1986 ; De Wit et al., 1992) voire de collisions successives d'arcs océaniques (Spray, 1985 ; Ludden et al., 1986 ; Hoffman, 1989 ; Taira et al., 1992). La structuration à petite échelle de ces régions présente, d'après ces auteurs, des caractéristiques résolument modernes. Ce serait en particulier le cas, dans le craton archéen d'Afrique du Sud (ceinture de Limpopo) dont les ressemblances avec la chaîne Himalayenne ont récemment été proposées (Wilks, 1988 ; Treloar et al., 1992). Si la tendance actuelle est de plutôt considérer la tectonique archéenne comme représentative de zones de collisions modernes, d'autres auteurs ont proposé des modèles bien différents.

Nous présentons les principales structures d'échelle crustale qui ont été décrites dans les cratons archéens. Ensuite, nous rappelons les différentes idées émises pour expliquer leurs origines.

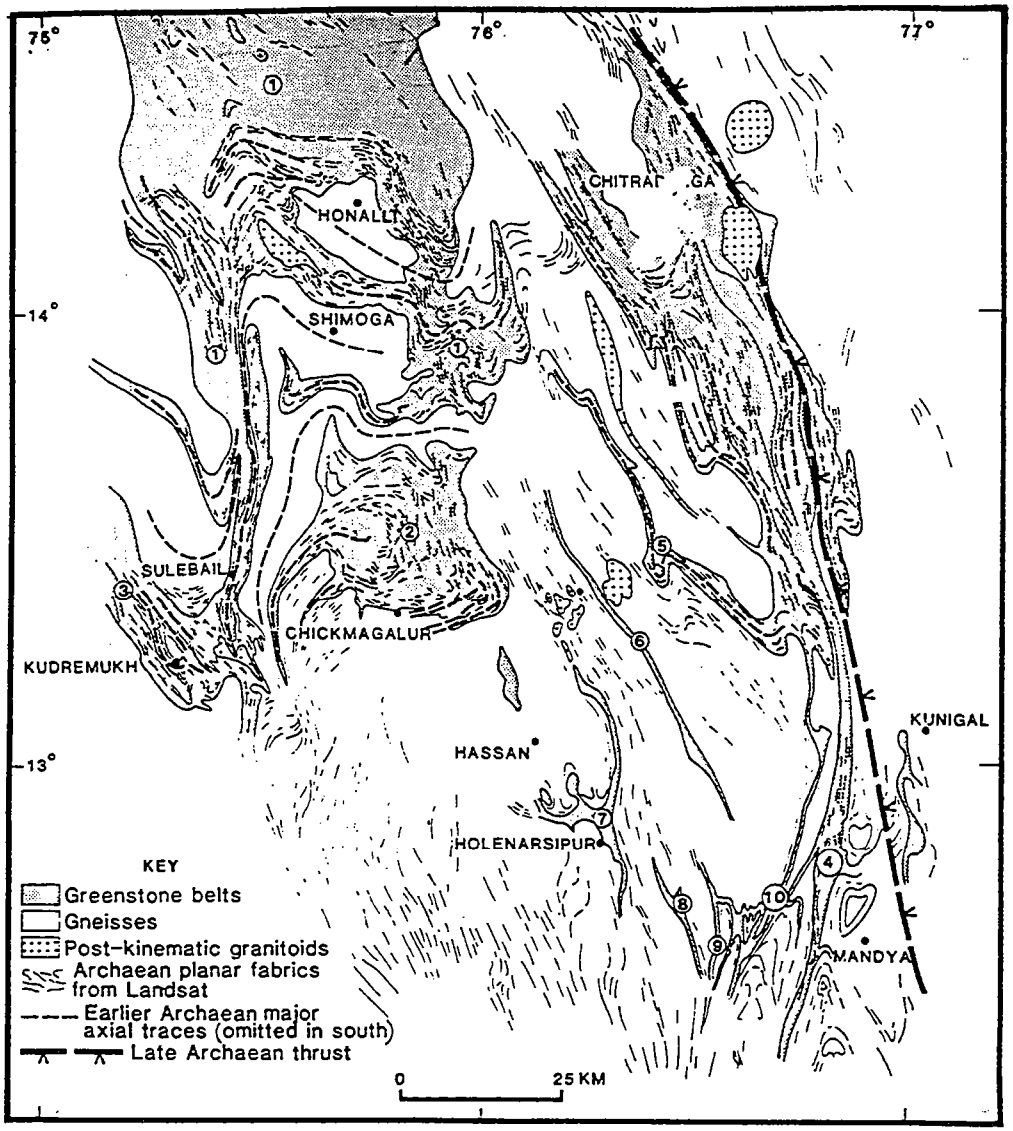

Fig. B. 5. Reconnaissance structural map of part of the western sub-block of the northern Archaean block, based on field data, published maps and interpretation of 1/500 000 photographic and 1/100 000 digitally enhanced Landsat images. Numbers 1-10 are Archaean supracrustal belts : 1-Shimoga-Goa ; 2-Bababudan ; 3-Kudremukh-West Coast ; 4-Chitradurga ; 5-Bommanahalli ; 6-Nuggihalli ; 7-Holenarsipur ; 8-Krishnarajpet ; 9-Hadanur ; 10-Nagamangala, from Dury et al., (1984).

3. 1. Structures d'échelle crustale

Seules les structures dont les dimensions ont une réalité cartographique sont présentées ici. Une exception concerne toutefois les structures tangentielles profondes. En effet, il n'a jamais été décrit dans la littérature de telles structures d'âge archéen dont la réalité cartographique soit indiscutable. Néanmoins, certains auteurs ont suggéré leur présence en domaines profonds (Bridgewater, 1974 ; Coward, 1976 ; Myers, 1984).

Structures en dômes-et-bassins

Les structures en dômes-et-bassins sont présentes sur la quasi-totalité des cratons archéens, aussi bien dans les domaines métamorphiques de haut grade (Windley & Bridgewater, 1971) que dans les domaines métamorphiques de plus bas grade (McGregor, 1951). Leurs dimensions et leurs formes sont très variables, de l'ordre d'une centaine de km (Fig. B. 3) jusqu'à la dizaine de km (Fig. B. 4). L'interprétation de ces structures est problématique. Pour certains, elles résultent de l'interférence de plis régionaux (ex : Snowden, 1984 ; Drury et al., 1984 ; Fyson, 1984 ; Myers & Watkins, 1985), pour d'autres, elles sont la conséquence du développement d'instabilités gravitaires de type diapirique (Collins, 1989 ; Ramsay, 1989 ; Bouhallier et al., 1993 ; Jelsma et al., 1993).

Structures d'interférence

Des structures d'interférence autres que celle en dômes-et-bassins ont été suggérées à une échelle régionale (Myers, 1984 ; Drury et al., 1984). Ce type de structures a été, par exemple, invoqué pour expliquer l'organisation parfois très complexe de l'interface entre le socle gneissique et les ceintures de roches vertes. C'est en particulier le cas dans le craton de Dharwar (Inde du Sud) où des interférences de type "champignons" (Ramsay, 1967) ont été décrites, d'après une étude satellitaire sur images LANDSAT (Drury, 1984). Ces structures d'interférence ont été associées au développement de nappes ou de plis isoclinaux déversés vers le Nord puis replissés lors de phases de raccourcissement tardives Est-Ouest (Fig. B. 5).

Fig. B. 6. Interpreted structural summary map of the Laverton-Wiluna region in the central Norseman-Wiluna belt illustrating the distribution of the main shear zones, faults and lags. Note the approximate location of the cross-section shown in Figure B. 16 , from Hammond & Nisbet, (1992).

Structures décrochantes

Les décrochements sont très largement représentées sur l'ensemble des cratons archéens (Fig. B. 6). Ils marquent le plus souvent la fin de l'évolution tectono-métamorphique intracontinentale des domaines archéens. Ces structures sont parfois très abondantes, et de part leur caractère tardif, rendent difficile l'étude des structures qui leur sont antérieures. Elles sont, de plus, souvent responsables de la juxtaposition de domaines métamorphiques de grade très différents et parfois, à l'origine de structures d'interférence (Drury et al., 1984).

Nappes superficielles

Des structures tangentielles impliquant de grandes quantités de matériel volcano-sédimentaire ont été décrites dans plusieurs provinces archéennes (Bickle et al., 1980 ; De Wit, 1982 ; De Wit & al., 1987a et b ; Camiré & Burg, 1993). A l'intérieur de certaines ceintures de roches vertes, des répétitions stratigraphiques correspondant en fait à l'empilement tectonique de nappes superficielles ont été remarquées (Fig. B. 7). Le déversement de plis isoclinaux, associé au développement de nombreuses zones mylonitiques a, par exemple, été observé dans la ceinture de roches vertes de Selukwe au Zimbabwe (Stowe, 1984). De part la quantité d'aplatissement très importante relevée sur l'ensemble de l'architecture, ces structures superficielles ont été interprétées en terme de nappes résultant d'un étalement d'origine gravitaire. Cotteril (1979) suggère même la présence de structures syn-sédimentaires de type "slump" affectant des roches saturées en eau, non encore consolidées.

Des structures superficielles similaires ont pu être décrites dans la ceinture de roches vertes de Barberton en Afrique du Sud (De Wit, 1982 ; Jackson et al., 1987). Ces auteurs relèvent l'existence d'olistostromes, de séquences stratigraphiques inversées ainsi que la juxtaposition de sédiments de faible et forte épaisseur d'eau (Fig. B. 8). L'ensemble de ces observations suggère des déplacements horizontaux d'une grande quantité de matière.

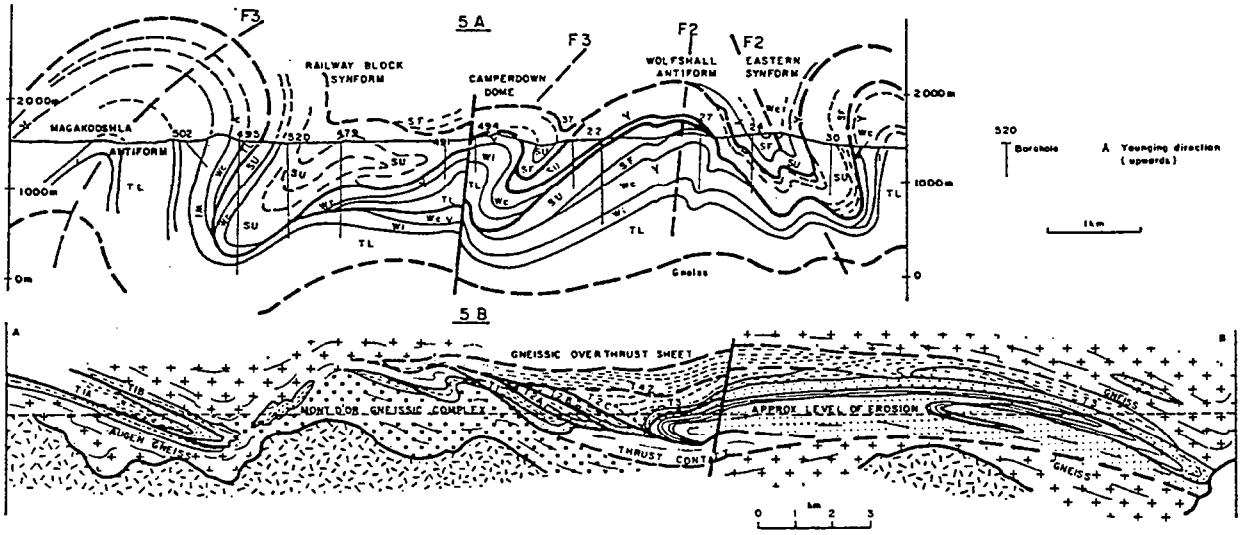

Fig. B. 7. Cross section drawn through the railway block synform normal to the F3 fold axes, illustrating the downward facing sequence. SF = Selukwe Formation ; SU = Selukwe Ultramafic Complex ; Wc = Wandler formation conglomerate ; Wi = Wander banded iron formation ; TL = Tibilikwe formation, from Stowe, (1984).

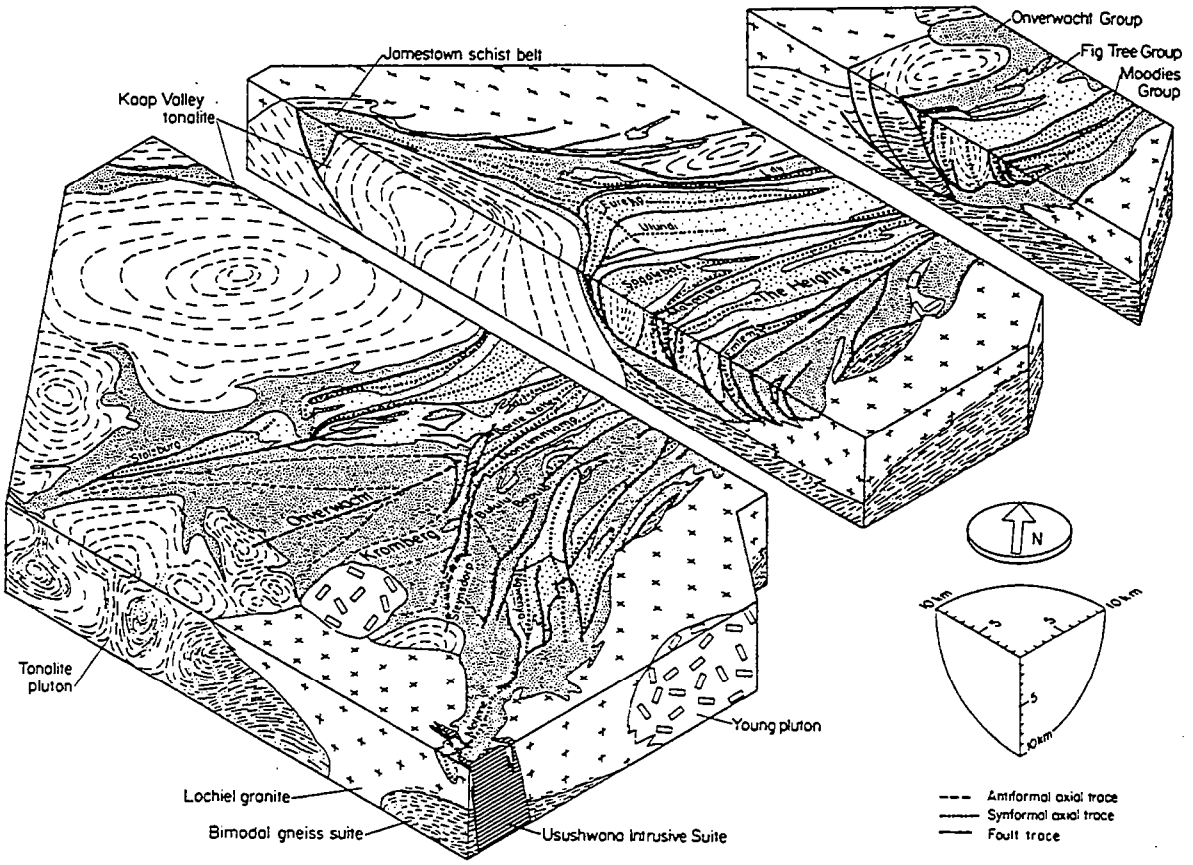

Fig. B. 8. Isometric exploded block diagram of the main part of the Barberton greenstone belt and surrounding area compiled from surface mapping by Reimer (1967), Anhaeusseur (1976), Heinrichs (1980) and Urie (1968, 1969, 1970, 1971). Deep structure is schematic, based on Darracot (1975) and Fripp et al. (1980). Basal Onverwacht thrust may be folded by later diapirism, from Jackson et al., (1987).

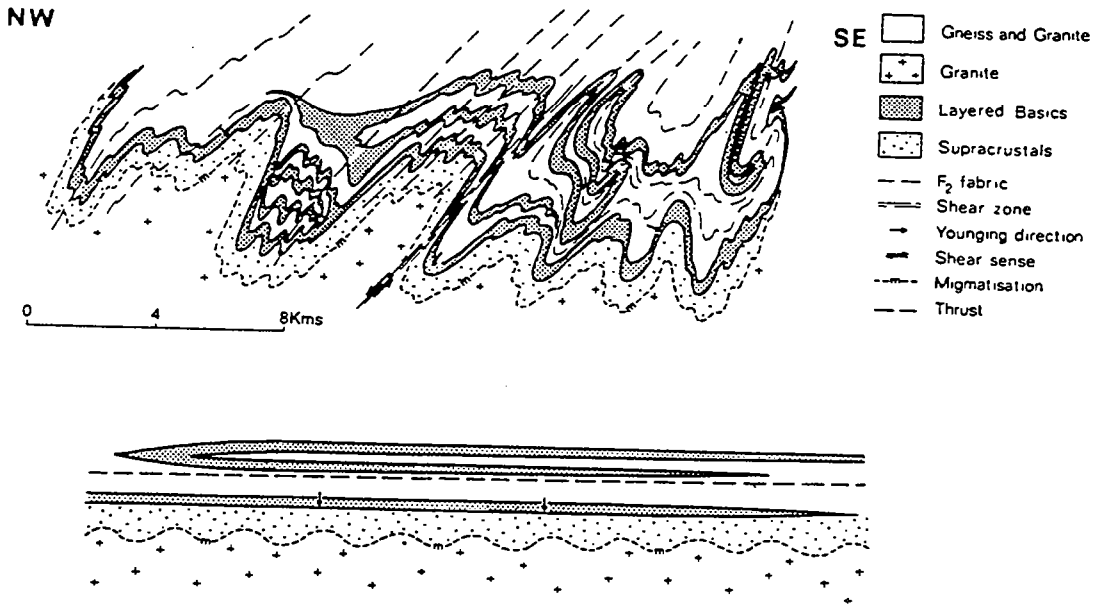

Fig. B. 9. Profile through the structures in the central part of the Limpopo belt, between Banes Drift and Pikwe. Arrows show youging directions. Lower section shows the form of the structure prior to F2 and F3 Limpopo deformation. The lowermost layer of basic and supracrustals faces downwards into migmatitic granite. The gneisses stratigraphically below the layered basics show deformation events pre-dating the first structures in the supracrustal rocks and may represent an earlier basement, from Coward et al., (1976).

Nappes profondes

A la différence des structures tangentielles superficielles, les structures tangentielles profondes sont extrêmement mal documentées. Elles ont été par exemple suggérées au Groenland d'après des considérations géochronologiques (Bridgwater, 1974). Les faits structuraux sont en fait très pauvres. Les intercalations successives de roches de natures différentes (amphibolites, métapélites, quartzites etc..) associées à une déformation régionale très forte ont amené certains auteurs à proposer l'existence de nappes replissées (Myers, 1976, 1984, Chadwick & Nutman, 1979). La cinématique de ces structures n'est toutefois pas connue.

Dans les faits, l'interprétation sur l'origine des structures observables dans les domaines archéens profonds se résume le plus souvent à discuter la nature de marqueurs supposés initialement horizontaux (le plus souvent associés à une foliation) et dont on ne peut que difficilement caractériser la cinématique et la géométrie originelle. De plus, ces structures primaires sont reprises lors de déformations successives tardives, parfois très intenses (Coward et al., 1976).

Malgré ces difficultés, un certain nombre de travaux ont pu argumenter la présence de structures tangentielles archéennes profondes (Coward et al., 1976). Il s'agit, dans tous les cas, de plis isoclinaux à plan axial faiblement penté (Fig. B. 9). Curieusement, ces structures anciennes ont été systématiquement rapportées à l'existence de structures chevauchantes majeures (ex : Biclkle et al., 1980). La seule chose qu'il soit possible de dire à ce propos, est que l'on puisse effectivement envisager l'existence d'une déformation régionale ancienne, affectant les domaines profonds du socle, et dont les caractéristiques structurales sont marquées par un très fort raccourcissement vertical. Des processus tectoniques aussi différents que l'extension crustale ou le diapirisme régional (Ramberg, 1967) peuvent aussi rendre compte de telles observations. Néanmoins, la plupart des domaines profonds archéens ne présentent pas (ou plus ?) ces structures à l'affleurement. Les structures et la foliation que l'on voit sont verticales, associées à une déformation globalement homogène et souvent très intense (Choukroune et al., in press).

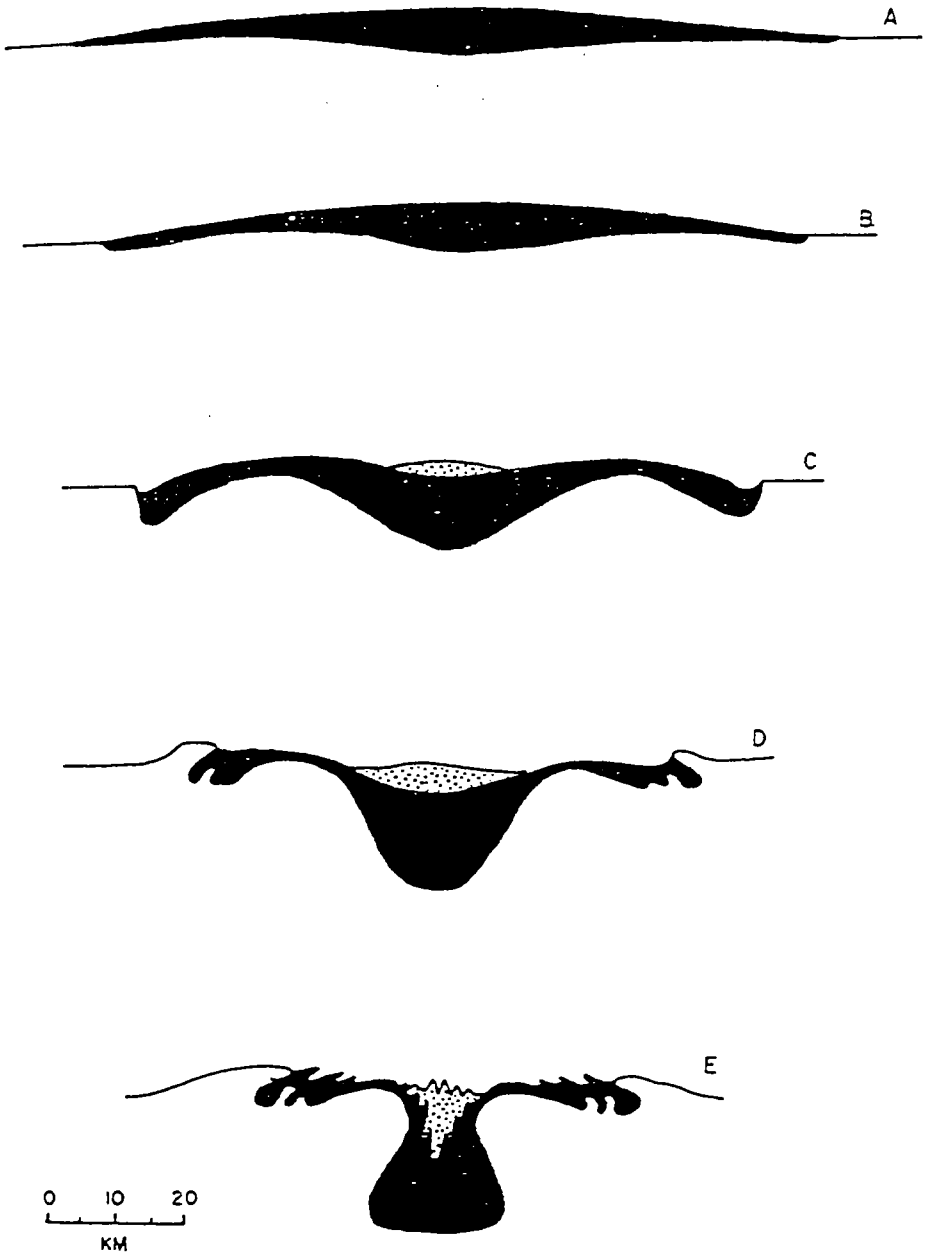

Fig. B. 10. Schematic representation of the stages of the deformation of a greenstone belt overlying a sialic crust, from the initial (A) to the final (E) configurations. Note the lateral shortening. Black represents the volcanic succession, and the stipple represents later "calc-alkaline" volcanic rocks and detrital sediments, from Gorman et al., (1978).

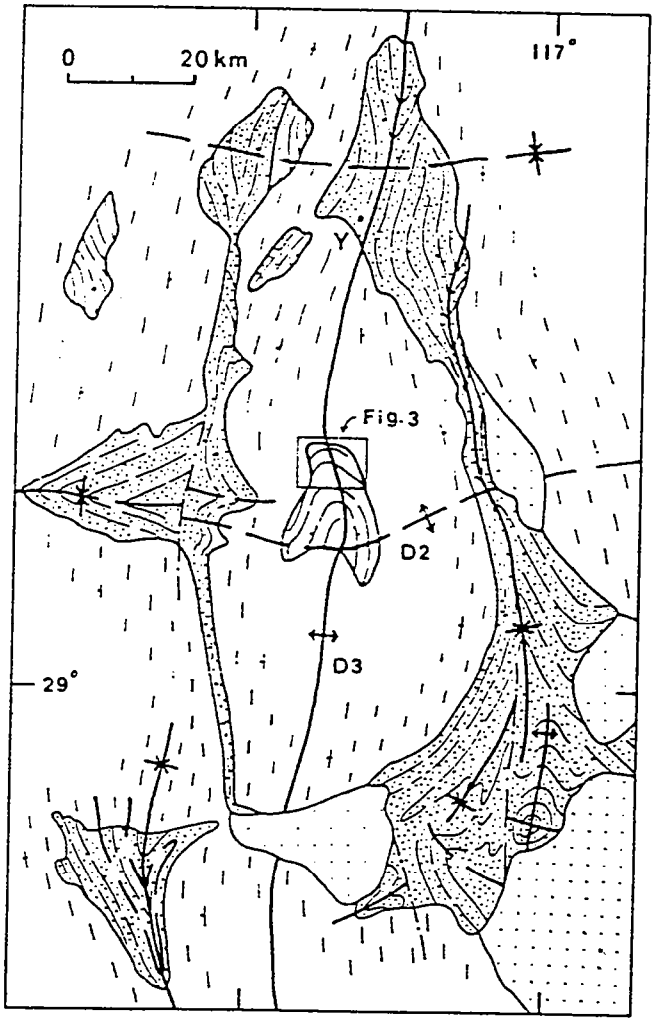

Fig. B. 11. Simplified geologic map of granite-greenstone terrain near Yalgoo (Y). Stipple with form lines of bedding = greenstones ; white with form lines of banding = pegmatite-anded gneiss ; white with short lines indicating D3 foliation where developed = recrystallized monzogranite ; crosses = post tectonic granitoid intrusions. Dips of bedding, banding, and foliation range from 65° to 90°. Thick continuous and broken lines indicate inferred major D3 and D2 fold axial traces, respectively. Dot-dash line = major fault, from Myers & Watkins, (1985).

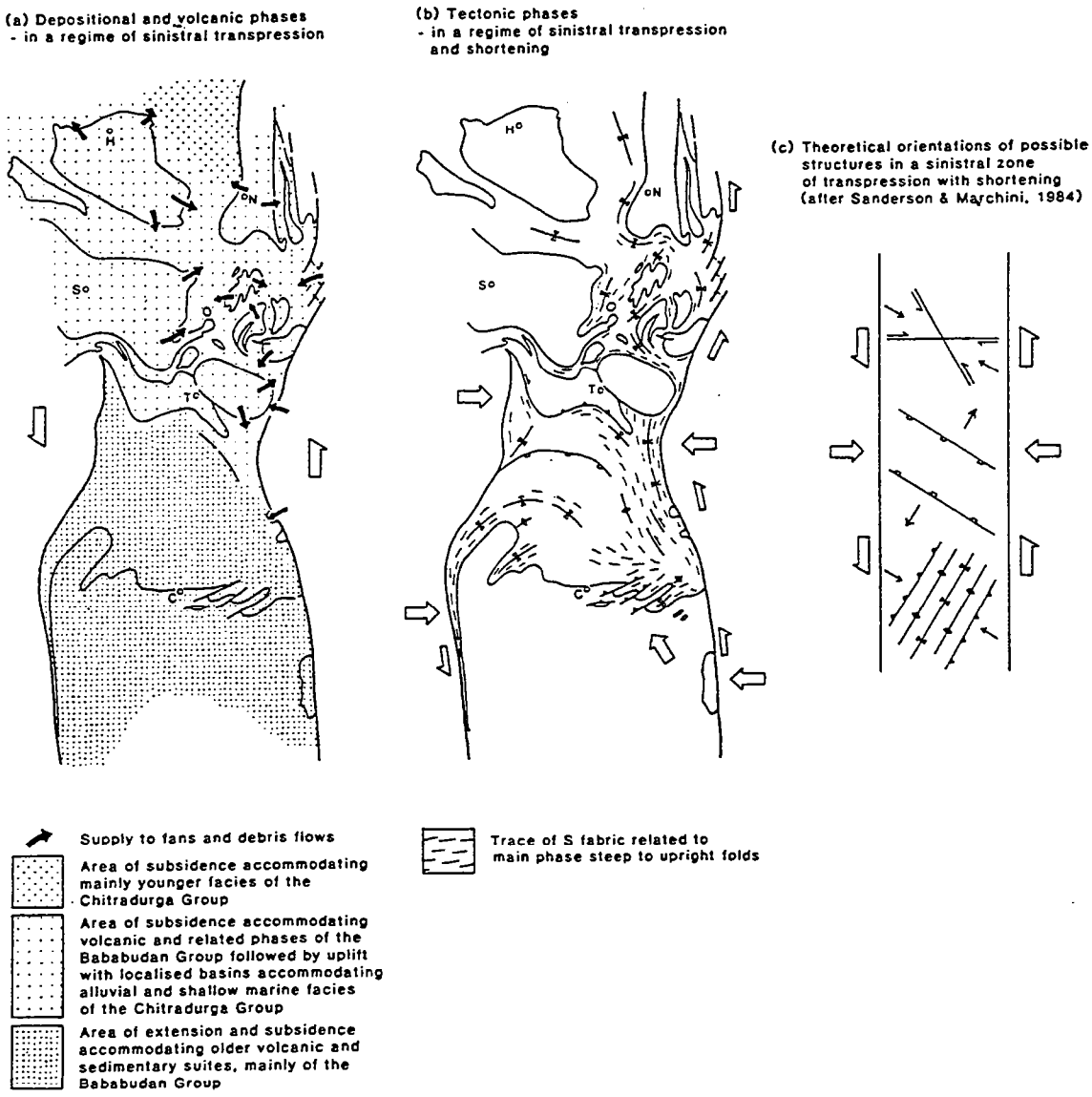

Fig. B. 12. Summary models of (a) the depositional and volcanic phases and (b) the structure of the Bababudan-Nallur basin compared with (c) the orientation of structures predicted in a zone of sinistral transpression with shortening after Sanderson & Marchini (1984). Note that in (a) the relative positions of the cover-basement boundaries are for for convenience based on present distributions, the original spatial relations being unknown, and in (b) the finite tectonic relations are indicated, from Chadwick et al., (1989).

3. 2. Mécanismes

Le diapirisme

Les instabilités gravitaires de type Raleigh-Taylor correspondent à un mécanisme physique connu depuis la fin du siècle dernier (Rayleigh, 1893). Ce phénomène physique, lié à la perturbation locale de la distribution des densités d'un multi-couche a été proposé par Wegmann (1935), puis par Eskola (1949) comme l'agent fondamental de la formation des dômes gneissiques. Dès 1951, MacGregor reprend cette idée pour expliquer la déformation observée dans le craton archéen de Rhodhésie. Il suggère que l'enfoncement d'une surcharge locale de coulées volcaniques basiques denses reposant sur un socle granito-gneissique plus léger (sagduction) soit le moteur des déformations observées à la fois dans le socle et dans la couverture volcanique. Ce concept a été, par la suite, amélioré et généralisé à d'autres cratons archéens (Anhaeusseur, 1969, 1973 ; Glikson, 1971, 1972 ; Drury, 1977 ; Schwerdtner et al., 1979).

Gorman et al. (1978), en se basant sur les expériences de Ramberg (1967, 1971, 1973), propose un modèle évolutif représentant les différents stades de la sagduction d'une ceinture de roches vertes (Fig. B. 10). Ce modèle présente des structures chevauchantes, périphériques aux zones subsidentes, dont la cinématique s'accorde avec le développement du diapir. Suivant un scénario similaire, Mareshal et West (1980) produisent des modèles numériques de l'évolution thermo-mécanique d'une croûte de composition granitique recouverte d'une épaisse couche de laves. Ils démontrent qu'il est tout à fait possible d'envisager, d'un point de vue thermo-mécanique, une origine diapirique pour le développement des ceintures de roches vertes.

Plissements superposés

Les interférences de plis ont été proposées en alternative au diapirisme pour expliquer l'organisation régionale des ceintures de roches vertes (ex : Snowden & Bickle, 1976 ; Fyson, 1984 ; Myers & Watkins, 1985). Ce mécanisme suppose la superposition de deux phases de déformation issues de deux raccourcissements régionaux (Fig. B. 11). Les quantités de raccourcissement nécessaires pour rendre compte de l'amplitude des struc-

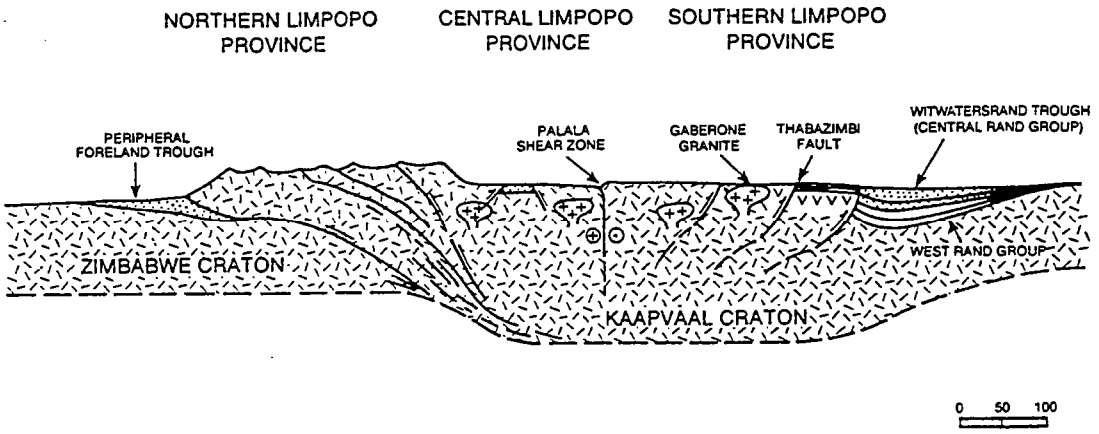

Fig. B. 13. Cross section through the Kaapval and Zimbabwe Cratons across the Limpopo Province, a product of the collision between the two cratons at approximately 2.7 ago. It is suggested in this diagram that the upper Witwatersrand strat were deposited in a foreland basin on the cratonward side of on uplifted plateau overlying continent greatly thickened (similar to Tibet) in the Kaapvaal/Zimbabwe collision, from Burke et al., (1986).

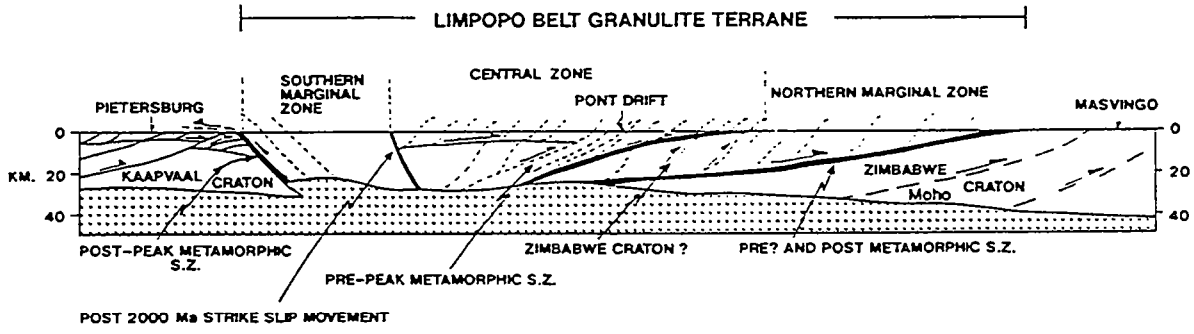

Fig. B. 14. Crustal profile across the Limpopo Belt based mainly on the geophysical data of De Beer and Stettler (1992), from Roering et al., (1992).

-tures observées sont très importantes et ce pour les deux épisodes tectoniques distincts.

Décrochements en contexte compressif

Des modèles transpressifs (ex : Swager et al., 1989 ; Chadwick et al., 1989) ont parfois été proposés pour rendre compte et de l'histoire subsidente et des déformations observées lors du développement des ceintures de roches vertes (Fig. B. 12). Platt (1980), construit un schéma évolutif des ceintures de roches vertes de l'Archéen d'Australie de type intra-continentale en contexte décrochant. Il propose que la déformation contemporaine de la mise en place des dômes-et-bassins soit en fait l'expression de plis en échelon, associés à de grandes zones de décrochements ductiles.

Epaississement crustal par empilements

Ce processus tectonique a surtout été invoqué pour expliquer le réajustement isostatique de domaines granulitiques archéens développés sur de très grandes surfaces et dont les mohos, sismiquement plats, sont détectés entre 30 et 40 km de profondeur.

Un processus tel que l'épaississement par empilements d'unités crustales peut être effectivement à l'origine de ce réajustement isostatique. Il nécessite un raccourcissement régional important et a été invoqué, par exemple, pour expliquer la présence de la ceinture granulitique du Limpopo (Fig. B. 13 & B. 14) entre les cratons archéens du Kaapval et du Zimbabwe (Coward & Fairhead, 1980 ; De Wit et al., 1992 ; Van Reenen et al., 1992). Ce modèle s'appuie sur des observations de terrain, des données géophysiques et géochronologiques dont une synthèse a récemment été publiée (Van Reenen et al., 1992).

Des chevauchements consécutifs à un raccourcissement régional ont aussi été proposés, par exemple, pour la province du Yilgarn en Australie (Fig. B. 15). Leur reconnaissance est basée sur la présence de répétitions stratigraphiques et de plis isoclinaux affectant les ceintures de roches vertes (Swager & Griffin, 1990). Ces mêmes structures tangentielles, dont les zones de décollements basales se localisent généralement au niveau d'interfaces

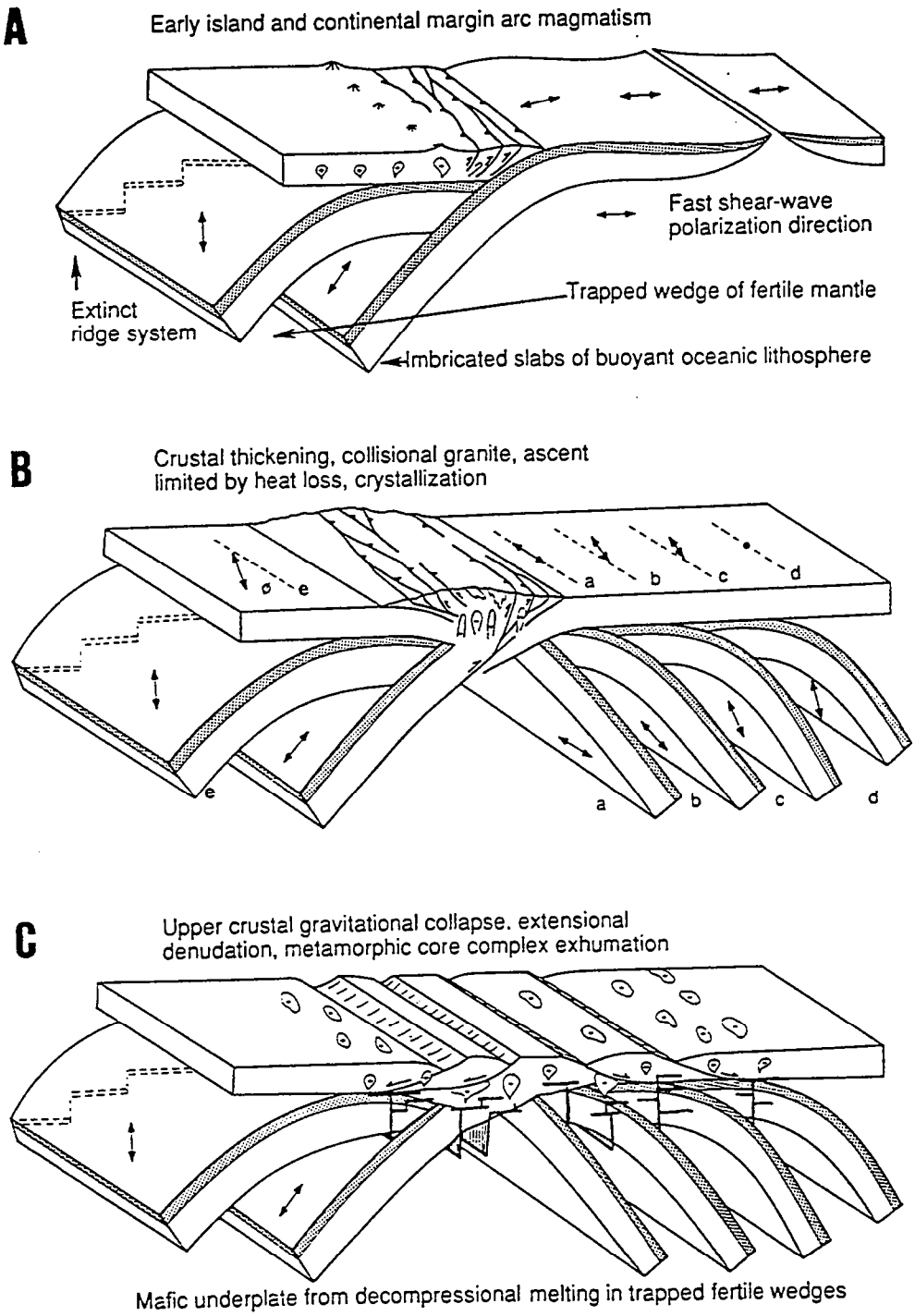

Fig. B. 15. General tectonic model, from Kusky, (1993).

lithologiques, ont été rapportées aux effets d'un raccourcissement régional majeur dans les ceintures de Barberton en Afrique du Sud (De Wit, 1982) ou de Selikwe au Zimbabwe (Stowe, 1984). L'environnement géodynamique de ces structures tangentielles a été comparé à celui de domaines océaniques obductés sur une croûte continentale.

Le domaine granulitique du craton Archéen de Dharwar a aussi été présenté comme le résultat d'un réajustement isostatique consécutif à un empilement d'unités structurales. Dans ce cas, l'épaississement est déduit de la géométrie des ceintures de roches vertes censée représenter des plis et des nappes charriés vers le Nord.

Extension post-épaississement

L'extension post-orogénique constitue une étape importante de l'évolution intra-continentale des domaines de collision (Dewey, 1988). Ce phénomène, dont la dynamique apparait clairement associée à relaxation thermique des zones continentales épaissies et au développement des "metamorphic core complexes", a souvent été décrit dans les zones orogéniques d'âge phanérozoïque (ex : Van den Driessche & Brun, 1991 ; Gautier et al., 1993).

Bien qu'aucune preuve pétrologique d'épaississement crustal n'ait été fourni, un modèle de ce type a récemment été proposé pour les provinces archéennes d'Australie et du Canada (Kusky, 1993, fig. B. 15).

Extension ante-épaississement

Sur cette même province du Yilgarn, précisément là où le modèle précédent a été en partie construit, un épisode extensif majeur, cette fois-ci précédant la séquence de déformation liée à un raccourcissement régional a été suggéré (Fig. B. 16, Hammond & Nisbet, 1992). Cette proposition repose, en ce qui concerne les caractéristiques structurales, sur (i) la présence de zones mylonitiques faiblement pentées entre les ceintures de roches vertes et le socle gneissique, (ii) la géométrie des linéations et la présence de critères cinématiques indiquant un déplacement général des séries vers le Sud, (iii) et finalement la présence de gradients métamorphiques très forts dans les ceintures de roches vertes.

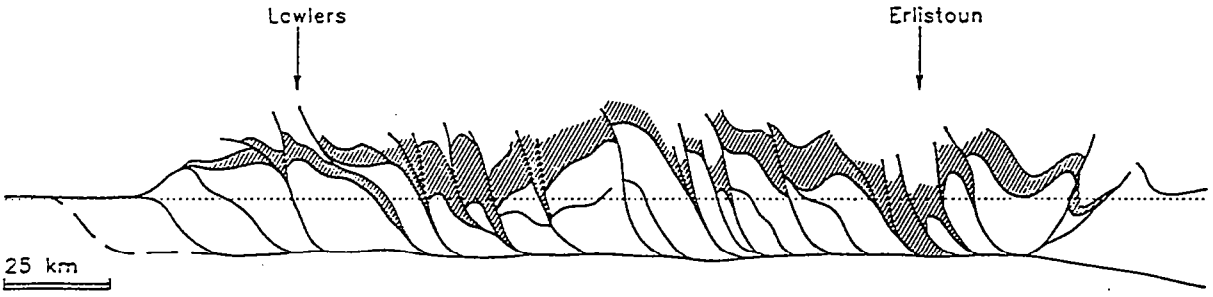

Fig. B. 16. Simplified sketch section illustrating the style of large-scale thrust imbrication envisaged for D2 shortening. Hatching denotes greenstone, the dotted line represents the approximate present level of exposure, and the section is drawn without vertical exageration, from Hammond & Nisbet, (1992).

OBJECTIFS ET MÉTHODES

Le travail que nous présentons dans cette thèse a comme objectif principal de ***caractériser l'évolution tectono-métamorphique d'un segment de croûte continentale archéenne*** . Le terrain d'étude est le craton archéen de Dharwar, dans le Sud de l'Inde. Ce craton a été choisi car (i) les conditions d'affleurement permettent d'accéder aux différents niveaux structuraux d'un même et unique segment de croûte continentale archéenne ; (ii) il est à priori exempt de toute déformation post-archéenne.

Les axes de recherche précis développé dans le cadre de ce travail ont été définis en référence aux questions fondamentales suivantes :

- Quelles sont, à l'échelle de la croûte, les structures et les champs de déformation qui caractérisent le craton archéen de Dharwar ?
- Quelle sont l'étendue et la représentativité de ces structures sur l'ensemble du craton ?
- Les structures des domaines métamorphique de plus haut grade (Hb-granulite faciès) et celles des domaines métamorphiques de plus bas grade (Amphibolite faciès) sont-elles complémentaires ?

Les méthodes structurales utilisées consistent à recueillir puis à intégrer sur cartes des données ponctuelles relatives à la déformation afin de reconnaître et de caractériser les grandes structures crustales d'une région donnée. Pour une grande part, cette méthode repose sur le travail d'analyse effectué sur le terrain. Le report sur cartes des paramètres relatifs aux déformations finies et incrémentales nécessite une couverture spatiale importante. Dès lors que la zone d'étude est définie, l'acquisition des données peut débuter : en plus des caractéristiques lithologiques et pétrographiques, on relève sur chaque station les données suivantes relatives à la déformation :

- l'orientation des axes principaux de l'ellipsoïde de la déformation finie,
- son intensité,
- Le type de l'ellipsoïde de la déformation finie et les textures significatives,
- les régimes de la déformation (coaxial ou non coaxial).

Ainsi, à chaque station étudiée, est attribué un ensemble de paramètres relatifs à la déformation. Leur intégration en carte, et par

conséquent dans l'espace permet la construction des champs de déformation, d'où est déduit la nature des structures de dimension régionale. Cette démarche est simple et son efficacité a été démontrée dans l'étude des domaines orogéniques récents et protérozoïques.

Cinq mois de missions sur le terrain ont été nécessaires pour couvrir et étudier en détail une surface de près de 1300 km^2. Ces cinq mois de missions nous ont permis de construire la première carte, jamais réalisée, des trajectoires de la déformation à l'échelle de croûte archéenne du Sud de l'Inde. Cette carte permet de dégager une image globale de l'évolution structurale de la croûte moyenne et inférieure du craton archéen de Dharwar. Les données structurales et leurs interprétations seront exposées et développées dans la suite de cette thèse sous la forme de trois articles publiés et/ou soumis.

Si elle nous renseigne sur la géométrie et la cinématique des structures, la démarche cartographique ne nous livre que très peu d'informations sur les conditions physiques de la déformation. C'est pour cette raison que nous y avons associé une étude pétrologique des conditions du métamorphisme. Ainsi, après un échantillonnage systématique des différentes lithologies métamorphiques, celles présentant les assemblages de plus faible variance (nombre maximal de phases minérales pour un minimum de constituants chimiques) ont été retenues pour une étude approfondie (analyse microsonde, analyse topologique et thermo-barométrie). Les données et leurs interprétations seront exposées et développées dans la suite de cette thèse sous la forme d'une publication.

Partie D

LE CRATON ARCHÉEN DE DHARWAR (INDE)

1. CONTEXTE GÉOLOGIQUE ET TRAVAUX ANTÉRIEURS

1. 1. La zone d'étude

Le craton Archéen de Dharwar ("Karnataka nucleus") se situe dans la partie méridionale de la péninsule indienne où il couvre une surface de près de 205 000 km2 (Fig. D. 1). Il appartient à un ensemble de trois nuclei archéens qui sont du Nord vers le Sud : le Singhbhum nucleus (SN), le Jeypore-Bastar nucleus (JBN) et le Karnataka nucleus (KN). Il est recouvert au Nord par les coulées volcaniques des trappes du Deccan ainsi que par une série de bassins d'âge protérozoïque (bassins de Kaladgi, de Badami et de Bhima). Le graben de Godavari, montrant plusieurs périodes de réactivation (Subba Raju et al., 1978 ; Rogers, 1986), le limite au Nord-Est tandis qu'à l'Est, le craton constitue l'avant-pays de la chaîne protérozoïque des Eastern Ghats (Kaila & Tewari, 1982). La mer arabique le borde à l'Ouest tandis qu'au Sud (Fig. D. 2), de grandes discontinuités structurales le juxtaposent avec un ensemble de roches granulitiques dont l'âge a récemment été précisé dans l'intervalle 2.55-2.51 Ga (Peucat et al., 1993).

L'ensemble des travaux et résultats présentés dans le cadre de cette thèse proviennent tous des régions situées à l'Ouest du batholite du Closepet, approximativement entre les latitudes 11°30' et 13°30'.

1. 2. Les unités lithologiques en présence

La composition lithologique de la croûte continentale archéenne du craton de Dharwar se résume à trois grands types de roches. Dans le secteur étudié, ce sont par ordre d'abondance :

- des gneiss (les gneiss "Péninsulaires"),
- des ceintures de roches vertes (roches volcaniques et sédimentaires),
- des plutons granitiques tardifs.

Remarque : Le domaine granulitique ne constitue pas en soit un domaine lithologique distinct. Ce domaine se compose, en fait, des trois unités lithologiques évoquées précédemment à la différence près qu'elles ont développé des paragenèses granulitiques.

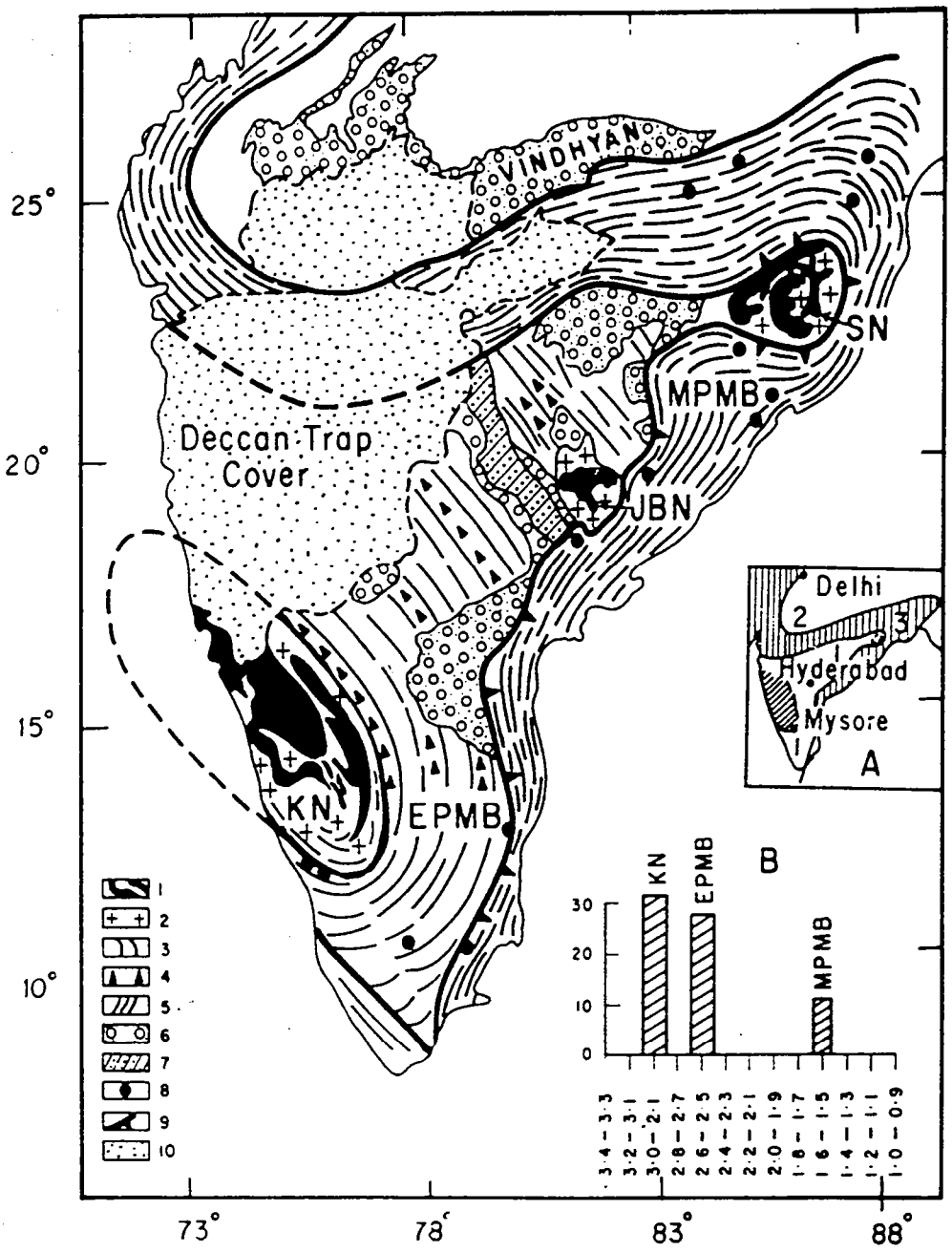

Fig. D .1. Generalized geological map of Peninsular India. KN - Karnataka nucleus, SN - Singhbhum nucleus, JBN - Jeypore-Bastar nucleus, EPMB - early Proterozoic mobile belt, MPMB - middle Proterozoic mobile belt ; 1 - schist belts within nucleii, 2 - Tonalitic gneisses, 3 - Granodiorites-granulites of EPMB, 4 - Granites-K in EPMB, 5 - Granulites and gneisses of MPMB, 6 - Middle Proterozoic sedimentary basins, 7 - Gondwana sediment of Godavari rift valley, 8 - Anorthosites emplaced along the EPMB-MPMB contact, 9 - Eastern Ghat Sukinda-singhbhum thrusts, 10 - Deccan trap cover ; modified from Radhakrishna & Naqvi, (1986).

Les gneiss péninsulaires

Près des deux-tiers du craton sont constitués de cet ensemble lithologique (Fig. D. 2) qui est, des trois, de loin le plus mal connu. En fait, il regroupe tout ce qui n'est pas assimilable à l'un des deux autres ensembles. Ainsi, y ont été regroupées des roches ortho- et paragneissiques (Janardhan et al., 1978, Naqvi et al., 1983b, Rogers et al., 1986). Des études ont cependant permis d'établir quelques caractéristiques de première importance des gneiss péninsulaires. Par exemple, il a pu être montré que ces gneiss étaient, pour l'essentiel, orthodérivés (Swami Nath & Ramakrishnan, 1981) et appartenaient à une lignée de type TTG (Bhaskar Rao et al., 1983). De plus, les rapports initiaux $^{87}Sr/^{86}Sr$ sont souvent très bas (Beckinsale et al., 1980 ; Monrad, 1983 ; Stroh et al., 1983 ; Taylor et al., 1984 ; Rogers et al., 1986, Meen et al., 1992), ce qui atteste soit d'une origine directement mantélique soit d'une origine par fusion de protolithes à faible temps de résidence crustale (Rogers et al., 1986). Les plus anciens de ces gneiss ont été, jusqu'à présent, reconnus dans la région d'Holenarsipur et ont fourni des âges de 3358+/- 66 Ma et 3315+/-54 Ma par la méthode Rb-Sr sur roche totale (Beckinsale et al., 1980, 1982).

Différents faciès gneissiques peuvent être macroscopiquement distingués sur le terrain (photos a, c, f, k, n, o, annexe). Pétrographiquement et géochimiquement, il est parfois possible de différencier certains de ces faciès gneissiques, sans que pour autant des différences d'âge significatives aient pu jusqu'alors être avancées (Monrad, 1983). L'absence d'une cartographie détaillée de ces différents faciès constitue un obstacle important pour la compréhension globale de l'histoire magmatique et tectono-métamorphique des gneiss péninsulaires à l'échelle du craton.

Les ceintures de roches vertes

Les ceintures de roches vertes du craton de Dharwar ont été abondamment étudiées (Swami Nath & Ramakrishnan, 1981, Radhakrishna & Ramakrisnan, 1990). Les constituants de ces ceintures, regroupés dans la littérature sous le terme général de roches supracrustales, sont principalement des volcanites ultrabasiques (komatiites), basiques et acides, et des sédiments clastiques. La distribution des ceintures de roches vertes n'est pas uniforme à l'échelle du craton de Dharwar (Fig. D. 2 et D . 3). Ainsi, à l'Est du batholite du Closepet, les ceintures supracrustales

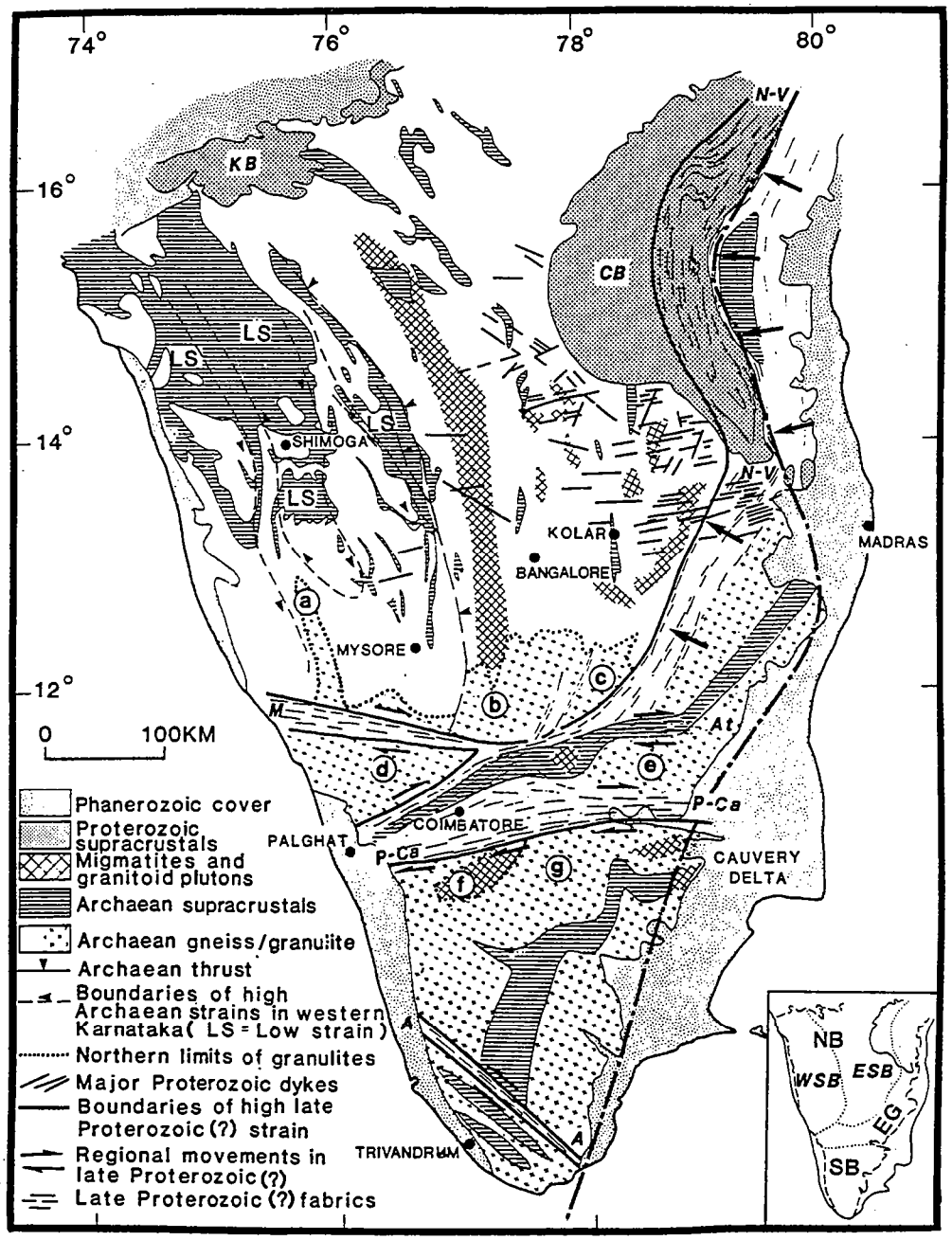

Fig D. 2. Tectonic map of South India. Bold dot-dash line indicates the western limit of a positive Bouguer gravity anomaly (Kaila & Batia, 1981). The mid-Proterozoic Cuddapah and Kaladgi basins are indicated by CB and KB ; late-Proterozoic zones of high strain are : N-V, Nallamalai-Velikonda ; M-B, Moyar-Bhavani ; At, Attur ; P-Ca, Palghat-Cauvery ; A, Achankovil ; lower case letters a-g are granulite massifs referred to in the text : a - Coorg ; b - Biligirirangan (B-R) ; c - Shevroi ; d - Nilgiri ; e - Kollimalai ; F - Anaimalai ; g - Palni. The inset shows the main Archaean blocks in South India : EG - Eastern Ghats ; NB - northern block ; WSB - western sub-block ; SB - southern block ; from Drury et al., (1984).

sont relativement peu abondantes, alors qu'à l'Ouest, elles développent de grands bassins, avec toutefois une tendance à disparaître lorsque l'on se dirige vers le Sud (Fig. D. 2 et D. 3). Dans les bassins au Nord-Ouest du Closepet, les séquences supracrustales présentent des variations latérales de puissance très importantes, depuis quelques centaines de mètres jusqu'à plusieurs kilomètres (Chadwick et al., 1985a et b).

Les études régionales ont conduit à la distinction et à la reconnaissance de deux types de ceintures : le type "Sargur" et le type "Dharwar" (Viswanatha & Ramakrishnan, 1976, Swami Nath et al., 1976). Le type Sargur représenterait une génération de roches supracrustales antérieure au type Dharwar. Le type Sargur a été défini à l'extrême Sud du craton (Fig. D. 3). Il se caractérise par l'abondance des séquences volcaniques basiques et ultrabasiques, ainsi que par un métamorphisme de haut à moyen grade et une déformation intense. Le type Dharwar a été défini lui à l'extrême Nord du craton (Fig. D. 3). Il se caractérise par la présence de faciès volcano-détritiques et méta-sédimentaires plus abondants que dans le type Sargur, ainsi que par un métamorphisme de bas à moyen grade et une déformation d'intensité plutôt modérée.

A ce stade, il convient de souligner que la notion "Sargur plus ancien que Dharwar" repose uniquement sur des différences de nature lithologique, de grade de métamorphisme et d'intensité de la déformation. En l'absence de données radiochronologiques, il ne peut pas être exclu qu'une partie des ceintures de type Sargur soit en fait, constituée de faciès lithologiques du type Dharwar incorporés tectoniquement dans des niveaux structuraux plus profonds. Ceci étant, l'existence d'au moins deux générations de ceintures de roches vertes n'est sans doute pas qu'une vue de l'esprit. En effet, dans plusieurs endroits du craton de Dharwar, il est fait état de la présence de discordances stratigraphiques et tectoniques mettant en contact deux générations de ceintures de roches vertes (Chadwick et al., 1981, Viswanatha et al., 1982). Dans les cas où ces discordances ont été observées, la génération la plus ancienne a été systématiquement attribuée au type "Sargur" (Chadwick et al., 1981, Viswanatha et al., 1982).

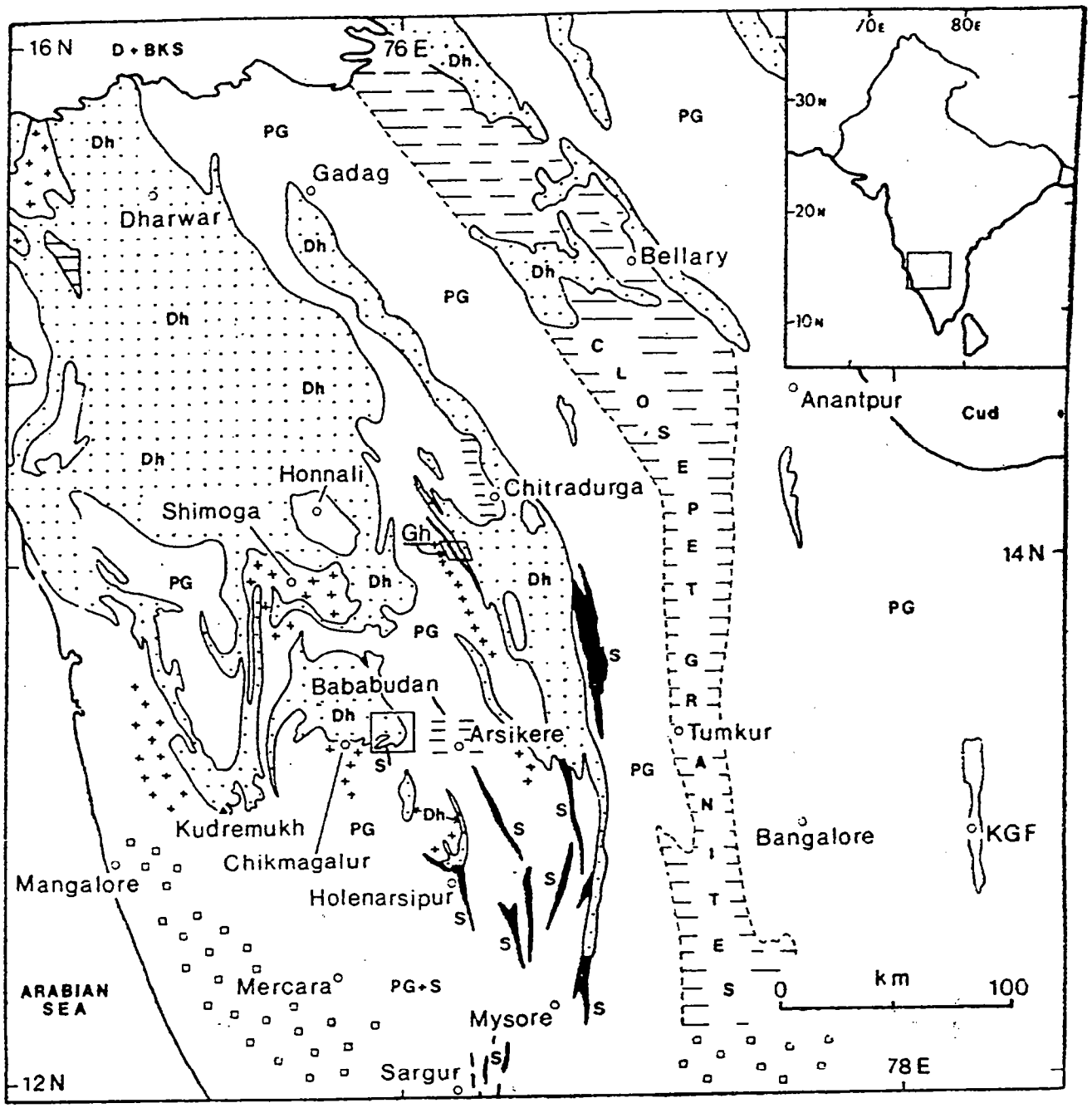

Fig. D. 3. Locality map showing the regional geological setting of southeast Bababudan and Ghatti Hosalli (Gh) within the Karnataka craton. Dh, Dharwar Supergroup ; PG, Peninsular gneisses ; S, Sargur Group. Horizontal ruling : younger granitic s.l. intrusions. Crosses : older intrusion., ca. 3000 Ma. Squares : areas of granulite facies. D + BKS, Deccan basalts and older Bhima-Kaladgi sequences ; Cud, Cuddapah basin unconformably overlying late Archaean terrane. KGF, Kolar Gold fields. Geology based on GST reports and Swami Nath et al., (1976), from Chadwick et al., (1981).

Les granites tardifs

Le dernier grand ensemble lithologique du craton de Dharwar est constitué d'une série de plutons granitiques tardifs, dont l'apparition marque une étape importante dans l'histoire tectonométamorphique de la région. Daté aux environs de 2.5-2.6 Ga (Crawford, 1969 ; Beckinsale et al., 1982 ; Buhl et al., 1983 ; Grew & Manton, 1984 ; Friend & Nutman, 1991 ; Peucat et al., 1993a), cet épisode granitique constitue le dernier grand événement de production de croûte continentale juvénile dans le craton de Dharwar (Martin et al., 1993 ; Peucat et al, 1993b ; Jayananda et al., 1994). La manifestation la plus spectaculaire de ce dernier épisode de création de croûte est la mise en place du batholite du Closepet, vaste corps linéaire s'étendant sur près de 400 km depuis les Trapps du Deccan au Nord jusqu'à l'isograde du faciès granulite au Sud (Fig. D. 2). Ce batholite comprend différents faciès pétrographiques, le plus répandu étant un faciès porphyroïde gris à phénocristaux de feldspaths-K (Jayananda et al., 1992). Les résultats isotopiques montrent que le batholite du Closepet est constitué à 80% de matériel juvénile (Jayananda et al., 1994) et à 20% de matériel recyclé provenant de la fusion des gneiss péninsulaires encaissants (Friend, 1983, Newton, 1990 ; Jayananda & Mahabaleswar, 1991).

1. 3. Les âges

L'évolution tectono-métamorphique du craton de Dharwar s'étend de 3.4 Ga à 2.2 Ga (Swami Nath & Ramakrishnan, 1981 ; Naqvi & Rodgers, 1983 ; Radakrisna & Ramakrishnan, 1990). Au moins trois périodes principales de formation de croûte continentale ont pu être, jusqu'à présent, reconnues. La première aux environs de 3.3 Ga (Venkatasubramanian & Narayanaswamy, 1974c ; Beckinsale et al, 1980, 1982 ; Nutman et al., 1993), la seconde aux environs de 3.0 Ga (Venkatasubramanian & Narayanaswamy, 1974a, Rajagopalan et al., 1980 ; Beckinsale et al., 1982 ; Bhaskar Rao et al., 1983, Monrad, 1983 ; Stroh et al., 1983) et la troisième aux environs de 2.5-2.6 Ga (Crawford, 1969, Venkatasubramanian & Narayanaswamy, 1974a et b ; Beckinsale et al., 1982 ; Buhl et al., 1983 ; Grew & Manton, 1984 ; Taylor et al., 1984 ; Rogers, 1986 ; Peucat et al., 1989, 1993a et b ; Friend et Nutman, 1991). Pour certains, l'événement 3.0 Ga serait contemporain d'un événement métamorphique majeur, de haut grade, vraissemblablement granulitique

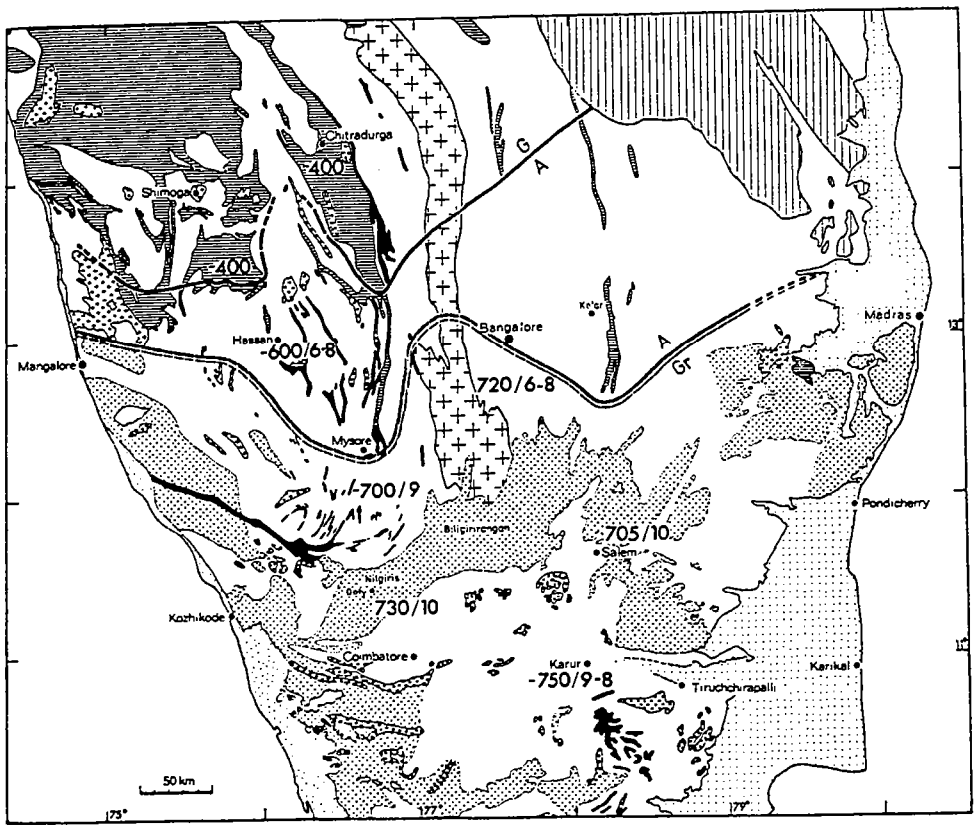

Fig. D. 4. Geological map of the Precambrian of the South Indian shield compiles on the basis of geological maps published by the Geological Survey of India, from Raith et al., (1982).

(Callahan & Rogers, 1987 ; Meen et al., 1992 ; Nutman et al., 1993). Cet événement métamorphique ancien serait à l'origine de l'appauvrissement de la croûte inférieure en certains LILE (U, Rb, etc..) ainsi qu'en H_20. Seules quelques régions suffisamment fertiles comme la région du Closepet ont pu produire postérieurement des liquides granitiques aux environs de 2.5-2.6 Ga (Meen et al., 1992). Le troisième épisode de formation de croûte continentale, dont fait partie le batholite du Closepet, est marqué par une séquence d'événements magmatiques et métamorphiques bien datés (Peucat et al., 1989, Peucat et al., 1993). Cette période correspond à la formation d'une croûte juvénile essentiellement granitique dont l'âge est compris entre 2.55 et 2.53 Ga et à laquelle succède, 10 à 30 Ma plus tard, le développement d'un événement métamorphique majeur atteignant dans la partie Sud du craton le faciès granulite (Peucat et al., 1993).

En ce qui concerne les ceintures de roches vertes, les âges les plus anciens ont été obtenus par la méthode U-Pb sur zircon et vont de 3.35 à 3.0 Ga (Nutman et al., 1992 ; Peucat et al., in prep). Des âges beaucoup plus récents (compris entre 2.7 et 2.2 Ga) ont aussi été publiés. Ces âges plus récents ont été obtenus par la méthode Rb-Sr et sont interprétés soit comme des âges de mise en place soit comme des âges de métamorphisme (Bhaskar Rao et al., 1992). Dans tous les endroits ou des études isotopiques ont été conduites, les résultats montrent que les unités supracrustales sont systématiquement plus jeunes que les gneiss avoisinants (Drury et al., 1983, 1986 ; Taylor et al., 1984 ; Gupta et al., 1988 ; Bhaskar Rao et al., 1992 ; Nutman et al., 1992 ; Peucat et al., in prep).

1. 4. Architecture générale

L'orientation régulière et globalement Nord-Sud des grandes structures cartographiques présentes dans le craton de Dharwar (i.e. ceintures de roches vertes ; batholite du Closepet ; grande zones de décrochements...) est un des faits les plus significatifs de ce craton (Fig. D. 2 et D . 3). Cette orientation préférentielle est vraissemblablement le résultat de grands décrochements Nord-Sud, dont le fonctionnement a parallélisé l'ensemble des structures préexistantes (Drury & Holt, 1980 ; Drury et al., 1984). Ces décrochements, en s'anastomosant, individualisent des zones lenticulaires de moindre déformation, séparées par des zones linéaires de déformation intense.

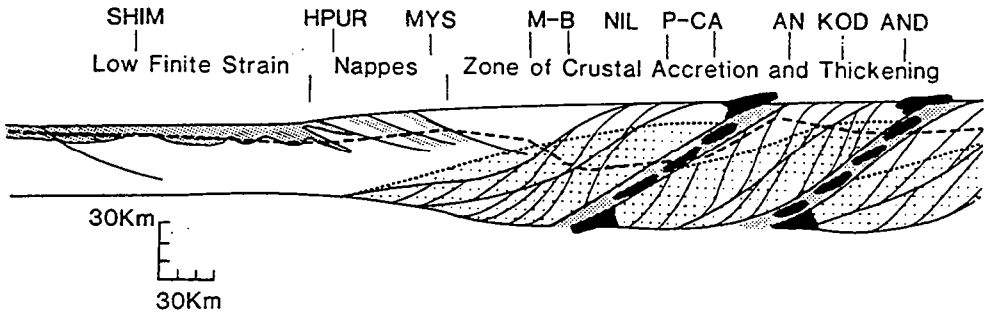

Fig. D. 5. A sketch crustal section from north to south illustrating a model for late-Archaean crustal shortenig and thickening in South India before the development of major transcurrent shear belts. The blod pecked line represents the depth of presently exposed rocks after crustal thickening, and indicates the large vertical displacements associated with the Moyar-Bhavani (M-B) and Palghat-Cauvery (P-C) shear zones. Stippled units are Archaean supracrustal rocks, black units represent possible tectonized relics of marginal basin crust and now eroded "ophiolites", crosses indicate the possible distribution of granulites. The sigmoidal crustal underthrusts associated with crustal thickening are based on Shackleton (1981) and Coward (1983). Abbreviations : SHIM-Shimoga ; HPUR-Holenarsipur ; MYS-Mysore ; NIL-Nilgiris ; AN-Anaimalais ; KOD-Kodaikanal ; AND-Andipatti. Vertical and horizontal scale bars are 30 km ; from Drury et al., (1984).

Dans les ceintures de roches vertes en forme de bassin (partie Nord-Ouest du craton ; Fig. D. 3), les premiers dépôts apparaissent nettement discordants par rapport à la foliation des gneiss du socle. D'après Chadwick et al. (1989), ces bassins seraient d'anciennes zones fortement subsidentes générées par une tectonique régionale transpressive (Chadwick et al., 1989). Plus au Sud, les ceintures de roches vertes deviennent linéaires et s'anastomosent fréquemment (ex : régions d'Holenarsipur, de Krishnaraspet ou de Kunigal). A l'approche des zones granulitiques, la surface occupée par les lithologies supracrustales se réduit, jusqu'à disparaître presque totalement (Fig. D. 3).

L'autre trait majeur du craton de Dharwar est la présence d'une transition progressive et continue depuis le faciès "schistes verts" au Nord jusqu'au faciès "granulite" au Sud (Fig. D. 4). Les tracés cartographiques des isogrades de ce métamorphisme régional apparaissent globalement Est-Ouest et définissent donc un angle très fort avec la direction globalement Nord-Sud des grandes structures précédemment décrites (i.e. ceintures de roches vertes ; batholite du Closepet ; grande zones de décrochements...). Aucune discontinuité tectonique majeure, telle que chevauchement ou décrochement, n'étant associée au franchissement des limites isogrades, tous les auteurs s'accordent pour relier la transition progressive et continue des conditions du métamorphisme à un seul et même événement thermique (Pichamuthu, 1961, 1962, 1967 ; Shackleton, 1976 ; Raith et al., 1982, 1983 ; Raase et al., 1986). Ainsi, les franchissements d'isogrades traduisent à l'échelle régionale la mise à l'affleurement de niveaux structuraux de plus en plus profonds lorsque l'on se dirige vers le Sud du craton. L'évolution barométrique des paragenèses métamorphiques qui marquent ces isogrades confirme cette vue. En effet, on assiste à une augmentation progressive des pressions du Nord vers le Sud, les estimations allant de 2-3 kbar au Nord jusqu'à 7-8 kbar au Sud (Harris & Jayaram, 1981 ; Janardhan et al., 1982 ; Raith et al., 1982 ; Hansen et al., 1984 ; Raase et al., 1986). La plus belle illustration de cette zonéographie des niveaux structuraux de la croûte archéenne est obtenue au voisinage des épontes du batholite du Closepet. Au Nord de la latitude 13°, les figures d'intrusion entre les roches gneissiques encaissantes et le batholite sont nettes et franches. Progressivement, vers le Sud, les contacts deviennent plus diffus en raison d'une migmatisation plus ou moins avancée des gneiss encaissants. Finalement, à l'extrême Sud de la zone d'étude, les différents faciès granitiques qui composent le batholite, laissent place aux

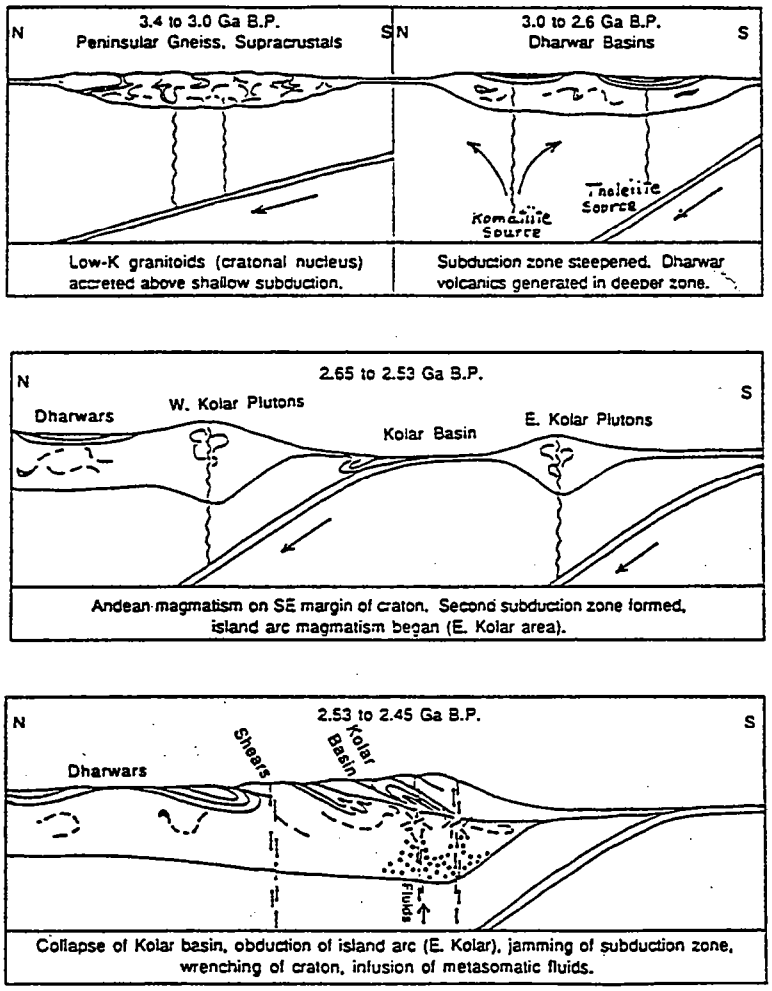

Fig. D. 6. Interpretation of the evolution of the Dharwar craton in terms of consistent northward subduction in the late Archaean, from Newton (1990a).

charnockites tandis que les gneiss encaissants, jusqu'alors migmatitiques deviennent granulitiques.

1. 5. Les modèles

Plusieurs schémas évolutifs généraux ont été avancés pour expliquer l'histoire tectonométamorphique du craton de Dharwar. Parmi les modèles proposés (Drury et al., 1984 ; Gopalakrishna et al., 1986 ; Radakrishna & Naqvi, 1986 ; Krogstad et al., 1989 ; Newton, 1990a), un seul, toutefois, intègre des données structurales d'échelle cartographique (Drury et al., 1984). Ce modèle repose, en ce qui concerne l'aspect tectonique, sur une étude satellitaire effectuée sur des images LANDSAT (Drury & Holt, 1980 ; Drury, 1983a ; Drury et al., 1984). Ces auteurs proposent que l'histoire ancienne du craton soit marquée par une tectonique de nappes à vergence Nord (Fig. D. 5), antithétiques de l'empilement général d'une chaîne de collision. Dans le craton de Dharwar, cette collision continentale s'exprimerait par la mise en place de vastes plis couchés déversés vers le Nord, repris ensuite par de grands décrochements Nord-Sud. Ces deux épisodes tectoniques, parce qu'ils nécessitent deux phases de raccourcissement régional distinctes dans le temps et dans l'espace, seraient à l'origine du développement de nombreuses structures d'interférences d'échelle cartographique. Pour tenir compte des variations barométriques du métamorphisme régional, ce modèle suppose par ailleurs que l'épaississement soit modéré au Nord (3 kbar au plus). Ainsi, le réajustement isostatique aurait peu joué, à la différence des régions méridionales où les pressions enregistrées sont significativement plus importantes (10-11 kbar). La vergence de la chaîne supposerait donc la convergence puis la collision Nord-Sud de deux plaques lithosphériques continentales, la fin de l'évolution intra-continentale étant marquée par un serrage final Est-Ouest. Ce modèle ne fait toutefois pas l'unanimité. Chadwick et al. (1989), en particulier, ont contesté l'existence, sur le terrain, d'anciens plis couchés d'échelle régionale même repris lors de phases de serrage. D'après ces auteurs, le développement intra-continental de bassins volcano-sédimentaires transpressifs localisés dans la partie Nord du craton (bassins de Bababudan, de Chitradurga, de Sandur, etc..) serait contemporain d'une déformation régionale importante marquée par de grands décrochements Nord-Sud. Toujours d'après Chadwick et al. (1989), les variations spatiales et temporelles importantes du taux de subsidence à l'intérieur de chacun des bassins transpressif seraient compatible avec un

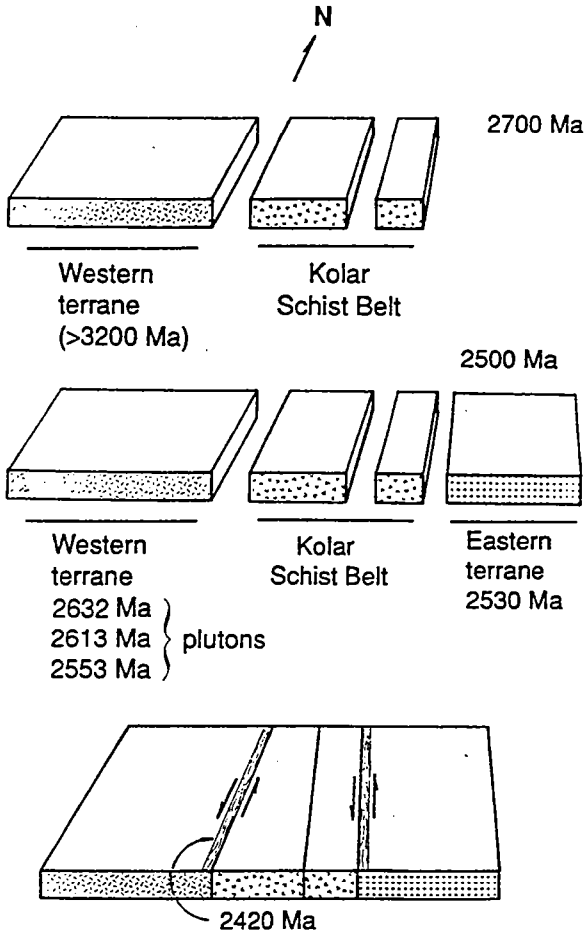

Fig. D. 7. Block diagram schematically showing the evolution of the Kolar schist Belt and surrounding gneisses. The age of older continental basement on the west is based on inherited zircons, isotopic signatures, and sporadic fragments of older crust occuring as xenoliths and tectonic inclusions in the westen gneisses. The age of the schist belt is based on Sm-Nd, Pb-Pb and Rb-Sr isochrons. The ages of gneisses are U-Pb zircon ages. The minimum age of the infered suture (2420 Ma) is based on ^{40}Ar-^{39}Ar mineral and Pb-Pb mineral-whole rock ages, from Krogstad et al. (1989).

développement de ces bassins en contexte intra-cratonique (Chadwick et al., 1985a et b, 1989). Néanmoins, ces deux modèles s'accordent pour considérer que la fin de l'évolution tectono-métamorphique du craton archéen de Dharwar est marquée par le développement de grandes structures régionales décrochantes.

Plus récemment, d'autres modèles sont apparus dans la littérature. Ainsi, Newton (1990a) reprend le schéma général de Drury et al., (1984) mais en y ajoutant un contexte ante-collisionnel. D'après cet auteur, une collision Nord-Sud d'âge 2.5 Ga entre une marge active et un arc insulaire serait à l'origine de l'ensemble des caractéristiques du craton de Dharwar (Fig. D. 6). L'idée d'un contexte géodynamique de type convergence lithosphérique précédant une collision figure également dans le modèle proposé par Krogstad et al., (1989) ; toutefois, d'après ce deuxième groupe d'auteurs, la convergence des blocs lithosphériques et la collision n'aurait pas été Nord-Sud mais Est-Ouest (Fig. D. 7). L'antagonisme directionnel affiché par ces deux modèles (convergence Nord-Sud vs. convergence Est-Ouest) illustre parfaitement le caractère fragmentaire et peu fiable des données structurales existant actuellement sur le Sud de l'Inde.

Le dernier modèle en date est l'oeuvre de Martin et al. (1993b), Peucat et al. (1993b) et Jayananda et al. (1994). D'après ces auteurs, l'anomalie thermique responsable de l'événement granulitique à 2.5 Ga ne serait pas liée à une collision continentale, mais à l'arrivée en base de croûte d'un panache mantélique. Toujours d'après ces auteurs, un événement de type panache expliquerait le caractère basse pression du métamorphisme régional à 2.5 Ga ainsi que les caractéristiques pétrologiques et géochimiques des magmas granitiques qui se mettaient en place à cette époque (batholite du Closepet).

2. PRÉSENTATION DES RÉSULTATS DE CE TRAVAIL

2. 1. Structuration interne de la croûte continentale Archéenne : l'exemple de la région d'Holenarsipur (Karnataka, Inde du Sud)

Dans un premier temps, nous nous sommes attachés à reconnaître et à caractériser le ou les types de structures d'échelle régionale impliquées dans la croûte archéenne du craton de Dharwar. La première région choisie a été le secteur d'Holenarsipur et ce pour deux raisons : (i) cette région était jusu'alors totalement inconnu d'un point de vue tectonique ; or, la région d'Holenarsipur est le lieu où se trouve préservé les plus anciennes roches constitutives du craton de Dharwar (3.35 Ga, Beckinsale et al., 1980) ; (ii) cette région était considérée jusqu'alors comme exempte de toute déformation décrochante tardi-archéenne (Drury et al, 1984). D'après les travaux de Raith et al., (1982), la région d'Holenarsipur appartient au domaine de métamorphisme régional de l'amphibolite faciès (Fig. D. 4).

2. 2. Diapirism, bulk homogeneous shortening and transcurrent shearing in the Archaean Dharwar craton : the Holenarsipur area, South India

DIAPIRISM, BULK HOMOGENEOUS SHORTENING AND TRANSCURRENT SHEARING IN THE ARCHAEAN DHARWAR CRATON : THE HOLENARSIPUR AREA, SOUTH INDIA

by

Hugues Bouhallier, Pierre Choukroune and Michel Ballèvre

Laboratoire de Tectonique, Géosciences Rennes (UPR CNRS 4661), 35042 Rennes Cedex (France)

ABSTRACT.

Qualitative strain data are spatially integrated in order to define Archaean foliation trajectories, and variations in strain intensity and ellipsoid type, in the Holenarsipur area, Dharwar Craton, southern India. The study provides constraints on the bulk geometry, the progressive deformation and the kinematic history of this region of Archaean continental crust. Two major structural events have shaped the study area : (i) a regional diapiric event contemporaneous with a magmatic event, (ii) a later sinistral transcurrent ductile shear event which has locally reorientated both foliations and stretching lineations. The entire Holenarsipur supracrustal belt underwent a common tectonometamorphic history that included two metamorphic events. Each event corresponds temporally to a distinct strain field. The first, a regional amphibolite facies event, was contemporaneous with the main tectonic event and probably with the intrusion of Halekote trondhjemites. The second occurred under greenschist-facies conditions and was restricted to a late transcurrent shear zone at the eastern boundary of the greenstone belt. The strain pattern prior to transcurrent shearing cannot be explained by a thrusting event unless all trace of this event had been erased by the diapirism. We interpret all structures older than the transcurrent shearing to be the direct result of vertical movements linked to body forces, augmented by minor horizontal crustal shortening.

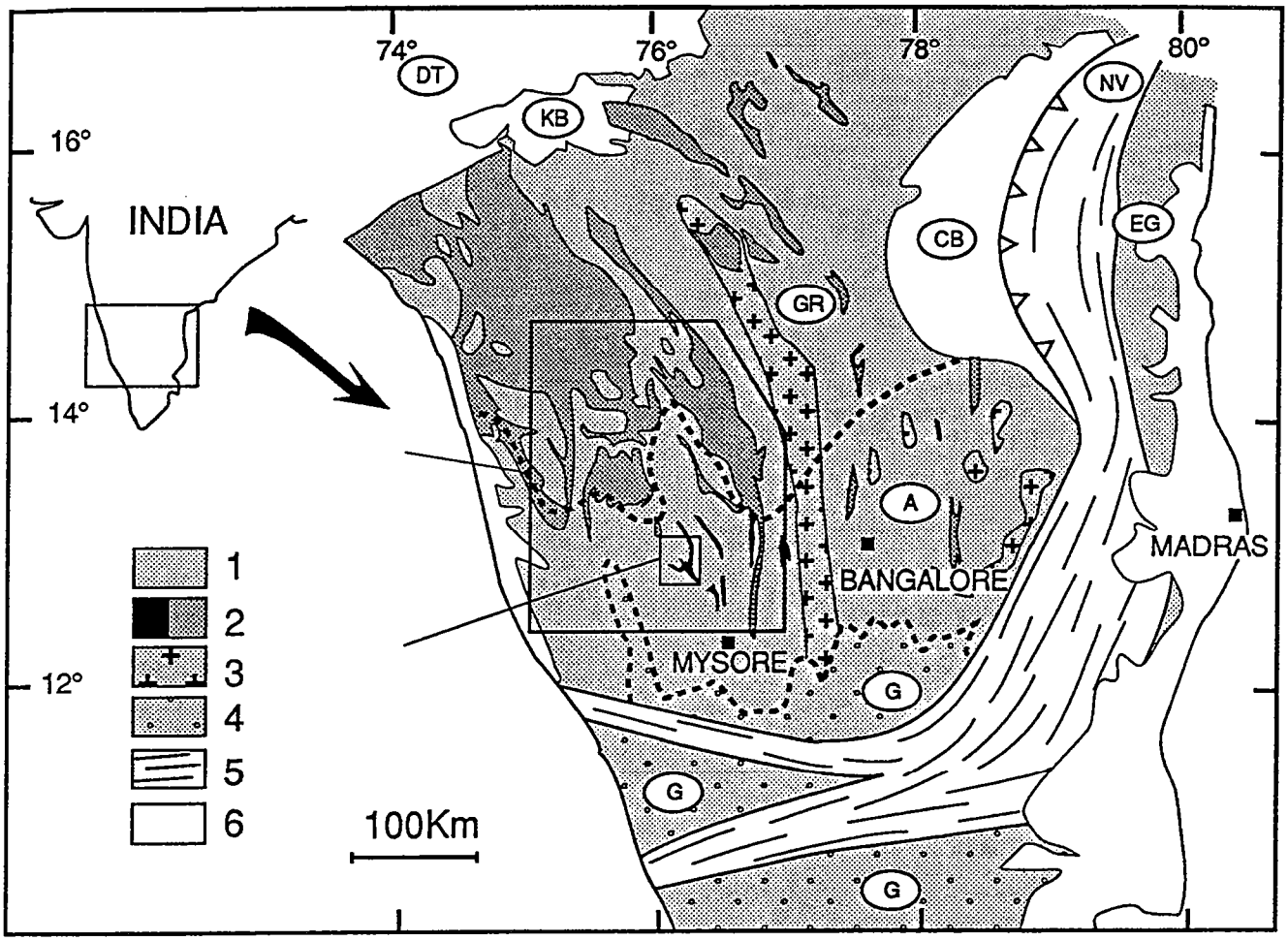

Fig. D. 8. Map of the Dharwar craton (South India) showing areas mentioned in the text and the area of detailed investigations.

1 : Archaean TTG ; **2** : Archaean supracrustals (Dharwar unit is in light grey , Sargur unit is in dark) ; **3** : Closepet granite ; **4** : granulite facies ; **5** : Proterozoic strained zones (EG : Eastern Ghats, NV : Nallamalai-Velikonda) ; **6** : Proterozoic basins (CB : Cuddapah basin, KB : Kaldagi basin) and Cenozoic rocks (DT : Deccan traps). GR, A, G represent, respectively greenschist, amphibolite and granulite zones of metamorphism according to Drury et al., (1984) and Raase et al., (1986).

Fig. D. 8. Carte du craton de Dharwar (Inde du Sud) montrant les régions citées dans le texte et la zone des investigations.

1 : TTG archéennes ; **2** : roches supracrustales archéennes (l'unité de Dharwar est en gris léger, l'unité de Sargur en foncé) ; **3** : granite de Closepet ; **4** : faciès granulite ; **5** : zones de déformation protérozoïque (EG : Eastern Ghats, NV : Nallamalai-Velikonda) ; **6** : bassins protérozoïques (CB : Cuddapah basin, KB : Kaldagi basin) et roches cénozoïques (DT : Deccan traps). GR, A, G représentent, respectivement les faciès schistes verts, amphibolite et granulite du métamorphisme régional d'après Drury et al., (1984) et Raase et al., (1986).

INTRODUCTION

The tectonic evolution of Archaean domains and their related thermal regime are still fiercely debated (Fyfe, 1974 ; West and Mareschal, 1979 ; Mareschal and West, 1980 ; Platt, 1980 ; England and Bickle, 1984 ; Richter, 1985). One of the most contentious issues is the question of whether horizontal or vertical tectonics prevailed during this period in Earth history.

The type of structural data needed to constrain the tectonic evolution of the Archaean crust are in fact very scarce. Because of the excellent and continuous outcrop of Archaean rocks in southern India, which exposes a wide variety of Archaean terrains, the Dharwar craton is an ideal target for detailed structural investigations. In this region, classic Archaean lithologies, including tonalitic, trondhjemitic and granodioritic granitoids and gneisses (TTG) as well as greenstone belts are well exposed and essentially unaffected by Proterozoic or Phanerozoic deformation.

This paper presents the results of a detailed field study of the Holenarsipur area (Fig. D. 8) during which field data of the type needed to constrain the deformation were gathered. These data were used to construct foliation trajectories from which we infer finite strain maps and the qualitative strain ellipsoid type. Qualitative strain gradients and kinematic indicators were then used to define the structural evolution of this Archaean province. These maps and structural data provide the basis required to discuss the kinematic history and the role of vertical or horizontal movements during the tectonic evolution of the region.

GEOLOGICAL SETTING

The Dharwar craton (Fig. D. 8)

Archaean rocks of South India have been the subject of many recent studies (Swami Nath and Ramakrishnan., 1981 ; Naqvi and Rodgers, 1983 ; Drury et al., 1984 ; Mukhopadhyay, 1986 ; Radhakrishna and Naqvi, 1986 ; Rogers, 1986 ; Rogers et al., 1986 ; Radhakrishna and Ramakrishnan., 1990 ; Naha et al., 1990 ; Newton, 1990 ; Naha et al., 1991). These terrains consist mainly of linear and arcuate low- to high-grade volcano-sedimentary belts ("greenstone", "supracrustal" or "schist" belts) surrounded by larger regions of high-grade infracrustal rocks and associated low-K tonalitic, trondhjemitic and granodioritic rocks (TTG series) with ages between 3.35

Ga and 2.5 Ga (Crawford, 1969 ; Venkatasubramanian, 1975 ; Beckinsale et al,. 1980, 1982 ; Monrad, 1983 ; Stroh et al., 1983 ; Taylor et al., 1984 ; Drury et al., 1986 ; Taylor et al., 1988 ; Meen et al., 1992). The greenstone belts have been divided into two types (Swami Nath et al., 1976) on the basis of differences in metamorphic grade and structural evolution. The Sargur type, which contains highly deformed sedimentary and mafic igneous rocks intruded by trondhjemites, is largely restricted to the southern part of the craton. The Dharwar type, which is mainly present in the northern part of the shield, is only slightly deformed or undeformed when not affected by late shearing. Although contacts between Sargur and Dharwar rocks are very scarce, there is some evidence that the Dharwar type uncomformably rests upon rocks of the Sargur type and the TTG series (Chadwick et al., 1981 ; Viswanatha et al., 1982). The southernmost boundary of the Bababudan belt is perhaps the best place to observe contacts between the two supracrustal units (Chadwick et al., 1981). There, Sargur supracrustal rocks, which display a strong vertical foliation, are unconformably overlain by a basal conglomerate that opens the thick and gently-dipping Dharwar supracrustal sequence (Srinivasan and Ojakangas, 1986). Further east, Dharwar supracrustals uncomformably overlie the Chikmagalur granodiorite, which is dated at 3.08 ± 0.11 Ga using the Rb-Sr method and at 3.17 ± 0.45 Ga with the Pb-Pb method (Taylor et al., 1984). The major unconformity between an older Sargur unit and a younger Dharwar unit has been recently confirmed in the Jayachamarajapura area (Venkata Dasu et al., 1991).

A characteristic feature of the Dharwar craton is the transition from a low- to medium-grade granite-greenstone terrain in the north to a high-grade granulitic terrain in the south. Paleopressures in gneissic and mafic rocks increase from about 3 kbar in central Karnataka to ~8-9 kbar in the Sargur area (Harris and Jayaram, 1981 ; Janardhan et al., 1982 ; Raith et al., 1982 ; Hansen et al., 1984 ; Raase et al., 1986). According to previous studies (Pichamuthu, 1962 ; Shackelton, 1976 ; Raith et al., 1982 ; Raase et al., 1986), the southward P-T gradient is not linked to any particular tectonic features or breaks and is perpendicular to the general N-S structural trend of the craton (Drury and Holt, 1980).

A gradual and continuous progression from high structural levels in the north to deeper levels in the south is well illustrated in the Closepet granite, a late Archaean batholith dated around 2.5 Ga (Crawford, 1969 ; Friend and Nutman, 1991). This enormous granitoid body extends for almost 400 km from north to south of the craton, generally following the

regional structural trend (Fig. D. 8). In the north, Closepet granites clearly intrude TTG gneisses and greenstone belts, while, further south, migmatization has affected the TTG gneisses at deeper structural levels (Friend, 1983 ; Jayananda and Mahabaleswar, 1991). The southernmost part of the Closepet batholith, which represents the deepest structural level in this heterogeneous granitic complex, is affected by a granulite-facies overprint (Janardhan et al., 1979 ; Friend, 1981 ; Hansen et al., 1987 ; Stähle et al., 1987).

The strong N-S-trending fabric of the Dharwar craton is partly the result of a late Archaean transcurrent ductile shearing episode (Drury and Holt, 1980 ; Drury, 1983 ; Drury et al., 1984 ; Chadwick et al., 1989) and is contemporaneous with the emplacement of the Closepet granite (Jayananda and Mahabaleswar, 1991) which has been dated at 2.5 Ga (Friend and Nutman, 1991) and with the development of migmatites and charnockites.

The Holenarsipur area.

Holenarsipur (Fig. D. 9), in the central, medium-grade terrain of the Dharwar craton, is one of the oldest greenstone belts of the craton (Hussain and Naqvi, 1983). This region exhibits the two classical lithologies of Archaean granite-greenstone terrains : (i) several generations of intermediate to acid plutonic rocks constituting a TTG infracrustal sequence, composed mainly of strongly strained gneisses, here described as "Gorur gneisses" and (ii) a mafic to ultramafic volcano-sedimentary supracrustal (greenstone) sequence (Naqvi et al., 1983b). The gneisses, which yielded Rb-Sr and Pb-Pb ages between 3.35 Ga (Beckinsale et al., 1980, 1982) and 3.305 Ga (Taylor et al., 1988) are intruded by 3.1-3.0 Ga trondhjemitic plutons (Beckinsale et al., 1982 ; Bhaskar Rao et al., 1983 ; Monrad, 1983 ; Stroh et al., 1983 ; Taylor et al., 1984 ; Meen et al. 1992).

The mafic and ultramafic volcano-sedimentary sequence of the Holenarsipur greenstone belt is now metamorphosed to amphibolite facies, but original rock types include sediments (pelite, sandstone, conglomerate, banded iron formation), volcanics (basalt and rhyolite), and mafic-ultramafic intrusions (dunite, peridotite, gabbro, anorthosite).

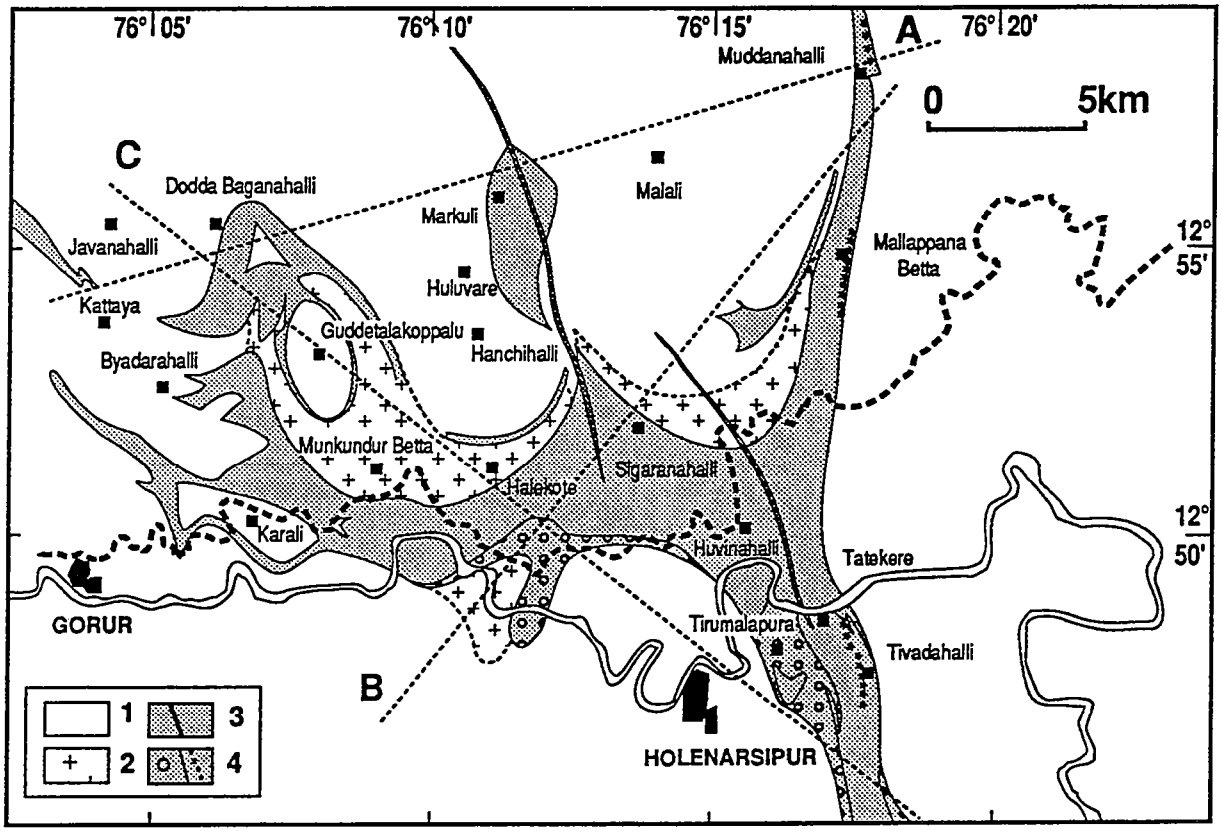

Fig. D. 9. Geological map of the Holenarsipur area (Karnataka). **1** : TTG (Peninsular Gneisses) ; **2** : trondhjemitic intrusions of Halekote type ; **3** : supracrustal rocks intruded by doleritic dykes ; **4** : supracrustal rocks with (i) Kyanite-Staurolite association (represented by circles), (ii) conglomeratic levels (represented by stars).

Fig. D. 9. Carte géologique de la région d'Holenarsipur (Karnataka). **1** : TTG (Gneiss Péninsulaires) ; **2** : intrusions trondhjémitiques de type Halekote ; **3** : roches supracrustales intrudées par des dykes doléritiques ; **4** : roches supracrustales avec (i) l'association disthène-staurotide (représentée par des cercles), (ii) niveaux conglomératiques (représentés par des étoiles).

The supracrustal sequence has been the subject of controversy (Swami Nath and Ramakrishnan, 1981) surrounding (i) lithological and geochemical differences in supracrustal rocks between the northern and southern parts of the belt, (ii) the significance of conglomeratic horizons within the belt, (iii) differences in metamorphic grade of the supracrustal rocks. These differences lead some authors to distinguish two units of supracrustal rocks (Sargur and Dharwar) within the Holenarsipur belt. The mafic and quartzitic lithologies, metamorphosed under greenschist to albite-epidote-amphibolite facies were said to represent the Dharwar unit, while ultramafic and pelitic lithologies, metamorphosed under amphibolite facies, were attributed to the Sargur unit. These units were thought by Viswanatha and Ramakrishnan (1975), Chadwick et al. (1978) and Ramakrishnan and Viswanatha (1981) to be separated by a conglomeratic horizon, but Sreenivas and Srinivasan (1968), Naqvi et al., (1978), Hussain and Naqvi (1983) interpret the same horizon as an "intraformational conglomerate" rather than an unconformity at the base of the supposedly younger unit. Furthermore, the latter authors point out that lithological differences within the belt do not prove the existence of two supracrustal units. Lithological differences could be simply the result of sedimentological, volcanic, tectonic and metamorphic variations during the development of a single volcano-sedimentary belt (Srinivasan, 1988).

STRUCTURAL DATA.

Previous studies

Three phases of deformation in the "Sargur part" (SgD1, SgD2 and SgD3) and three phases of deformation in the "Dharwar part" (DhD1, DhD2, Dhd3) of the Holenarsipur belt have been described by Chadwick et al. (1978) : they suggest that either Sargur and Dharwar rocks have undergone the same deformation history or rotation of the deformed older "Sargur" structures (SgD1 SgD2 and SgD3) into parallelism with younger ones (DhD1 and DhD2) can explain the great similarity of both structures and fabrics in the "Dharwar" and "Sargur" units. In the same study, the synkinematic intrusion of the Halekote trondhjemite is argued.

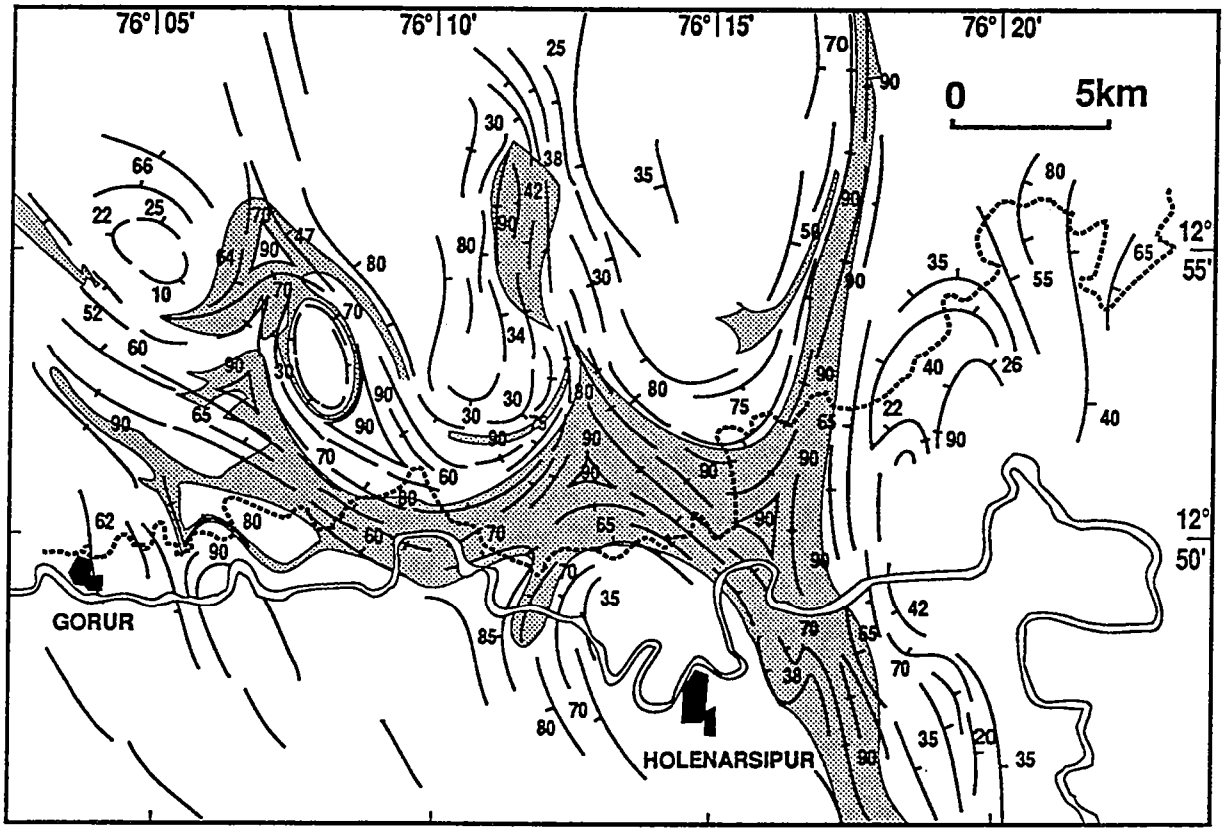

Fig. D. 10. Map of foliation trajectories in the Holenarsipur area (Karnataka).

Fig. D. 10. Carte des trajectoires de la foliation dans la région d'Holenarsipur (Karnataka).

More recently, Drury et al. (1984, 1986) proposed that the Holenarsipur belt was shaped by large mushroom-type fold interferences (Ramsay, 1967), the earliest recumbent isoclinal folds being refolded by upright open folds with N-S axial traces. They also considered that the deformed supracrustal belt represents a rotated and sheared allochthonous or parautochthonous thrust toward the North. This thickening event would be necessarily younger than 2.62 Ga, the age of the Holenarsipur belt according to the Sm-Nd method (Drury et al., 1986). However, no detailed structural map or data were presented to support this hypothesis.

Structures and foliation trajectories.

Foliation and folds.

The main structural feature in the Holenarsipur area is a regional foliation that affects both supracrustal and infracrustal rocks. This foliation (S1) is characterised by a strong variability in dip and strike (Fig. D. 11a). In quarries south of Javanahalli (Fig. D. 9), leucocratic veins intrude TTG gneisses. Some of these veins crosscut the S1 foliation and are undeformed. Others are folded and/or stretched in the S1 foliation.

Banded iron formation and associated mafic rocks NE of Markuli are folded, and have an axial-planar cleavage parallel to the regional foliation (S1). S1 is refolded in some places, particularly in areas where foliation trajectories define triple junctions but also in the eastern part of the belt (South of Tirumalapura). In the triple junctions, fold axes are always subvertical while in eastern areas, the axes of late folds are vertical or plunge steeply to the North.

Foliation trajectories.

Foliation trajectories (Fig. D. 10) reveal dome and basin structures with supracrustal rocks in synforms (e. g. Markuli synform) and infracrustal rocks in elliptical domal antiforms (e.g. the Javanahalli, Holenarsipur, Hanchihalli, Guddetalakoppalu, Javanahalli and Malali domes). At contacts between supracrustal and infracrustal rocks, the foliation is strongly developed and steeply dipping, whereas in the central part of the domal structures, it is less pronounced and has very shallow dips. At these places the intrusive rocks are more isotropic.

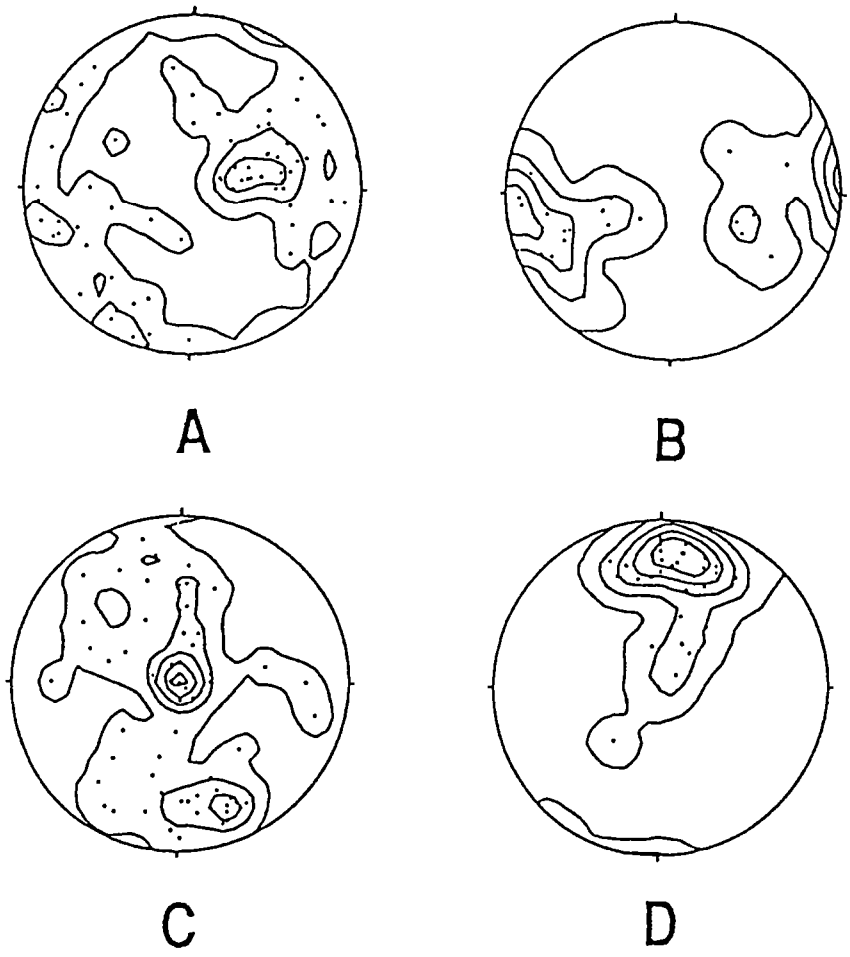

Fig. D. 11. Stereograms with projection onto the lower hemisphere. **a** : poles to foliations around domes ; **b** : poles to foliations in the easternmost branch of the greenstone belt ; **c** : stretching lineations around domes : **d** : stretching lineations in the easternmost branch of the greenstone belt.

Fig. D. 11. Diagrammes stéréo (projection sur l'hémisphère inférieur). **a** : pôles des plans de foliation autour des dômes ; **b** : pôles des plans de foliation dans la branche Est de la ceinture de roches vertes ; **c** : lineations d'étirement autour des dômes : **d** : lineations d'étirement dans la branche Est de la ceinture de roches vertes.

The foliation is generally parallel to major lithological boundaries but in places (e.g. North of Holenarsipur, Fig. D. 10) there are low-angle relationships between the S1 foliation plane and the contact between supra- and infracrustal rocks.

Between elliptical domes, a triangular arrangement of vertical S1 foliations defines triple junctions (Brun, 1983a). These are present in both supracrustal (e.g. near Sigaranahalli and Huvinahalli, where a "late" crenulation has been previously described by Chadwick et al. (1978)), and infracrustal rocks (e.g. near Byadarahalli). Triple junctions are preferred sites for trondhjemitic intrusions (e.g. Munkundur Betta and near Dodda Baganahalli) and quartz-tourmaline veins that indicate major channelised fluid circulation (e.g. South-West of Sigaranahalli). Some of these trondhjemitic bodies have been dated at 3.031±0.012 Ga (Meen et al., 1992).

The S1 trajectory map also shows a highly foliated linear zone along the eastern boundary of the supracrustal belt. Here, the foliation is always nearly vertical with a 170° strike (Fig. D. 11b). This linear belt appears significantly different from the surrounding areas characterised by dome and basin patterns.

Stretching lineations.

At map scale (Fig. D. 12), the stretching lineation L1 has a mean 170° direction except at the southeasternmost boundary of the greenstone belt where lineations are clustered around 010° (Fig. D. 11d). Furthermore, lineations, like foliations, gradually change from a gently plunging attitude in the core of the domal structures to a vertical position near the contact between supra- and infracrustal rocks (e.g. South of Hanchihalli dome). In supracrustal rocks, stretching lineations are generally downdip (fine examples are seen along the Gorur canal), except at the linear, easternmost boundary of the supracrustal belt where they are mainly horizontal or plunge gently northward (Fig. D. 11d). Within the triple junctions, stretching lineations are well developed and are always vertical.

Strain ellipsoid type and fabrics.

The finite strain ellipsoid shape was estimated using four different types of rock fabric, each easily distinguishable in the field. These were (i) planar fabrics in which the foliation plane is better developed than the stretching lineation, (ii) planar-linear fabrics in which both foliation planes and stretching lineations are equally developed, (iii) linear fabrics that

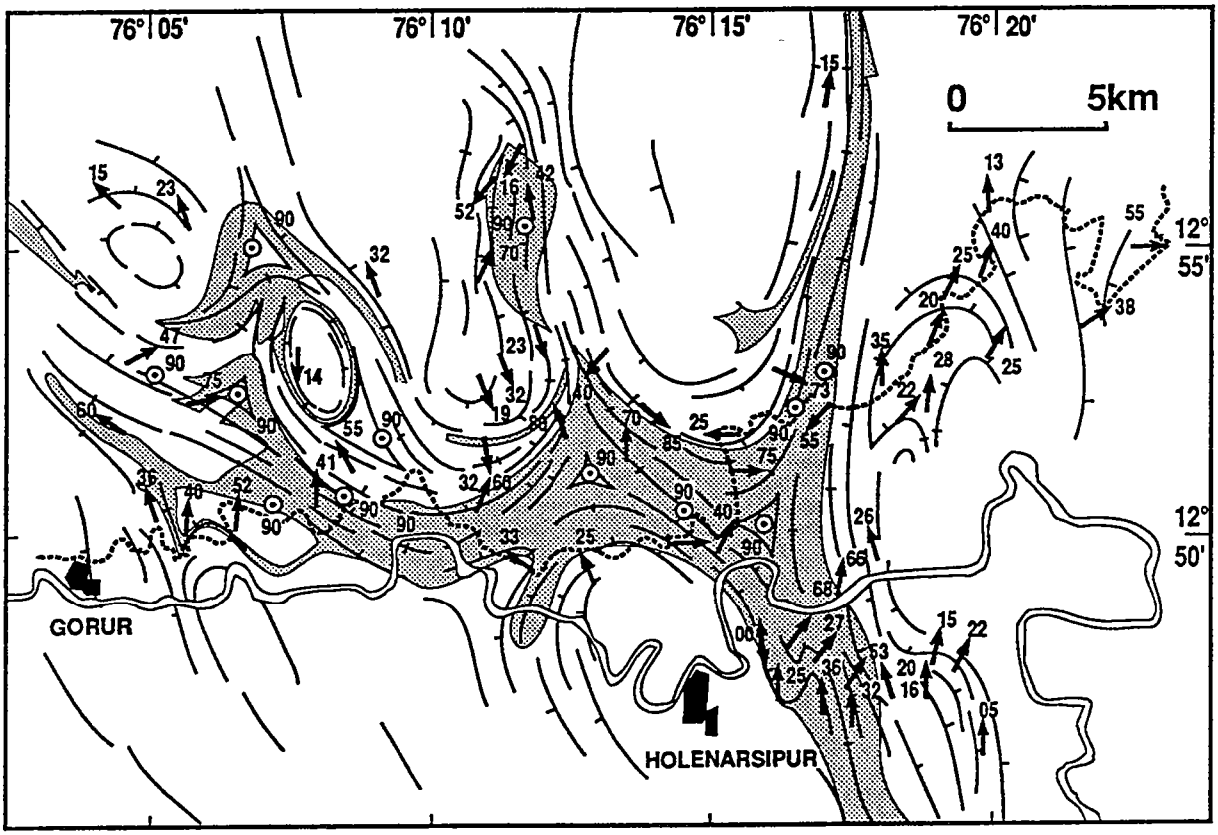

Fig. D. 12. Map of stretching lineations in the Holenarsipur area.

Fig. D. 12. Carte des linéations d'étirement dans la région d'Holenarsipur.

contain no evident foliation, being characterised by a stretching lineation and "pencil splitting", (iv) areas in which fabric is absent or poorly developed. Although these fabric distinctions do not provide a direct measure of strain intensity, they qualitatively define the shape of the finite strain ellipsoid (i.e. apparent flattening or constriction) (Flinn, 1965 ; Schwerdtner et al., 1976).

Our map reveals a high variability in the distribution of fabric types throughout the map area (Fig. D. 13). Particularly significant are the following observations :

- There are poorly developed fabric zones within the central parts of the domes (e.g. Holenarsipur, Javanahalli, Guddetalakoppalu and Malali domes) and in one case, within a foliation triple junction (Mukundur Betta).

- Planar fabrics characterise two-thirds of the studied area. This fabric occurs in the areas where the S1 foliation plane exhibits the largest variations in dip. It dominates the vertical foliation sectors, and is ubiquitous throughout the supracrustal belt, except near its eastern boundary.

- Planar-linear fabric zones occur in two different settings. First, they show an almost triangular distribution around foliation triple junctions (e.g. Dodda Baganahalli, Byadarahalli, Sigaranahalli, Huvinahalli and Mukundur Betta triple junctions). Second, planar-linear fabrics characterise the linear zone along the eastern N-S boundary of the belt.

- Linear vertical fabric zones are invariably confined within the foliation triple junctions. Linear horizontal fabrics are rare (north of the Markuli synform and east of Tivadahalli in the southern branch of the belt).

Strain regimes.

Shear bands and other obvious kinematic indicators (Choukroune et al., 1987) are restricted to supracrustal rocks in the vicinity of the TTG-greenstone contacts. Two distinct areas are outlined by analysis of sense and direction of the shearing. One area, which includes the dome-and-basin terrain that makes of Holenasipur belt and its surroundings, displays kinematic criteria indicative of vertical displacement. The second area, which is restricted to the linear easternmost part of the greenstone belt, is dominated by horizontal displacements.

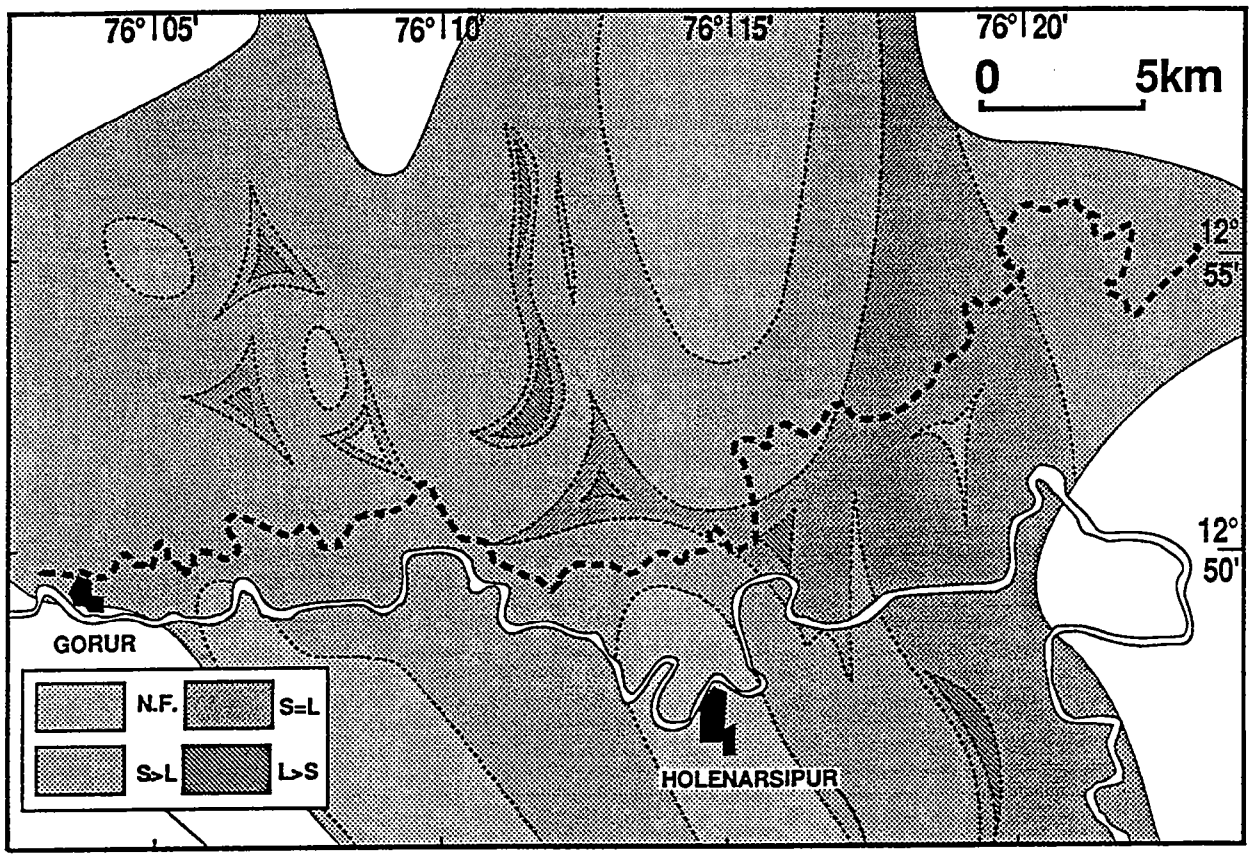

Fig. D. 13. Map of fabrics in the Holenarsipur area.**N.F.** : zone with no fabric ; **S>L** : zone where planar fabric is more developed than linear fabric ; **S=L** : zone where both planar and linear fabrics are equally developed ; **L>S** : zone where linear fabric is more developed than planar fabric.

Fig. D. 13. Carte des fabriques dans la région d'Holenarsipur.**N.F.** : zone sans fabrique ; **S>L** : zone où la fabrique planaire est davantage développée que la fabrique linéaire ; **S=L** : zone où la fabrique est plano-linéaire ; **L>S** : zone où la fabrique linéaire est davantage développée que la fabrique planaire.

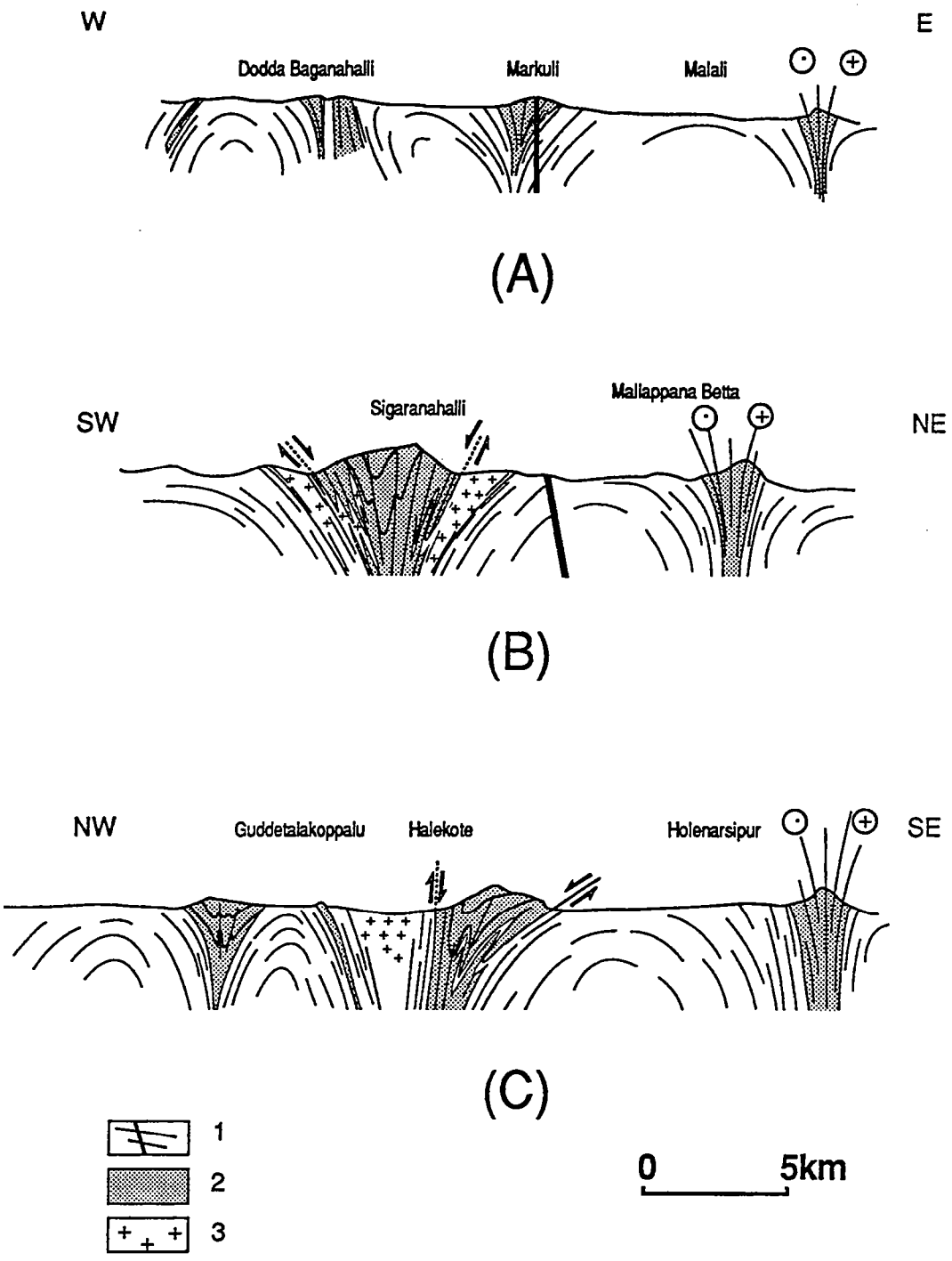

Fig. D. 14. Cross-sections in the Holenarsipur area (localization on Fig. IV. 2. 2). **1** : TTG (Peninsular Gneisses) with later doleritic dykes ; **2** : greenstone belt ; **3** : syntectonic intrusions of Halekote type.

Fig. D. 14. Coupes dans la région d'Holenarsipur (localisation des coupes sur la Fig. IV. 2. 2). **1** : TTG (gneiss Péninsulaires) avec des dykes doléritiques tardifs ; **2** : ceinture de roches vertes ; **3** : intrusions syn-tectoniques de type Halekote .

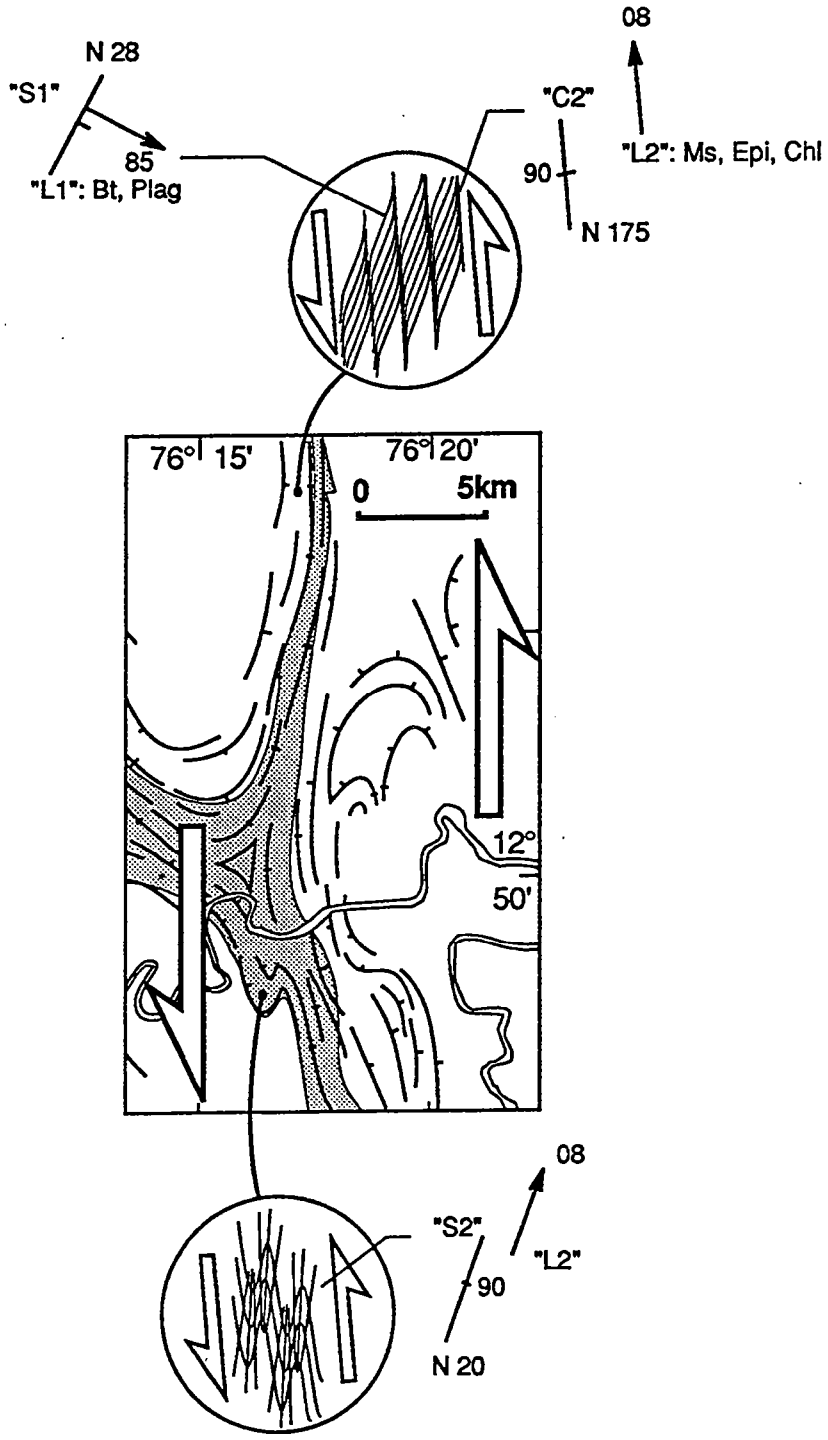

Fig. D. 15. Situation and schematic representation of significant late microstructures due to the sinistral shearing along the eastern border of the Holenarsipur greenstone belt. The shears and related low-grade metamorphism postdate the earlier regional deformation and amphibolite facies linked to the main event (doming). The considered area is located on **Fig. D. 16)**

Fig. D. 15. Localisation et représentation schématique des principales microstructures liées au décrochement senestre de la bordure Est de la ceinture de roches vertes d'Holenarsipur. Les cisaillements et le métamorphisme de bas-grade sont postérieurs à la déformation régionale de l'amphibolite faciès, liée à l'événement principal (doming). La région considérée est positionnée sur la **Fig. D . 16).**

Kinematic criteria in the first area always indicate a downward displacement of the supracrustal belt relative to the TTG basement (Fig. D. 14). Consistent criteria such as shear bands, rotated boudins, asymetric folds are observed near Karali (along the canal) and east of Halekote. In these examples, the sense of shearing in the supracrustal rocks implies a normal shearing towards the central part of the greenstone belt (Fig. D. 14b and 14c). These data rule out the possibility of interpreting the greenstone-gneiss relationships as folds which affect the interface between two formations with strongly different viscosities. Indeed, this latter model would result in opposite shear senses as those actually observed along the greenstone-gneiss interface.

The second area displays sinistral ductile slip at all scales (Fig. D. 15). This is the only region where asymmetric sets of sinistral shear bands (indicative of a non-coaxial regime) provide evidence of horizontal shearing. In this linear zone, the stretching lineation is subhorizontal, and asymmetric folds affect the S1 foliation. The geometries of these folds are also consistent with a sinistral shear along this zone (Fig. D. 15). These brittle-ductile structures invariably affect the regional foliation and consequently postdate the main structural event.

The direction and sense of shearing in the Holenarsipur transcurrent zone are compatible with what was described in surrounding areas of the Dharwar craton (Fig. D. 16) (Drury, 1983 ; Chadwick et al., 1989 ; Jayananda and Mahabaleswar, 1991).

Metamorphism and deformation.

According to Ramakrishnan et al. (1981), two different greenstone belts are present in the Holenarsipur area, each of them having recorded specific P-T history. According to Naqvi et al. (1983 a), the Holenarsipur greenstone belt was affected by a single amphibolite-facies regional metamorphic event. Our observations are consistent with this interpretation. However, we are able to distinguish a second event at greenschist facies, restricted to the eastern shear zone, during a late phase of deformation.

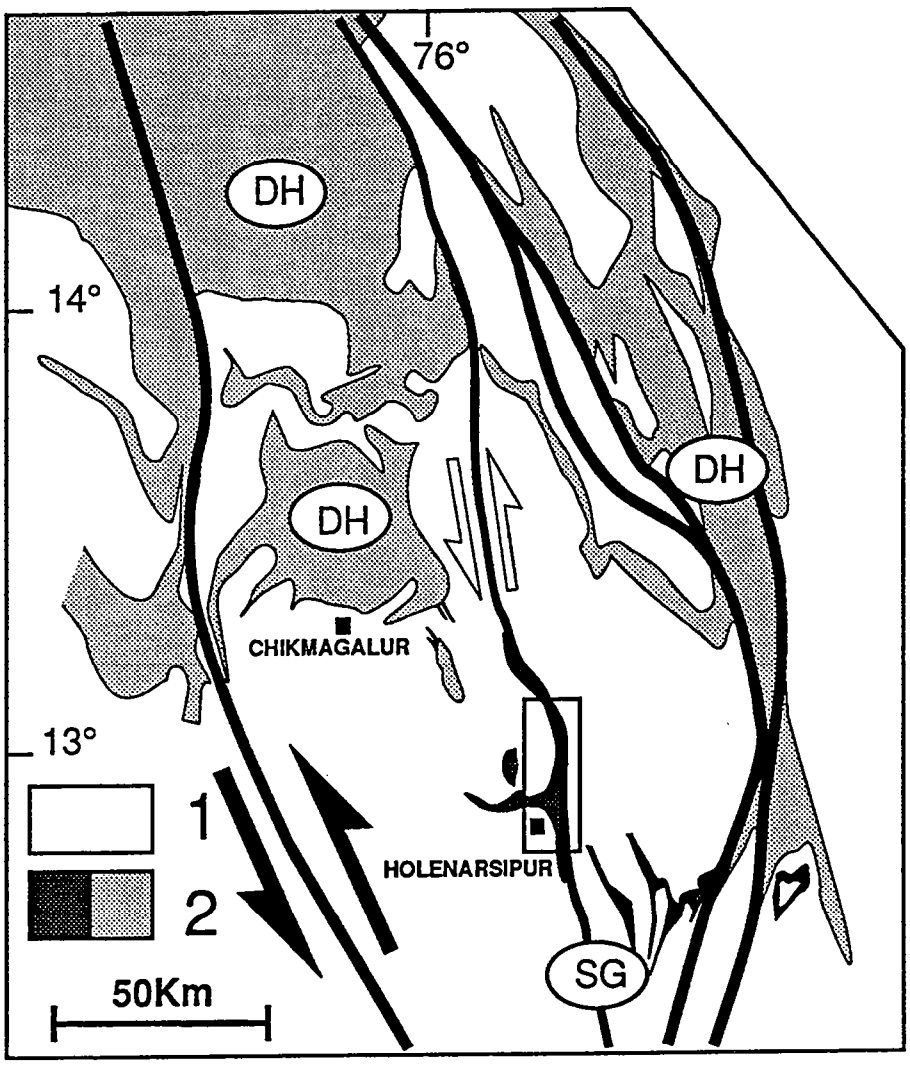

Fig. D. 16. Location of transcurent shear zones around the Holenarsipur area. **1** : TTG (Peninsular Gneisses) ; **2** : supracrustal rocks of Sargur unit (SG) in dark grey, of Dharwar unit (DH) in light grey. The sinistral shear which bounds the Holenarsipur greenstone belt is situated in a consistent regional pattern of late (post-doming) transcurrent deformation which affected the Dharwar craton around 2.5 Ga.

Fig. D. 16. Situation géographique des zones de cisaillement décrochantes autour de la région d'Holenarsipur. **1** : TTG (gneiss péninsulaires) ; **2** : roches supracrustales de l'unité de Sargur (SG) en gris foncé, de l'unité de Dharwar (DH) en gris clair. La zone de cisaillement senestre qui borde la ceinture d'Holenarsipur appartient à une organisation régionale de cisaillements transcurrents tardifs (post-doming) qui ont affecté le craton de Dharwar aux environs de 2.5 Ga.

Critical relationships between metamorphism and the regional foliation, as revealed by field and thin section observations, are as follows :

In the mica schists, the long axes of staurolite, kyanite and biotite are always parallel to the regional foliation. These minerals are scattered within the foliation plane when the fabric is planar (flattening strain) and oriented parallel to the stretching lineation when the fabric is linear or planar-linear (constrictive or plane strain). Thin sections display well–preserved garnets with spiral inclusions trails. Minerals such as quartz, biotite, and opaques delineate the matrix foliation. Opaque inclusions in garnets design internal sigmoidal foliations linked with the matrix foliation : this clearly indicates that the garnets in mica schists grew during the main tectonic event and demonstrates the synkinematic character of these minerals.

In amphibolites, garnets display similar synkinematic relationships to the main structural event : internal rotated foliation in garnets is linked with the matrix foliation. The shape fabric of amphiboles is related to the finite strain ellipsoid type : well developed "garbenschiefer" are only found in planar fabric areas (e.g. East of Halekote) meanwhile amphiboles are oriented parallel to the stretching direction in more linear fabric areas.

These observations lead to the conclusion that, in the greenstone belt, the regional metamorphism under amphibolite-facies conditions was contemporaneous with the regional foliation that we shall argue to be the result of dome and basin formation.

The metamorphic grade that accompanied the late tectonic event (numerous sinistral shear bands and asymmetric folds that affect the regional foliation) can be documented in gneissic rocks adjoining the easternmost part of the belt. For example, gneissic granitoids near Muddanahalli display two distinct parageneses. The first consists of quartz, feldspar, biotite and opaque minerals oriented parallel to the regional foliation (strike - 028°, dip - 85°E) and a down-dip stretching lineation (plunge - 085°). The second paragenesis comprises chlorite, epidote, quartz and biotite which outline horizontal striations in shear bands (strike - 180°, dip - 90°) that are observable all along the eastern boundary of the greenstone belt.

Furthermore, thin sections perpendicular to the regional foliation plane display the following features :

- the foliation plane is well preserved far from the shear bands.
- shear bands affect the older foliation plane.

- broken and disrupted feldspars, sheared biotites and plastically deformed quartz are observed in the shear bands ;

- chlorite and epidote are stable within the shear bands.

These observations show that a greenschist-facies metamorphism is linked to the development of shear bands and post foliation folds localized at the eastern boundary of the greenstone belt (Fig. D. 16).

In summary, the Holenarsipur greenstone belt clearly underwent two metamorphic events, each related to a distinct strain field. The first event, which was of regional extent and under amphibolite-facies conditions, was contemporaneous with the main tectonic deformation. The second lower-grade metamorphic event (greenschist facies) was restricted to a late transcurrent shear zone at the eastern boundary of the belt.

The relative timing of the deformation and magmatism

Trondhjemites, which are very well exposed north and west of Halekote (Mavinakere Betta and Mukundur Betta), can be seen to intrude the older granitoid gneisses (e.g. in quarries N-E of Kattaya.) To the east of Huluvare and west of Guddetalakoppalu, where the supracrustal rocks were attributed to the Dharwar unit, and to the south of Munkundur Betta along the canal, where the supracrustal material was considered to be a part of the Sargur unit, quartzofeldspathic veins spatially related to the Halekote plutons intrude, and are folded, boudinaged and foliated together with the supracrustal rocks. A younger, undeformed group of aplitic and pegmatitic veins cut across the foliation, and consequently postdate the main tectonic event.

At map scale, the granitoid material is seen to be located (i) along the contacts between TTG and supracrustal rocks, and (ii) in the triple junction points. This material is invariably affected by plastic deformation near the contacts with supracrustal rocks (e.g. south of Halekote and Munkundur Betta, north of Sigaranahalli). The deformation fabric evolves progressively, being most pronounced at the margins and diminishing progressively towards the virtually isotropic centres of the intrusions. Extended outcrops, in particular around Munkundur Betta, provide continuous cross sections from the central part of the trondjhemitic body, where the fabric is isotropic, to the boundaries, where the deformation fabric is well developed.

As it was proposed before (Chadwick et al., 1978), such relationships, which are present both in outcrop (veining), and at map scale (strain

patterns and strain gradients), indicate that, at least a part of granitoid intrusions are, in a broad sense, syntectonic.

INTERPRETATION AND DISCUSSION OF STRUCTURAL DATA.

The key observations pertaining to the structural evolution of the Holenarsipur area are :

1)- the entire Holenarsipur greenstone belt underwent the same tectono-metamorphic history.

2)- the entire belt was intruded by a magmatic phase which can be reasonably correlated with the 3.1-3.0 Ga old Halekote trondhjemite. The trondhjemites are oriented generally parallel to the foliation trajectories.

3)- foliation trajectories outline elliptical domes of gneissic material, separated and surrounded by supracrustal rocks.

4)- foliation trajectories define triple junctions where linear vertical tectonites are preferentially located, some of which are marked by superimposed structures (such as post-foliation folds with vertical axes). It is important to notice that some of these areas are preferential sites of fluid circulation (quartz- and tourmaline-bearing veins).

5)- when S1 is vertical, the stretching lineation L1 is also generally vertical. The exception is in a narrow N-S vertical zone at the eastern boundary of the Holenarsipur greenstone belt, where L1 is horizontal and the strain high. This narrow zone is the locus of a non-coaxial deformation associated with retrograde crystallization.

Points 1 and 2 cast considerable doubt on the hypothesis that two different supracrustal series were separated by a tectonic episode. The entire supracrustal belt in the Holenarsipur area was strained with the intrusive trondhjemitic bodies dated at 3.1-3.0 Ga. If the intruding magmatic phase observed in the greenstones is contemporaneous with the trondhjemite emplacement, the Holenarsipur belt is older than 3.1-3.0 Ga and should be assigned to the Sargur unit. If it is not the case, the trondhjemite emplacement could predate the regional deformation and metamorphism.

Nevertheless, point 4 is a strong argument in favour of syntectonic trondhjemite emplacement. Thus, if the age for the Halekote trondhjemite is 3.0 Ga. (Beckinsale et al., 1982 ; Bhaskar Rao et al., 1983 ; Monrad, 1983 ; Stroh et al., 1983 ; Taylor et al., 1984 ; Meen et al., 1992 ;), it is also the age of the main tectonic and metamorphic episode. In that case, the Sm-Nd age of 2.62 Ga for supracrustal rocks (Drury et al., 1986) must be considered dubious. On the opposite, if this last age is acceptable, one will have to

reconsider the age of the major tectonometamorphic event as well as the syntectonic character of the trondhjemite.

Strain trajectories due to the first tectono-metamorphic event are typical of bulk deformation **resulting from interference between diapiric domes and regional shortening** (Brun, 1983a and b). Here, this shortening direction is 060-070° as documented by the orientation of the great axis of the elliptical gneissic domes (Fig. D. 10). No earlier deformation can be recognized, and no evidence was found to support Drury et al.'s (1984) assertion that major thrusts affected the studied area.

Lastly, point 5 clearly indicates that transcurrent deformation affected the eastern boundary of the Holenarsipur belt after the major tectonic episode. This major shear zone is similar to those described in the Chitradurga and Bababudan areas (Drury et al., 1984 ; Chadwick et al., 1989). The whole Dharwar craton apparently underwent a transcurrent shearing event during late Archaean, probably at the same time as the Closepet granite emplacement at 2.5 Ga (Jayananda and Mahabaleswar, 1991). At this stage of knowledge, we cannot argue for the relative timing between the regional shortening of initially more or less round-shaped domes and the transcurrent event.

CONCLUSIONS

Foliation trajectories, strain intensity variations and ellipsoid type variations have been defined by spatial integration of qualitative punctual strain data. These constrain the bulk geometry, the progressive deformation and the kinematics of part of the Archaean Dharwar craton. Such bulk geometry is the result of the interference between diapiric domes and moderate horizontal crustal shortening. This interpretation has not previously been proposed for southern India but has been inferred in other Archaean domains such as in Canada (Drury, 1977 ; Schwerdtner, 1984), South Africa Craton (Anhaeusser, 1984 ; Ramsay, 1989) and Australia (Hickman, 1984 ; Delor et al., 1990).

The approach explains not only the observed regional strain field, but also the location of superimposed structures, some of which are merely the result of progressive deformation (from flattening to constriction) at localities where doming and regional shortening interfere.

In addition to this major tectono-metamorphic event, the eastern boundary of the Holenarsipur belt was later the locus of heterogeneous deformation. This event was accompanied by non-coaxial strain which

contrasts sharply with the previous regional coaxial strain of the earlier event. Thus, we propose that two major structural and metamorphic events have shaped the Holenarsipur area : (i) a regional diapiric event, which could have occured around 3.0 Ga, (ii) a later transcurrent ductile shear event, which had locally reoriented both foliation and stretching lineation, at 2.5 Ga. If it is correct, this result enhance the overly simplified representation of the regional metamorphic isograde at craton scale, which necessarily cannot take into account the whole of a complex tectonometamorphic history.

Lastly, it is possible to discard some hypotheses that appear incompatible with the observations and interpretations presented above. For instance basin and dome patterns cannot be interpreted as fold interference patterns considering the kinematic indicators. Major thrusting, as postulated by Drury et al. (1984), cannot explain the described strain pattern, unless thrust-related deformation had been completely erased by the doming event. This seems highly improbable. We infer that all structures, including the transcurrent shearing, are the direct result of a combination of vertical relative movements linked to body forces, and crustal shortening due to boundary forces.

2. 2. Caractérisation du métamorphisme associé aux structures diapiriques de la région d'Holenarsipur (Karnataka, Inde du Sud)

L'étude structurale menée sur le secteur d'Holenarsipur révèle l'existence d'un champ d'instabilités gravitaires d'origine diapirique. Ces structures sont marquées cinématiquement par les évidences de déplacements relatifs verticaux de la couverture dense ("greenstones") par rapport à son environnement de gneiss TTG migmatitiques plus léger. Il apparait aussi que les points triples situés dans les zones de connection entre les différentes branches de la "greenstone belt" possèdent des caractéristiques structurales particulières (fabrique linéaire de type constrictif verticale, déformation non-coaxiale intense), différentes de celles observées dans les branches linéaires de la "greenstone belt". Ces deux zones (points triples et branches linéaires), marquées par une cinématique verticale, ont fait l'objet d'une étude pétrologique détaillée des conditions du métamorphisme.

GRAVITATIONAL COLLAPSE AND FLUID CHANNELLING WITHIN ARCHAEAN DIAPIRIC TRIPLE POINT : EVIDENCE FROM P-T CONDITIONS OF METAPELITES FROM HOLENARSIPUR GREENSTONE BELT, (KARNATAKA, SOUTH INDIA)

BOUHALLIER Hugues
Laboratoire de tectonique
Géosciences Rennes (UPR 4661-CNRS)
Université de Rennes I
35042 Rennes Cedex
France

and

GUIRAUD Michel
Laboratoire de Minéralogie, URA CNRS N°736
Muséum National d'Histoire Naturelle,
61 rue Buffon, 75005 Paris
France

ABSTRACT

Recent structural studies have documented diapiric instabilities within the Archaean Dharwar craton in the Holenarsipur area (South India). Diapiric strain fields are characterized by the occurence of linear troughs of supracrustals connected at foliation triple points. We have studied the P-T-X evolution recorded by metapelites in these two different settings. Our results show that linear troughs and foliation triple points underwent the same peak conditions of metamorphism estimated at 7-8 kbar and 600°C. However values of X_{H_2O} are different between troughs (X_{H_2O}=0.9) and triple points (X_{H_2O}=0.5). We also show that foliation triple points have recorded the prograde history from 470°C to 600°C and from 3 to 7-8 kbar and underwent some metasomatism during this prograde evolution. These results support the diapiric instabilities model.

Key words : Archaean, diapiric structures, metapelites, fluid channelling, South India

INTRODUCTION

Diapiric instabilities which are the result of density inversion of dense mafic and ultramafic series overlying a lighter sialic basement have been inferred in numerous Archaean areas (MacGregor, 1951 ; Drury, 1977 ; Gorman *et al.*, 1978, Schwerdtner 1980 ; Bronner, 1981 ; Hickman, 1984 ; Anhaeusser, 1984 ; Talbot, 1987 ; Collins, 1989 ; Ramsay, 1989, Delor *et al.*, 1991 ; Jelsma *et al.*, 1993). The diapiric structures of the Dharwar craton (South India) have been recently documented in the vicinity of Holenarsipur following the results on detailed strain field analysis and associated kinematics studies (Bouhallier *et al.*, 1993). Regional structures are characterized by linear troughs of dense mainly mafic rocks which connect at specific triple junction areas. These structures are surrounded by a lighter migmatitic sialic basement. Triple junctions are characterized by intense non-coaxial strain with kinematic criteria indicative of the vertical downward motion of the denser material relative to the adjacent migmatitic basement.

The main goal of this paper is to constrain the P-T-X evolution of supracrustal rocks. The study focuses on interbedded pelites because these are evenly distributed within troughs and triple points and provide a number of mineral equilibria sufficient to estimate P-T-X evolution with a reasonable precision.

Abbreviations :

And : andalusite ; Bi : biotite ; Cd : cordierite ; Chl : chlorite ; Ctd : chloritoid ; Cz : clinozoizite ; Epi : epidote ; Gt : garnet ; Ilm : ilmenite ; Ky : kyanite ; Mu : muscovite ; Qtz : quartz ; Ru : rutile ; Sill : sillimanite ; St : staurolite.

GEOLOGICAL SETTING

The geological evolution of the Dharwar craton (Swami Nath & Ramakrishnan, 1981 ; Naqvi & Rogers, 1983 ; Radhakrishna & Ramakrishnan, 1990) took place between 3.4 Ga and 2.2 Ga. At least three main periods of sialic continental crust production have been recognized : around 3.4 Ga, 3.0 Ga and 2.5 Ga (Crawford, 1969 ; Venkatasubramanian, 1975 ; Beckinsale *et al.*, 1980, 1982 ; Bhaskar Rao *et al.*, 1983 ; Monrad, 1983 ; Stroh *et al.*, 1983 ; Taylor *et al.*, 1984 ; Taylor *et al.*, 1988 ; Peucat *et al.*, 1989, 1993 ; Friend & Nutman, 1991 ; Meen *et al.*, 1992 ; Jayananda *et al.*, in press). The central part of the Dharwar craton displays the common Archaean bimodal association of infra- and supracrustal rocks (Fig. D. 17). The infracrustal rocks are principally tonalite-trondhjemite-granodiorite gneisses and represent at least two-third of the area of the Dharwar craton. The Peninsular Gneisses have yielded Rb-Sr whole rock isochrons at 3358±66 Ma and 3315±54 Ma (Beckinsale *et al.* ; 1980 ; 1982). Supracrustal units are mainly composed of ultramafic and mafic metavolcanics and sedimentary rocks. In the northern part of the craton, they constitute broad and large units that unconformably overlie the TTG gneisses whereas in the South, they are mainly in the form of cusp-shaped or elongated synforms. In both cases, geochronology data confirmed that they are systematically younger than the adjacent TTG gneisses (Drury *et al.*, 1983, 1986 ; Taylor *et al.*, 1984 ; Gupta *et al.*, 1988 ; Bhaskar Rao *et al.*, 1992 ; Nutman *et al.*, 1992).

The Dharwar craton, north of the Moyar shear zone, is characterized by a low- to medium-grade metamorphism in the granite-greenstone terrain in the North and a high-grade granulite facies metamorphism in the South (Fig. D. 17). Pressures recorded in gneisses and/or mafic rocks are about 3 kbar in supracrustals in the northern part of the craton, and about 8-9 kbar in both supracrustals and infracrustals in the South (Harris & Jayaram, 1981 ; Janardhan *et al.*, 1982 ; Raith *et al.*, 1982 ; Hansen et al., 1984 ; Raase *et al.*, 1986). Pichamuthu, (1962), Raith *et al.*, (1982, 1983) and Raase et al., (1986) have interpreted this change in metamorphic grade as one broad event characterized by a southward increase in P-T conditions from greenschist to granulite facies. According to them, the display of different P-T conditions is due to a post-metamorphic tilting of the overall craton rather than a true metamorphic gradient. This hypothesis is substantiated by the occurrence of a late Archaean batholith, namely the Closepet granite, which shows a gradual and continuous progression from shallow structural levels in the North to deeper ones in the South. The southernmost part of

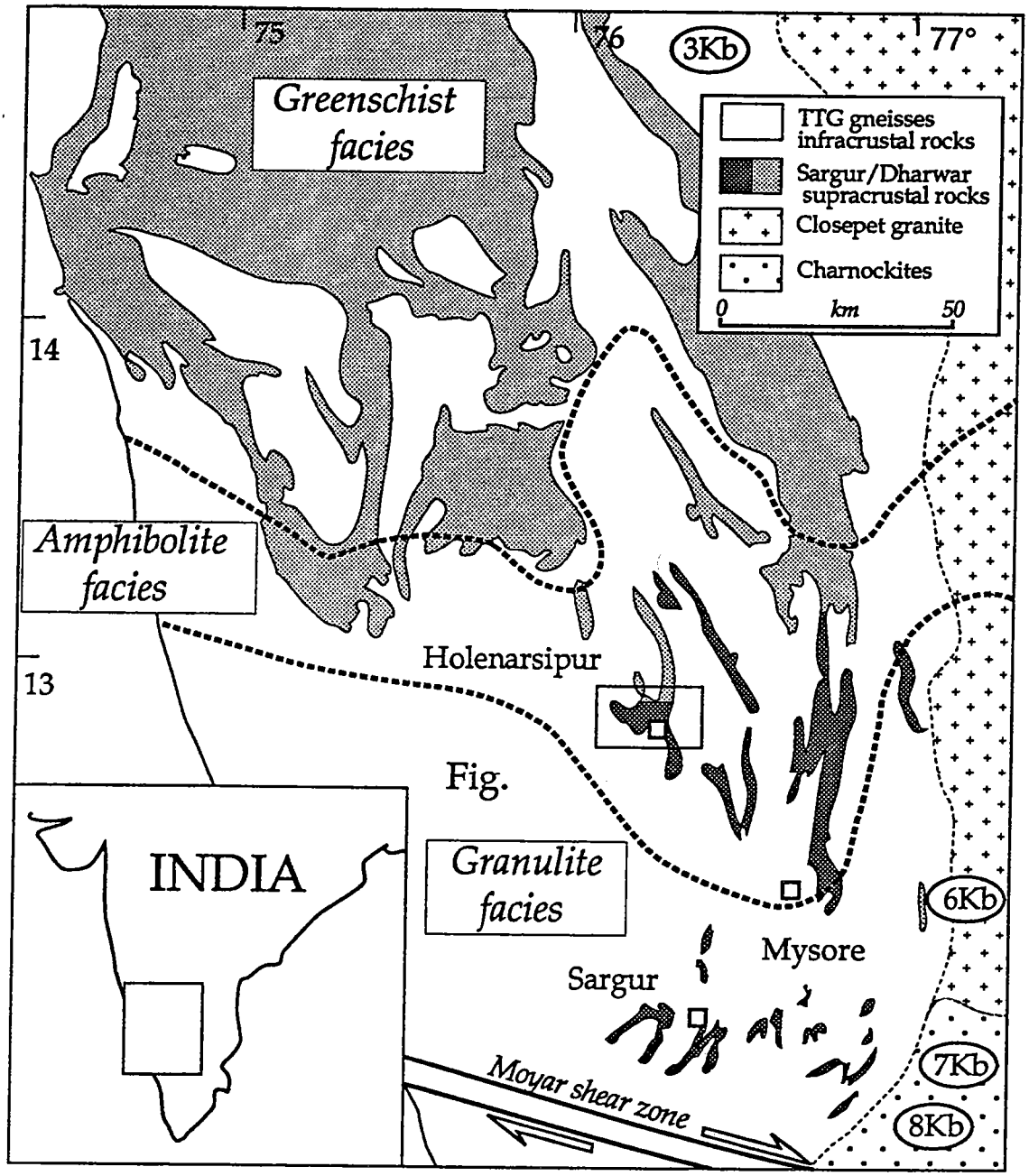

Fig. D. 17. Geology of the western part of Dharwar craton, southern India. Metamorphic facies boundaries (dotted lines) are taken from Raase *et al.* (1986). Palaeopressures in rectangles are from Hansen *et al.* (1984), Harris & Jayaram (1982), and Raith *et al.* (1988).

Fig. D. 17. Géologie de la partie ouest du craton de Dharwar (Inde du Sud). Les isogrades du métamorphisme (en pointillé) sont tirés de Raase *et al.* (1986). Les paléopressions dans les rectangles sont d'après Hansen *et al.* (1984), Harris & Jayaram (1982), et Raith *et al.* (1988).

the Closepet batholith, which represents the deepest structural level in this heterogeneous granitic complex, is affected by the granulite-facies metamorphism (Janardhan *et al.*, 1979 ; Friend, 1981, 1983 ; Hansen *et al.*, 1984, 1987 ; Stähle *et al.*, 1987). The granulite facies metamorphism has been dated at 2.51± 0.01 Ga (Peucat *et al.*, 1993) which is also the age of the Closepet granite (Crawford, 1969 ; Friend & Nutman, 1991, Jayananda *et al.*, in press).

The supracrustals have classically been divided into two types (Swami Nath *et al.*, 1976) matching the general feature of the craton (Fig. D. 17). (i) The Sargur type, mostly restricted to the southern part of the craton, is characterized by amphibolite to granulite facies metamorphism and contains highly deformed sedimentary and mafic igneous rocks ; (ii) the Dharwar type, mainly present in the northern part of the shield, is only slightly deformed, except in late shear zones (Chadwick *et al.*, 1989), and is metamorphosed at greenschist to amphibolite facies conditions. The Sargur unit is considered to be older than the Dharwar unit. Both types underwent the same event at 2.5 Ga (Raith *et al.*, 1982) but it remains unclear whether the Sargur and Dharwar types belong to the same or different supracrustal units and whether there was a metamorphic event prior to the 2.5 Ga event. Both types are supposed to be juxtaposed over a fairly large area in the amphibolite zone near Holenarsipur : the Sargur group is located south of the Hemavati river, and the Dharwar group, north of the river (Ramakrishnan & Viswanatha, 1981 ; Hussain & Naqvi, 1983). The distinction between the Sargur and Dharwar groups rests only on lithological and metamorphic differences, and in spite of detailed mapping, no clear cut unconformity has been identified between the two groups (Hussain & Naqvi, 1983). Moreover, this distinction is supported neither by structural evidence (Chadwick *et al.*, 1978, 1981, Bouhallier *et al..*, 1993) nor by the Sm-Nd isotopic studies by Drury *et al.*, (1986). Bouhallier *et al.*, (1993) have pointed out that parallelism of strain trajectories (Fig. D. 18a), the repartition of fabric types (Fig. D. 18b), strain intensity variations and kinematic indicators in supracrustal rocks are neither consistent with the concept that two tectonometamorphic events are preserved in the supracrustal rocks (Hussain & Naqvi, 1983) nor with the presence of early E-W recumbent structures deformed by N-S upright folded (Drury *et al.*, 1984). Bouhallier et al. proposed that the whole Holenarsipur area was shaped by an intense diapiric event created by the heating of the entire continental crust which in turn provoked gravitational instabilites due to the density contrast between the denser supracrustal rocks and the lighter Peninsular

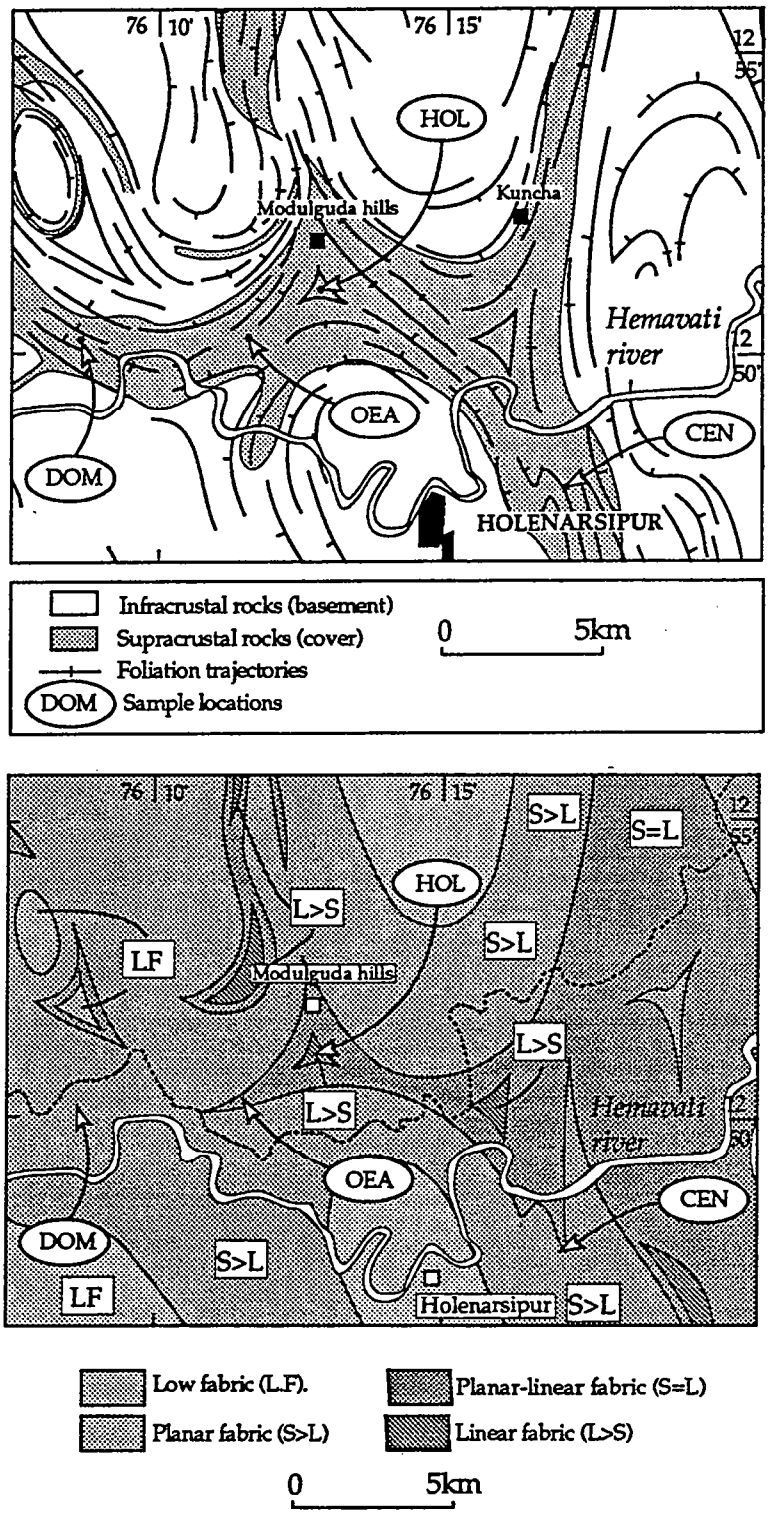

Fig. D. 18. After Bouhallier *et al.*, 1993 ; (a) : Foliation trajectories map and samples locations in the Holenarsipur area. Infracrustal rocks (basement) crop out as elliptical domes whereas supracrustal rocks (cover) display linear troughs connected at triple points embedded in the migmatitic TTG basement ; (b) : Structural map of fabric in the Holenarsipur area. Sample locations have been added.

Fig. D. 18. D'après Bouhallier *et al.*, 1993 ; (a) : Carte des trajectoires de la foliation et localisation des échantillons dans la région d'Holenarsipur. Les roches infra-crustales affleurent sous la forme de dômes elliptiques tandis que les roches supracrustales (couverture) sont disposées en synformes linéaires, connectés en points triples et ennoyés dans le socle migmatitique de TTG ; (b) : Carte structurale des fabriques de la région d'Holenarsipur. Les emplacements des échantillons ont été ajoutés.

gneisses. Evidence for these gravitational instabilities includes the occurrence of linear troughs connected by triple junctions characterized by intense vertical constriction, and kinematic criteria pointing to downward motion of the supracrustals relative to the TTG basement.

PETROGRAPHY

Four samples of pelitic rocks have been studied (Fig. D. 18a and Fig. D. 18b) : two from linear troughs (CEN and DOM), one centered on a triple junction (HOL) and one (OEA) in an intermediate position between HOL and DOM.

1- Garnet-chloritoid schists (HOL sample, Fig. D. 19)

Iyengar (1971) was first to describe the garnet-chloritoid schist in the area of Holenarsipur. The rocks consist, in decreasing amount, of chlorite, garnet, chloritoid, ilmenite and quartz. Chloritoid and garnet occur as centimetre scale porphyroblasts within a matrix composed of large and automorphic crystals of chlorite. Garnet and chloritoid represent sometimes up to 30% of the whole rock. Hand specimens display a penetrative plano-linear fabric. Chloritoids and oblate strained garnets outline a strong vertical stretching lineation. Garnets are either intensely flattened within the foliation plane or their deformation is weak or negligible. In thin section, the matrix foliation or external schistosity Se, (Spry, 1969) is outlined by chlorite and ilmenite. Porphyroblasts of garnet and chloritoid have preserved inclusion trails which mark an internal schistosity Si - rotated in the case of garnets - continuous with Se. Furthermore, rotation of garnets has developed pressure shadows which are filled by coarse scattered chlorites attesting to syn-tectonic growth of the assemblage *Gt+Ctd+Chl*. However, some garnets overgrew the external schistosity under more-or-less static conditions which indicates that the metamorphism has partly outlasted the main deformational event. Furthermore, in some places, chlorite fills cracks created by the boudinage of chloritoid. The nature of inclusions in minerals is worth noting : chlorite inclusions are randomly distributed within chloritoid but are found only in the core of garnets. More important, quartz occurs only as inclusions within chloritoid and even a careful search using the electron microprobe failed to reveal its presence in the matrix and in grains of garnet. By contrast, ilmenite is observed in garnet, chloritoid and matrix. Thus, the paragenetic evolution in HOL is characterized by the transformation of the early paragenesis *Ctd+Chl+Qtz* into the later

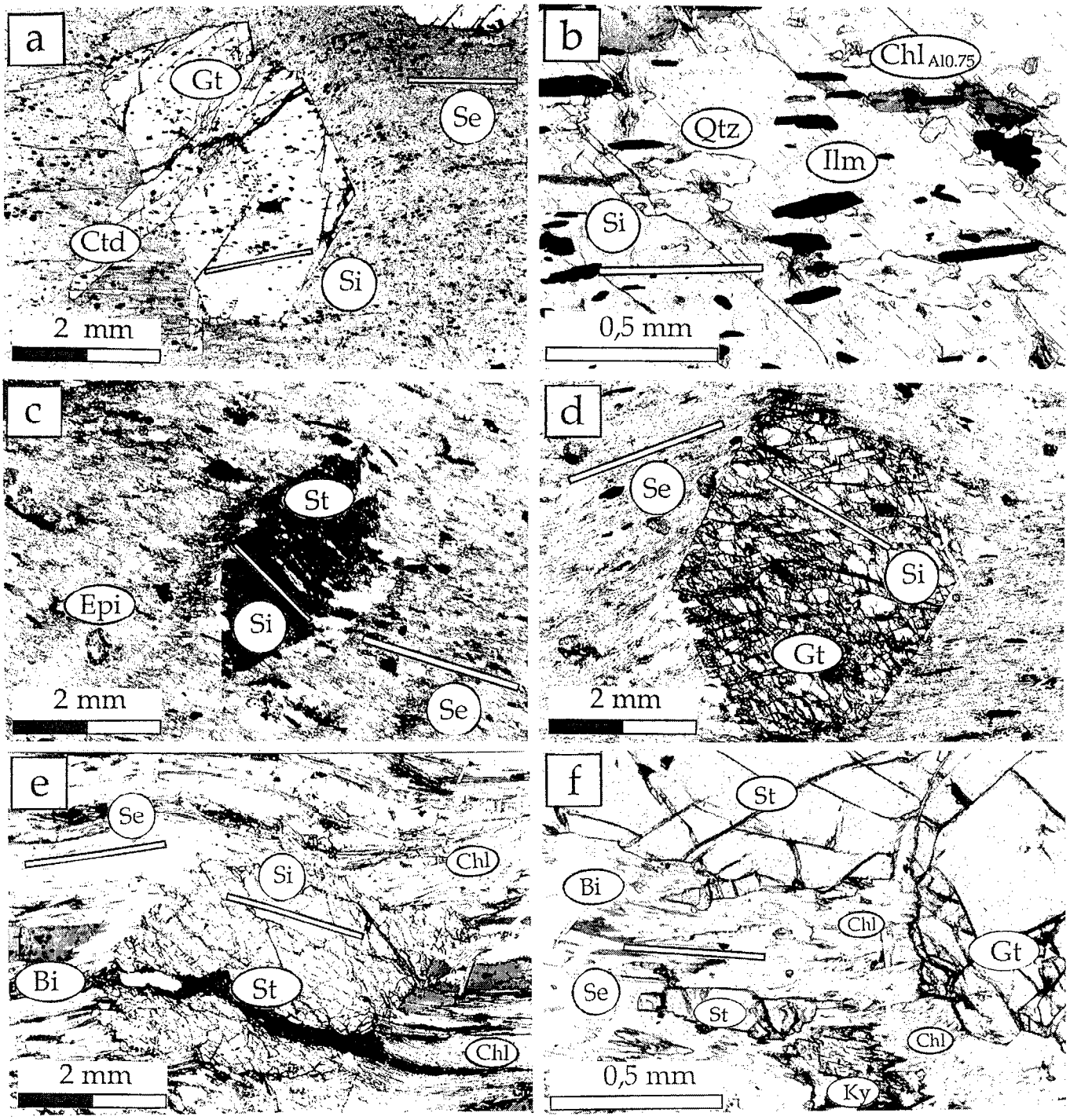
a
Gt
Se
Ctd
Si
2 mm
b
Chl Al0.75
Qtz
Ilm
Si
0,5 mm
c
St
Epi
Si
Se
2 mm
d
Se
Si
Gt
2 mm
e
Se
Si
Chl
Bi
St
Chl
2 mm
f
St
Bi
Chl
Gt
Se
St
Chl
0,5 mm
Ky

Fig. D. 19. (a) Photomicrograph of HOL showing garnet (Gt) and chloritoid (Ctd) overgrowing the external schistosity *(Se)* under more-or-less static conditions. *Se* is outlined by chlorite ($Chl_{Al0.85}$) and numerous grains of ilmenite. *Si* is outlined by chlorite ($Chl_{Al0.75}$) only in the core of garnet and numerous grains of ilmenite throughout the garnet. (b) Photomicrograph of HOL showing *Si* made of inclusions of quartz (Qtz), ilmenite (Ilm) and chlorite ($Chl_{Al0.75}$) in the chloritoid. (c) Photomicrograph of OEA showing chlorite, staurolite (St), epidote (epi), white mica, quartz and ilmenite. Staurolite are entirely retrogressed into chlorite, sericite and quartz but have preserved numerous inclusions of epidote, ilmenite and quartz. The matrix foliation *(Se)* is outlined by chloritised biotite, chlorite, epidote, ilmenite, quartz and white mica. Porphyroblasts of staurolite have preserved an internal and sigmoidal schistosity outlined by quartz, epidote and ilmenite continuous with the external schistosity. (d) Photomicrograph of OEA showing chlorite, garnet (Gt), epidote, white mica, quartz and ilmenite. Garnet has preserved numerous inclusions of epidote, ilmenite and quartz. The matrix foliation *(Se)* is outlined by chloritised biotite, chlorite, epidote, ilmenite, quartz and white mica. Porphyroblasts of garnet have preserved an internal and sigmoidal schistosity outlined by quartz, epidote and ilmenite continuous with the external schistosity. Asymetric pressure shadows are mainly filled with chlorite, quartz and white mica. (e) Photomicrograph of CEN showing biotite (Bi), staurolite (St), chlorite (Chl), white mica, quartz, and rutile. The matrix foliation *(Se)* is outlined by biotite, white mica, chlorite, rutile and quartz. Patterns of inclusions within staurolite define an internal and sigmoïdal schistosity *(Si)* continuous with the external schistosity. Staurolite is flanked by pressure shadows filled with biotite, chlorite and quartz. (f) Photomicrograph of DOM showing biotite (Bi), staurolite (St), garnet (Gt), chlorite (Chl), kyanite (Ky) white mica, quartz, and rutile. The matrix foliation *(Se)* is outlined by staurolite, biotite, white mica, chlorite and quartz.

Fig. D. 19. (a) Photo de l'échantillon HOL montrant le grenat (Gt) et le chloritoïde (Ctd) post-cinématiques croissant de manière plus ou moins statique. *Se* est marquée par la chlorite ($Chl_{Al0.85}$) et de nombreux grains d'ilménite. *Si* est marquée par la chlorite ($Chl_{Al0.75}$) seulement au coeur du grenat et par de nombreux grains d'ilménite à travers la totalité du grenat. (b) Photo de l'échantillon HOL montrant Si marquée par des inclusions de quartz (Qtz), ilmenite (Ilm) et de chlorite ($Chl_{Al0.75}$) dans le chloritoïde. (c) Photo de l'échantillon OEA montrant la chlorite, la staurotide (St), l'épidote (epi), le mica blanc, le quartz et l'ilmenite. La staurotide est complètement rétromorphosée en chlorite, en séricite et en quartz mais a préservé de nombreuses inclusions d'épidote , d'ilménite et de quartz. La foliation matricielle *(Se)* est marquée par de la biotite chloritisée, de la chlorite, de l'épidote, de l'ilménite, du quartz et du mica blanc. Les porphyroblastes de staurotide ont préservés une schistosité interne sigmoïdale marquée par le quartz, l'épidote et de l'ilménite continue avec la schistositée externe. (d) Photo de l'échantillon OEA montrant la chlorite, le grenat (Gt), l'épidote, le mica blanc, le quartz et l'ilménite. Le grenat a préservé de nombreuses inclusions d'épidote, d'ilménite et de quartz. La foliation matricielle *(Se)* est marquée par de la biotite chloritisée, de la chlorite, de l'épidote, de l'ilménite, du quartz et du mica blanc. Les porphyroblastes de grenat ont préservés une schistosité interne sigmoïde marquée par le quartz, l'épidote et l'ilménite continue avec la schistosité externe *(Se)*. Les ombres de pression sont principalement remplis avec de la chlorite, du quartz et du mica blanc. (e) Photo de l'échantillon CEN montrant la biotite (Bi), la staurotide (St), la chlorite (Chl), le mica blanc, le quartz, et le rutile. La foliation matricielle *(Se)* est marquée par de la biotite, du mica blanc, de la chlorite, du rutile et du quartz. Les alignements d'inclusions dans la staurotide définissent une schistosité interne sigmoïdale *(Si)* continue avec la schistosité externe *(Se)*. La staurotide abrite des ombres de pression remplies avec de la biotite, de la chlorite et du quartz. (f) Photo de l'échantillon DOM montrant de la biotite (Bi), de la staurotide (St), du grenat (Gt), de la chlorite (Chl), du disthène (Ky) du mica blanc, du quartz, et du rutile. La foliation matricielle *(Se)* est marquée par la staurotide, la biotite, le mica blanc, la chlorite et le quartz.

paragenesis*Ctd+Chl+Gt*. The disappearance of quartz and the appearance of garnet constitute the most relevant features.

2- Garnet-staurolite-epidote metapelites (OEA sample, Fig. D. 19)

The rock contains biotite, chlorite, staurolite, garnet, epidote, white mica, quartz and ilmenite in decreasing amount. Thin sections display garnet (< 2mm) which appears restricted to specific lithological layers. Staurolite occurs as a large centimetre-scale porphyroblasts entirely retrogressed to chlorite, sericite and quartz. However, numerous inclusions of garnet, epidote, ilmenite and quartz remain in staurolite crystals. Garnet displays several types of inclusions such as epidote, ilmenite, staurolite and quartz. The matrix consists of chloritised biotite, chlorite, epidote, ilmenite, quartz and white mica. Porphyroblasts of garnet and staurolite have preserved an internal schistosity outlined by quartz, epidote and ilmenite. The internal schistosity is continuous with the external schistosity for the staurolite but discontinuous for garnet. However, both minerals are syn-tectonic since staurolite has been observed as inclusion in garnet ; the disruption between the internal and external schistosity could then be explained by strong ductility contrast between rotated garnets and matrix. In summary, the paragenetic evolution in OEA is characterized by an early equilibrium between St, Gt, Bi, Chl, Cz, Wm and Qtz.

3- Staurolite-kyanite metapelites (CEN sámple, Fig. D. 19)

The rock contains biotite, staurolite, kyanite, chlorite, white mica, quartz, plagioclase and rutile in decreasing amount. These pelitic layers display a strong dip foliation associated with planar-linear or planar fabrics. Stretching lineation is always marked by well orientated crystals of kyanite and phyllosilicates excepted in the case of planar fabric where prismatic crystals (as kyanite and staurolite) are randomly distributed in the flattening plane. In thin section, staurolite occurs as centimetre scale porphyroblasts frequently twinned and imbricated with large crystals of kyanite which is the aluminosilicate only represented in the rocks. Porphyroblasts are idiomorphic and frequently kinked. The matrix foliation (Se) is outlined by biotite, white mica, chlorite, rutile and quartz. Patterns of inclusions within staurolite define a sigmoidal internal schistosity (Si) continuous with the external schistosity. Porphyroblasts of staurolite are flanked by pressure shadows filled with biotite, chlorite and quartz. The syn-tectonic character for this assemblage can be therefore unambiguously emphasized. Scarce porphyroblasts of plagioclase preserve white mica and quartz in inclusions.

Quartz, is present in the matrix as well as in kyanite and staurolite. Chlorite is mainly associated with staurolite. Rutile, abundant in the matrix is also included in staurolite and kyanite. In summary, the paragenetic evolution in CEN is characterized by an early equilibrium between St, Ky, Bi, Chl, Wm and Qtz.

4- Garnet-staurolite-kyanite metapelites (DOM sample, Fig. D. 19)

Garnet-staurolite-kyanite metapelite was previously reported by Jayaram (1899, 1910). The rocks contain biotite, staurolite, kyanite, garnet, chlorite, white mica, quartz, rutile and ilmenite in decreasing amount. Kyanite and staurolite occur as idioblastic minerals and are reacting with biotite to chlorite and white mica. Garnet, kyanite and staurolite are contemporaneous since these phases are generally observed imbricated together. Furthermore, these phases display patterns of inclusions which define a sigmoidal internal schistosity (Si) continuous with the external schistosity and attest for the syn-tectonic character of this assemblage. The matrix is composed of biotite, quartz, white mica, ilmenite and rutile. Rutile, ilmenite and quartz are included in kyanite, staurolite and garnet. However, it is worth noting that rutile is often rimmed by ilmenite in the matrix. Meanwhile, there are two generations of biotite : the first one grows parallel to the foliation and the other one cuts across the foliation. In summary, the paragenetic evolution in DOM is characterized by an early equilibrium between Gt, St, Ky, Bi, Chl, Wm and Qtz.

MINERAL CHEMISTRY

Mineral analyses were performed with the electron microprobe at the Service Microsonde Ouest, Brest. Analytical conditions were 15 kV accelerating voltage, 10 nA sample current and 6 seconds counting time. Natural minerals were used as standards. Chemistry of coexisting phases has been investigated in detail in four samples, i.e. one garnet-chloritoid schist (HOL), one garnet-staurolite-epidote metapelite (OEA), one staurolite-kyanite metapelite (CEN) and one garnet-staurolite-kyanite metapelite (DOM). However, it has been very difficult to analyze the primary phases in OEA because of the extensive retrogression it underwent.

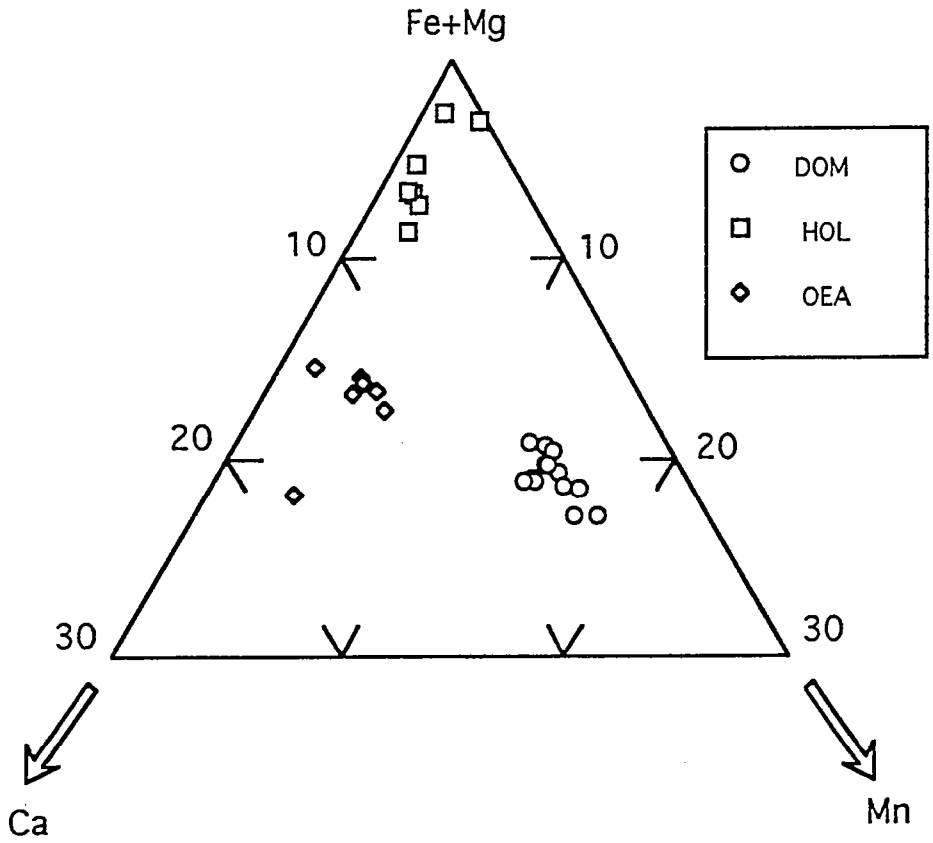

Fig. D. 20. Ternary Fe+Mg, Ca, Mn diagram for garnets.

Fig. D. 20. Diagramme ternaire Fe+Mg, Ca, Mn pour les grenats.

Tableau 1

Garnet					
	HOL		OEA	DOM	
	35 C	34 R	13 C	30 C	8 R
SiO2	37.11	36.75	37.65	37.80	37.53
TiO2	0.0	0.0	0.09	0.01	0.0
Al2O3	20.42	20.69	20.86	20.94	20.85
Cr2O3	0.05	0.0	0.0	0.11	0.14
Fe2O3	0.0	0.24	1.42	1.46	1.72
MgO	0.46	0.51	0.94	3.73	2.9
FeO	39.95	40.06	33.59	28.67	29.32
MnO	0.9	0.69	1.68	6.1	7.49
CaO	1.77	1.76	6.34	2.46	2.1
Na2O	0.03	0.0	0.0	0.1	0.02
K2O	0.0	0.0	0.0	0.04	0.01
Total	100.70	100.70	102.56	101.41	102.08
Si	3.026	2.998	2.979	2.987	2.973
AlIV	0.0	0.002	0.021	0.013	0.027
Al VI	1.963	1.988	1.925	1.937	1.920
Ti	0.0	0.0	0.005	0.001	0.0
Cr	0.003	0.0	0.0	0.007	0.009
Fe3+	0.0	0.15	0.084	0.087	0.103
Mg	0.056	0.062	0.111	0.44	0.342
Fe2+	2.724	2.733	2.223	1.894	1.942
Mn	0.062	0.048	0.112	0.408	0.502
Ca	0.154	0.154	0.538	0.209	0.178
Na	0.005	0.0	0.0	0.015	0.003
K	0.0	0.001	0.0	0.004	0.001
Total	7.993	8.00	8.00	8.00	8.00
Xalm	0.91	0.91	0.74	0.64	0.66
Xpy	0.02	0.02	0.04	0.15	0.12
Xgro	0.05	0.05	0.18	0.07	0.06
Xspe	0.02	0.02	0.04	0.14	0.17
XFe	0.98	0.978	0.952	0.812	0.85

Table 1. Representative garnet analyses and structural formulae. C : core ; R : rim.

Table 1. Analyses et formules structurales des grenats. C : coeur ; R : bordure.

Tableau 2

Chloritoid		
	HOL	
	40 C	22 R
SiO2	24.60	24.31
TiO2	0.0	0.01
Al2O	39.37	40.08
Cr2O	0.14	0.09
MgO	0.79	0.79
FeO	27.25	27.80
MnO	0.13	0.01
CaO	0.0	0.01
Na2C	0.0	0.01
K2O	0.0	0.0
H2O	7.14	7.19
Total	99.42	100.30
Si	1.032	1.012
AlIV	0.0	0.0
Al VI	1.946	1.968
Ti	0.0	0.0
Cr	0.005	0.003
Mg	0.049	0.049
Fe2+	0.956	0.968
Mn	0.004	0.0
Ca	0.0	0.0
Na	0.0	0.001
K	0.0	0.0
OH	2.0	2.0
Total	5.993	6.002
XFe	0.951	0.952

Table 2. Representative chloritoid analyses and structural formulae. C : core ; R : rim.

Table 2. Analyses et formules structurales du chloritoïde. C : coeur ; R : bordure.

Tableau 3

Chlorite

	HOL				CEN	DOM
	37	30	94	159	110	7
	I Ctd	Mat C	Mat R	Mat R	Mat	Mat
SiO2	22.73	22.38	21.42	22.34	25.93	25.65
TiO2	0.05	0.05	0.05	0.08	0.11	0.08
Al2O3	22.14	23.12	25.67	25.64	23.49	23.38
Cr2O3	0.04	0.00	0.0	0.08	0.11	0.28
MgO	4.67	4.61	3.87	3.94	19.35	18.34
FeO	39.10	37.67	36.94	37.41	17.68	20.31
MnO	0.06	0.05	0.15	0.0	0.19	0.26
CaO	0.0	0.00	0.01	0.04	0.0	0.0
Na2O	0.01	0.03	0.0	0.03	0.02	0.0
K2O	0.04	0.02	0.0	0.01	0.05	0.0
H2O	10.65	10.63	10.71	10.91	11.77	11.78
Total	99.49	98.56	98.82	100.48	98.70	100.08
Si	2.556	2.523	2.397	2.454	2.64	2.609
AlIV	1.444	1.477	1.603	1.546	1.36	1.391
Al VI	1.491	1.595	1.783	1.773	1.458	1.412
Ti	0.004	0.05	0.004	0.007	0.008	0.006
Cr	0.004	0.0	0.0	0.007	0.009	0.022
Mg	0.783	0.774	0.646	0.644	2.936	2.781
Fe2+	3.678	3.552	3.458	3.436	1.505	1.728
Mn	0.006	0.005	0.014	0.0	0.016	0.022
Ca	0.0	0.0	0.002	0.005	0.0	0.0
Na	0.002	0.007	0.0	0.006	0.004	0.0
K	0.006	0.003	0.0	0.001	0.006	0.0
OH	8.0	8.0	8.0	8.0	8.0	8.0
Total	17.97	17.941	17.906	17.88	17.944	17.972
XFe	0.824	0.821	0.843	0.842	0.339	0.383
XAlM1	0.745	0.795	0.89	0.886	0.729	0.706

Table 3. Representative chlorite analyses and structural formulae. I : in inclusion ; Mat : in matrix ; C : core ; R : rim.

Table 3. Analyses et formules structurales de s chlorites. I : en inclusion ; Mat : en matrice ; C : coeur ; R : bordure.

Tableau 4

Staurolite

	CEN		DOM	
	92	102	48	23
	C	R	C	R
SiO2	27.86	28.14	28.08	27.71
TiO2	0.68	0.53	0.67	0.69
Al2O3	53.63	53.21	53.29	54.23
Cr2O3	0.4	0.29	0.45	0.14
MgO	2.07	1.59	1.93	1.77
FeO	13.01	13.31	13.28	13.32
MnO	0.47	0.61	0.39	0.31
CaO	0.0	0.02	0.05	0.0
Na2O	0.0	0.01	0.0	0.03
K2O	0.0	0.02	0.0	0.01
Total	98.12	97.73	98.14	98.21
Si	8.036	8.158	8.106	7.986
AlIV	0.0	0.0	0.0	0.014
Al VI	18.234	18.184	18.132	18.404
Ti	0.148	0.116	0.145	0.149
Cr	0.091	0.066	0.102	0.033
Mg	0.89	0.687	0.83	0.759
Fe2+	3.139	3.227	3.207	3.211
Mn	0.115	0.15	0.096	0.075
Ca	0.0	0.006	0.014	0.0
Na	0.0	0.006	0.0	0.018
K	0.0	0.007	0.0	0.005
Total	30.653	30.608	30.632	30.652
XFe	0.779	0.824	0.794	0.809

Table 4. Representative staurolite analyses and structural formulae. C : core ; R : rim.

Table 4. Analyses et formules structurales de la staurotide. C : coeur ; R : bordure.

Tableau 5

	Epidote	
	OEA	
	5	10
	C	R
SiO2	38.81	39.63
TiO2	0.07	0.07
Al2O3	27.95	27.95
Cr2O3	0.0	0.09
Fe2O3	8.18	7.58
MgO	0.0	0.13
FeO	0.0	0.0
CaO	23.93	23.71
MnO	0.0	0.0
Na2O	0.01	0.0
K2O	1.94	1.95
Total	100.91	101.11
Si	2.994	3.039
Al	2.542	2.527
Ti	0.004	0.004
Cr	0.0	0.006
Fe3+	0.475	0.437
Mg	0.0	0.008
Mn3+	0.0	0.0
Ca	1.978	1.948
Na	0.0	0.0
K	0.001	0.0
OH	1.0	1.0
Total	8.994	8.968
XFe3+	0.47	0.45

Tableau 6

	Biotite		White mica		Biotite		White mica
	DOM		DOM		CEN		CEN
	59	3	41	61	90	96	109
	C	R			R	C	
SiO2	36.13	36.17	45.26	46.93	37.48	37.77	46.08
TiO2	1.89	1.79	0.78	0.32	1.5	1.83	0.38
Al2O3	18.99	20.49	36.89	35.82	20.39	19.98	36.17
Cr2O3	0.54	0.34	0.29	0.13	0.16	0.24	0.04
MgO	11.68	11.69	0.44	0.57	13.11	14.05	0.62
FeO	15.92	15.88	0.79	0.77	13.39	11.82	0.89
MnO	0.17	0.06	0.0	0.03	0.0	0.09	0.12
CaO	0.0	0.03	0.0	0.0	0.0	0.0	0.0
Na2O	0.19	0.25	1.47	1.20	0.47	0.35	1.52
K2O	9.55	9.33	9.25	9.95	8.9	8.77	9.26
H2O	3.99	4.05	4.52	4.54	4.09	4.10	4.52
Total	99.05	100.08	99.69	100.26	99.49	99.00	99.60
Si	2.713	2.677	3.001	3.094	2.742	2.756	3.056
AlIV	1.287	1.323	0.999	0.906	1.258	1.244	0.944
Al VI	0.394	0.464	1.884	1.877	0.501	0.475	1.883
Ti	0.107	0.1	0.039	0.44	0.083	0.1	0.019
Cr	0.032	0.02	0.015	0.017	0.009	0.014	0.002
Mg	1.308	1.29	0.043	0.078	1.43	1.528	0.061
Fe2+	1.0	0.983	0.044	0.059	0.819	0.721	0.049
Mn	0.011	0.004	0.0	0.0	0.0	0.006	0.007
Ca	0.0	0.003	0.0	0.008	0.0	0.0	0.0
Na	0.028	0.036	0.189	0.154	0.067	0.05	0.195
K	0.915	0.881	0.783	0.787	0.831	0.816	0.783
OH	2.0	2.0	2.0	2.0	2.0	2.0	2.0
Total	9.795	9.779	8.997	9.016	9.74	9.71	9.0
XFe	0.433	0.432			0.364	0.321	

Table 5. Representative epidote analyses and structural formulae. C : core ; R : rim.

Table 5. Analyses et formules structurales de l'épidote. C : coeur ; R : bordure.

Table 6. Representative mica analyses and structural formulae. C : core ; R : rim.

Table 6. Analyses et formules structurales des micas. C : coeur ; R : bordure.

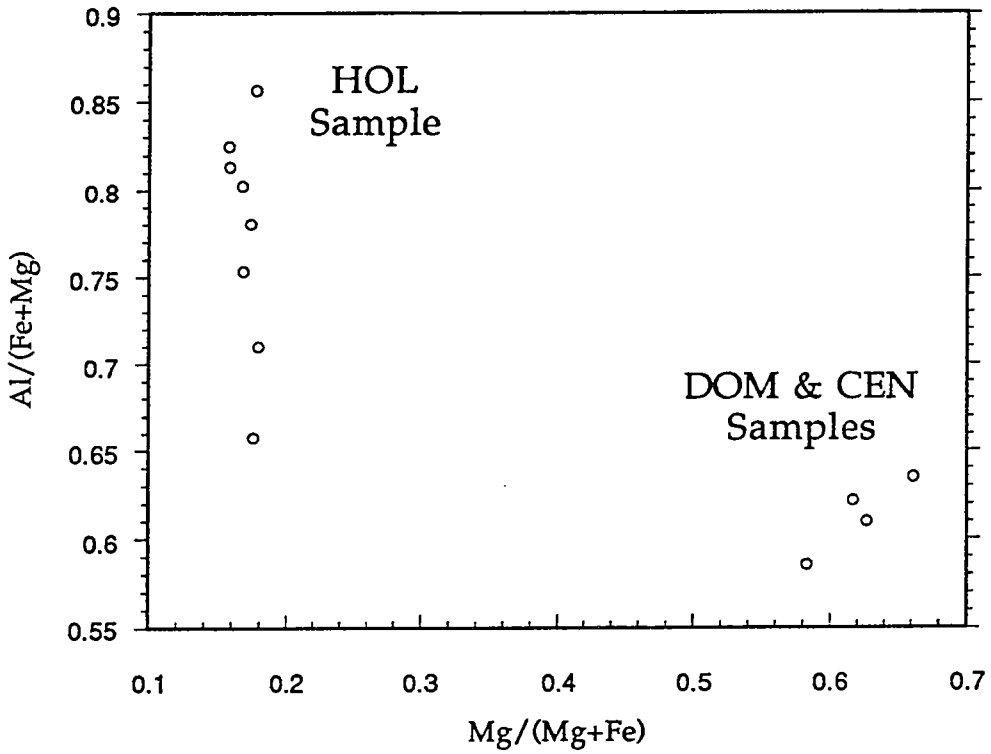

Fig. D. 21. Al/(Fe+Mg) vs Mg/(Fe+Mg) for chlorites compositions. All Fe is Fe^{2+}. Note that the Tchermakitic substitution is well developped for chlorites in HOL sample compared to DOM and CEN samples.

Fig. D. 21. Al/(Fe+Mg) vs Mg/(Fe+Mg) pour la composition des chlorites. Tout le Fe est Fe^{2+}. Remarquer la substitution tchermakitique bien développée dans l'échantillon HOL par rapport aux échantillons DOM et CEN.

Garnet (Table 1, Fig. D. 20). Garnet in HOL is almandine $Alm_{91-95}Py_{2-3}Gro_{2-5}Spe_{1-3}$ with a constant X_{Fe} (Fe/Fe+Mg)=0.97. Grossular and almandin contents display small irregular variations which do not exceed 5 % mol. Recalculated formulae generally show the lack of ferric iron. No significant zoning has been detected. Garnet in OEA is mainly almandine-grossular $Alm_{74-79}Py_{4-6}Gro_{14-18}Spe_{2-4}$ with X_{Fe} almost constant around 0.94. Garnet in DOM is almandine-spessartine-pyrope $Alm_{64-68}Py_{10-16}Gro_{5-7}Spe_{13-18}$ and X_{Fe} varies from 0.81 to 0.87. Garnet is slightly zoned : from core to rim, X_{Fe}, X_{Alm} and X_{Spe} increase whereas X_{Py} decreases. Recalculated formulae generally show a small amount of Fe_2O_3, homogeneously distributed (1 - 3 wt %).

Chloritoid (Table 2). Chloritoid in HOL is unzoned and contains only negligible amounts of MnO and Cr_2O_3 (less than 0.15 % wt%). TiO_2 is absent. Fe^{3+} content recalculated on the basis of stoichiometry is always very low. X_{Fe} is high and constant at 0.95.

Chlorite (Table 3, Fig. D. 21). Chlorites in HOL belong to the daphnite-Fe-Amesite solid solution with a high and almost constant X_{Fe} (X_{Fe} = 0.82 - 0.85). However, they vary strongly with respect to X_{AlM1} and it has been found that primary chlorite included within garnet or chloritoid is significantly less aluminous (X_{AlM1}=0.75-0.76) than the chlorite in the matrix (X_{AlM1} in the range 0.80-0.91). Chlorites in OEA are formed by the retrogression of biotite and therefore are characterized by the presence of K_2O (between 1 and 3 wt%). X_{Fe} is in the range 0.62-0.65. Chlorite compositions in CEN and DOM are homogeneous : X_{Fe} and X_{AlM1} are respectively around 0.34 and 0.73 for CEN and around 0.37-0.38 and 0.70-0.71 for DOM. Excepted K_2O in OEA, any other component such as MnO, Cr_2O_3 and TiO_2 is in negligible amount in all the analyzed chlorites.

Staurolite (Table 4). No analysis has been obtained in OEA since this phase has been completely retrogressed into sericite and chlorite. Staurolite in CEN and DOM is characterized by low MnO and TiO_2 contents (less than 0.7 wt %) and trivial amounts of Cr_2O_3 and ZnO. X_{Fe} ranges between 0.76 and 0.82 in CEN and between 0.79 and 0.84 in DOM. No zoning is observed

Epidote (Table 5). The $Fe^{3+}/(Fe^{3+} + Al^{3+})$ ratio in OEA epidotes is in the range 0.45 - 0.48. Neither zoning nor difference between epidotes in inclusions and in matrix has been detected.

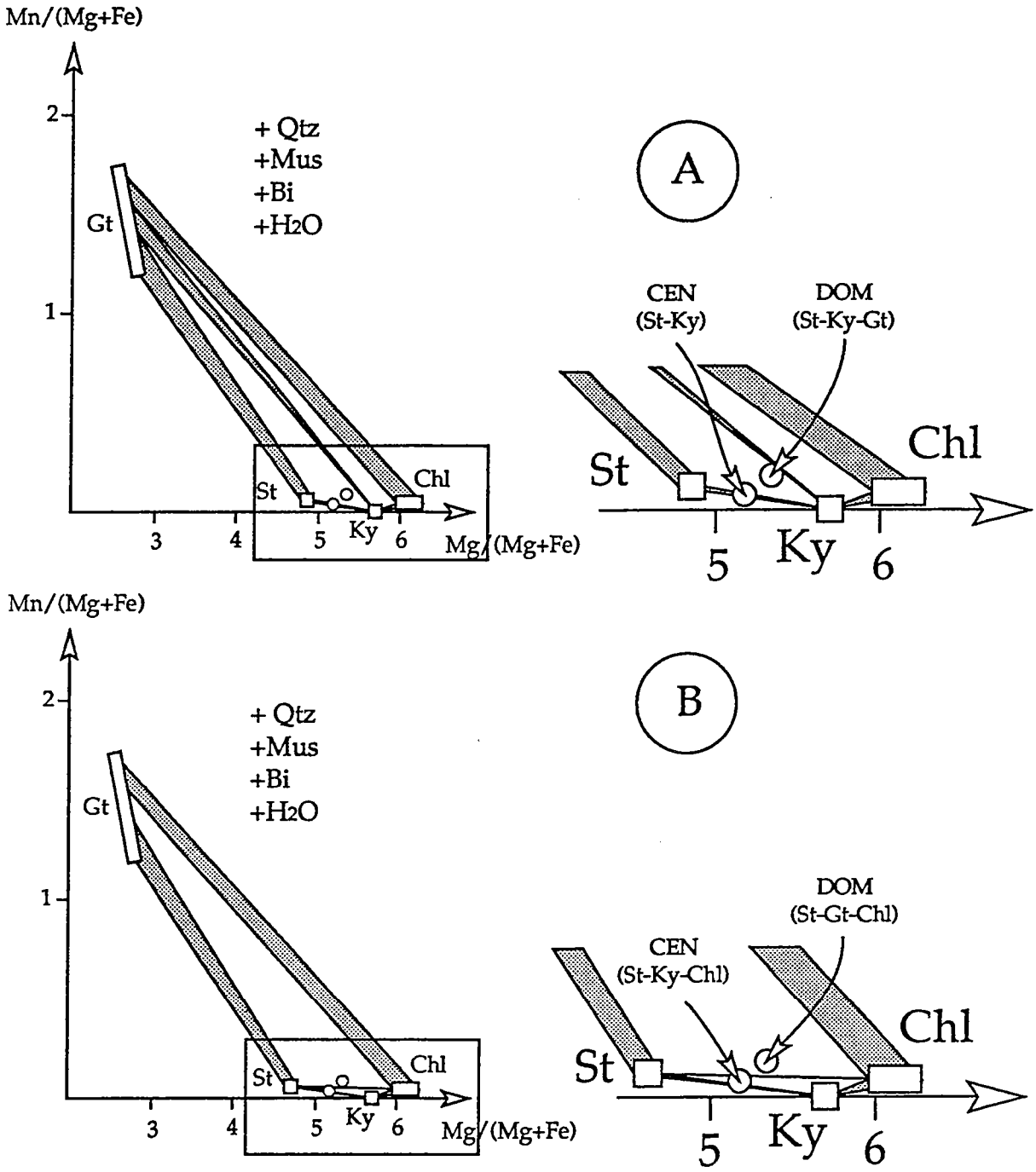

Fig. D. 22. Compatibility diagram for the staurolite-kyanite (CEN) and staurolite-kyanite-garnet (DOM) assemblages. Phases are projected from quartz, muscovite and biotite onto the $Fe_{0.75}\ Al_{0.25}$ - $Mn_{0.75}\ Al_{0.25}$ - $Mg_{0.75}\ Al_{0.25}$ plane. H_2O is assumed to be in excess. Topologies A and B are respectively at higher and lower temperature sides of the Mn-KFMASH reaction Ky + Gt = St + Chl.

Fig. D. 22. Diagramme de compatibilité pour les assemblages staurotide-disthène (CEN) et staurotide-disthène-grenat (DOM). Les phases sont projetées à partir du quartz, de la muscovite et de la biotite sur le plan $Fe_{0.75}\ Al_{0.25}$ - $Mn_{0.75}\ Al_{0.25}$ - $Mg_{0.75}\ Al_{0.25}$. H_2O est supposée en excès. Les topologies A et B sont respectivement des côtés haute et basse températures de la réaction Ky + Gt = St + Chl du système Mn-KFMASH.

Biotite (Table 6). No reliable analyse of biotite in OEA has been obtained ; analyses are characterized by low K_2O content due to retrogression into chlorite. The X_{Fe} value for these analyses is in the ranges of 0.62-0.65. Biotite in CEN is characterized by homogneous compositions : X_{Fe} is in the range of 0.32 - 0.38 and X_{AlM1} in the range 0.21-0.25. Biotite compositions in DOM are also homogeneous in X_{Fe} (0.42-0.45), regardless of the position of the biotite with respect to the foliation. However, there is a variation with respect to X_{AlM1} : X_{AlM1} is around 0.20 for post-tectonic biotite whereas it ranges between 0.16 to 0.34 for syn-tectonic biotites.

White mica (Table 6). All analysed white micas in the samples are muscovite. The ranges of the paragonite content (Na/Na+K) and the phengite content (Si on the basis of 10 Oxygens in the structural formulae) are respectively 0.10-0.20 and 3.06-3.09 in CEN, and 0.11-0.21 and 3.0-3.1 in DOM.

Ilmenites. ilmenites in HOL have a low MnO content (less than 0.8 wt%). Recalculation of analyses on stoechiometry shows that Fe_2O_3 in ilmenites included in garnets or chloritoid is 3 to 4 wt% whereas it never exceeds 1.5 wt% in the ilmenites of the matrix. Ilmenites in OEA have a very low MnO content (less than 0.3 wt %). Recalculation of analyses shows less than 2 wt % Fe_2O_3. Ilmenite in DOM contains between 1 and 3 wt% MnO. Recalculation of analyses do not show any ferric iron.

Plagioclase in CEN has anorthite content in the range of 31 to 41 mol. %.

Kyanite in CEN and DOM has negligible amounts of Fe_2O_3 and Cr_2O_3.

PHASE RELATIONSHIPS AND CONDITIONS OF METAMORPHISM

From the mineral chemistry, phase relationships in DOM and CEN samples can be described together within the Mn-KFMASH system (MnO - K2O - FeO - MgO - Al2O3 - SiO2 - H2O). The observation in thin section of the two samples shows that staurolite, kyanite, biotite, muscovite, chlorite and garnet for DOM are all syn-kinematic ; however, textures involving chlorite, garnet, kyanite and staurolite suggests that chlorite formed after the other phases. The parageneses have been represented in the compatibility diagram Mn-Fe-Mg projected from quartz, muscovite and biotite onto the $Fe_{0.75}\ Al_{0.25}$ - $Mn_{0.75}\ Al_{0.25}$ - $Mg_{0.75}\ Al_{0.25}$ plane. H_2O is assumed to be in excess (Fig. D. 22). Chlorite would then form by the Mn-KFMASH reaction *Gt+Ky=St+Chl* and/or the KFMASH reaction *Ky=St+Chl*. The relevant part of the petrogenetic grid in Mn-KFMASH and KFMASH (Fig. D. 23a) has been calculated using the version 2.2b of

THERMOCALC (Powell & Holland, 1988). All the activity models are based on ideal mixing on site as for the KFMASH grid of Holland and Powell (1990). The conditions of formation for the observed parageneses are given by the two equilibria *St+Chl=Gt+Ky+Bi* and *St+Chl=Ky+Bi* and therefore are comprised between 580 and 630°C and between 5 and 10 kbar assuming $P(H_2O)$=PTOTAL, (Fig. D. 23a). However, the P-T conditions have been calculated more precisely by using average P-T estimation in THERMOCALC. All activities are calculated on the basis of ideal mixing on site, excepted for garnets for which the activity model of Newton & Haselton (1981) has been used. The details of the calculations are given in appendix A and are presented in Fig. D. 23b. The results for $X_{H_2O}=1$ are : in CEN all the compositions are homogeneous and lead to T=614±16°C and P=8.4±1.9 ; for DOM, the estimation varies according the celadonite content from T=599±12°C and P=8.6±1.6kbar to T=597±15°C and P=5.7±2.2 kbar. Therefore, the conditions for DOM and CEN can be reasonably estimated at T around 580-620°C and P at around 7-8 kbar.

Given that epidote and garnet contain Fe^{3+} in not negligible amount, phases relationships in OEA metapelite should be described within the Ca-KFMASHTO system ($CaO - K_2O - FeO - MgO - Al_2O_3 - Fe_2O_3 - SiO_2 - H_2O - TiO_2$). The paragenesis within this system is *Gt+St+Mu+Bi+Chl+Ep+Ilm+Qtz* and correponds to a divariant assemblage if H_2O is supposed to be in excess. Moreover, as there is no good probe analysis of the minerals excepted garnet and epidote, the P-T conditions for this paragenesis are difficult to assess using straight geothermometry/geobarometry as for DOM and CEN samples. However, these conditions should be restricted to the P-T location of the Ca-KFMASH reaction *Gt+Chl=Ep+St+Bi* for activities of clinozoisite and andradite respectively in epidote and garnet analysed in the thin section. The P-T location of this equilibrium shown in Fig. D. 23b is consistent with the P-T estimation obtained on DOM and CEN samples. Moreover, the calculation gives X_{Gro} in the range 0.16 to 0.18 which corresponds to the analyzed values (appendix B).

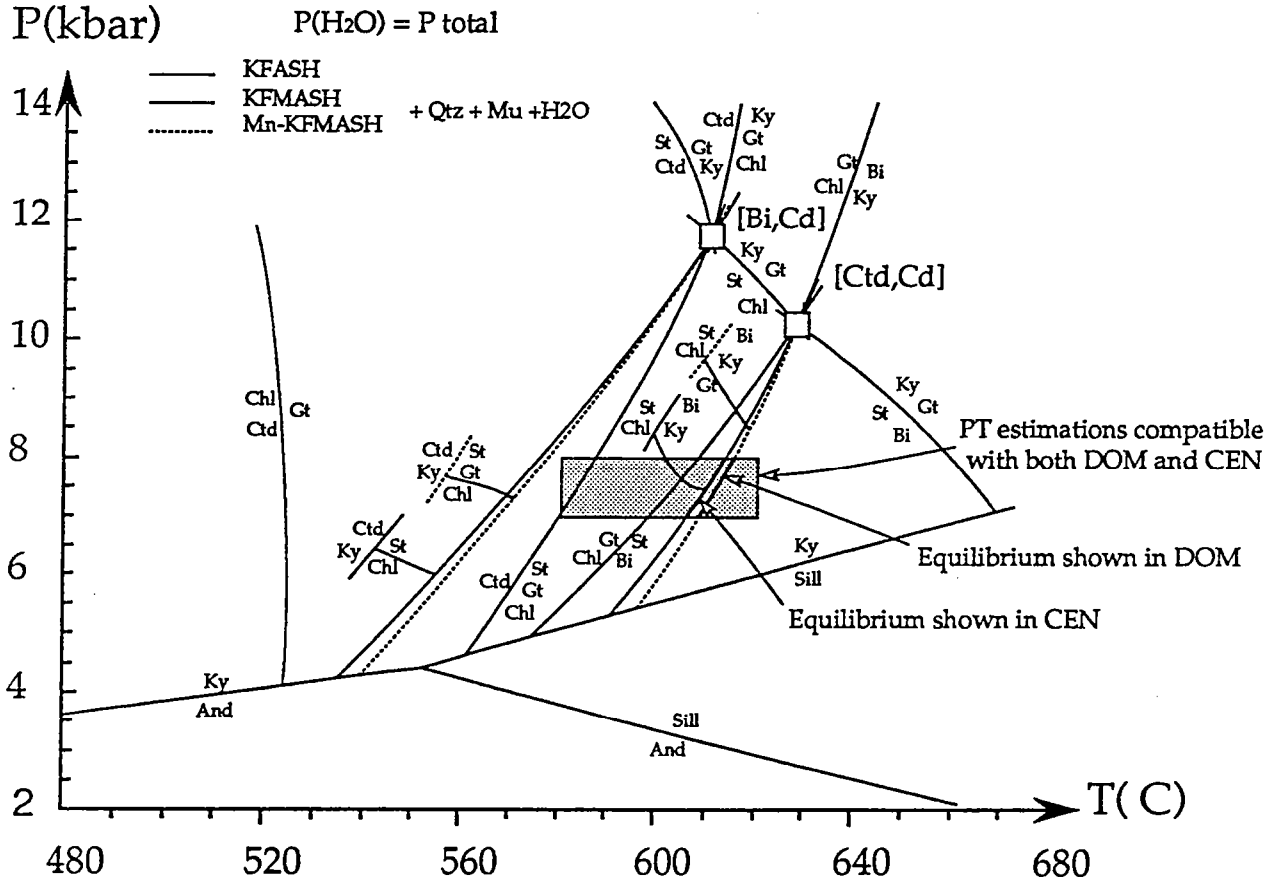

Fig. D. 23. (A). Relevant P-T diagram for KFMASH system with additional KFASH and Mn-KFMASH reactions assuming $P(H_2O)=P(total)$. All calculations have been performed using the version 2.2b of THERMOCALC (Powell & Holland, 1988).

Fig. D. 23. (A). Diagramme P-T pour le système KFMASH avec en plus certaines réactions des systèmes KFASH et Mn-KFMASH en considérant $P(H_2O)=P(total)$. Tous les calculs ont été réalisés avec la version 2.2b de THERMOCALC (Powell & Holland, 1988).

Phases relationships in HOL schist can be described within the FMASHT system (FeO - MgO - Al_2O_3 - SiO_2 - H_2O - TiO_2). From thin section observation and mineral chemistry, quartz and low Al chlorite belong to an early paragenesis preserved as inclusions in chloritoid (paragenesis I : *Ilm+Ctd+Chl*$_{Al0.75}$*+Qtz*), whereas high Al chlorite belong to the main paragenesis displayed by the matrix minerals (paragenesis II : *Ilm+Ctd+Gt+Chl*$_{Al0.85}$). Phases are projected from ilmenite and chloritoid onto the Si - $Fe_{0.66}$ $Al_{0.33}$ - $Mg_{0.66}$ $Al_{0.33}$ plane assuming H_2O in excess (Fig. D. 24). This diagram shows that a_{SiO_2} is different in parageneses I and II : a_{SiO_2} =1 for the quartz-bearing paragenesis I whereas it is less than 1 for garnet in equilibrium with high Al chlorite. Therefore, a_{SiO_2} is a parameter which has to be taken into account in assessing the conditions of metamorphism. Moreover, parageneses I and II are trivariant in the FMASH system and there are not enough independent reactions for the estimation of P and T to be straightforward. However, it is possible to calculate theoretically isopleths for compositional variables and compare them to the analyses. We studied X_{AlM1} in chlorite in the assemblage garnet + chloritoid + chlorite with respect to P, T ,$\log a_{SiO_2}$ and X_{H_2O}. All calculations have been performed using the phase diagram calculations option in THERMOCALC. The results are compiled and given in Fig. D. 25. Isopleths in T versus $\log a_{SiO_2}$ are very narrow and constitute a potential geothermometer. As quartz is present in paragenesis I ($Chl_{Al0.75}$ + Ctd + Qtz), $\log a_{SiO_2}$ is fixed and is equal to zero. However, we need to fix $\log a_{SiO_2}$ for paragenesis II ($Chl_{Al0.85}$ + Ctd + Gt) in which quartz is absent. As the structural level is the same for HOL, DOM, CEN and OEA (Bouhallier et al., 1993), pressure is assumed to be the same for all the samples during the metamorphic event corresponding to the crystallization of minerals in the matrix (paragenesis II for HOL). This pressure has been well constrained around 7-8 kbar in DOM and CEN. Furthermore, chlorite in paragenesis II for HOL is characterized by x_{AlM1}=0.85±0.05 which leads to $\log a_{SiO_2}$=-0.8 to -1 at X_{H_2O}=1 and for P=7.5 kbar. This value implies that T is comprised between 650 and 680°C, a range of values significantly higher than the previous estimations on DOM, CEN and OEA (T=580-620°C).

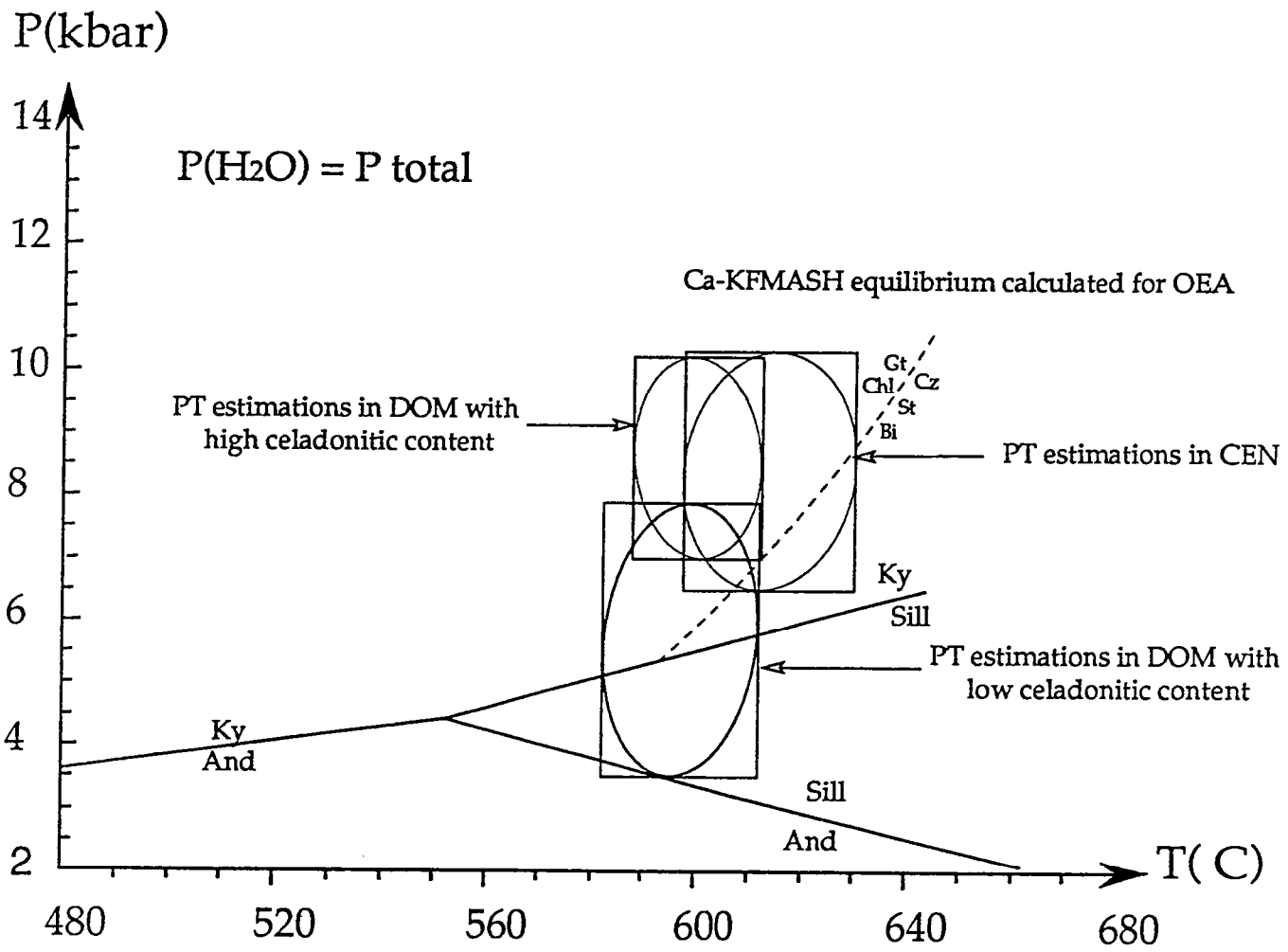

Fig. D. 23. (B). Diagram showing THERMOCALC average P-T estimations in DOM and CEN with additional Ca-KFMASH reaction observed in OEA assuming $P(H_2O)=P(total)$, quartz and muscovite in excess. Location of equilibrium shown in OEA is compatible with the average P-T estimations given by DOM and CEN

Fig. D. 23. (B). Diagramme P-T montrant les estimations P-T établies avec THERMOCALC sur les échantillons DOM et CEN avec, en plus, la réaction du système Ca-KFMASH observée dans l'échantillon OEA considérant $P(H_2O)=P(total)$, ainsi que le quartz et la muscovite en excès. Le calcul de l'équilibre observé dans l'échantillon OEA est compatible avec les estimations P-T données par DOM et CEN.

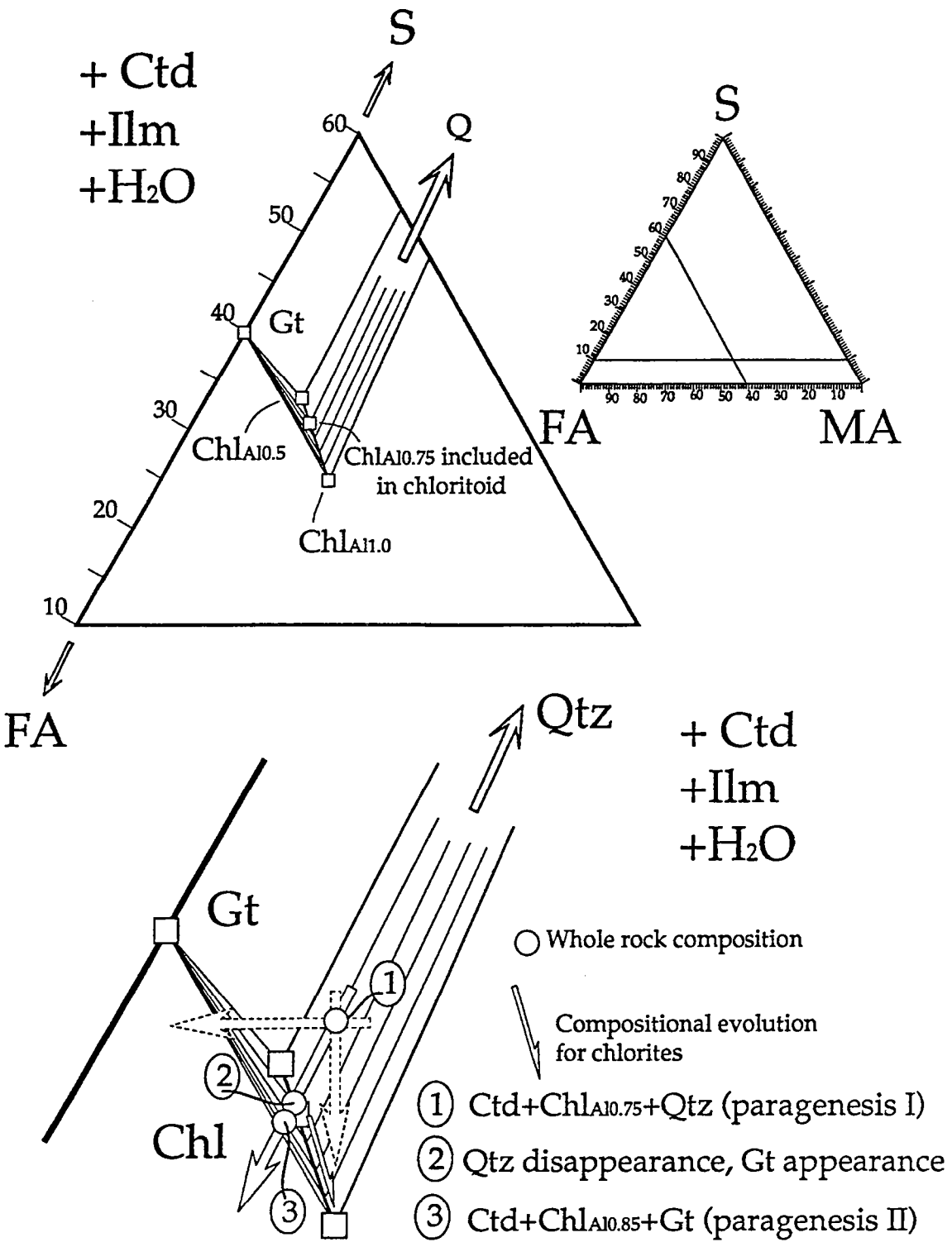

Fig. D. 24. Compatibility diagram for the chloritoid-garnet-chlorite (HOL) rocks assemblage ; phases are projected from ilmenite and chloritoid onto the Si - $Fe_{0.66}$ $Al_{0.33}$ - $Mg_{0.66}$ $Al_{0.33}$ plane assuming H_2O in excess. Arrows represent possible paths for change in equilibrium volume composition.

Fig. D. 24. Diagramme de compatibilité pour l'assemblage chloritoïde-grenat-chlorite (HOL) ; les phases sont projetées à partir de l'ilménite et du chloritoïde sur le plan Si - $Fe_{0.66}$ $Al_{0.33}$ - $Mg_{0.66}$ $Al_{0.33}$ en considérant H_2O en excès. Les flèches représentent les chemins possibles pour le changement de la composition du volume d'équilibre.

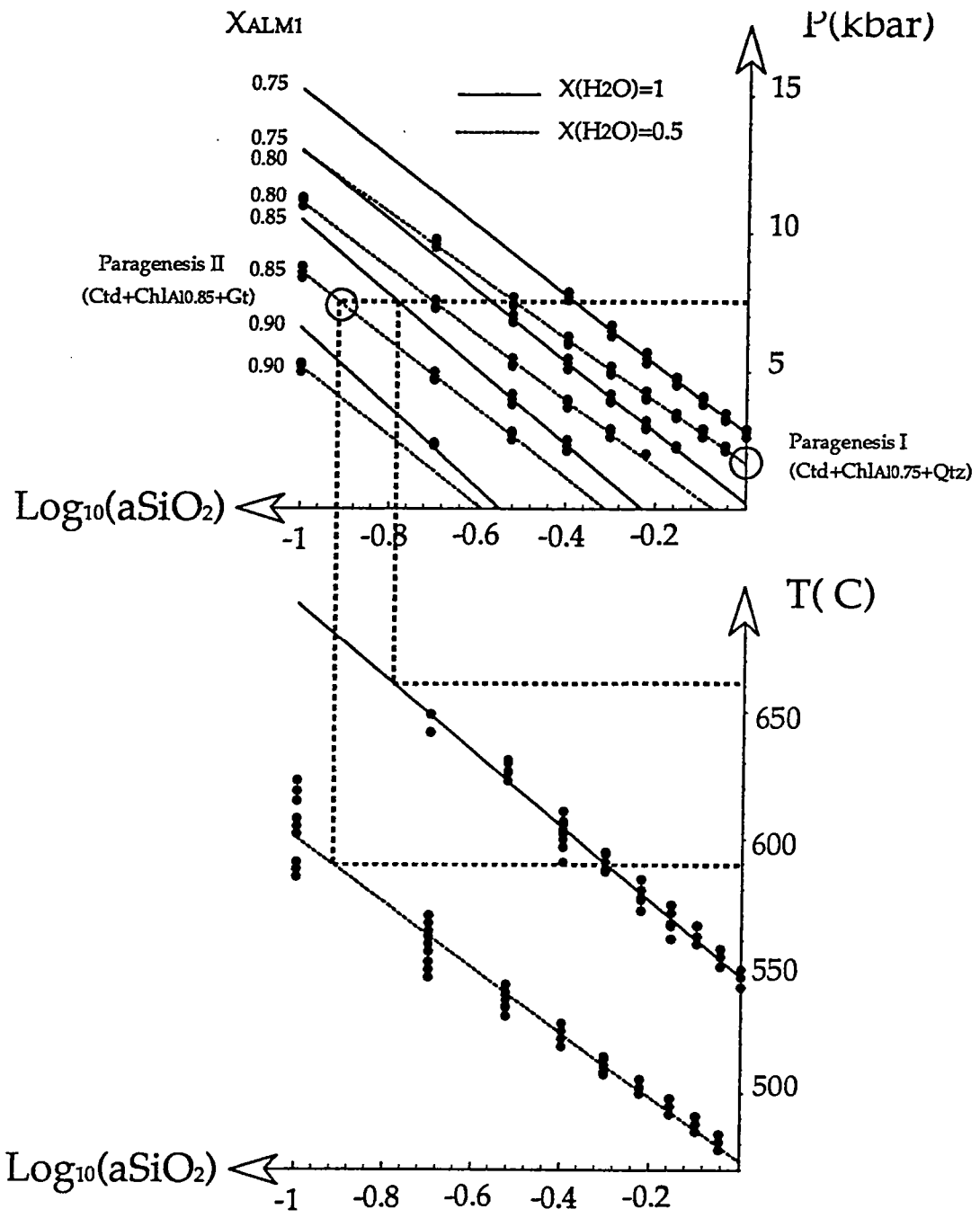

Fig. D. 25. Isopleths calculations of chlorites (X_{AlM1}) for the trivariant assemblage garnet + chloritoid + chlorite with respect to P, T ,log_{aSiO2} and X_{H_2O} in the FMASH system. All calculations (dots) have been obtained using phase diagram calculations of THERMOCALC. X_{AlM1}=0.75 in paragenesis I ($Chl_{Al0.75}$ + Ctd + Qtz) and in the FMASH reaction $Chl_{Al0.75}$ + Ctd + Qtz = Gt ; XAlM1=0.85 in paragenesis II ($Chl_{Al0.85}$ + Ctd + Gt) ;

Fig. D. 25. Calculs des isopleths pour les chlorites (X_{AlM1}) de l'assemblage trivariant grenat + chloritoïde + chlorite en fonction de P, T ,log_{aSiO2} et X_{H_2O} dans le système FMASH. Tous les calculs ont été réalisés avec la procedure "phase diagram calculations" de THERMOCALC. X_{AlM1}=0.75 pour la paragenèse I ($Chl_{Al0.75}$ + Ctd + Qtz) et pour la réaction $Chl_{Al0.75}$ + Ctd + Qtz = Gt du système FMASH ; XAlM1=0.85 pour la paragenèse II ($Chl_{Al0.85}$ + Ctd + Gt) ;

DISCUSSION

The difference between the estimated temperature in paragenesis II for HOL and the three other samples is significant at X_{H_2O}=1. However, Fe-Mg exchange between garnet and chlorite (Ghent *et al.*, 1987 ; Grambling, 1990) gives T in the range 530-600°C at P=7.5 kbar for the HOL sample. All the estimations can be made consistent if X_{H_2O} is taken into account. If we consider the isopleths calculated at X_{H_2O}=0.5 (Fig. D. 25), at P=7.5 kbar, $\log a_{SiO_2}$=-0.9-1.1 corresponding to T around 600°C, a value consistent with the estimation for DOM, CEN and OEA. In consequence, we have investigated the effect of X_{H_2O} on the P-T estimation for DOM and CEN and compared them to the estimation for HOL (Fig. D. 26). Common area for T-X_{H_2O} conditions of DOM and CEN has been obtained using average T estimations of THERMOCALC at different X_{H_2O} whereas common area for T-X_{H_2O} conditions of HOL has been built for X_{AlM1}=0.85 using Fig. D. 25. Pressure has been fixed in the range of 7-8kbar. The common area to all the samples for P-T-X_{H_2O} conditions is located at T about 500°C and X_{H_2O} about 0.1. However, classical geothermometry based on Fe-Mg exchange between garnet and biotite (Ferry & Spear, 1978 ; Hodges & Spear, 1982 ; Perchuk & Lavrent'eva, 1983 ; Williams & Grambling, 1991) give T in the range 500 to 580°C at P=7.5kbar, and THERMOCALC using average P-T on H_2O absent reactions in DOM leads to the estimation T=603±40°C and P=8.7±1.8kbar. Therefore, the value of X_{H_2O} cannot be lower than 0.5 in DOM and CEN (Fig. D. 26). Consequently, the difference in X_{H_2O} between HOL and the other samples at identical P-T conditions is significant. For example, assuming homogeneous P-T conditions of 7-8kbar and 580-620°C at the final stage of the diapiric evolution within all the supracrustal rocks, the fluid phase composition is X_{H_2O}=0.5 at the triple point (HOL) whereas it is X_{H_2O}=0.9 in the troughs (DOM and CEN).

Isopleths in Fig. D. 25 can also be used to estimate the P-T path followed by the HOL sample : the chlorite in equilibrium with quartz indicates that the conditions of stability for paragenesis I (ChlAl0.75 + Ctd + Qtz) were P at about 2-3kbar and T at about 470-550°C. Also, it should be noted that all the phases in this sample are close to the Fe end-members and therefore that garnet formed by the FASH reaction *Chl + Qtz + Ctd = Gt* which lies at around 520°C (Fig. D. 22). Therefore, primary conditions corresponding to paragenesis I should lie at a lower temperature than the temperature of this reaction. An estimation of T at about 470°C and X_{H_2O}=0.5 for the

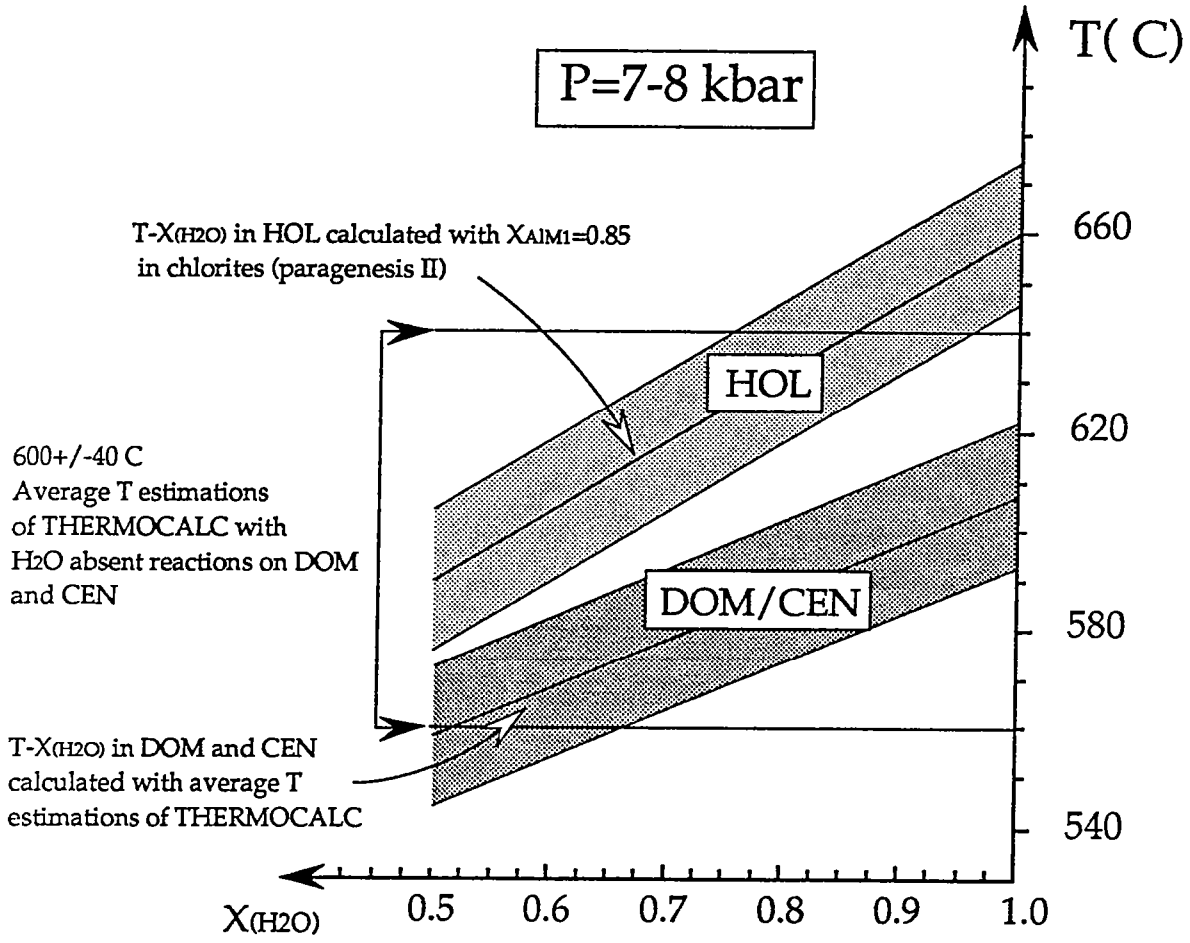

Fig. D. 26. Diagram showing the difference in X_{H_2O} at 7.5 kbar between samples in triple point (HOL) and the other samples in the troughs (DOM and CEN). Average P-T estimations with H_2O absent reactions gives 603±40°C and P=8.7±1.8kbar on DOM and CEN. T-X_{H_2O} for HOL has been obtained from Fig. 9 with X_{AlM1}=0.85 and P=7.5kbar. T-X_{H_2O} for DOM and CEN has been obtained using average P-T of THERMOCALC at different X_{H_2O}.

Fig. D. 26. Diagramme montrant la différence de X_{H_2O} à 7.5 kbar entre l'échantillon du point triple (HOL) et ceux des branches linéaires (DOM et CEN). Les estimations P-T calculées par la procédure "average P-T" sur les réactions sans H_2O donnent 603±40°C et P=8.7±1.8 kbar sur les échantillons DOM et CEN. T-X_{H_2O} pour l'échantillon HOL a été obtenu d'après la Fig. 9 avec X_{AlM1}=0.85 et P=7.5kbar. T-X_{H_2O} pour les échantillons DOM et CEN a été obtenu en utilisant la procédure "average P-T" de THERMOCALC pour differentes valeurs de X_{H_2O}.

paragenesis I in HOL on the basis of Al isopleth is thus consistent with this result.

The HOL sample presents another feature : as chloritoid and ilmenite have the same compositions in parageneses I and II, the compatibility diagram in Fig. D. 24 is valid for both parageneses and implies that the composition of the equilibrium volume changes with the P-T evolution. The way the composition changes can be discussed : it could be a change in X_{Fe} at almost constant Al/Fe+Mg ratio (horizontal dotted arrow) or a change in Al/Fe+Mg ratio at almost constant X_{Fe} (vertical dotted arrow), or a mix of the two paths (solid arrow). However, the path followed by the equilibrium composition should be consistent with two features : firstly, chlorites in matrix should always be more Al-rich than those included in chloritoid and secondly, chlorites included in chloritoid should have an almost homogeneous and nearly constant composition. For example, a change across X_{Fe} (horizontal dotted arrow) would imply that the whole range of chlorites (low and high Al) would be present within the garnet and the matrix. Following this hypothesis, the composition of chlorites included in chloritoid and in equilibrium with quartz should evolve toward more Si-rich compositions before garnet appears. This feature is not consistent with the observations. On the opposite, Si content in the rock decreasing with the P-T evolution (solid arrow) is more consistent with the observations. Predicted compositional evolution for chlorites in that case matches the measured compositions. This decreasing in Si content could be explained by higher solubility of Si over Al in a metamorphic fluid phase streaming through the rocks.

Relations between fluid circulation and fabrics in supracrustals.

Fabrics have been mapped in detail in the Holenarsipur area (Bouhallier et al., 1993). These maps show that foliation triple points are specific areas where the fabrics are intense, linear and vertical (Fig. D. 18a and Fig. D. 18b). On the opposite, fabrics in the linear troughs are less developed, planar or planar-linear with various orientation of the mineral lineation from down-dip to nearly horizontal. The fluid composition in foliation triple points is apparently controlled by external buffering with X_{H_2O}=0.5. Moreover, the difference in X_{H_2O} between metamorphic fluid phase in the foliation triple point and the other samples of the linear troughs at identical P-T conditions is significant, X_{H_2O} being systematically higher in the linear troughs than in the foliation triple point. A explanation for the compositional heterogeneity of fluids and Si metasomatism in

supracrustals could be a difference in rock permeability related to the nature and the orientation of the fabrics : the vertical structures characteristics of these triple points would constitute preferential zones for fluid transfer and metasomatic processes through the Archaean crust. This feature is corroborated by the occurrence of numerous tourmaline-bearing veins intensely developed and strictly localized at foliation triple points.

Relations between P-T evolution and structural evolution in supracrustals.

The gravitational collapse of supracrustal rocks in the Holenarsipur area has been documented in the light of structural observations (Bouhallier et al., 1993). Nevertheless, the amount of supracrustals subsiding with respect to the surrounding sialic rocks is unknown. At the triple points, the recording of a prograde evolution from 3 to 7-8 kbar shows that diffusion rates were not sufficient to erase the primary compositions of the metamorphic phases during burial. On the contrary, the homogeneity of the mineral compositions in the parageneses of metamorphic rocks within the linear troughs shows that diffusion at the final stage of the structural evolution of the linear troughs has been almost sufficient to erase primary compositions. A possible explanation, consistent with diapiric experimental models (Dixon, 1975 ; Dixon & Summers, 1983) is that the burial of supracrustal rocks within foliation triple points was much faster than in the linear troughs. This feature fits in with the idea that the studied foliation triple point of supracrustals in the Holenarsipur area corresponds to a overturned diapiric stem connected with linear subsiding troughs (Bouhallier et al., in prep).

2. 3. Evolution structurale 3D des parties moyenne et inférieure de la croûte continentale archéenne du craton de Dharwar (Karnataka, Inde du Sud)

Dans cette troisième partie, nous utilisons la caractéristique majeure du craton de Dharwar qui est de mettre à l'affleurement, du Nord vers le Sud, des niveaux structuraux de plus en plus profonds. A l'instar de ce qui à été fait dans la région d'Holenarsipur (amphibolite faciès) nous présentons ici les champs de déformation du secteur de Gundlupet. Ceci nous permet de reconnaître et caractériser les grandes structures crustales de ce domaine métamorphique (Hb-granulite faciès) que nous comparons avec celles du secteur d'Holenarsipur.

STRAIN PATTERNS IN ARCHAEAN DOME-AND-BASIN STRUCTURES : THE DHARWAR CRATON (KARNATAKA, SOUTH INDIA)

H. BOUHALLIER and P. CHOUKROUNE

Laboratoire de Tectonique
Géosciences Rennes (UPR 4661-CNRS)
Université de Rennes I
35042 Rennes Cedex

ABSTRACT - Models simulating the role of gravity in the earth's crust are the main source of criteria for field identification of diapirs. After a short review of the distribution of finite strains in experimental diapir models, we describe an example where differential erosion of a tilted craton provides 3D geometrical information of patterns in a diapiric system (as Raleigh-Taylor instabilities) at various depth within the Archaean continental crust (Dharwar craton, South India). This natural example is consistent with all field identification criteria expected from experimental models ; but also some peculiar structural features which are not predicted by the models are also observed. These features, such as triple junctions of strain trajectories, result from i) the progressive deformation of diapiric domes or sagducted basins, ii) interferences between diapiric structures (body forces) and iii) superimposition of diapiric strain field on a regional horizontal shortening (boundary forces).

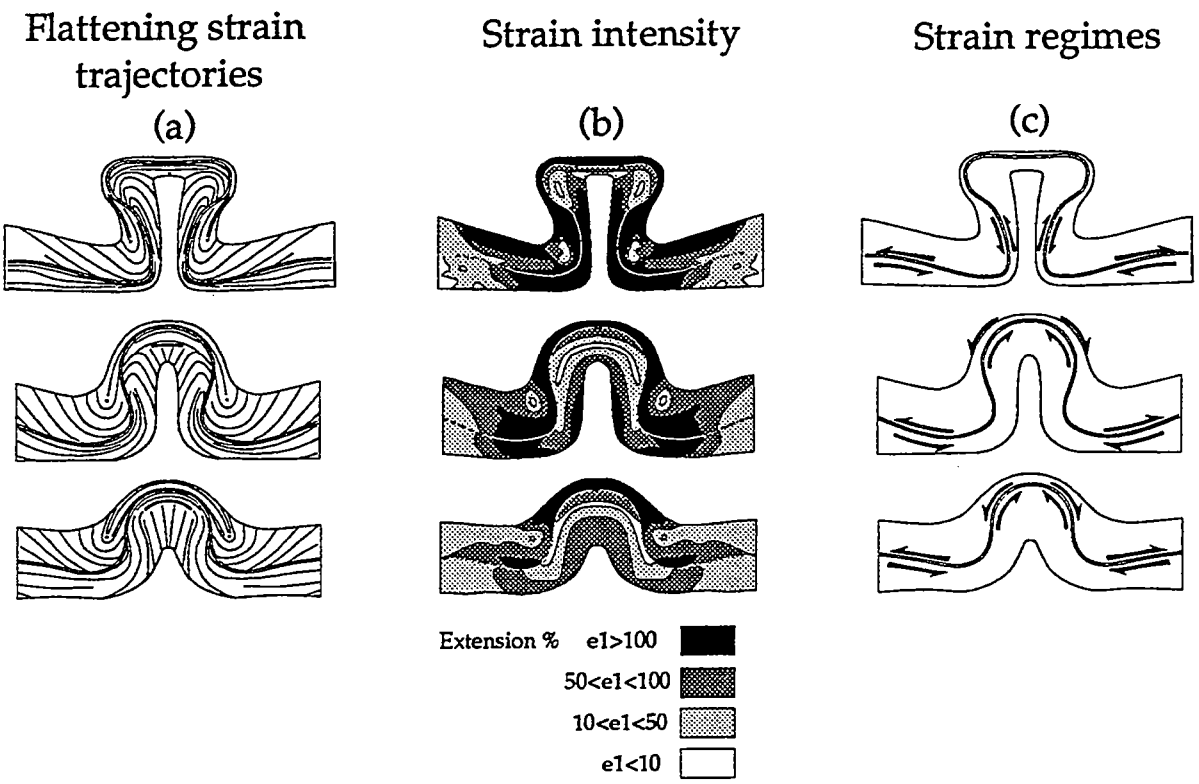

Fig. D. 27. Strain characteristics at three succesive stages showing the evolution of cylindric diapiric dome (ridge), from Dixon, (1975) : (a) flattening plane, (b) strain intensity, with *e1* as finite principal extension, (c) strain regimes.

INTRODUCTION

Field indicators of diapirism have been the subject of debates (e. g. Stephasson, 1977 ; Schwerdtner et al.,1978, Platt,1980, Coward, 1981,Brun et al,1990). Experimental modellings of diapirism (Ramberg, 1967, Fletcher, 1972, Dixon, 1975, Woidt, 1978, Dixon & Summers, 1983, Talbot *et al.*, 1991) can be divided into two sets. The first set was devoted to the relationships between mechanical properties of material used and shapes and periodicity of diapiric bodies at different stages of their evolution. The second set was designed to define the strain field into and around diapiric bodies.

These experiments were justified by the fact that low density occur frequently layers in the earth crust and by the observation of this material now cropping out in circular or elliptical structures intruding material of higher density. Well known examples are granites, migmatitic gneiss domes, salt domes (Jackson & Talbot, 1989), etc...

All structural levels of the Earth crust was supposed to be able to undergone a diapiric evolution. At depth, opposite relationships between low density material (partially or totally melted) and more dense surroundings are expected (Talbot et al., 1991). In the upper parts, salt domes represent the results of similar processes.

The results of the analogical approach were fundamental to define what are the relevant structural features which can be expected in field and they introduced some basic criteria of diapiric motion ; nevertheless the use of experimental results for interpretation of natural examples is generally difficult essentially because experiments provided 2D results, and because conditions imposed by experiments made difficult to introduce effects such as ballooning (volume change), interference between diapiric structures and interference between diapirism and tectonics. Furthermore, kinematic indicators can provide local information about the deformation history in normal rocks situation whereas models provides information about the total strain only.

In this paper we first summarize the main results provided by experiments published in the literature, then we describe natural strains associated with diapiric structures in the Dharwar craton where structures of various scale can be observed from upper- to lower-structural levels. Indeed, this area displays a continuous cross-section of the Archaean crust from greenschist facies to the North to granulite facies to the South (Rama Rao, 1936 ; Pichamuthu, 1962) with a combined increase of pressures from 3 kbar to the North to 7-8 kbar to the South. Two areas showing dome-and-basin structures have ben studied in detail, one in the amphibolite facies (Holenarsipur area), and the other in the hornblende-granulite facies (Gundlupet area).

We shall first recall the main results obtained with experimental models. Then, we shall examine how peculiar structural features or strain field characteristics observed in the natural example, fit (or not) with the model's predictions. We shall lastly propose an explanation to their presence and examine their compatibility in term of Raleigh-Taylor instabilities evolution : we want to argue that the observed differences with model's predictions are the result of interferences between diapiric domes (body forces), superimposition of domes and regional shortening (surface forces), or can be explained by the proper evolution of doming (progressive deformation).

PRESENT KNOWLEDGE OF DIAPIRIC STRAIN FIELD FROM ANALOG MODELLING

Geometry of diapiric structures

Many experiments have been done to define the shape of domes during the evolution of gravitational instabilities (initiation, amplification, locking and their periodicity according to parameters such as density,viscosity and relative thickness ratios of the buoyant and overburden layers (Ramberg, 1967 ; Talbot, 1974 ,1977 ; Woidt, 1978)

Analogue models which lead to quantify strain throughout diapiric structures are very scarce (Dixon, 1975, Dixon & Summers, 1983). Main informations provided by these models are as follows (Fig. D. 27).

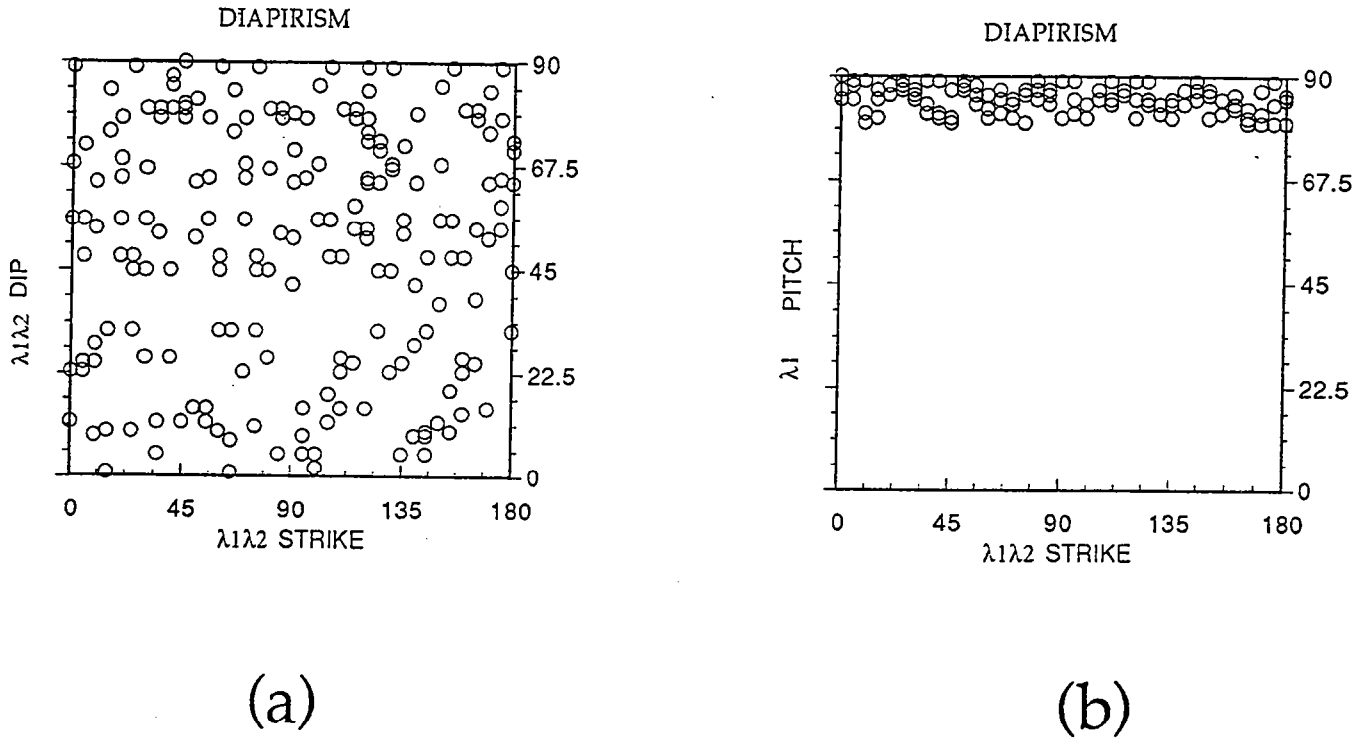

Fig. D. 28. (a) λ1λ2 dip vs. λ1λ2 strike and (b) λ1 pitch vs. λ1λ2 strike expected in the case of diapirism.

Strain trajectories (Fig. D. 27a)

The first information given by experiments is that flattening strain trajectories trend parallel with, or at low angle to the overburden-intrusion interface.

In the buoyant layer, first stages of diapirism are marked by flattening trajectories which are vertical in the inner part of the dome and horizontal at the top. Within more mature diapiric structures, strain trajectories display two antiformal structures which are diverging from the core of the dome. Between them, a nearly horizontal isotropic line (Brun, 1983) appears at the top of the dome. During the evolution of the diapir, this isotropic line migrates downward with a progressive reduction in length.

In the overburden, flattening planes are deformed in double synformal structures on both sides of the dome. At more evolved stages, these synforms are amplified and their axial planes, which run parallel to the dome boundary, become vertical and subsequently overturned. A zone of low strain bounded by a triangular pattern of flattening strain trajectories appears in the inner part of the synformal structures (Brun, 1983). This peculiar zone (also named isotropic point) is almost motionless throughout the deformation.

Strain intensity (Fig. D. 27b)

In the buoyant layer the highest strained zone is first located into the core of the dome and is affected by a vertical stretching. During the amplification of the structure, this vertical-stretching zone moves upwards and the highest strain marked by strong horizontal stretching, occur at the top of the dome The limit between the upper zone of horizontal stretching and the lower zone of vertical extension is an area of lower strain. In the most evolved diapirs, this region of low strain becomes smaller, and finally vanishes.

In the overburden the highest strains (horizontal stretching) are first located above the dome and extend progressively along the limbs to reach an other area of high strain developing near the roots of the dome. Zones of low strain are very restricted on both sides of the trunk.

In summary, models indicate that areas where highest strains occur, is mainly determined by the geometry of the overburden-source interface all along the diapiric evolution.

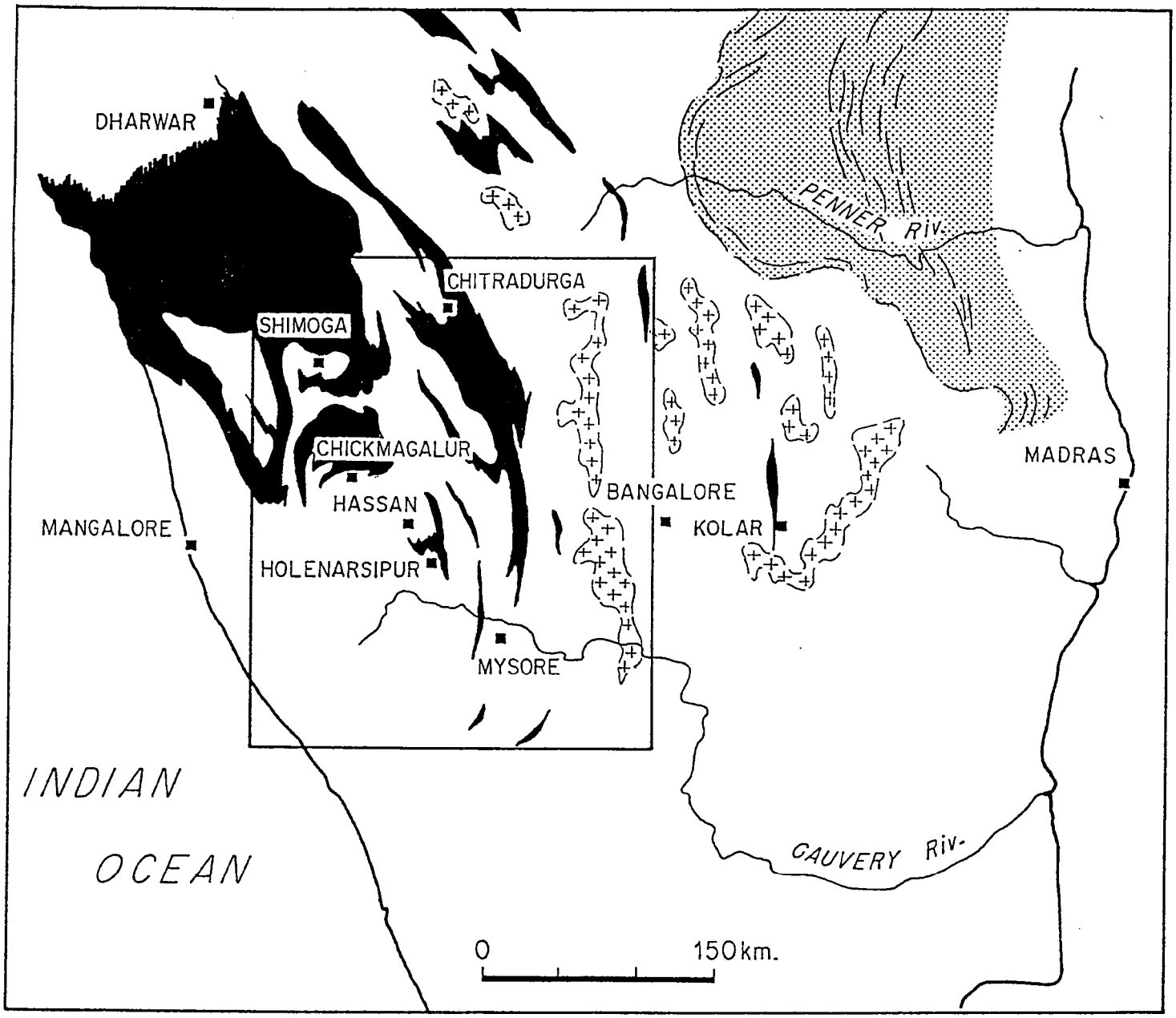

Fig. D. 29. Geological map of the Archaean Dharwar craton (South India). Archaean rocks are : greenstones in black, Closepet granite with crosses, and Peninsular gneisses in white. Proterozoic rocks are dotted.

Strain regimes (Fig. D. 27c)

In both buoyant layer and overburden buoyant layer, coaxial strain is expected at the top of the evolving dome, whereas its limbs undergo shearing deformation. The shear strain is maximum at the interface and increases during the amplification.

Fabrics and progressive deformation

Strain patterns observed in 2D experimental models of diapiric structures (Dixon, 1975) have been extrapolated to propose a 3D distribution of fabrics within radially symmetric domes. Thus, assuming uniaxial symmetry, one can expects a radial extension at the top of the dome. Consequently, rocks must exhibit a planar fabric, and a radial distribution of the principal stretching direction $\lambda 1$ in areas of flat foliation (Schwerdner et al.1978).

At a given stage of diapir evolution, domains with differing direction of stretching occur. For example, a domain of vertical stretching occurs into the roots of the buoyant layer, whereas horizontal stretching affects its top (Fig. 27). It is interesting to consider the geometric evolution of an area situated near the boundary between these two distinct domains ; because of the downwards motion of this boundary during the maturation of the diapir, one area initially stretched vertically will progressively move in a zone affected by horizontal stretching. One can expect that rocks deformed in this way would recorded this evolution and exhibit overprinted fabrics. Indeed, the first vertical flattening planes must be progressively folded and affected by a superimposed horizontal foliation leading to a constrictive bulk strain and a linear horizontal fabric.

Most authors emphasize that the vertical stretching in the core of the buoyant layer can represent a vertical planar fabric under conditions of plane flow or a vertical linear fabric under conditions of radial flow. Regions in the lower parts and on each side of the central axis of the dome are expected to exhibit a planar fabric. Areas along the interface between source and overburden are affected by a non coaxial deformation : L-S fabrics parallel to the interface, with vertical maximum stretching direction, are there expected.

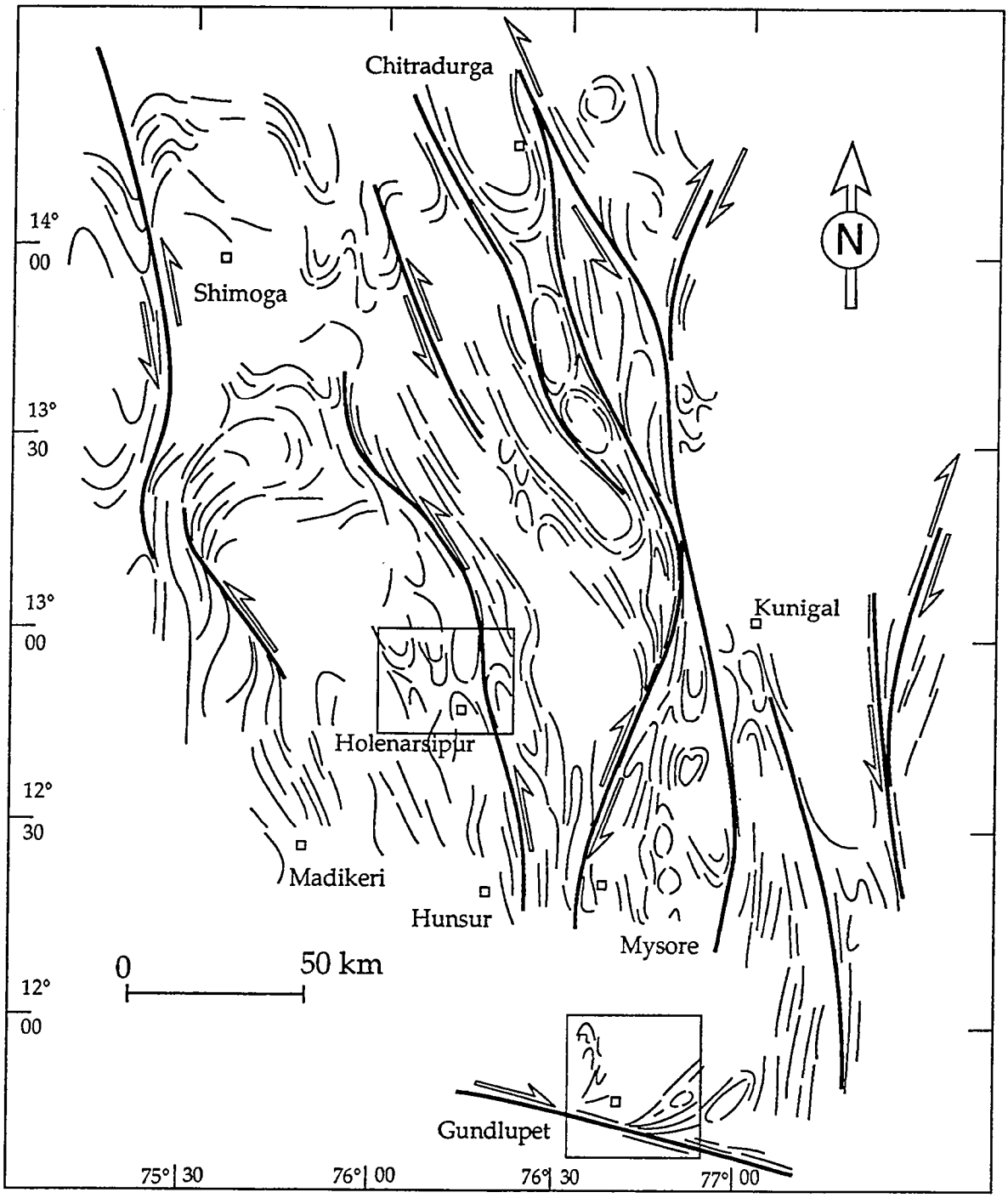

Fig. D. 30. Structural map of the western part of the Archaean Dharwar craton (South India).

Another remarkable example of superimposed fabrics due to progressive deformation of the sagducted overburden is shown by Dixon & Summers (1983). An early horizontal planar fabric is expressed in the overburden above the buoyant layer and is affected by horizontal shortening as the elements migrate into the most subsiding regions. Natural rocks deformed in this way should display overprinted fabrics with the two flattening planes defined by two perpendicular foliations. The first one which is horizontal should be crenulated or folded by the second one which is vertical. Again total strains are there expected to be of constriction type with horizontal $\lambda 1$.

A part of above inferences deduced from experiments can be summarized on diagrams showing pitches of $\lambda 1$ are presented versus the strike of $\lambda 1\lambda 2$ plane, or dip of $\lambda 1\lambda 2$ planes versus strike of $\lambda 1\lambda 2$ planes : first, dome geometry implies that all strikes and dip of $\lambda 1\lambda 2$ are possible (Fig. D. 28a) ; second, irrespective of the attitude of the $\lambda 1\lambda 2$ planes, the pitches of $\lambda 1$ direction must be equal to 90° (Fig. D. 28b) : this characteristic is probably one of the most important consequences of diapiric processes explored by experimental way.

STRAIN PATTERN IN THE ARCHAEAN CRUST OF DHARWAR CRATON, (SOUTH INDIA)

Geological setting

In the Dharwar craton (Swami Nath & Ramakrishnan, 1981 ; Naqvi & Rodgers, 1983 ; Radhakrishna & Ramakrishnan, 1990) the two classical Archaean lithologies are exposed : the tabular, linear and curved low- to high-grade volcano-sedimentary series ("greenstone", "supracrustals" or "schist" belts) are surrounded by larger regions of high-grade infracrustal rocks and associated low-K tonalitic, trondhjemitic and granodioritic rocks (TTG series) which ages vary between 3.35 Ga and 2.5 Ga (Crawford, 1969 ; Venkatasubramanian, 1975 ; Beckinsale et al,. 1980, 1982 ; Monrad, 1983 ; Stroh *et al.*, 1983 ; Taylor *et al.*, 1984 ; Drury *et al.*, 1986 ; Taylor *et al.*, 1988 ; Peucat *et al.*, 1989 ; Meen *et al.*, 1992 ; Peucat *et al.*, 1993) (Fig. D. 29).

At the scale of the craton , Landsat satellite images reveal a strong north-south trending fabric which partly results from a late Archaean transcurrent ductile shearing episode (Drury & Holt, 1980 ; Chadwick et al., 1989) (Fig. D. 30). This episode is considered to be contemporaneous with

the emplacement of the large Closepet batolith (Jayananda & Mahabaleswar, 1991) dated at 2.5 Ga (Crawford, 1969 ; Friend & Nutman, 1991 ; Jayananda *et al.*, 1994). Areas located between these discrete linear shear zones (such as Holenarsipur and Gundlupet areas) are convenient targets to investigate the tectonic style of the Archaean crust prior to shearing.

The main characteristic of the Dharwar craton is the transition from a low- to medium-grade granite-greenstone terrain to the North, to a high-grade granulitic terrain to the South. From North to South, paleopressures in gneissic and mafic rocks increase from about 3 kbar in the North and central Karnataka to 8-9 kbar in the Sargur area (Harris & Jayaram, 1981 ; Janardhan *et al.*, 1982 ; Raith *et al.*, 1982 ; Hansen *et al.*, 1984 ; Raase *et al.*, 1986). According to Pichamuthu, (1962), Raith *et al.*, (1982), (1983), Raase *et al.*, (1986), the Archaean craton, North of the Moyar shear zone, is affected by one metamorphic event dated around 2.5 Ga (Grew & Manton, 1984 ; Peucat *et al.*, 1989, 1993). These authors have attributed this feature as due to a postmetamorphic tilting of the overall craton. The southernmost part of the Closepet batolith represents the deepest structural level in this heterogeneous granitic complex ; It is affected by a granulite facies overprint (Janardhan *et al.*, 1979 ; Friend, 1981 ; Hansen *et al.*, 1987 ; Stähle *et al.*, 1987).

Geological background of the Holenarsipur and the Gundlupet areas

Holenarsipur area (see location on Fig. D. 30), in the central medium-grade terrain of the Dharwar craton (Raith *et al.*, 1982), displays one of the oldest "greenstone belts" of the craton (Hussain & Naqvi, 1983, Peucat *et al.*, in prep.). The surrounding gneisses, which yielded Rb-Sr and Pb-Pb ages between 3.35 Ga (Beckinsale *et al.*, 1980, 1982) and 3.305 Ga (Taylor *et al.*, 1988), are intruded by 3.1-3.0 Ga trondhjemitic plutons (Beckinsale *et al.*, 1982 ; Bhaskar Rao *et al.*, 1983 ; Monrad, 1983 ; Stroh *et al.*, 1983 ; Taylor *et al.*, 1984 ; Meen *et al.* 1992). The trondhjemites also intrude supracrustal rocks (Chadwick *et al.*, 1978, Bouhallier *et al.*, 1993). Recent geochronological data obtained on supracrustal rhyolites yielded an age of 3.3 Ga (Peucat *et al.*, in prep).

Recently, Bouhallier *et al.* (1993) have proposed that the observed structural strain field in the Holenarsipur area was consistent with a diapiric event locally overprinted by transcurrent shear zones. In the supracrustal units, only one progressive tectonometamorphic event has been preserved. This event is probably related to the emplacement of the Closepet batholith at 2.5 Ga.

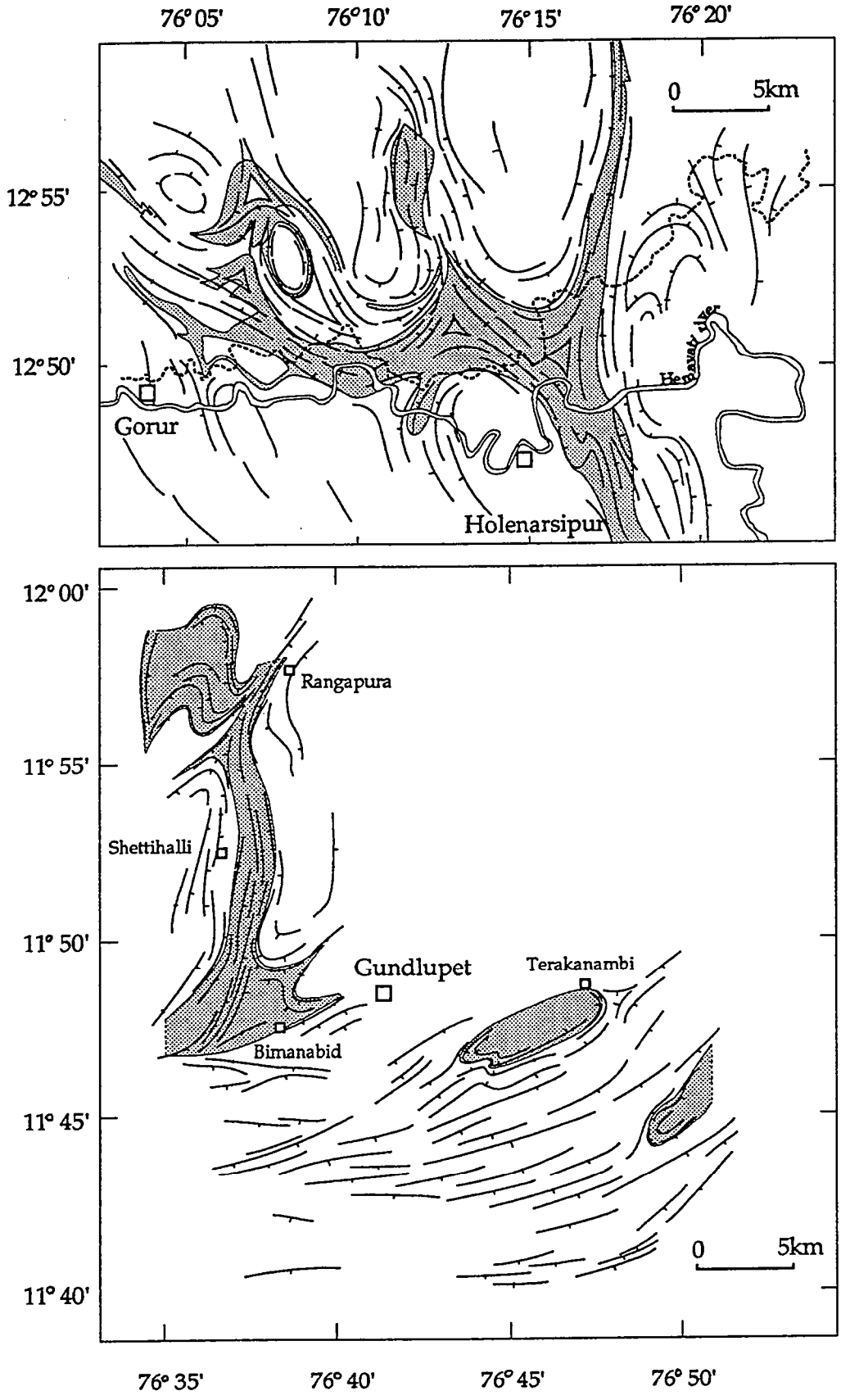

Fig. D. 31. Map of foliation trajectories in the Holenarsipur and Gundlupet areas (Karnataka).

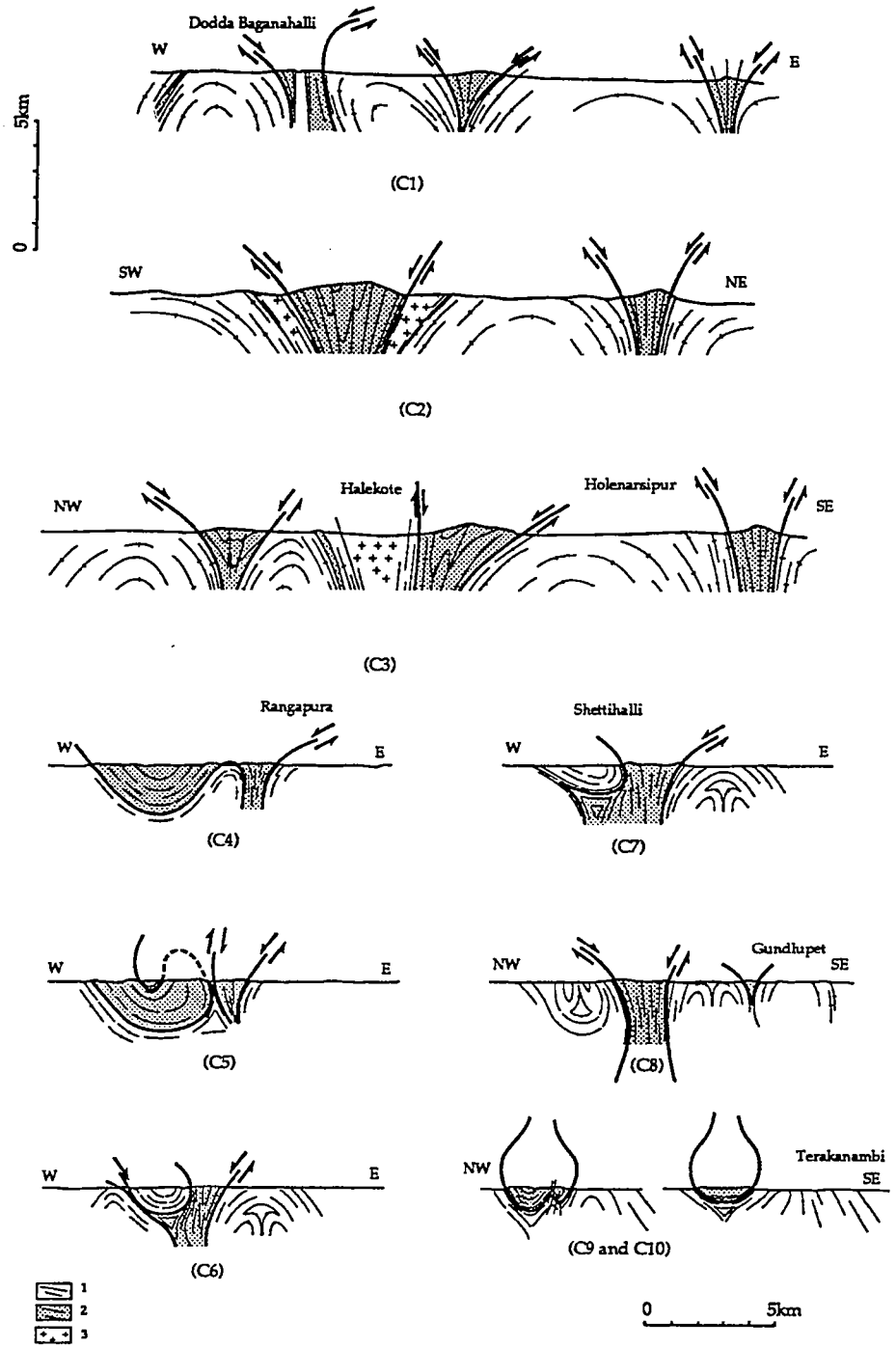

Fig. D. 32. Cross-sections in the Holenarsipur and Gundlupet areas (localization on Fig. D 36). 1 : TTG (Peninsular Gneisses) ; 2 : greenstone belt ; 3 : syntectonic intrusions of Halekote type.

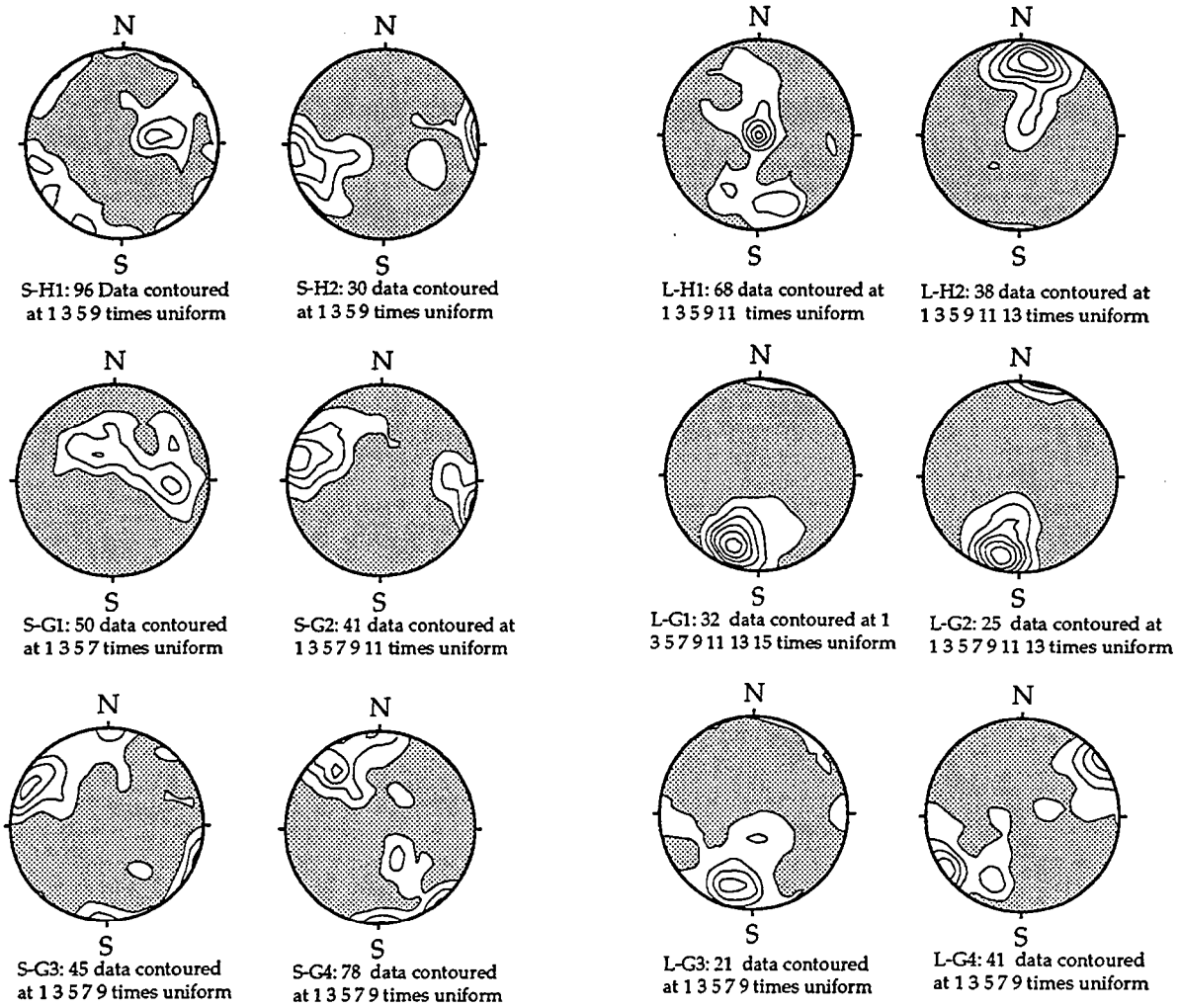

Fig. D. 33. Stereograms with projection onto the lower hemisphere. **S-H1** : poles to foliations around domes ; **S-H2** : poles to foliations in the easternmost branch of the greenstone belt ; **S-G1** : poles to foliation West of Rangapura ; **S-G2** : poles to foliation South of Rangapura ; **S-G3** : poles to foliation West of Gundlupet ; **S-G4** : poles to foliation South of Terakanambi ; **L-H1** : stretching lineations around domes ; **L-H2** : stretching lineations in the easternmost branch of the greenstone belt ; **L-G1** : stretching lineations West of Rangapura ; **L-G2** : stretching lineations South of Rangapura ; **L-G3** : stretching lineations West of Gundlupet ; **L-G4** : stretching lineations South of Terakanambi.

In the Gundlupet area, (Swami Nath & Ramakrishnan, 1981) (see location on Fig. D. 30) greenstones and TTG sequences, display metamorphic parageneses which are indicative of upper amphibolite to transitional hornblende-granulite grade metamorphism (Janardhan *et al.*, 1979). There, structures are comparable with those recognized in the neighbouring area of Sargur (Chadwick *et al.*, 1978 ; Viswanatha and Ramakrishnan, 1975). Regional dome-and-basin patterns (Janardhan *et al.*, 1979) are deformed by a major dextral transcurrent shear zone (Drury & Holt, 1980). This shear zone separates the Sargur area to the North from the Khondalite-Charnokites terrains to the South. P-T estimations of surrounding gneissic and mafic areas North of the shear zone and Est of the Gundlupet area, have been estimated at about 700-750 °C / 8 kbar (Janardhan *et al.*, 1982 ; Raith *et al.*, 1983 ; Hansen *et al.*, 1984 ; Raase *et al.*, 1986). As in the Holenarsipur area, the main metamorphic and deformation events seem to be related to the 2.5 Ga event (Gruau et al. in prep.).

Foliation trajectories

Maps of $\lambda 1\lambda 2$ trajectories in the Dharwar craton reveal extensive dome-and-basin structures (Fig. D. 31, 32, 33). The $\lambda 1\lambda 2$ trajectories of the two studied areas reveal that supracrustal rocks (cover) coincide with $\lambda 1\lambda 2$ synforms and infracrustal rocks (gneissic basement) with elliptical $\lambda 1\lambda 2$ antiforms. In the hornblende-granulite zone of Gundlupet, the $\lambda 1\lambda 2$ trajectories in the infracrustal gneissic basement, locally define a elliptical synform shape (e.g. north of Shettihalli).

Some important structural features appear constant for both areas. $\lambda 1\lambda 2$ trajectories are parallel to the contact between supra- and infracrustal rocks and are always associated with an increase of strain toward the contact. In both areas, strike and dip of $\lambda 1\lambda 2$ are strongly variable. In the Holenarsipur area, contacts between supracrustal and infracrustal rocks, are generally steeply dipping ; whereas some are flat-lying in the Gundlupet area, especially around the supracrustal basins south and south-east of Terakanambi. There, in the inner parts of the basins, contacts between infra- and supracrustal rocks are sub-horizontal, parallel to $\lambda 1\lambda 2$. Another significant feature observable both in the Holenarsipur and Gundlupet areas is that regions of infracrustal rocks, where $\lambda 1\lambda 2$ is sub-horizontal, are always restricted within the central parts of the elliptical gneissic antiforms.

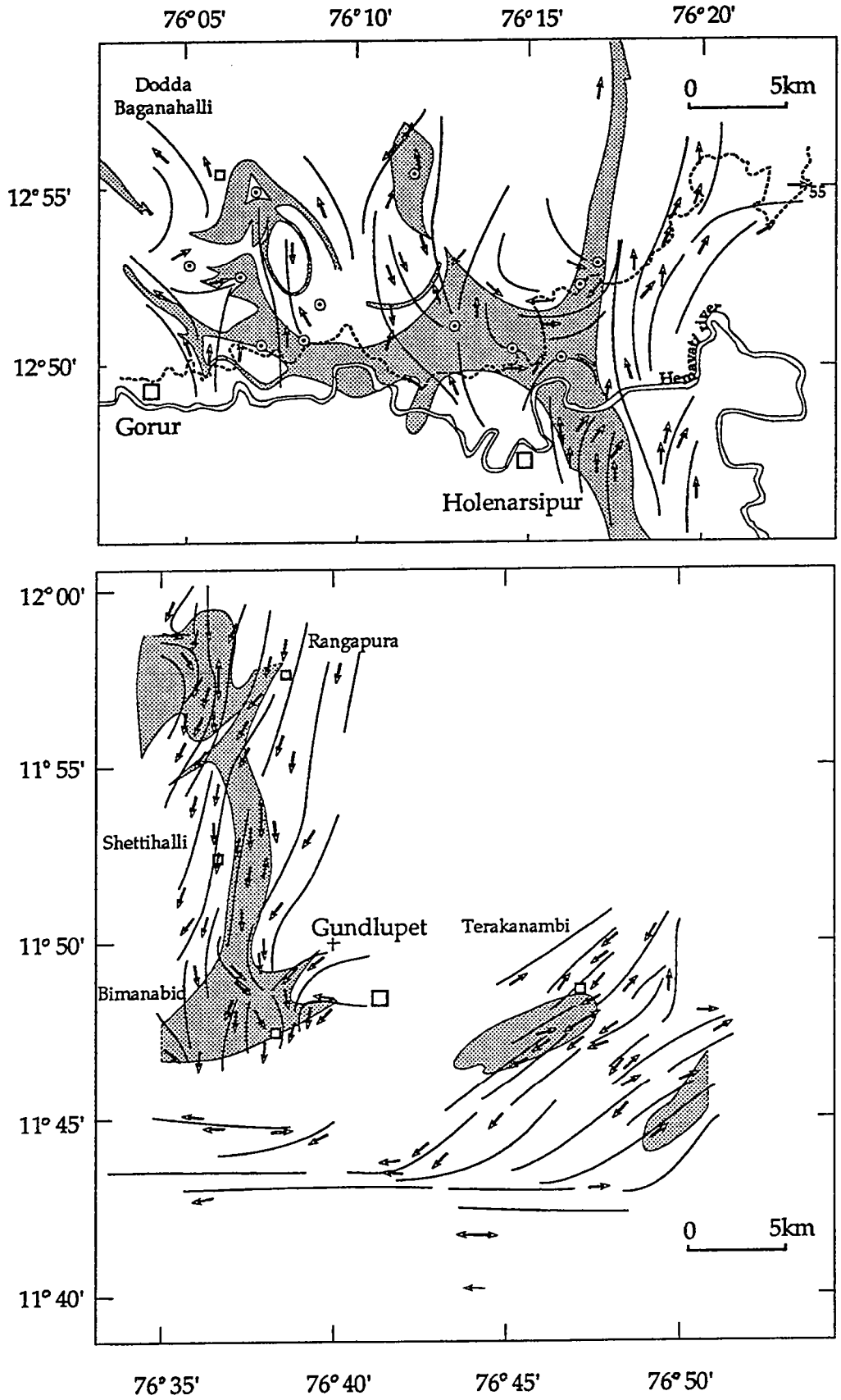

Fig. D. 34. Map of stretching lineation trajectories in the Holenarsipur and Gundlupet areas.

Furthermore, specific dome-in-dome structures which recall those observed in the buoyant layer in experiments can be observed east of the Holenarsipur area (Fig. D. 31) and are suspected in the Gundlupet area.

The most significant differences between the two studied areas are : i) flat lying foliations in supracrustal rocks have been observed within the central parts of elliptical supracrustal basins (south of Terakanambi), whereas they are totally lacking in the Holenarsipur area, and ii) $\lambda 1\lambda 2$ trajectories in infracrustal rocks have define synformal closure of migmatitic gneisses in the Gundlupet area, but not in the Holenarsipur area.

Vertical foliation triple points constitute probably the most interesting features outlined by $\lambda 1\lambda 2$ trajectories. In the Holenarsipur area, they occur between three elliptical domes where triangular arrangements of vertical $\lambda 1\lambda 2$ foliations define characteristic triple junctions. These specific areas are present both in supracrustal (e.g. near Sigaranahalli and Huvinahalli) and infracrustal rocks (e.g. near Byadarahalli). In the triple junctions, fold axes are always subvertical associated with an intense vertical crenulation.

In the Gundlupet area, terminations of elliptical synformal closures display moderately dipping S_1 foliations which also define triple junctions. These are also present in both supracrustal (e.g. north of Shettihalli) and infracrustal rocks (e.g. east of Terakanambi). In triple junctions areas, fold axes are moderately to gently dipping and are associated with an intense horizontal crenulation. In both Holenarsipur and Gunlupet areas the crenulation is localized within triple junctions and is associated with an increase of strain.

Stretching direction (Fig. D. 34)

In both areas studied, $\lambda 1$ trajectories trend parallel to the axial planes of the main regional structures and cut across the supra- infracrustal interface at several places. Nevertheless, significant differences occur in the geometry and distribution of $\lambda 1$ between Holenarsipur and Gundlupet areas. In the Holenarsipur area (Fig. D. 34), plunge and pitch are generally strong in the supracrustal rocks, except at the linear easternmost boundary of the supracrustal belt. Histogram shows the predominance of high pitches of lineation (Fig. D. 35) whereas pitch of $\lambda 1$ versus orientation of

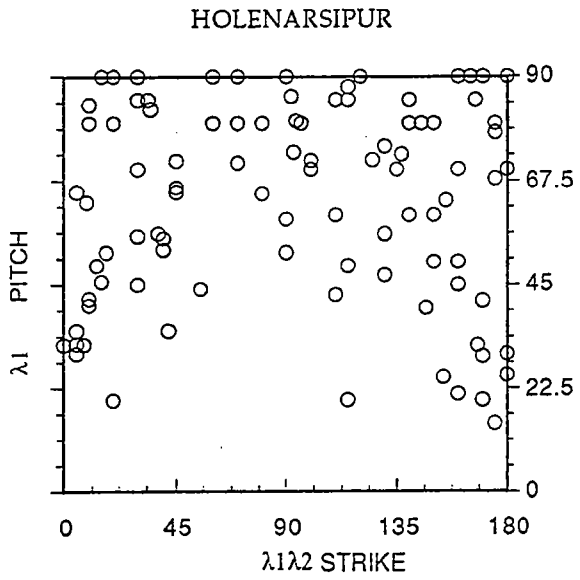

(b)

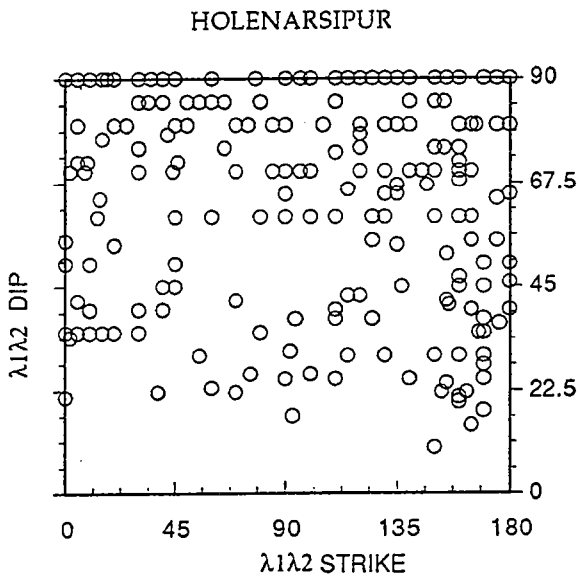

(a)

Fig. D. 35. (a) λ1λ2 dip vs. λ1λ2 strike and (b) λ1 pitch vs. λ1λ2 strike in the case of regional scale structures in Holenarsipur. It appears that the lowest pitches of lineations are confined to NS foliation planes associated with strike-slip motions.

$\lambda 1\lambda 2$ (strike) shows that the pitch are higher for a nearly E-W foliation attitude (Fig. D. 35). In the gneissic basement, $\lambda 1$ is less well marked and is scattered around 170°E. $\lambda 1$ like $\lambda 1\lambda 2$, gradually changes from a gently dipping attitude in the core of the domal structures to a vertical position near the contact between supra- and infracrustal rocks.

In the Gundlupet area (Fig. D. 34), $\lambda 1$ is evenly marked in supra- and infracrustal rocks and is generally moderately plunging (e.g. east of Shettihalli). North of Shettihalli, $\lambda 1$ associated with the gneissic synformal closure is downdip and parallel with the supra- infracrustal interface. Same relationships can be observed South of Terakanambi at the vicinity the synformal closures of the supracrustal basins. In the central part of the basins, $\lambda 1$ is well-marked, horizontal and strikes 60E.

In the Holenarsipur and Gundlupet areas, $\lambda 1$ trajectories are converging towards supracrustal foliation triple points (Fig. D. 34). This is well illustrated around Sigaranahalli and Huvinahalli in the Holenarsipur area, and north of Bimanabid in the Gundlupet area. Within these triple junctions, stretching lineations are very well-developed and vertical. Nevertheless, $\lambda 1$ trajectories in the Gundlupet area are not invariably converging towards foliation triple points. This is especially the case within the triple junction zones where $\lambda 1$ is gently plunging (e.g. in supracrustal rocks north of Shettihalli or in infracrustal rocks south of Terakanambi). In such zones, the stretching lineation is well-developped and parallel to the interface between supra- and infracrustal rocks.

Strain ellipsoid and fabrics (Fig. D. 36)

Fabric maps distinguishing (S) planar fabrics, (S-L) planar-linear fabrics, (L) linear fabrics, and areas in which fabric is absent or poorly developed, have been made. Although these fabric distinctions do not provide a direct measure of strain intensity, they define qualitatively the shape of the finite strain ellipsoid (Flinn, 1965 ; Schwerdtner et al., 1977).

The most significant feature is that maps reveal a strong variability in the distribution of fabric types throughout the studied areas. In the Holenarsipur area the results have been presented by Bouhallier et al., (1993) (Fig. D. 36) :

- Zones of poorly developed fabrics are located within the central parts of the domes

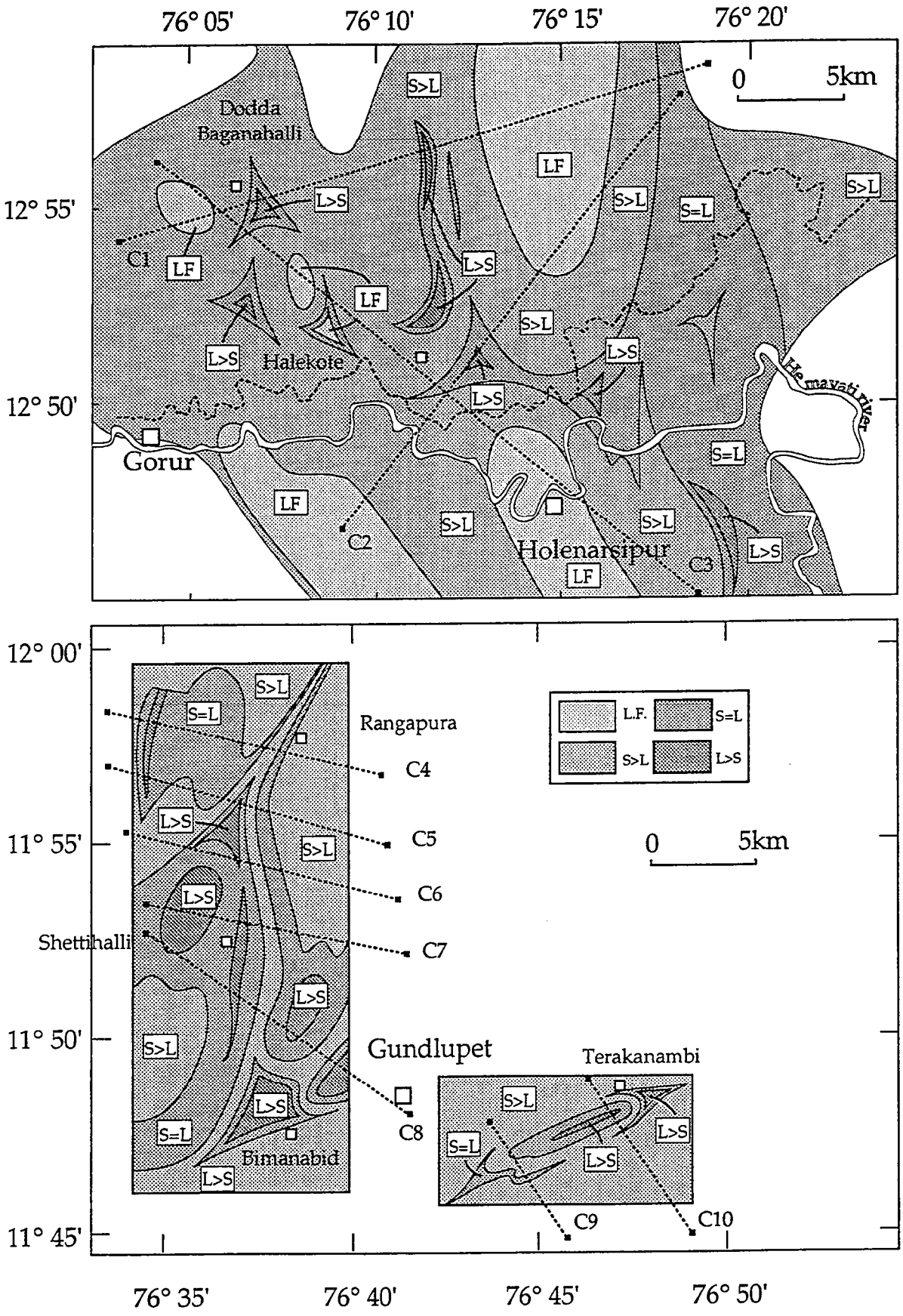

Fig. D. 36. Map of fabrics in the Holenearsipur and Gundlupet areas. **N.F.** : zone with no fabric ; **S>L** : zone where planar fabric is more developed than linear fabric ; **S=L** : zone where both planar and linear fabrics are equally developed ; **L>S** : zone where linear fabric is more developed than planar fabric.

- Planar fabrics occur in dome limbs, where the foliation is vertical and, especially at the interfaces between supra- and infracrustal rocks.

- Planar-linear fabric zones occur around foliation triple junctions (e.g. Dodda Baganahalli, Byadarahalli, Sigaranahalli, Huvinahalli and Mukundur Betta triple junctions), and along the linear zone along the eastern boundary of the Holenarsipur greenstone belt.

- Finally, linear horizontal fabrics are scarce (north of Markuli and east of Tivadahalli) and where they are vertical, they are located in the triple points.

In the Gundlupet area (Fig. D. 36), zones of poorly developed fabric are absent. In contrast, planar fabric zones are largely developed and cover half of the study area. They occur in the inner parts of gneissic domes (e.g. horizontal fabric south of Rangapura, vertical fabric south of Shettihalli), as well as in the central part of the linear synforms made of supracrustal rocks (e.g. vertical fabric east of Shettihalli). Planar-linear fabric zones are located at the vicinity of the cover-basement interface and occur in areas where $\lambda 1 \lambda 2$ exhibits the largest variations in dip. Furthermore, this fabric also occurs in the central parts of the supracrustal basins (e.g. west of Rangapura, south of Terakanambi). Where so, $\lambda 1 \lambda 2$ is horizontal, affected by small folds with an vertical axial planes indicating a superimposed horizontal shortening. Furthermore, zones of planar-linear fabrics show an almost triangular distribution around foliation triple junctions (e.g. north of Shettihalli and south-east of Terakanambi).

Zones of linear fabrics can be observed at each termination of the synformal closures (e.g. north of Shettihalli and south-east of Terakanambi). The lineation is moderately plunging toward the inner parts of the basins. Linear vertical fabric zones have been only observed in supracrustal rocks north of Bimanabid, whereas horizontal linear fabric zones occur in the inner parts of the supracrustal basins south-west of Terakanambi. The southernmost part of domes north-west of Gundlupet display small areas with strong fabric, gently plunging (20° SW), associated with numerous mesoscopic superimposed folding. These interference patterns are exclusively associated with the linear fabrics in gneisses. As soon as linear fabric evolves to planar-linear and planar fabrics, no zone of superimposed structures can be noticed.

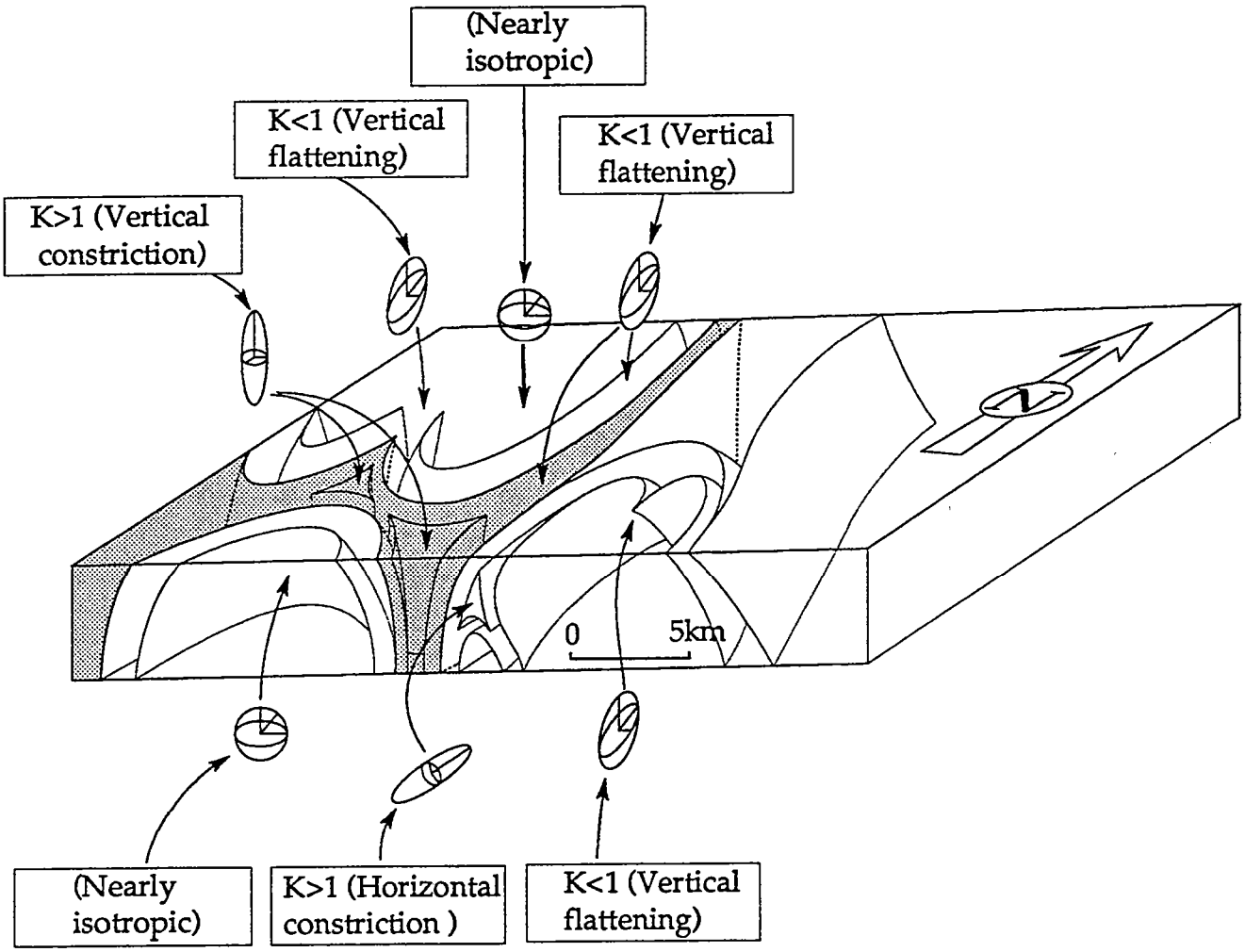

Fig. D. 37. Schematic bloc diagram in the Holenarsipur area showing (i) the 3D geometry of the greenstone-basement interface, (ii) the 3D geometry of the foliation triple point, (iii) their associated finite strain ellipsoids.

Strain regimes

The strain regimes were estimated using significant criteria of non-coaxial strain ; they characterize both areas, but are significantly more developed in the Holenarsipur area than in the Gundlupet area. In the Holenarsipur area, clear kinematic indicators are generally restricted to regions in the vicinity of the infra-supracrustal rocks interface. They always indicate a downward displacement of the supracrustal rocks relative to the infracrustal basement (Fig. D. 32) (Bouhallier et al., 1993). The linear easternmost part of the greenstone belt is dominated by horizontal sinistral displacements.

In the Gundlupet area, non-coaxial strain has been observed in two different settings. Firstly at the vicinity of the infra-supracrustal rocks interface north of Bimanabid, where kinematic criteria such as shear bands and asymmetric folds always indicate a downward displacement of the supracrustal rocks with respect to the infracrustal basement. Second, along a linear zone which affects both supra- and infracrustal rocks south-west of Rangapura. $\lambda 1$ is nearly horizontal. Shear bands seen in the gneisses, south of Rangapura are consistent with sinistral ductile shear. Elsewhere, strain regimes appear mainly coaxial.

In the triple points, strain regimes can be essentially discussed at some distance of the central axis of the S_1 foliation triple points which are vertical in greenstone belts. In such cases, the sense of shearing and the strain intensity attest to an important displacement of supracrustal rocks with respect with the infracrustal gneissic basement. This downward motion of greenstone material (called sagduction by Gorman et al., 1978), is locally recorded by the estimation of P-T conditions ; in the Holenarsipur area, greenstones in triple junctions display metamorphic assemblages showing a prograde evolution from 3 to 7kbar. (Bouhallier *et al.*, submitted).

FIELD DATA VERSUS ANALOG MODELS

Field data consistent with scaled models

In the light of our structural analysis, most of diapirism indicators expected from experiments appear to be reliable.These are in particular,

- foliation trajectories conformable with the cover-basement interface
- intensification of strain at the cover-basement interface

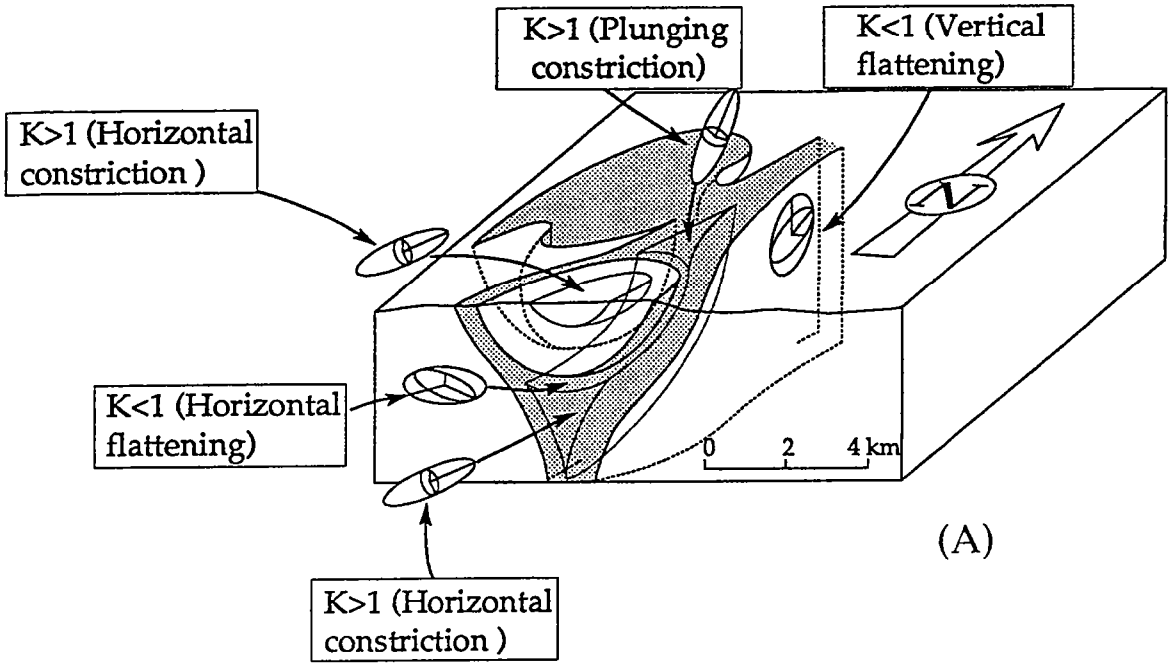

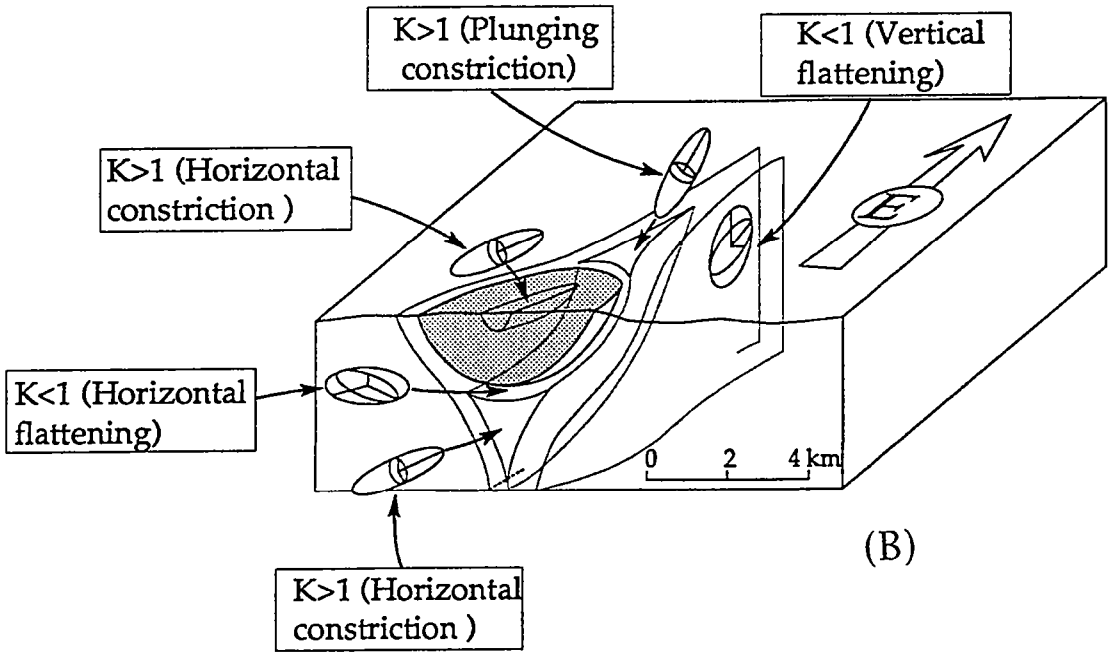

Fig. D. 38. Schematic bloc diagrams in the Gundlupet area showing (i) the 3D geometry of the greenstone-basement interface, (ii) the 3D geometry of the foliation triple point, (iii) their associated finite strain ellipsoids. (A) : West of Rangapura ; (B) : South of Terakanambi.

- lineation trajectories converging toward areas of non-coaxial vertical shearing

- high variability in the distribution of fabric types throughout the studied area.

- kinematic indicators showing a downward displacement of the supracrustal cover with respect to the TTG basement with opposite shear sense on both sides of a given dome

- high variability in the distribution of strain regimes throughout the studied area. Different type of fabrics are highly controlled by the dome and basins geometry.

- Specific domes in dome structures observed in the Holenarsipur area as those expected by experimental models (Dixon, 1975)

- Finally, the 3D shape of the supra-infracrustal rocks interface consistent with the 3D geometry and strain patterns of a diapiric net system (Talbot, 1991).

Specific structural features observed in the field, such as vertical linear fabric were also expected from experimental works. In models of diapiric sagduction, regions of linear vertical and constrictive fabric are expected in the zones where the subsidence of the denser overburden is the strongest (Dixon & Summers, 1983). This experimental data has been verified within the vertical foliation triple junctions of supracrustals, in both the Holenarsipur and Gundlupet areas. There, like in other similar situation (Brun et al.1981), fabrics are linear and vertical. Furthermore, evidences of non-coaxial regimes implying a downward displacement of the heavy supracrustal cover relative to the light migmatitic basement of gneisses are consistent with experimental observations and illustrate the gravitational collapse within this regions.

Another feature shown by strain maps and is that lineation trajectories are converging towards vertical foliation junctions (Fig. D. 31). This suggests that the high density supracrustal overburden tends to sink into the vertical triple junctions which act as wells. A systematic mapping of lineation strain trajectories associated with an increase of plunge should constitute a helpful tool to localize zones of maximal subsidence within areas expected to have underwent a diapiric evolution.

SAGDUCTED RIDGE (PLANE FLOW)
Incremental strain and fabric

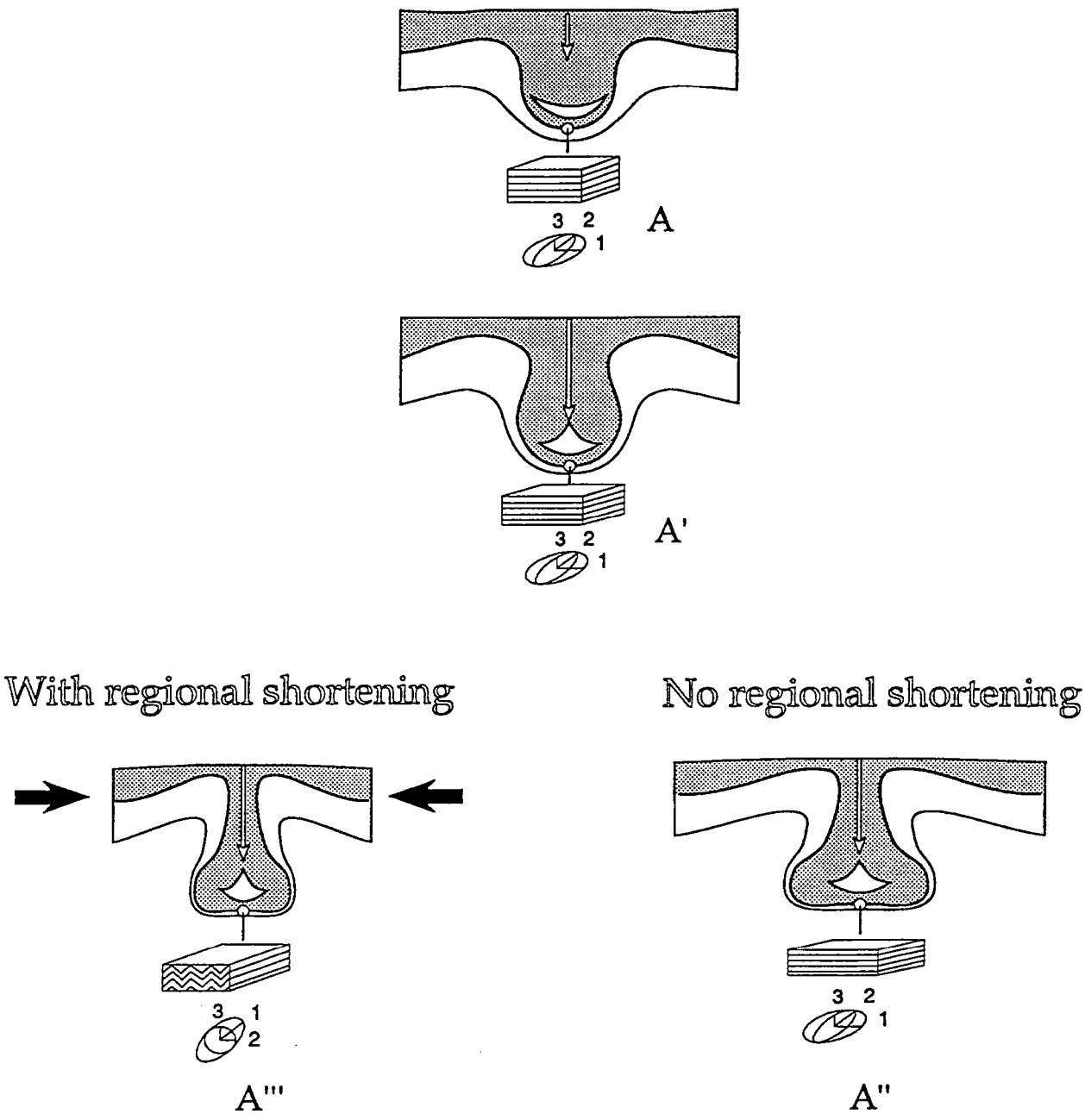

Fig. D. 39. Fabrics and associated strain ellipsoids of one specific area at three successive stages of the evolution of a sagducted greenstone belt (trough). The latest stage is supposed to be homogeneously and horizontaly shortened.

Unexpected field data and added effects

If most of structural features observed in the areas studied are consistent with experimental models of diapirs, some are not.

We have seen that horizontal displacements along regional transcurrent shear zones have occured in both areas studied. In the Holenarsipur area, the easternmost branch of the supracrustal belt is a linear and sinistral shear zone. In the Gundlupet area, evidence of horizontal shearing along vertical zones can also be observed. At smaller scale, shear zones appear organized along two major directions : dextral around 20E, and sinistral around 140E. They cut the Dharwar craton into lenses leading to elliptical domes and basins (Fig. D. 30). The ellipticity of domes between these zones is almost constant and suggests that strain was homogeneously moderate. Furthermore, the distribution of the regional transcurrent shear zones appears, at the scale of the craton, nearly regular and symmetric. It suggests that the overall craton has been coaxially strained with an almost E-W direction of regional shortening (Choukroune et al., 1987).

For a simple diapiric evolution, all pitches of $\lambda 1$ must be close to 90° irrespective the dip azimuth of foliation (Fig. D. 28). A diagram of the pitch of $\lambda 1$ versus attitude of $\lambda 1\lambda 2$ planes for the Holenarsipur area shows a scattering of pitches which clearly decreases when foliation strikes north-south (Fig. D. 35). A simple explanation in terms of interfering strain fields can be given. In the Holenarsipur area, the transcurrent shearing is north-south and one can expect that the effects of this shearing will be stronger along north-south foliation planes. The stretching direction in the N-S $\lambda 1\lambda 2$ planes will be preferentially reoriented by the shearing occuring during the diapiric evolution. On the opposite, a maximum of high $\lambda 1$ pitches resulting from the pure diapiric evolution are preserved within the E-W $\lambda 1\lambda 2$ planes where the effects of shear is minimal.

Horizontal triple junctions which were not directly predicted by experimental models can also be the result of interfering strain fields. Some of them are situated at the termination of the domes and sinking basins, some others are internal (Figs. D. 37 and 38).

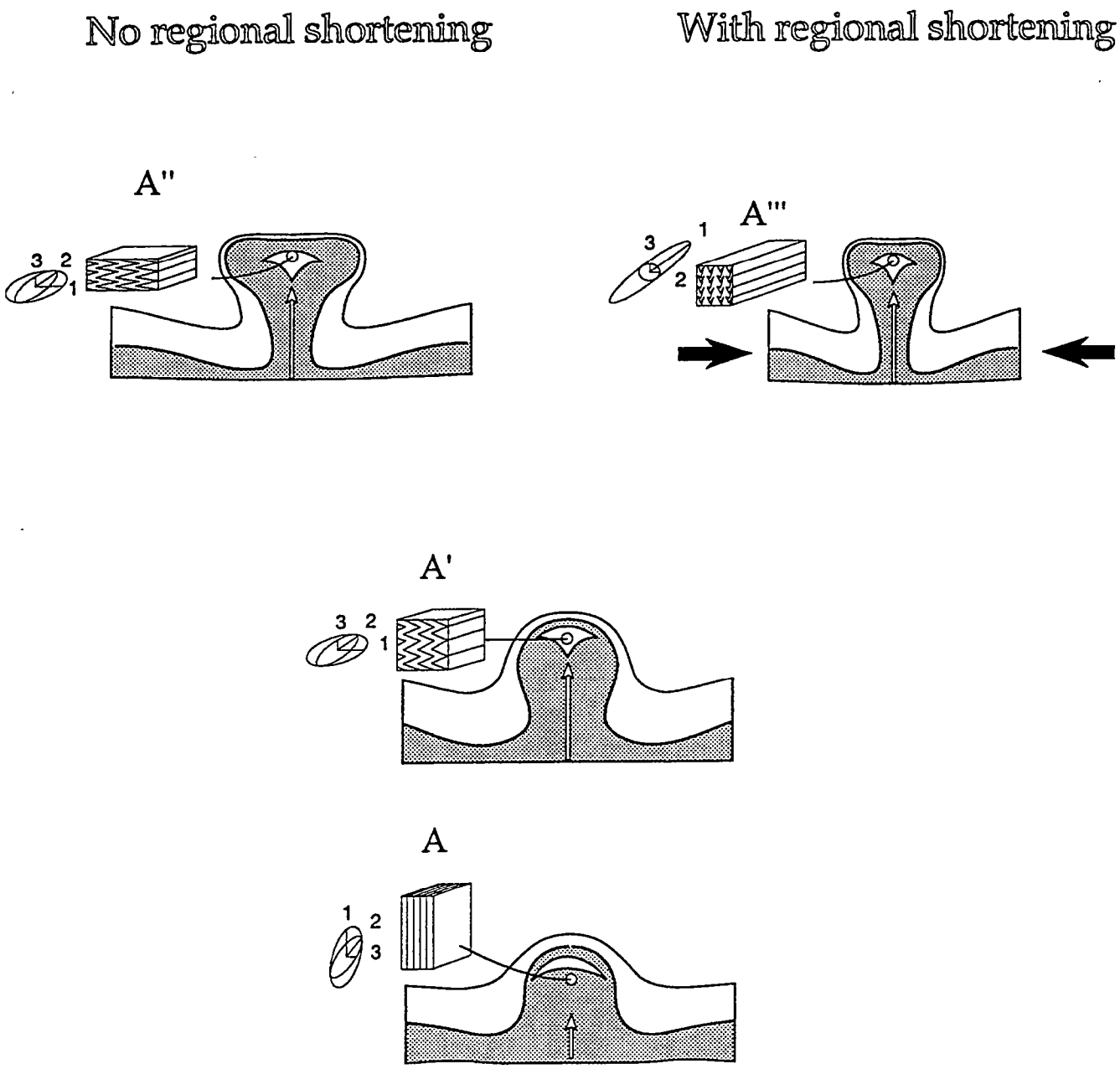

DIAPIRIC RIDGE (PLANE FLOW)
Incremental strain and fabric

Fig. D. 40. Fabrics and associated strain ellipsoids of one specific area at three successive stages of the evolution of a rising migmatitic dome (ridge). The latest stage is supposed to be homogeneously and horizontaly shortened.

The significance of outer horizontal triple junctions have been studied by Brun & Pons (1983). At the terminations of elliptical rising domes, at the terminations of the elliptical sinking basins, horizontal triple jonctions can result from simultaneous horizontal shortening due to regional deformation and vertical shortening due to vertical motion of the diapir or the sagducted bodies. This is the case of triple points situated, at the termination of supracrustal basins south of Terakanambi or north of the gneissic synformal closure north of Shettihalli, in the Gundlupet area (Fig. D. 38).

Horizontal triple junctions also develop within domes or basins. Two situations of superimposed structures have been observed near the top of the domes or near the bottom of sagducted basins. A first case is illustrated by the top of a dome situated N-W of Gundlupet. There, a vertical foliation is affected by folds with horizontal axial planes indicating vertical shortening. The resulting bulk strain is constriction with $\lambda 1$ sub-horizontal principal stretching.

A second situation is illustrated by the central part of the supracrustal basins south of Terakanambi (Gunlupet area). There, the fabric is planar-linear with $\lambda 1 \lambda 2$ horizontal and vertically crenulated. Resulting $\lambda 1$ is horizontal and parallel to the crenulation.

In order to explain the differences between the two situations, we have to explain why a vertical diapiric foliation can be vertically shortened, while an horizontal diapiric foliation can be horizontally shortened.

In the first case, the constriction area can be the simple consequence of diapiric motion. A given point situated in the domain of vertical flattening migrates into the domain of horizontal flattening when the diapir moves upward. In the second case, the folding of horizontal foliations can only be the result of superimposed horizontal regional shortening.

Figures D. 39 and D. 40 show fabrics associated with different stages of a sagduction and doming evolutions, with or without associated regional shortening. If we consider the deepest areas of sagducted supracrustals near the gneiss interface (Fig. D. 39), the fabric should be horizontal and planar in the case of a single diapiric evolution (A, A' and A" in Fig. D. 39), whereas superimposed planar-linear fabric (A"') are expected to result from regional shortening. We point up similar argument to explain superimposed linear fabric in the central parts of migmatitic gneissic domes west of Gundlupet (Fig. D. 40. Linear fabrics due the refolding of a vertical foliation do not imply regional shortening (A, A' and A", Fig. D. 40), whereas the refolding

of an horizontal foliation is considered to be the result of an horizontal regional shortening acting at least at the latest stage of the diapiric evolution (A"', Fig. D 40).

Lastly, we have to consider the vertical triple points mainly present in the Holenarsipur area. Models consider the strain field due to a single diapiric body. In the field, diapirs interfere. It was emphasized that final stages of diapir emplacements are often characterized by an increase of horizontal diameter called "ballooning effect" (Ramsay 1975, Holder 1979). The interference between various shortening directions linked to the horizontal spreading of two, three or four domes generate triple junction in which finite strain is of constriction type (Brun et al., 1981). Vertical triple junctions in greenstones situated between domes are the result of such a situation.

To summarize, two kinds of data have been described, i) those which infer a deviation from models results and ii) those which could not be predicted by modelling. The first kind concerns the scattering of $\lambda 1$ within vertical foliation planes in a given direction : they are the result of the interference between doming and regional shortening.

The second kind concerns the triple points and the location of constrictive strain : where these peculiar zones are vertical, they can be explained by the interference between spreading domes. Where these peculiar zones are horizontal and situated at the external tip of a dome and basin structure, they are the result of an interference with regional shortening.

Lastly, when these constrictional areas are horizontal and occupy the inner part of dome tops or basin bottoms, they can be the result of the progressive evolution of doming /sagducting processes, or the result of an interference with regional shortening. the choice between the two solutions can be easily made.

CONCLUSIONS

Data presented in this paper complete the previous knowledge of strain fields generated by diapiric structures. Most associated structures can be explained by vertical differencial motions. The internal tectonic style of the Archaean continental crust of Dharwar craton appears to result from interfering strain fields between Raleigh-Taylor diapiric structures (body forces) and horizontal regional shortening (boundary forces). However where the regional shortening did not erase the basical indicators of diapirism.

As these features are observed at different levels of the Archaean crust (from greenschist to granulitic facies) and over very large areas, one can say that the body forces were operating on a large scale at given periods of the evolution of the young continental crust. The observed patterns which characterize the supracrustal basins in the hornblende granulitic zone of the craton can only be interpreted in term of sinking drop-like blobs, whereas spoke patterns of linear "greenstone belts" in the amphibolitic zone represent subsiding troughs of the overburden (supracrustal cover) at a higher structural level. The difference in the shape of regional structures between the amphibolite and the hornblende-granulitic zones is probably only due to the fact that observations concern different horizontal sections of the same structures.

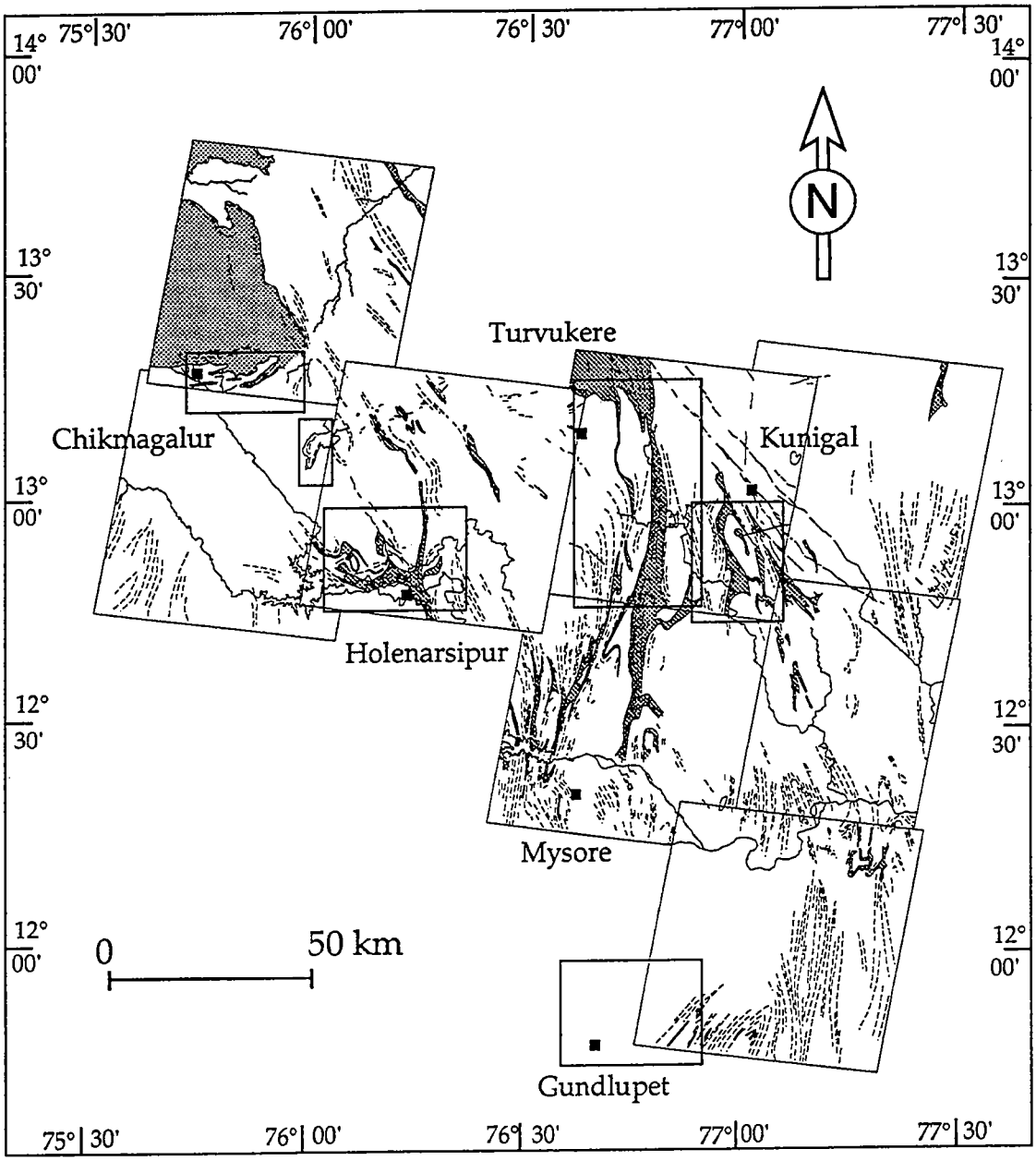

Fig. D. 41. Localisation des principaux secteurs d'études utilisés pour la synthèse structurale. Du Nord vers le Sud, on trouve les secteurs de : Chikmagalur-Sigegudha, d'Holenarsipur, de Turvukere, de Kunigal et de Gundlupet. Les limites cartographiques d'images satellitaires SPOT ont été reportées avec, en pointillé, l'orientation des principaux marqueurs texturaux.

2. 4. Données complémentaires

En plus des secteurs d'Holenarsipur et de Gundlupet, trois autres régions ont retenu notre attention. Ce sont, du Nord-Ouest vers le Sud-Est, les secteurs de Chikmagalur-Sigegudha, de Turvukere et de Kunigal (Fig. D. 41). Les résultats obtenus dans ces trois autres secteurs, couplés avec les quelques données structurales disponibles dans la littérature permettent de compléter l'organisation générale des structures impliquées dans la croûte continentale du craton de Dharwar.

Région de Chikmagalur

Les bassins présents dans la partie Nord du craton de Dharwar ont comme caractéristique remarquable de présenter des bordures monoclinales. A cela, il faut ajouter la présence quasi-systématique de zones mylonitiques et ultra-mylonitiques à la base des séries volcano-sédimentaires, c'est à dire à l'interface bassin-socle. Dans le bassin de Bababudan, les niveaux conglomératiques qui débutent le cycle volcano-sédimentaire sont intensément cisaillés et présentent des critères cinématiques qui indiquent un déplacement de la pile volcano-sédimentaire vers le centre du bassin. Dans le bassin de Bababudan comme dans celui de Sigegudha, des zones ultramylonitiques sont également observées plus haut dans les séries (Choukroune et Chardon, communication pers.). Dans les deux cas, le sens de déplacement des parties supérieures des piles volcano-sédimentaires apparaît aussi systématiquement dirigé vers le centre des bassins.

Le bassin volcano-sédimentaire de Bababudan a fait l'objet d'une cartographie détaillée. Son schéma évolutif global est résumé dans Chadwick et al., (1989). Ces auteurs proposent que l'ensemble des déformations qui affectent ce bassin soit le résultat d'une évolution intra-cratonique en contexte transpressif. En outre, ils démontrent la nature fortement subsidente du bassin, surtout lors des phases d'éruptions basaltiques. Ainsi, la subsidence au Sud apparaît rapidement compensée, au Nord, par la remontée puis l'érosion des premiers niveaux basaltiques, niveaux qui alimentent la sédimentation de cônes détritiques développés à l'intérieur du bassin sous faible tranche d'eau.

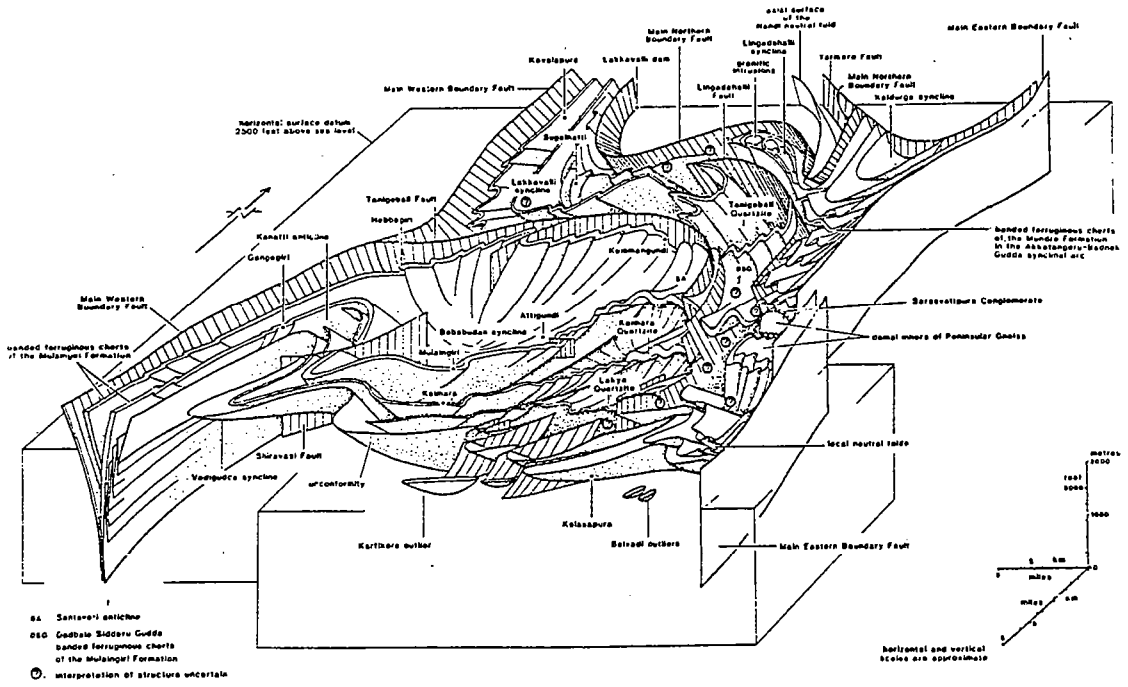

Fig. D. 42. Schematic representation of the structure of the Bababudan région, from Chadwick et al., (1985).

Toutefois, Chadwick et al. (1989) omettent de signaler un fait important dans leur analyse des structures présentes dans le bassin de Bababudan : les axes de plis mesurés dans la partie centrale du bassin ont tous une disposition radiale et plongent vers les régions de plus forte subsidence (Fig. D. 42). De plus, on retrouve dans la région centrale du bassin un niveau de décollement en faille normale avec le compartiment supérieur glissant vers le centre du bassin et dont la racine présente une forme arquée, analogue à une niche d'arrachement. Ainsi, superposée à une tectonique transpressive, il y a eu développement, dans le bassin de Bababudan, une tectonique de type gravitaire. L'analyse structurale du bassin de Bababudan est résumée et schématisée dans les Figures B. 12 et Fig. D. 42.

Les bassins volcaniques de Bababudan et de Sigegudha reposent sur un socle constitué de gneiss péninsulaires dans lesquels sont intrusives des granodiorites, comme celle de Chikmagalur datée à 3.1 Ga (Taylor et al., 1984). Les relations structurales entre le socle et les bassins sont présentées sur la figure D. 43. Une discordance structurale très nette est visible entre les trajectoires du plan principal d'aplatissement, cartées à la base des bassins et celles du socle gneissique. Des filons granodioritiques non déformés et attribués à la mise en place de la granodiorite de Chikmagalur recoupent, par endroits, la foliation des gneiss du socle (Chadwick et al., 1981). Par ailleurs, plusieurs niveaux volcaniques (rhyolites et basaltes) appartenant au bassin de Bababudan ont été datés aux environs de 2.7 Ga (Bhaskar Rao et al., 1992). Ces résultats indiquent un intervalle de temps minimum de 0.4 Ga entre l'âge de la déformation dans le bassin et celui affectant le socle gneissique. Dans cette partie nord du craton, l'événement le plus récent, c'est à dire celui qui a structuré les bassins, ne semble pas avoir été suffisamment intense pour affecter significativement le socle.

Secteur de Turvukere

Le secteur de Turvukere se situe à 50 km à l'Ouest de la ville d'Holenarsipur (Fig. D. 41). Ce secteur se compose des trois unités lithologiques habituellement reconnues dans le craton de Dharwar, à savoir des gneiss péninsulaires, des roches supracrustales (partie sud de la ceinture de Chitradurga) et des granites. Il n'existe pas de carte géologique détaillée de cette région. Néanmoins, l'appui satellitaire nous a permis de carter les limites entre les ceintures de roches vertes et le socle.

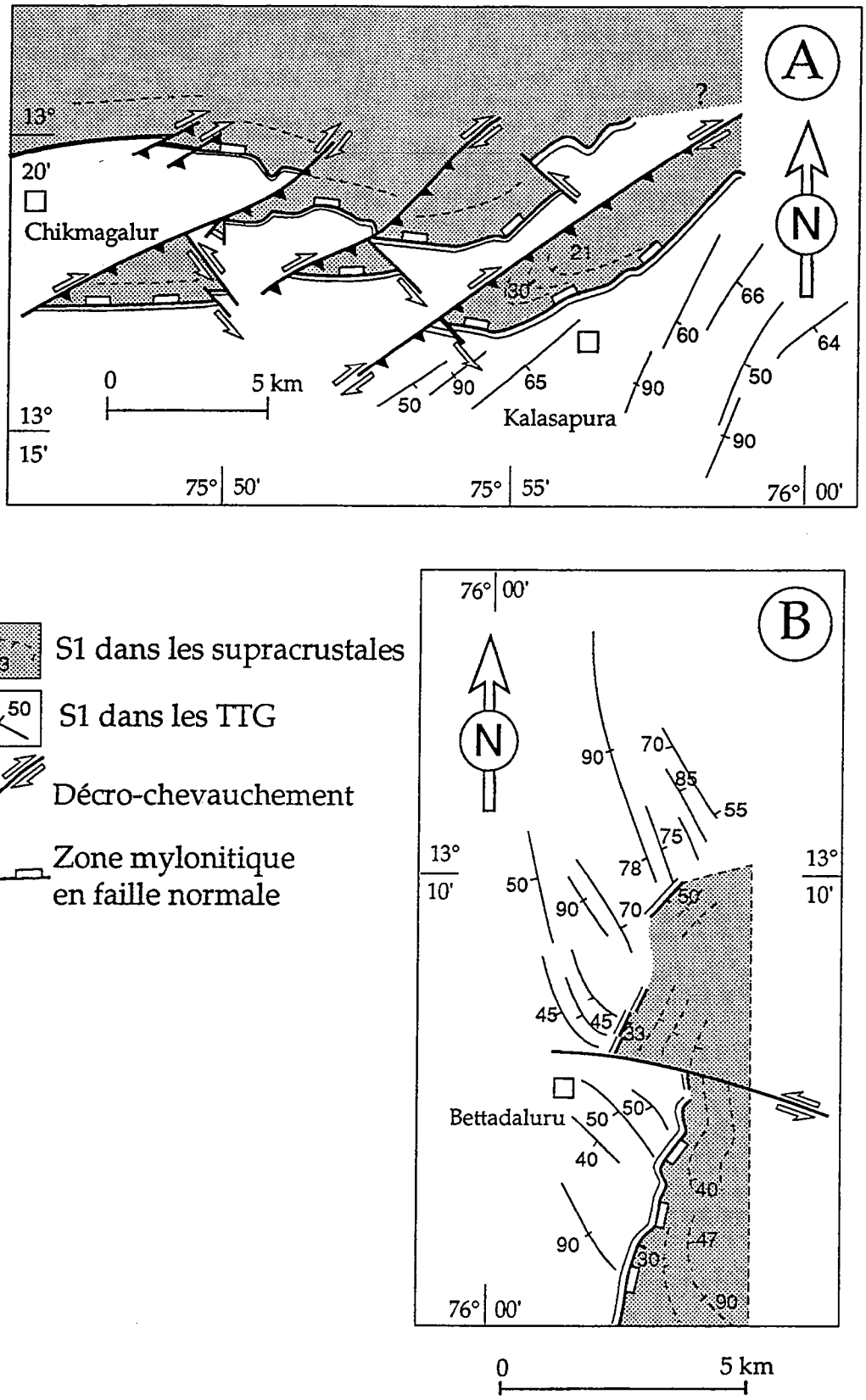

Fig. D. 43. (A) Carte structurale présentant les relations structurales entre la partie sud de la ceinture de roches vertes de Bababudan (en grisé) et son socle granito-gneissique (en blanc) dans la région de Chikmagalur. Les trajectoires du plan d'aplatissement dans le socle son syn- à post migmatitiques. (B) Carte structurale présentant les relations structurales entre la ceinture de roches vertes de Sigegudha (en grisé) et son socle gneissique sous-jacent.

Dans les gneiss péninsulaires, les trajectoires du plan principal d'aplatissement sont contemporaines du développement de nombreuses injections leucocrates **(photo)**, alors qu'elles sont synmétamorphes dans les roches supracrustales. Dans la région de Turvukere, les métabasaltes sont métamorphisés dans le faciès amphibolite (Raith et al., 1982). Dans ces roches, des minéraux tels que l'amphibole ou le plagioclase marquent la foliation et la linéation régionale (Figures D. 44 et D. 45). Dans le socle gneissique, les trajectoires du plan principal d'aplatissement soulignent très clairement la présence de structures en dômes, alors que dans les roches supracrustales les trajectoires du plan principal d'aplatissement sont parallèles à la direction d'allongement de la ceinture. L'ensemble des structures a une orientation globalement Nord-Sud.

Le secteur de Turvukere est marqué par la présence de grands cisaillements ductiles verticaux, présentant une cinématique dextre. Le mieux exprimé d'entre eux, affecte les terrains situés à l'Ouest de Beluru (Fig. D. 44 et D. 45). Ces cisaillements sont en outre jalonnés par plusieurs corps granitiques dont les faciès à phénocristaux évoquent très nettement certains faciès du batholite du Closepet. Parmi les structures les plus significatives observées dans ces granites, on peut noter la présence de structures C/S indiquant une cinématique dextre. Les plans C et S sont verticaux. De plus, l'orientation préférentielle des phénocristaux s'avère être parallèle à la linéation régionale, laquelle linéation tend à s'horizontaliser là où la déformation décrochante est la mieux exprimée (Fig. D. 45). Les dômes gneissiques qui n'ont pas été affectés par la déformation décrochante présente une linéation qui tend à se disperser autour d'une direction sub-méridienne ; c'est le cas notamment de celui situé dans la partie Sud-Est du secteur d'étude (Fig. D. 45).

Hormis la présence de grands décrochements ductiles dextres, le secteur de Turvkere se caractérise d'un point de vue structural par (i) l'intensification systématique de la déformation au voisinage de l'interface entre les ceintures de roches vertes et les gneiss péninsulaires, (ii) le parallélisme constant des trajectoires du plan principal d'aplatissement avec cette même interface (Fig. D. 44).

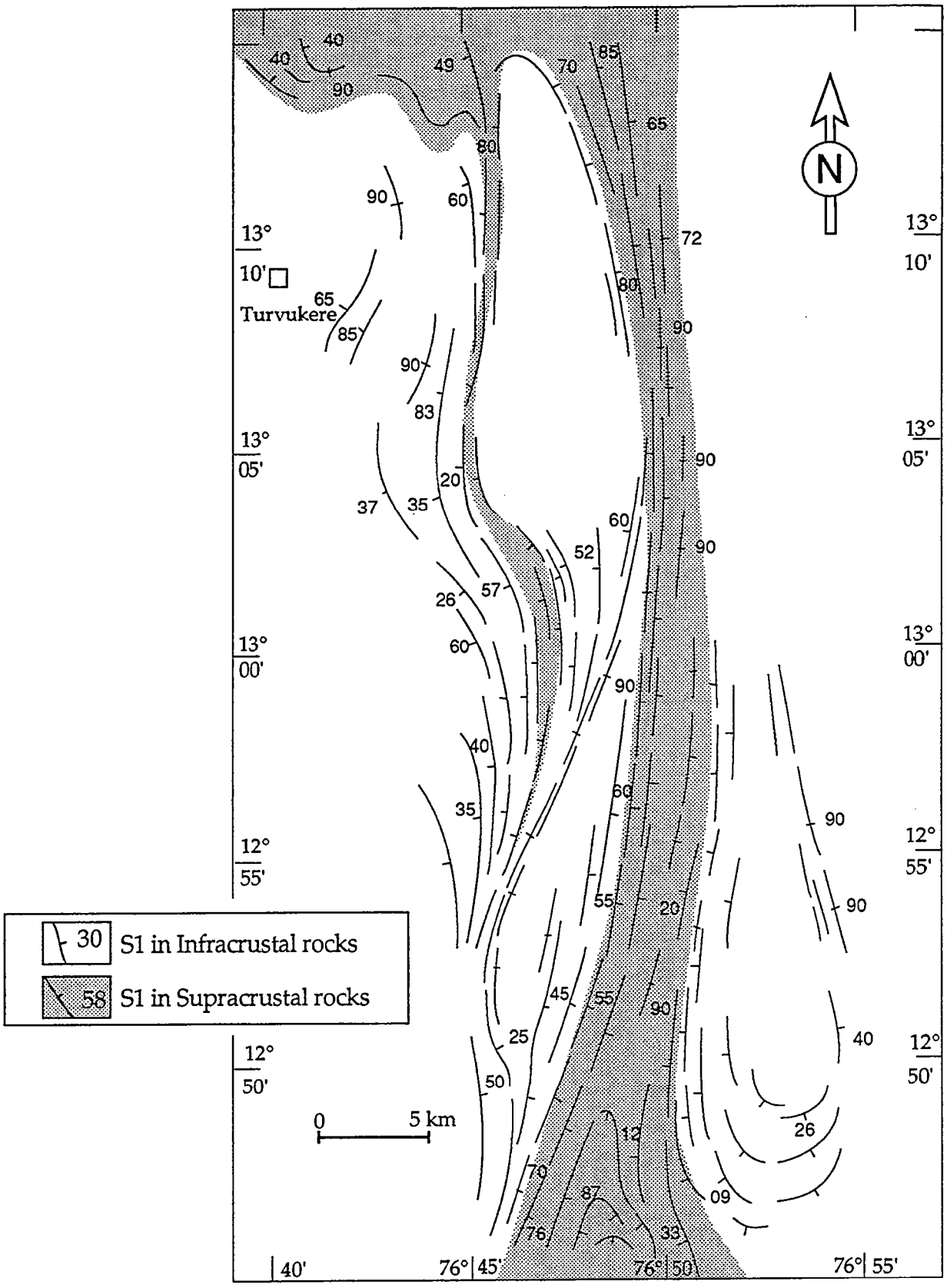

Fig. D. 44. Carte structurale présentant la foliation régionale du secteur de Turvukere. Les roches supracrustales (ceinture de roches vertes) sont en grisé ; Les TTG et les roches granitiques porphyroïdes en blanc. Les trajectoires du plan d'aplatissement correspondent à la foliation gneissique syn-migmatitique dans le socle et à la foliation métamorphique métamorphique de l'amphibolite faciès dans les roches supracrustales.

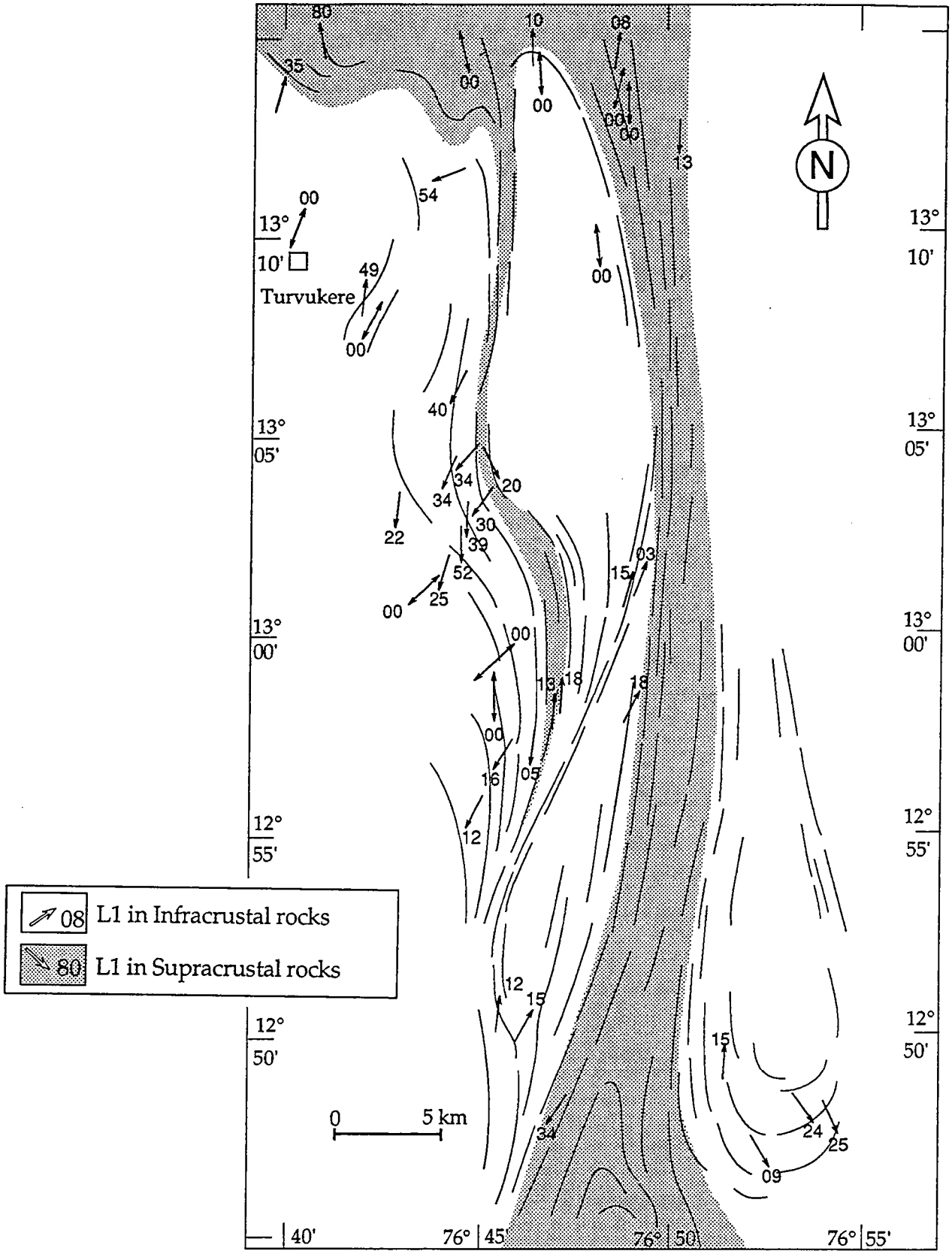

Fig. D. 45. Carte des linéations d'allongement du secteur de Turvukere. Les roches supracrustales (ceinture de roches vertes) sont en grisé ; Les TTG et les roches granitiques porphyroïdes en blanc. Les trajectoires du plan d'aplatissement correspondent à la foliation gneissique syn-migmatitique dans le socle et à la foliation métamorphique de l'amphibolite faciès dans les roches supracrustales.

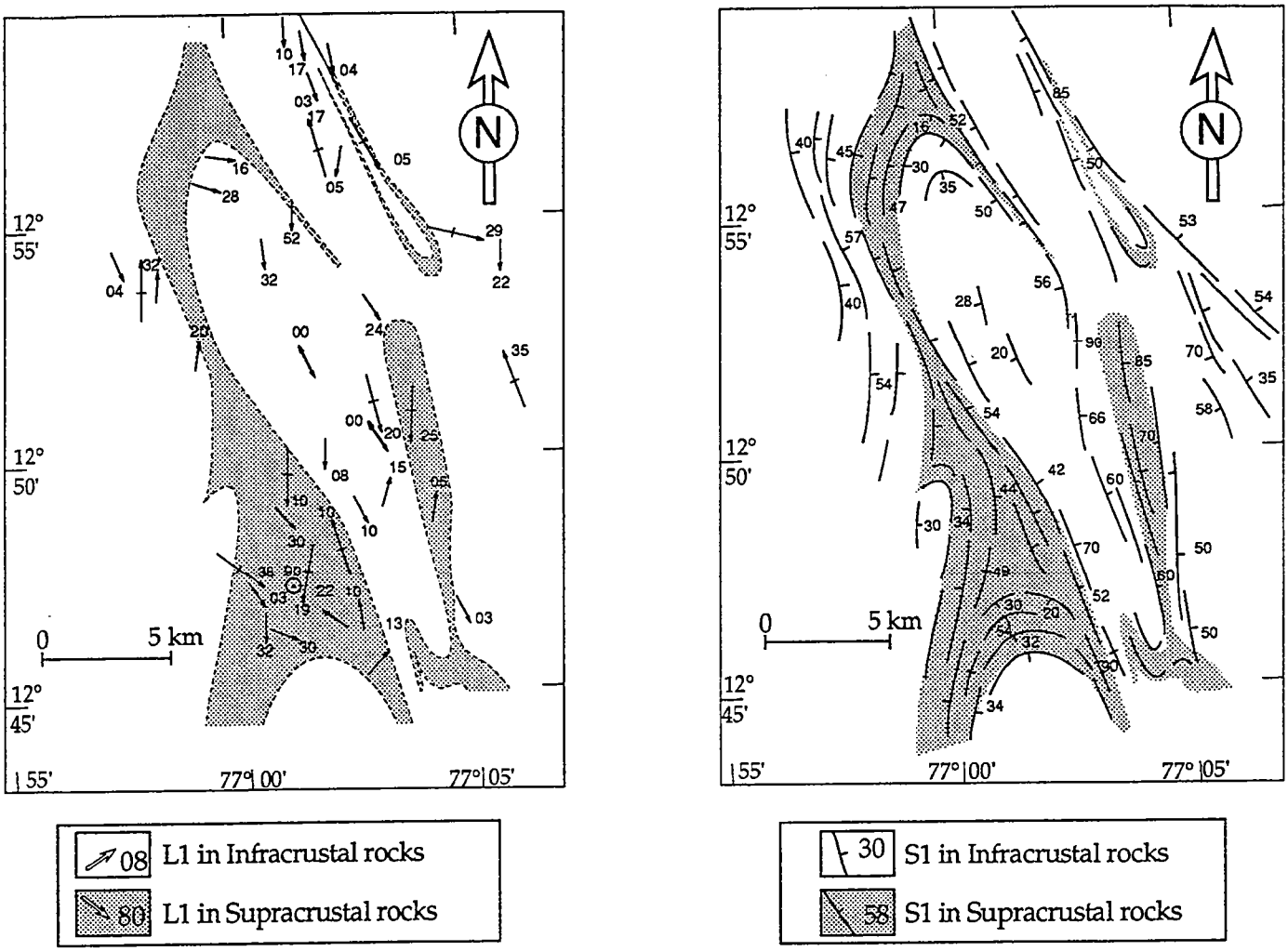

Fig. D. 46. (A). Carte structurale présentant la foliation régionale du secteur de Kunigal. Les roches supracrustales (ceinture de roches vertes) sont en grisé ; Les TTG et les roches granitiques porphyroïdes en blanc. Les trajectoires du plan d'aplatissement correspondent à la foliation gneissique syn-migmatitique dans le socle et à la foliation métamorphique de l'amphibolite faciès dans les roches supracrustales.

Fig. D. 46. (B). Carte des linéations d'allongement du secteur de Kunigal. Les roches supracrustales (ceinture de roches vertes) sont en grisé ; Les TTG et les roches granitiques porphyroides en blanc. Les trajectoires du plan d'aplatissement correspondent à la foliation gneissique syn-migmatitique dans le socle et à la foliation métamorphique de l'amphibolite faciès dans les roches supracrustales.

Secteur de Kunigal

Cette zone d'étude se situe au Sud-Est de la région de Turvukere (Fig. D. 41) et est constituée de gneiss péninsulaires et de roches supracrustales (ceinture de Kunigal). A l'inverse de celui de Turvukere, le secteur de Kunigal ne montre pas de massifs granitiques à phénocristaux à l'affleurement.

Les faits structuraux les plus significatifs du secteur de Kunigal sont les suivants :

- Dans la partie sud de la zone étudiée, l'interface entre roches supracrustales et gneiss péninsulaires présente des pendages divergents vers l'extérieur de la ceinture. En d'autres termes et contrairement à ce qui est observé dans les autres ceintures du craton, les branches Sud de la ceinture de Kunigal ne constituent pas des synformes mais des antiformes.

- Les trajectoires du plan principal d'aplatissement des gneiss péninsulaires situés dans la partie centrale de la ceinture dessinent un bassin ; dans les gneiss situés au Sud-Ouest de la zone étudiée, les trajectoires du plan principal d'aplatissement définissent une fermeture péri-synforme (Fig. D. 46a).

- Les trajectoires dans la ceinture de roches vertes font apparaître trois points-triples résultant de l'interférence associée au développement d'au moins trois bassins ou dômes de gneiss péninsulaires. Pour le plus méridional de ces points triples, nous avons pu vérifier que la linéation synmétamorphe, marquée macroscopiquement par l'alignement de minéraux comme les amphiboles et les plagioclases, était verticale et que la présence restreinte et localisée de nombreux plis à axes verticaux et de plans axiaux très dispersés attestait de la nature constrictive de ce secteur (Fig. D. 46b).

Les autres grands traits structuraux du secteur du Kunigal sont : (i) l'intensification systématique de la déformation au voisinage de l'interface entre les roches supracrustales et les gneiss péninsulaires, (ii) le parallélisme systématique des trajectoires du plan d'aplatissement avec cette même interface.

2. 5. Analyse géométrique des ceintures

Dans le craton de Dharwar, on assiste à une variation progressive et continue de la géométrie des ceintures de roches vertes du Nord vers le Sud. Au Nord, les roches volcano-sédimentaires occupent de grands bassins (jusqu'à 100 km de large) dont les limites cartographiques sont très irrégulières (formes souvent arquées et parfois convolutes). Dans la région centrale, les roches supracrustales forment, au contraire, des bassins linéaires (parfois plusieurs dizaines de km) et relativement étroits (d'une dizaine de km à quelques km). En outre, dans les régions d'Holenarsipur et de Turvukere, les interfaces au contact avec le socle gneissique sont soit fortement pentées, soit verticales. Une autre caractéristique majeure des ceintures de la région centrale du craton est qu'elles se connectent et s'anastomosent. Les zones de jonctions sont triangulaires (ceintures d'Holenarsipur, de Krishnarashpet et de Kunigal). Cet aspect en "réseau" se poursuit jusque dans le Sud du craton, dans le secteur de Gundlupet.

On peut facilement opposer à la largeur des bassins volcano-sédimentaires du Nord du craton, la forme étroite et elliptique des ceintures du Sud. Ce fait est particulièrement net dans la région de Sargur et/ou dans le secteur de Terakanambi (région de Gundlupet). Les bassins ne sont en fait que des cuvettes elliptiques, de forme parfois très allongée et dont la largeur ne dépasse jamais les 10 km. L'interface entre le socle gneissique migmatitique et les roches volcano-sédimentaires présente un pendage très variable depuis des valeurs très faibles dans la région de Terakanambi (secteur de Gundlupet) jusqu'à des pendages verticaux, voire renversés dans la région de Rangapura (secteur de Gundlupet).

Le secteur de Kunigal représente un secteur clé pour la compréhension de l'architecture globale de l'ensemble de ces ceintures ou bassins de roches vertes. Ainsi les branches linéaires ne sont plus des synformes, comme c'est par exemple le cas dans la région d'Holenarsipur, mais ont une géométrie d'antiformes. Ce fait est d'ailleurs très nettement souligné par les trajectoires du plan d'aplatissement dans le socle, trajectoires qui ne dessinent plus des dômes (ex : région d'Holenarsipur) mais des bassins (Fig. D. 46a).

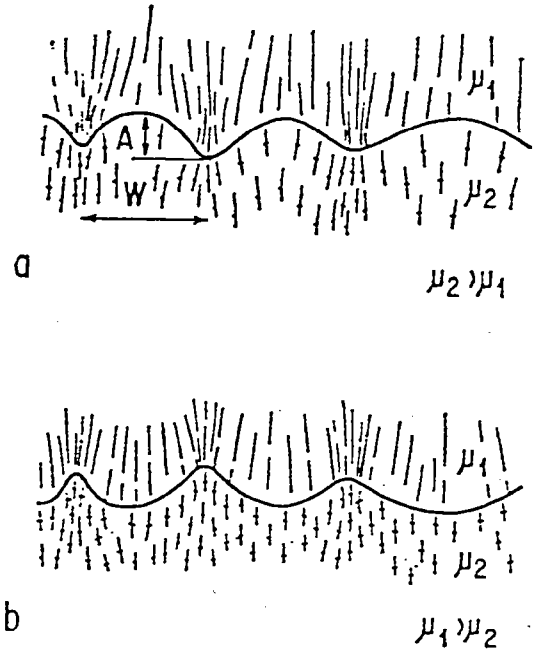

Fig. D. 47. Raccourcissement d'une interface simple. a) Plis et trajectoires de déformation dans le cas d'un socle plus compétent que la couverture. b) Plis et trajectoires de déformation dans le cas d'un socle moins compétent que la couverture, d'après Brun, (1983).

2. 6. Tests sur la signification des structures d'échelle cartographique du craton de Dharwar

Le problème de l'origine des structures en dômes-et-bassins peut être traité en utilisant les trois critères suivants : (i) les relations angulaires entre les trajectoires du plan d'aplatissement et l'interface socle-ceinture, (ii) la localisation des zones d'intensification de la déformation, (iii) la cinématique de l'interface socle-couverture (Brun, 1983, Schwerdtner & Lumbers, 1980). Brun (1983) reconnaît trois mécanismes principaux susceptibles de générer de telles structures.

Le raccourcissement

Le flambage d'une interface entre deux lithologies comme les ceintures de roches vertes et le socle gneissique peut donner conjointement naissance à des plis pincés en position synclinale et à des dômes gneissiques si le socle est l'unité de plus forte viscosité. Ce modèle impose que les trajectoires du plan d'aplatissement soient sécantes sur l'interface socle-ceinture (Fig. D. 47), ce qui n'est pratiquement jamais le cas pour l'ensemble des zones étudiées. De plus, les zones intensément déformées doivent être situées dans les plis pincés et être perpendiculaires à l'interface (Fig. D. 47), ce qui n'a jamais été observé pour les champs de déformation que nous avons cartés, sauf dans les zones de décrochements. Dans tous les autres cas, les zones intensément déformées sont systématiquement parallèles aux interfaces socle-ceintures.

Le plissement polyphasé a aussi été proposé pour expliquer l'origine des structures en dômes-et-bassins. En plus des deux caractéristiques présentées ci-dessus, incompatibles avec les champs de déformation du craton de Dharwar, le plissement polyphasé suppose le développement de deux champs de déformation distincts, caractérisés par des trajectoires du plan d'aplatissement recoupant l'interface socle-couverture et présentant chacun des relations (rapports de symétrie) avec la structure globale (Fig. D. 48).

Des modèles par plissements non-cylindriques ont aussi été proposés pour expliquer l'origine des structure en dômes-et-bassins (Platt, 1980, Coward, 1981 ; Kröner, 1984). Dans un modèle de type plis en échelons, en plus des deux critères caractéristiques du raccourcissement (trajectoires du plan d'aplatissement sécantes sur l'interface socle-ceinture ; zones

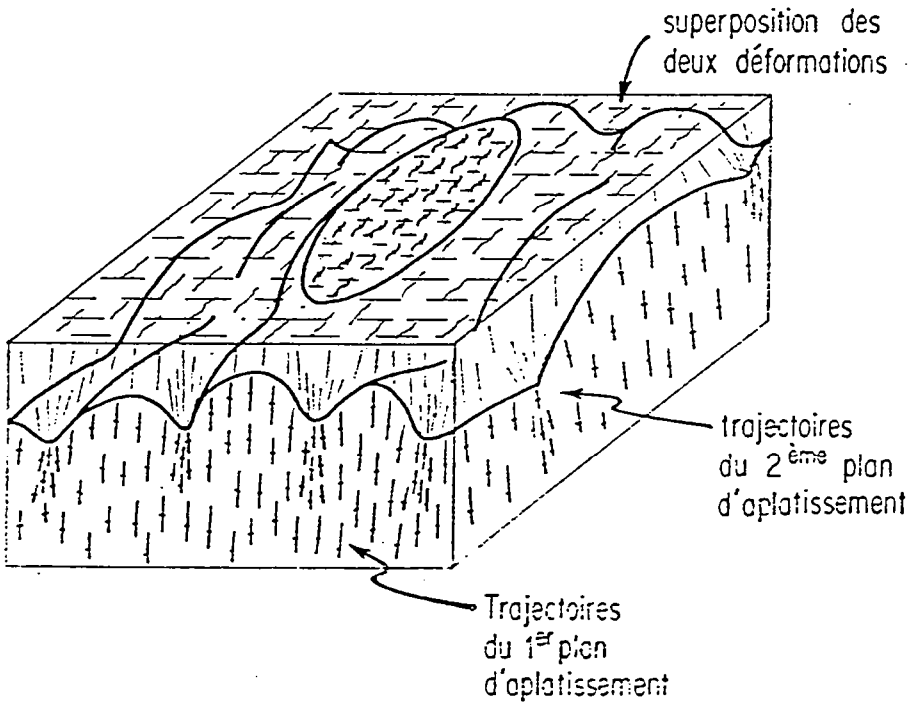

Fig. D. 48. Schéma d'un dôme issu de la superposition de deux déformations, d'après Brun, (1983).

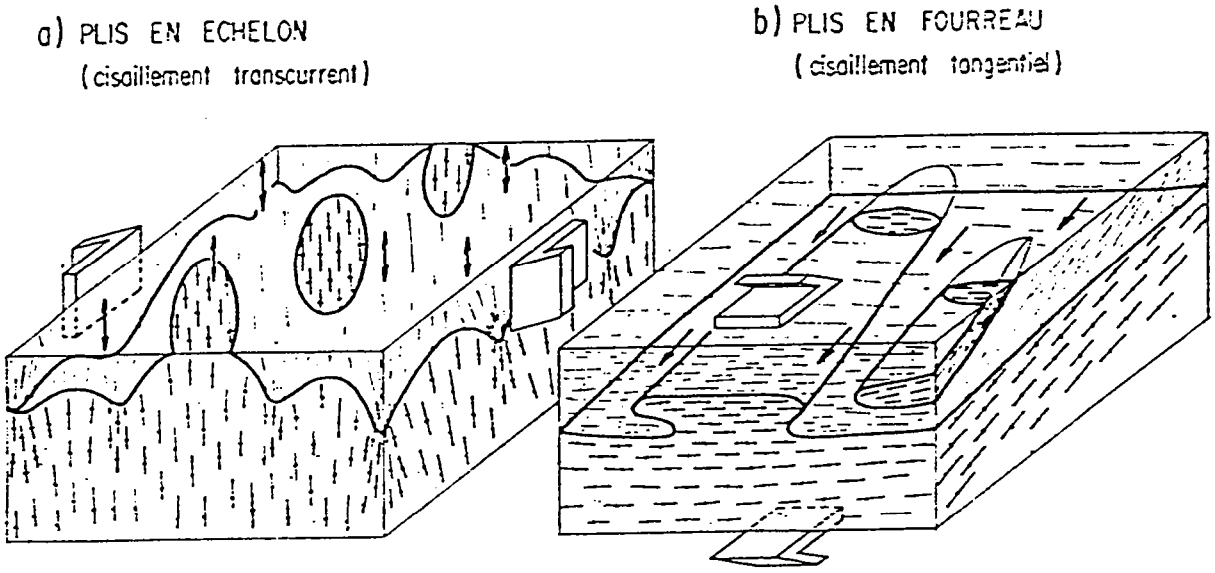

Fig. D. 49. Dômes assimilables à des plis non-cylindriques résultant d'un cisaillement a) transcurrent, et b) tangentiel. Traits fins : trajectoires du plan d'aplatissement ; flèches : direction principale d'étirement, d'après Brun, (1983).

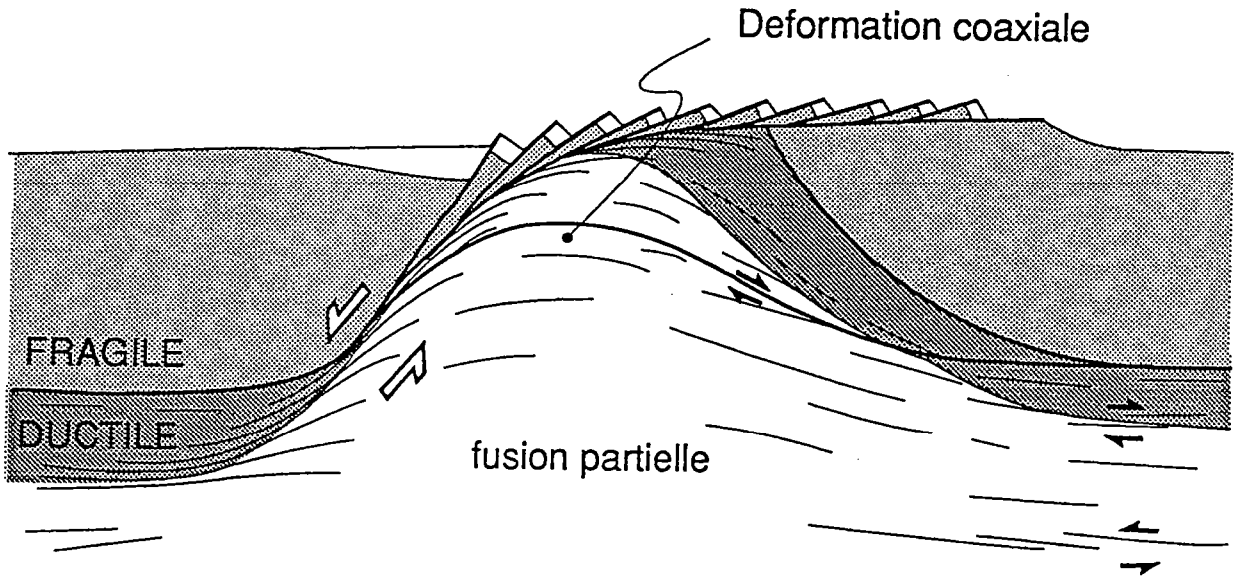

Fig. D. 50. Exemple de dôme extensif ("metamorphic core complexe"), Van den Driessche & Brun, 1991.

intensément déformées perpendiculaires à l'interface), un troisième doit être vérifié : la position systématiquement horizontale et parallèle de la linéation d'étirement avec la trace cartographique des dômes (Fig. D. 49a).

Dans un modèle de type plis en fourreaux (Fig. D. 49b), deux autres critères sont nécessaires : (i) la foliation régionale doit être peu pentée et être sécante sur les contours cartographiques des dômes ; (ii) l'ensemble de la région doit témoigner de la réalité d'un cisaillement tangentiel régional cohérent en sens et direction. Tous ces critères de reconnaissance sont incompatibles avec les champs de déformation régionaux cartés dans le craton de Dharwar.

La distension

Des structures à priori assimilables à des dômes extensifs, ont récemment été proposées dans l'Archéen d'Australie (Hammond & Nisbet, 1991). Dans un contexte extensif, les structures en dômes-et-bassins doivent être fortement asymétriques (Brun, 1983, Van den Driessche & Brun, 1991). En outre, le pendage de la zone de détachement représentée par l'interface socle-couverture (Fig. D. 50) ne peut excéder 60°, ce qui est contraire à la plupart de nos observations. Néanmoins, il est toujours possible de verticaliser cette interface au cours d'une phase de raccourcissement régionale postérieure à la phase extensive. Ceci implique la superposition de deux champs de déformation distincts, un relatif à l'épisode extensif, l'autre caractérisant l'événement compressif. Cependant l'observation de pendages socle-couverture à forte valeur (>60°) et renversés comme dans les régions de Kunigal et de Gundlupet exclut cette éventualité.

Le diapirisme

Ce modèle implique que deux critères soient vérifiés : (i) les trajectoires du plan d'aplatissement doivent s'adapter à l'interface socle-couverture, (ii) les zones d'intensité maximale de la déformation doivent se concentrer autour de l'interface socle-couverture. Ces deux caractéristiques sont vérifiées à toutes les latitudes du craton.

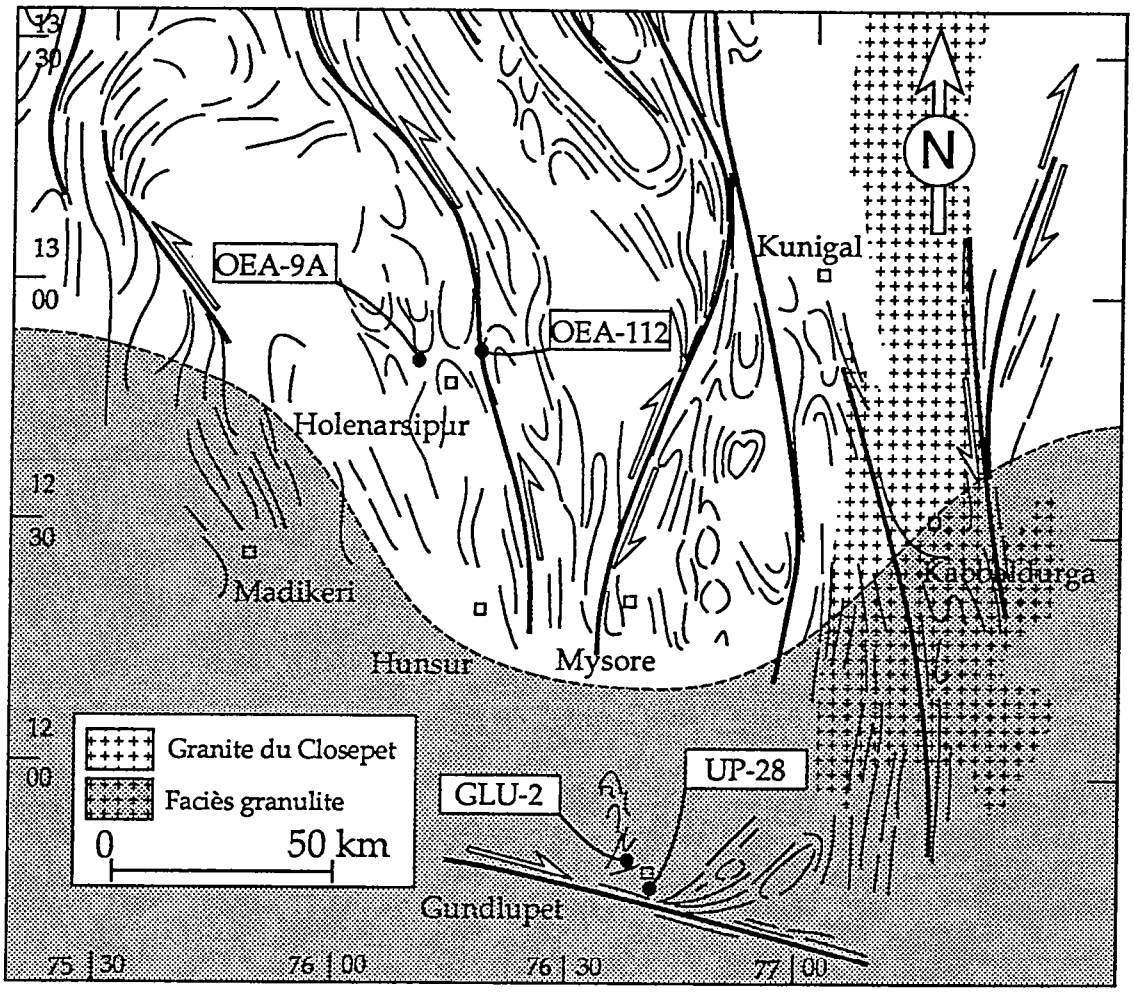

Fig. D. 51. Localisation des échantillons OEA 112, OEA 9A, GLU 2 et UP 28 dans le craton de Dharwar.

2. 7. Âge des structures

Les observations de terrain

Toutes les observations de terrain indiquent que la mise en place du batholite du Closepet a été contemporaine d'une déformation régionale importante. Les arguments sont les suivants : (i) une foliation régionale généralement sub-verticale et de direction Nord-Sud, marquée par l'alignement des phénocristaux des faciès porphyroïdes ; (ii) une organisation régulière de bandes de cisaillements verticales, dont le développement est parfois contemporain de la mise en place des matériaux granitiques ; en outre, nous avons pu observer des structures de type C/S attestant du caractère syn-tectonique (Berthé et al., 1978) des faciès porphyroïdes du batholite.

D'une façon générale, le plan d'aplatissement principal observé dans le batholite est parallèle à ses épontes Nord-Sud ainsi qu'à la foliation gneissique du socle encaissant. Sur le terrain, l'organisation spatiale des critères cinématiques montre deux populations de bandes de cisaillements verticales, l'une dextre et d'azimut N20 (photo q, annexe), l'autre senestre et d'azimut N160 (photo s, annexe). Ces dernières sont non seulement présentes dans les différents faciès granitiques du batholite mais se développent aussi dans les gneiss migmatitiques encaissants. Dans les gneiss encaissants, on observe l'injection préférentielle de veines granitiques leucocrates dans les bandes de cisaillements. Cependant, les veines les plus tardives cristallisent de façon statique et sont sécantes sur les bandes de cisaillements. Le développement des veines semble par conséquent syn- à post-tectonique.

A l'échelle d'un affleurement, seule l'une de ces deux familles de bandes de cisaillements est généralement exprimée. Par contre, à l'échelle régionale, il n'apparait pas de dominance d'une des deux populations.

En carte et d'après l'étude d'images satellitaires (Drury and Holt, 1980), la totalité du craton archéen de Dharwar est marquée par deux familles de décrochements régionaux d'importance égale et de distribution relativement homogène. Leur géométrie et leur cinématique implique une direction de raccourcissement régional Est-Ouest (Drury et al., 1984).

Il est frappant de constater que les deux directions de cisaillements verticales relevées sur le terrain dans le batholite du Closepet s'intègrent parfaitement dans cette organisation cinématique d'échelle régionale (Fig. D. 51). Ainsi, ces observations suggèrent (i) que la mise en place du

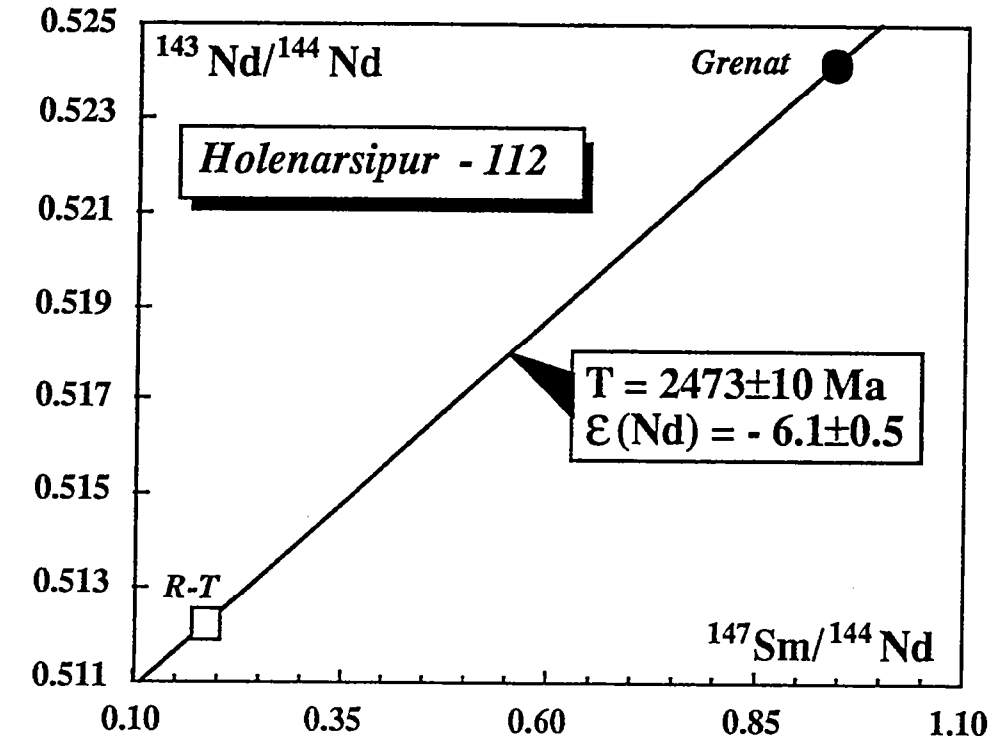

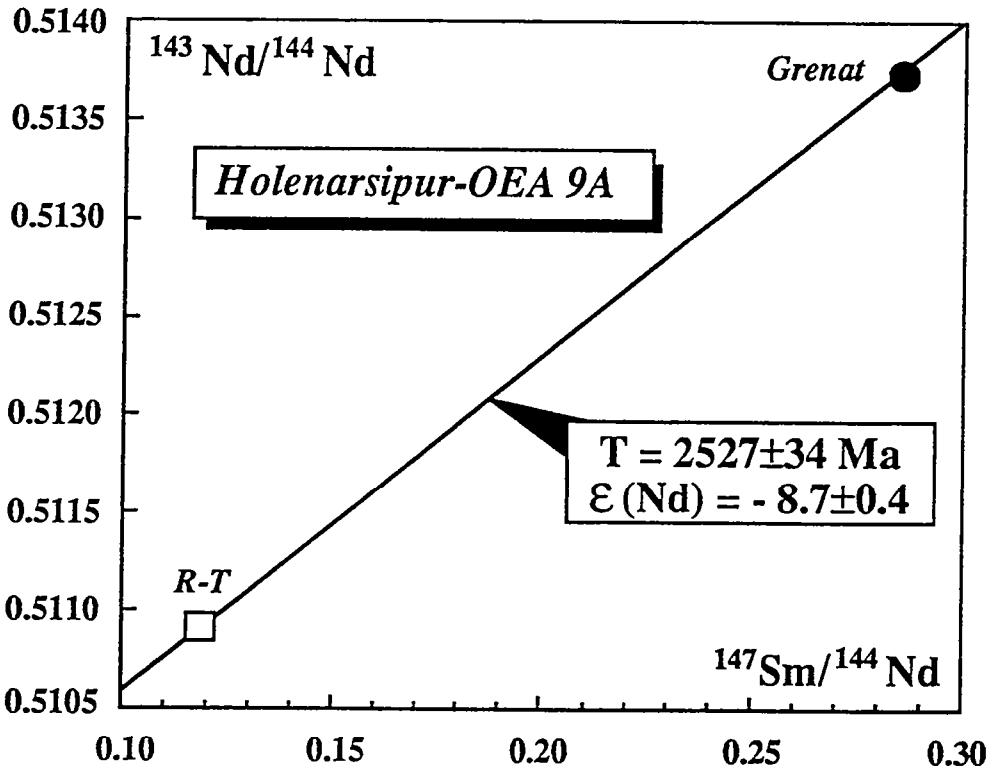

Fig. D. 52. Diagramme isochrone Sm-Nd pour les couples grenat-roche total des échantillons OEA 112 et OEA 9A (Secteur d'Holenarsipur).

batholite du Closepet a été contemporaine du développement de grands cisaillements décrochants, parfois senestres (N160), parfois dextres (N20), et (ii) que la géométrie et la cinématique de ces grandes structures d'échelle crustale s'intègrent parfaitement à l'ensemble des grands décrochements qui affectent la totalité du craton.

La zone de transition au Sud du batholite du Closepet (région de Kabbaldurga), zone marquant sur le terrain le franchissement de l'isograde amphibolites-granulites, se caractérise par la présence de "patches" granulitiques de taille variable (quelques cm à plusieurs dizaines de m). Ces derniers recristallisent soit de façon statique sur des gneiss migmatitiques, soit dans des bandes de cisaillements ductiles (photo r et t). De plus, le plan d'aplatissement principal des "patches", lorsqu'ils sont déformés, est systématiquement parallèle à la foliation régionale. Ainsi, le développement du faciès des granulites a été, au moins en partie, contemporain de la déformation régionale.

En résumé, le développement des grandes structures décrochantes N20 et N160, la mise en place du batholite du Closepet et le développement du métamorphisme régional granulitique sont les manifestations d'un seul et même continuum tectono-métamorphique.

Les données isotopiques

Si les données structurales obtenues dans les régions d'Holenarsipur et de Gundlupet sont concordantes et s'intègrent toutes dans un modèle de type instabilité gravitaire Raleigh-Taylor, les lacunes d'affleurements entre ces deux régions ne permettent pas d'assurer, sur la base des seuls arguments de terrains, que les déformations observées procèdent d'un même et unique événement tectonique. En outre, dans la région d'Holenarsipur se trouve posé le problème de la relation temporelle entre diapirisme et décrochement. C'est la raison pour laquelle un programme de datation radiométrique des paragenèses métamorphiques syn-diapiriques et syn-décrochements a été entrepris.

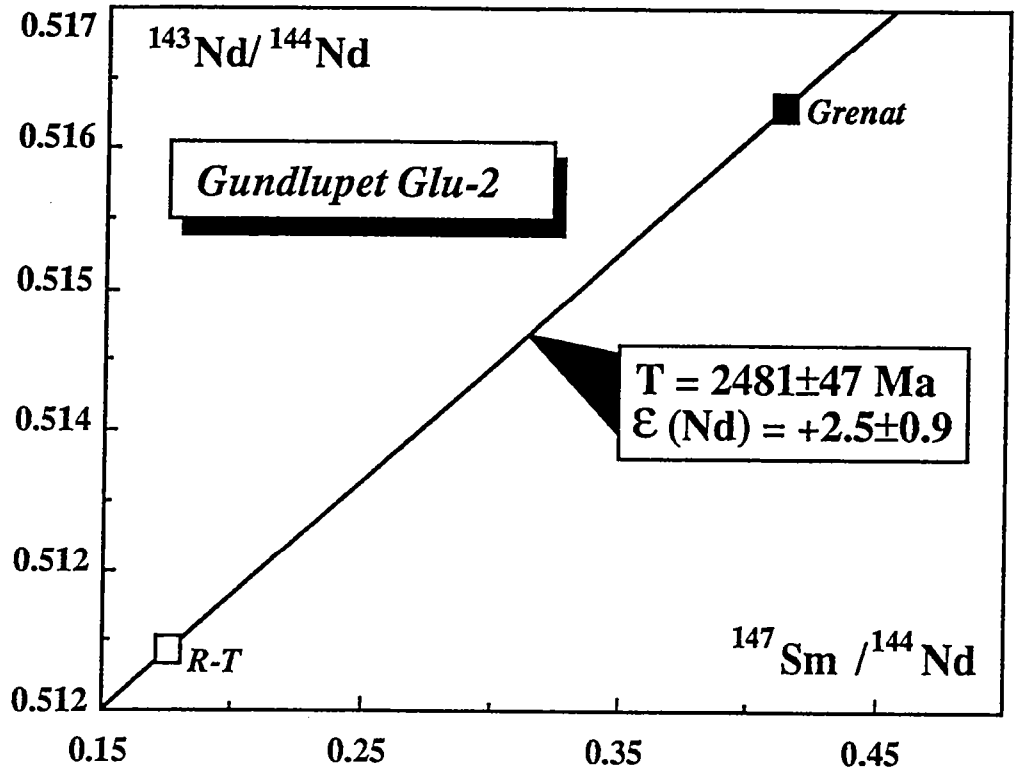

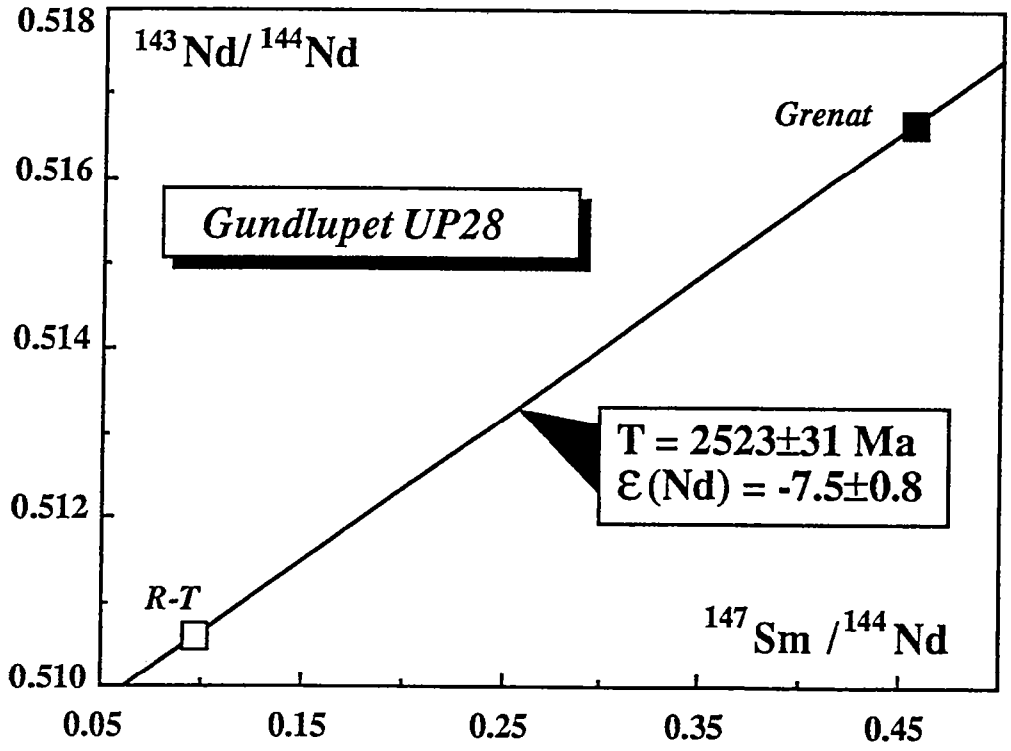

Fig. D. 53. Diagramme isochrone Sm-Nd pour les couples grenat-roche total des échantillons GLU 2 et UP 28 (secteur de Gundlupet).

Deux échantillons provenant de la ceinture d'Holenarsipur (112-OEA9A) et deux échantillons provenant de la ceinture de Gundlupet (GLU-2 et UP28) ont été analysés. Dans les quatre cas, les analyses ont porté sur les fractions roche-totale et sur des séparés de grenat. La méthode de datation utilisée est la méthode Sm-Nd.

L'échantillon OEA 112 a été prélevé dans la zone de décrochement senestre qui affecte la branche Est de la ceinture d'Holenarsipur (Fig. D. 51). Il s'agit d'un micaschiste à grenat, dont le plan d'aplatissement est vertical et orienté Nord-Sud. Les grenats présentent une foliation interne sigmoïdale marquée par l'alignement d'inclusions (quartz, opaques). La foliation interne passe en continuité à la foliation matricielle marquée par l'alignement de micas (principalement des chlorites et des biotites). Tous les porphyroblastes de grenat développent des zones abritées le plus souvent asymétriques. L'échantillon OEA 9A est une amphibolite à grenat foliée, dont la géométrie du plan d'aplatissement s'intègre parfaitement dans le champ de déformation régional diapirique du secteur d'Holenarsipur. Ce niveau basique est intercalé dans une métapélite, présentant une seule et même paragenèse syntectonique (cf : échantillon DOM). Les échantillons GLU-2 et UP-28 sont localisés dans la partie Sud du craton, dans le secteur de Gundlupet. Ces échantillons foliés présentent un plan d'aplatissement qui s'intègre parfaitement dans le champ de déformation régional diapirique inhérent à ce secteur. L'échantillon UP-28 est un gneiss migmatitique à grenats (photo). Les jus de fusion issus de la migmatitisation s'accumulent généralement entre les boudins de roches gneissiques résiduelles. Ces derniers sont systématiquement allongés parallèlement à la foliation régionale. Lorsque les jus migmatitiques sont injectés, ils sont plissés perpendiculairement à la foliation régionale. L'échantillon GLU-2 provient d'une série de roches mélanocrates basiques à grenats dilacérée parallèlement à la foliation régionale. Ces roches apparaissent en enclaves dans les gneiss migmatitiques précédents.

Les résultats isotopiques Sm-Nd présentés ici ont tous été obtenus au laboratoire de géochimie-géochronologie de Géosciences Rennes. Les procédures de dissolution et de séparation chimiques des échantillons, ainsi que les méthodes d'acquisition des rapports isotopiques du Nd sont décrites dans Gruau et al. (1992). Tous les rapports $^{143}Nd/^{144}Nd$ mesurés ont été normalisés à $^{146}Nd/^{144}Nd=0.7219$. Pendant la durée de cette étude, le sel de Nd La Jolla a donné un rapport $^{143}Nd/^{144}Nd$ moyen de 0.511844±4 (10 analyses). Les calculs isochrones ont été effectués en utilisant la méthode de

York (1969). La constante de désintégration du ^{147}Sm utilisée est 0.00654 Ga^{-1}.

Résultats et conclusions

Les résultats Sm-Nd sont présentés dans le Tableau 7 et reportés dans des diagrammes isochrones dans les figures D. 52 (Holenarsipur) et D. 53 (Gunlupet). Pour ce qui est de la région d'Holenarsipur (**Fig. D. 52**), les âges obtenus sont concordants et compris dans une fourchette 2470-2530 Ma. Aucune différence significative n'est observée entre l'échantillon provenant de la zone de décrochement (112 ; T=2473±10 Ma) et celui provenant de la zone de déformation diapirique (OEA 9A ; T= 2527±34 Ma). En ce qui concerne la région de Gunlupet (Fig. D. 53), la même concordance est observée (T=2481±47 et T=2523±31 Ma). De plus la fourchette des âges (2480-2520 Ma) est identique à celle obtenue pour les échantillons de la ceinture d'Holenarsipur.

Les âges Sm-Nd aux alentours de 2500±30 Ma définis par les quatre paires grenat/roche-totale analysées sont comparables aux âges U-Pb sur monazite (2510±10 et 2517±10 Ma) récemment obtenus par Peucat et al. (1993) pour des échantillons de gneiss et de charnockites provenant de la région de Krishnagiri (zone de transition amphibolite-granulite au Sud-Est de Bangalore). Ces âges sont aussi très proches de l'âge U-Pb sur zircon de 2513±5 Ma obtenu par Friend et Nutman (1991) pour la mise en place du granite du Closepet.

Comme pour tous les âges isotopiques sur minéraux, l'interprétation des âges grenat/roche-totale obtenus ici dépend de la connaissance de la température de blocage du système Sm-Nd dans le grenat. Les études récentes conduites par Mezger et al. (1992) montrent que cette température de blocage est ≥600 °C. D'après certains auteurs (Cohen et al., 1988 ; Jagoutz, 1988), cette température pourrait même avoisinée 800 à 900°C. De telles températures sont de l'ordre de, ou supérieures, aux températures déduites des assemblages métamorphiques présents dans les ceintures du sud de l'Inde (600±50°C). En conséquence, les âges de 2500±30 Ma que nous obtenons doivent être interprétés comme l'âge de cristallisation des paragenèses à grenat présentes dans les ceintures de Gunlupet et d'Holenarsipur. Une telle interprétation est cohérente avec les résultats obtenus par Peucat et al. (1993) sur les monazites des gneiss de Krishnagiri, étant entendu que le système U-Pb des monazites est censé se fermer lui-

aussi à T≥600 °C (Parrish, 1990). La similitude des âges monazites obtenus sur les granulites de Krishnagiri et des âges grenat/roche totale obtenus dans le cadre de cette étude permet en outre de considérer la cristallisation de ces grenats comme faisant partie intégrante de l'événement métamorphique régional à 2500 Ma responsable du développement du faciès granulite plus au sud (régions de Kabbaldurga et Krishnagiri).

En conclusion, les datations Sm-Nd des assemblages à grenat présents dans les ceintures d'Holenarsipur et de Gunlupet montrent que ces assemblages ont tous cristallisé vers 2500±30 Ma. Le caractère syn-diapirique et/ou syn-décrochement des paragenèses datées nous permet en outre (i) de relier les déformations de type instabilité gravitaire vues à Holenarsipur et à Gunlupet à un seul et même événement tectonique ; et (ii) d'établir le caractère quasi-synchrone des événements décrochants et diapiriques intervenant au niveau de la ceinture d'Holenarsipur.

N° Echant.	Fraction analysée	Sm (ppm)	Nd (ppm)	$^{147}Sm/^{144}Nd$ (1)	$^{143}Nd/^{144}Nd$ (2)
	Holenarsipur				
112	roche-totale	4.794	16.200	0.1789	0.512035±15
112	grenat	4.304	2.832	0.9214	0.524143±09
	Holenarsipur				
0EA 9A	roche-totale	2.060	10.300	0.1208	0.510927±05
0EA 9A	grenat	1.330	2.790	0.2885	0.513722±04
	Gunlupet				
GLU 2	roche-totale	2.470	8.480	0.1761	0.512430±4
GLU 2	grenat	1.990	2.910	0.4138	0.516319±8
	Gunlupet				
UP 28	roche-totale	2.270	14.52	0.0945	0.510556±5
UP 28	grenat	0.680	1.240	0.4584	0.516610±7

(1) L'erreur sur ce rapport est de ±0.2%.
(2) Les erreurs présentées sur ce rapport son les erreurs obtenues lors de l'analyse spectrométrique. Les vraies erreurs, intégrant les blancs de réactifs et les écrarts de reproductibilité sont estimées être de l'ordre de ±20.
(3) Valeurs calculées en prenant des rapports $^{143}Nd/^{144}Nd$ et $^{147}Sm/^{144}Nd$ pour la Terre Globale actuelle égaux à 0.512638 et 0.1967, respectivement.
(4) Ages modèles T_{DM} exprimés en millions d'années. Valeurs calculées en prenant des rapports $^{143}Nd/^{144}Nd$ et $^{147}Sm/^{144}Nd$ pour le Manteau Appauvri (DM) actuel égaux à 0.513151 et 0.2137, respectivement.

Table 7: Résultats isotopiques Sm-Nd pour les échantillons d'Holenarsipur et de Gunlupet

3. SYNTHÈSE : MODÈLE ÉVOLUTIF POUR LA CROÛTE CONTINENTALE ARCHÉENNE DU CRATON DE DHARWAR

Les modèles de l'évolution tectonique et métamorphique de la croûte continentale archéenne du craton de Dharwar reposent soit sur des considérations pétro-géochimiques (Krogstad et al., 1989, Newton, 1990) soit sur des études satéllitaires (Drury & Holt, 1980, Drury et al, 1984). Sur ces bases, les interprétations de ces différents auteurs convergent toutes vers une même hypothèse : l'évolution tectono-métamorphique du craton de Dharwar résulte d'une collision continentale avec un épaississement crustal d'origine tectonique (chevauchements).

L'étude présentée dans cette thèse repose principalement sur la construction puis l'interprétation des champs de déformation d'échelle cartographique. Cette approche, à laquelle nous avons joints une étude des conditions du métamorphisme ainsi qu'une étude géochronologique nous a permis d'établir les points suivants :

1 - Les champs de déformation sont le résultat de l'interférence entre (i) un développement d'instabilités gravitaires d'origine diapirique et (ii) un raccourcissement régional sub-horizontal de direction Est-Ouest.

2 - Les instabilités gravitaires affectent tous les niveaux structuraux étudiés (depuis le faciès des schistes verts au Nord jusqu'au faciès des granulites au Sud). Dans cette perspective, nous proposons que les variations de géométrie des ceintures de roches vertes du craton de Dharwar soient l'expression du développement d'un réseau d'instabilités gravitaires de type Raleigh-Taylor en partie connecté (Talbot et al., 1991).

3 - Les champs de déformation sont incompatibles avec la présence de structures chevauchantes ou d'empilements.

4 - L'ensemble de ces déformations (diapirisme et raccourcissement) caractérise un même événement tectono-métamorphique que nous avons daté aux environs de 2.5 Ga. Ce dernier est marqué par (i) un épisode de formation de croûte continentale juvénile (batholite du Closepet) et (ii) un métamorphisme régional parfois intense (migmatisation, granulitisation).

5 - L'étude pétrographique révèle que seules certaines zones diapiriques dont la subsidence a été la plus rapide, ont enregistré une évolution prograde avec une augmentation de pression de 3 à 7-8 kbar. De plus, ces régions montrent une hétérogénéité dans la composition de la phase fluide qui semble être associée à une différence de perméabilité

induite par la nature et l'orientation des textures des roches métamorphiques.

En résumé, la croûte continentale archéenne du craton de Dharwar, ne montre pas de structure tectonique susceptible d'avoir généré un épaississement crustal important. Sa déformation est due principalement à des forces de volume (diapirisme) et dans une moindre mesure à des forces de surface (décrochements).

Partie E

DISCUSSION

1. TECTONIQUE DE LA CROÛTE CONTINENTALE ARCHÉENNE: UN SCHÉMA ÉVOLUTIF SIMPLE

SOFT ARCHEAN LITHOSPHERE DURING PERIODS OF CRUSTAL GROWTH OR REWORKING

P. Choukroune, H. Bouhallier and N. T. Arndt
Géosciences, Université de Rennes 1,
Campus de Beaulieu, 35042 RENNES CEDEX, France

Abstract

Field observations, and an analysis of the strain field, have been carried out in Archean terranes of the Hebei province in the Dharwar craton of India, the Sino-Korean craton in China, and the Man shield in Ivory Coast.

Two broadly different situations can be recognized. In the Dharwar and Man Shields the deformation shows a range of characteristic features. The foliation trajectories outline dome-and-basin structures in which supracrustal rocks of greenstone belts invariably occupy the basins. The foliation trajectories are perturbed only by bands of transcurrent shearing. Variations in deformation directions depend essentially on the geometry of plutonic or migmatitic bodies within which the foliation invariably has a domal form. Changes in the intensity of deformation are essentially limited to boundaries between granitoids and supracrustal series. These changes are largely horizontal. Characteristics of the finite strain ellipsoid (the parameter k) vary extremely rapidly.

The second situation is manifested in the Hebei province where the Archean crust has deformed without the preservation of domes and basins. Here the deformation is characterized by a the presence of a foliation and a very strong vertical flattening which extends into catazonal domains. This deformation is homogeneous.To explain these observations we propose that this homogeneous deformation was superimposed on pre-existing dome-and-basin structure, obliterating the original geometry. The Hebei example represents a stage of deformation greater than that of the Ivory Coast, which in turn is greater than that in the India craton.

It is apparent that the Archean crust has specific characteristics that controlled the manner in which it deformed. During accretion, or reworking, it was dominated by body forces related to differences in the densities of the two major Archean lithological units - granitoid and greenstones. Deformation resulting from boundary forces then led to a second type of behaviour controlled by a vertical planar anisotropy induced during the first stage.

These characteristics are never reported in modern orogenic belts, which generally are marked by a uniform structural trend and vergence. We propose that Archean cratons completely lacked a rigid element during the accretion events responsible for their formation, that the thermal regime in these periods was quite unlike that of today, and that the continental crust formed or was reworked during episodes of enhanced mantle plume activity.

I. Introduction

The concept that Archean cratons have a structure fundamentally different from that of modern orogenic belts arose when it was noticed that these regions contain a great abundance of granitoids and felsic gneisses, and that metavolcanics and metasediments are commonly confined to discontinuous, often cusp-shaped belts between felsic bodies. McGregor (1951) popularized the concept in his description of the "gregarious" granites of the Rhodesian (now Zimbabwe) Craton, and the satellite view of the domes and basins of the Pilbara craton has become a geological classic. Nonetheless, the precise manner in which these structures formed, and, more specifically, whether they resulted from processes like those on the modern Earth, have long been subjects of debate (see for instance Fyfe ,1974, Platt, 1980). In the past five years a wave of papers has appeared in which it is argued that the model of plate tectonics can be adapted to Archean times, and that thrusting on a scale comparable to that seen in the Alpine chain and other modern mountain belts has contributed to the thickening of an Archean protocrust that formed part of a rigid lithosphere. These ideas have to reckon with certain remarkable lithologic, metamorphic and structural characteristics of Archean cratons, which, although sometimes ignored, are of immediate relevance to the question of how the Archean Earth operated.

(a) High-pressure low-temperature metamorphism has not been reported from regions older than 2.5 Ga.

(b) The volume of magmatic material in Archean terrains is exceptionally large: the Archean was without doubt a major period of continental crust formation (e.g. Taylor and McLennan 1985, Nelson and DePaolo, 1985).

(c) Neither oceanic crust, nor sutures, have been identified in Archean regions. In certain papers, typical greenstone belt volcanics are compared with mid-ocean ridge basalts (e.g. Helmstaedt et al, 1986, de Wit et al, 1987), but in our opinion, none of these reports is convincing (see also Bickle, this volume). On the other hand, the characteristic lithological duality of Archean granite-greenstone belts is absent from more modern regions: Archean sequences commonly comprise two assemblages of contrasting composition, a granitoid assemblage (TTG, or tonalite-trondhjemite-granodiorite) and volcano-sedimentary material (the greenstone belts).

(d) Many Archean terranes lack an obvious linear trend. This is especially noticeable in regions older than 3 Ga such as the Pilbara of Australia (Collins 1989) where the strain field is highly unusual, being marked by abrupt changes in strike and dip of the strain axes, and large variations in the axial planes of structures: a dome-and-basin geometry is characteristic and widespread. In younger regions, such as the Superior Province of Canada or the Yilgarn of Australia, linear belts are developed (e.g. Card 1990, Clowes et al, 1992) but the dome-and-basin geometry remains .

The debate about Archean dynamics can be phrased in terms of two extreme models. In the first, boundary forces are assigned a dominant role. The existence of rigid microcontinents is assumed, even at the earliest stages of accretion, and the margins of these continents are thought to deform during collisions comparable to those on the modern Earth. In the second model, the role of body forces is seen as more important. These forces, which act in the interiors of the protocontinents, result in vertical displacements related to gravitational instabilities that stem from crustal fusion and the density differences between the two major Archean lithologic assemblages, the granitoids and the greenstone belts.

In the following sections we describe three examples that may illustrate different stages of the deformation that has affected Archean continental crust. The three are the Dharwar craton in India, the Hebei province of the Sino-Korean craton in China, and the Man shield in West Africa. These examples provide evidence that the strain field had certain characteristics that were peculiar to this period of Earth history. We

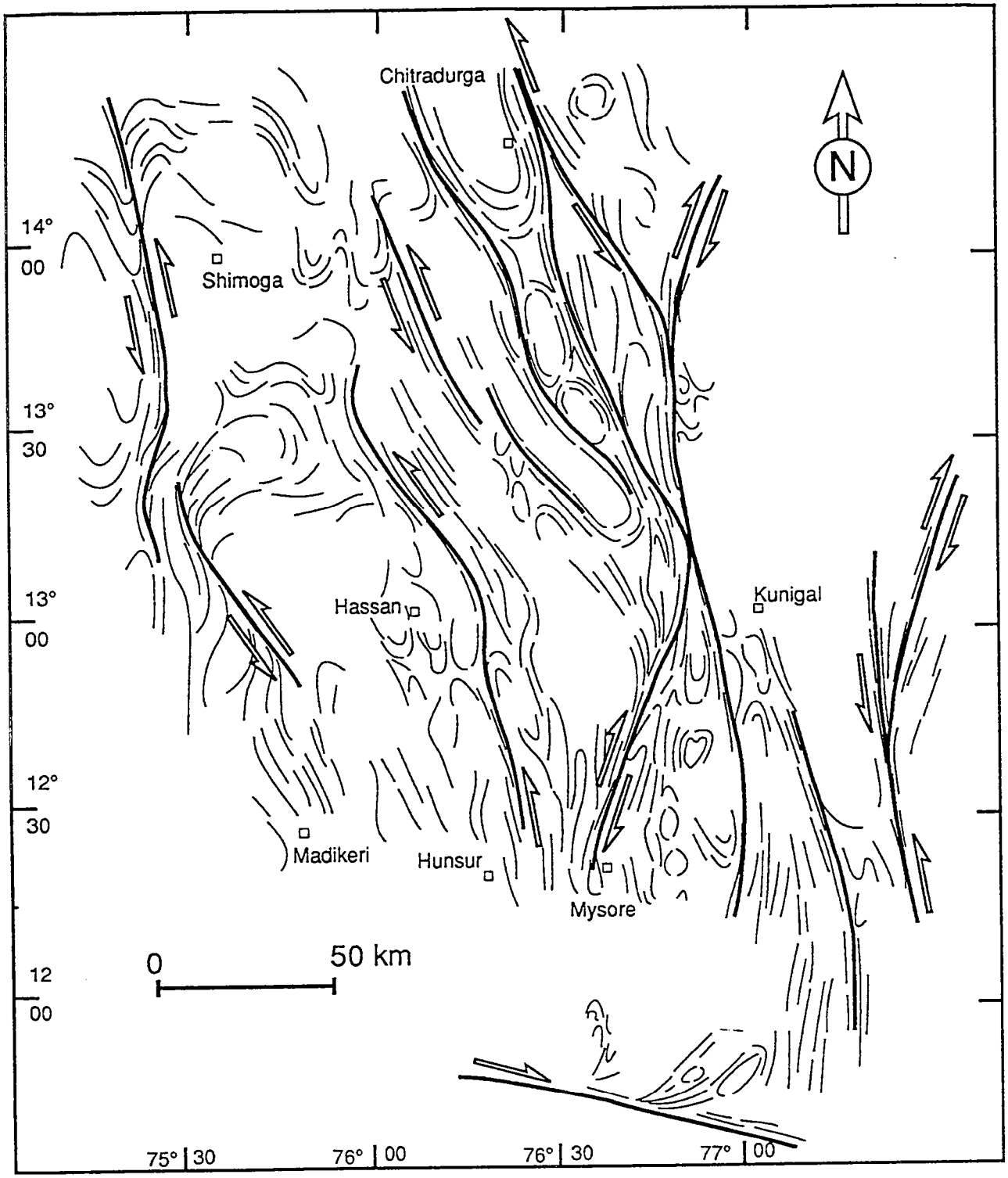

Fig. E. 1. (a) Structural map of the central Dharwar Craton showing domal structures affected by later transcurrent shearing.

Fig. E. 1. (a) Carte structurale de la partie centrale du craton de Dharwar montrant des structures en dômes affectées tardivement par un épisode cisaillant décrochant.

recognise that certain features that might be thought of as characteristic of the Archean cratons are also found in modern orogenic belts, but we emphasize that the scale of these structures is very different. We do not deny that thrusts are present in Archean terranes but will argue that where recognise that certain features that might be thought of as characteristic of the Archean cratons are also found in modern orogenic belts, but we emphasize that the scale of these structures is very different. We do not deny that thrusts are present in Archean terranes but will argue that where convincingly documented, these are relatively minor features not to be compared with those that characterize modern orogenic belts. Thus we will defend the idea that the tectonic processes active during the events that formed or reworked Archean continental crust were fundamentally different from those which dominate in modern orogenic domains.

II- Examples

1. The Dharwar craton

Lithologies

The Archaean terrains of southern India mainly consist of linear and arcuate, low- to high-grade volcano-sedimentary belts ("greenstone", "supracrustal" or "schist" belts) surrounded by larger regions of high-grade infracrustal rocks (Naqvi and Rodgers, 1983; Swami Nath and Ramakrishnan, 1981; Rhadakrishna and Naqvi, 1986). These are associated with low-K tonalitic, trondhjemitic and granodioritic gneisses (TTG series) with ages between 3.35 Ga and 2.5 Ga (Crawford, 1969; Venkatasubramanian, 1975; Beckinsale et al., 1980, 1982; Monrad, 1983; Stroh et al., 1983; Taylor et al., 1984; Drury et al., 1986; Taylor et al., 1988; Meen et al., 1992). The greenstone belts have been divided into two types (Swami Nath et al., 1976) on the basis of differences in metamorphic grade and structural evolution: the highly deformed Sargur type, and the less deformed Dharwar type (see Radhakrishna and Ramakrishnan, 1990). Although contacts between Sargur and Dharwar rocks are very scarce, there is some evidence that the Dharwar type rests uncomformably on rocks of the Sargur type and on TTG series gneisses (Chadwick et al., 1981; Viswanatha et al., 1982).

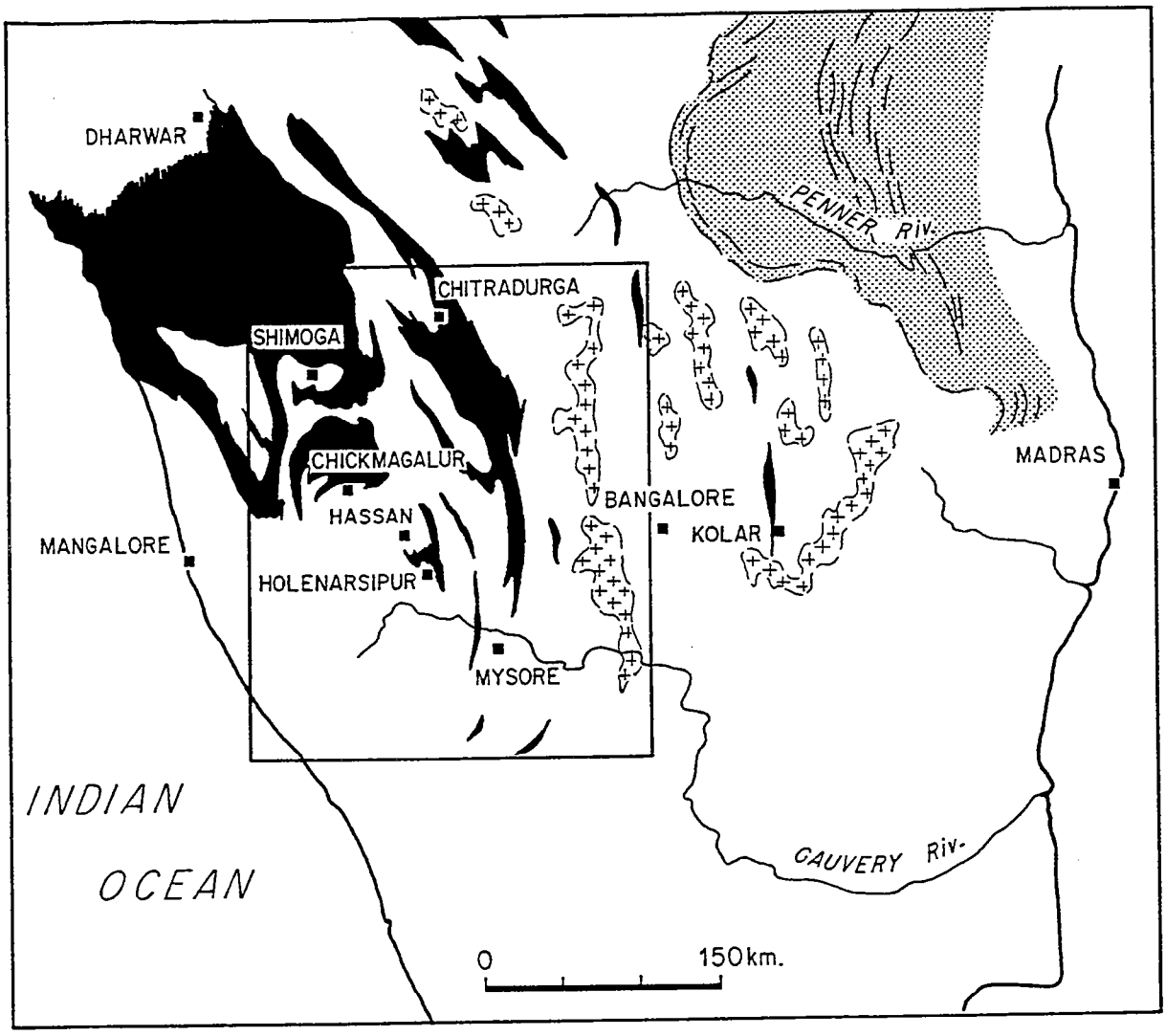

Fig. E. 1. (b) Geological map of the Dharwar craton showing the location of (a). Greenstone belts are black, late granitoids with crosses, Proterozoic belts with dotted pattern.

Fig. E. 1. (b) Carte géologique du craton de Dharwar indiquant la position de la figure (a). Les ceintures de roches vertes sont en noir, des granitoïdes tardifs marqués par les croix, les ceintures protérozoïques en pointillé.

Metamorphism

A characteristic feature of the Dharwar craton is the transition from a low- to medium-grade terrain in the north to a high-grade granulitic terrain in the south. Paleopressures in gneissic and mafic rocks increase from about 3 kbar in central Karnataka to ~8-9 kbar in the Sargur area (Harris and Jayaram, 1981; Janardhan et al., 1982; Raith et al., 1982; Hansen et al., 1984; Raase et al., 1986). The southward P-T gradient is perpendicular to the general N-S structural trend of the craton (Drury and Holt, 1980).

The Closepet granite, a late Archaean batholith dated around 2.5 Ga (Crawford, 1969; Friend and Nutman, 1991, Jayananda et al., 1992), extends for almost 400 km from north to south of the craton, and is clearly linked to a period of major migmatization that affects the surrounding gneisses and supracrustal rocks (Friend, 1983). The southernmost part of the Closepet batholith is overprinted by granulites (Janardhan et al., 1979a,1982; Friend, 1981,1983; Hansen et al., 1987; Stähle et al., 1987).

Structure

The strong N-S-trending fabric of the Dharwar craton is partly the result of a late Archaean transcurrent ductile shearing episode (Fig. E. 1) (Drury and Holt, 1980; Drury, 1983; Drury et al., 1984; Chadwick et al., 1989) that was contemporaneous with the emplacement of the Closepet granite (Jayananda and Mahabaleswar, 1991). Here we describe the Holenarsipur and the Gunlupet areas, two complementary areas that typify of the structural evolution of the craton.

(1) Holenarsipur Belt.

Holenarsipur is a cusp-shaped greenstone belt surrounded by domes of felsic gneisses, in the central medium-grade part of the Dharwar craton, (Hussain and Naqvi, 1983). Several generations of intermediate to felsic plutonic rocks comprise a TTG infracrustal sequence. These rocks, which have now been transformed into highly strained gneisses, are grouped together in the Holenarsipur region under the term "Gorur gneisses". Mafic to ultramafic volcano-sedimentary supracrustal units make up the second lithology (Naqvi et al., 1983b).

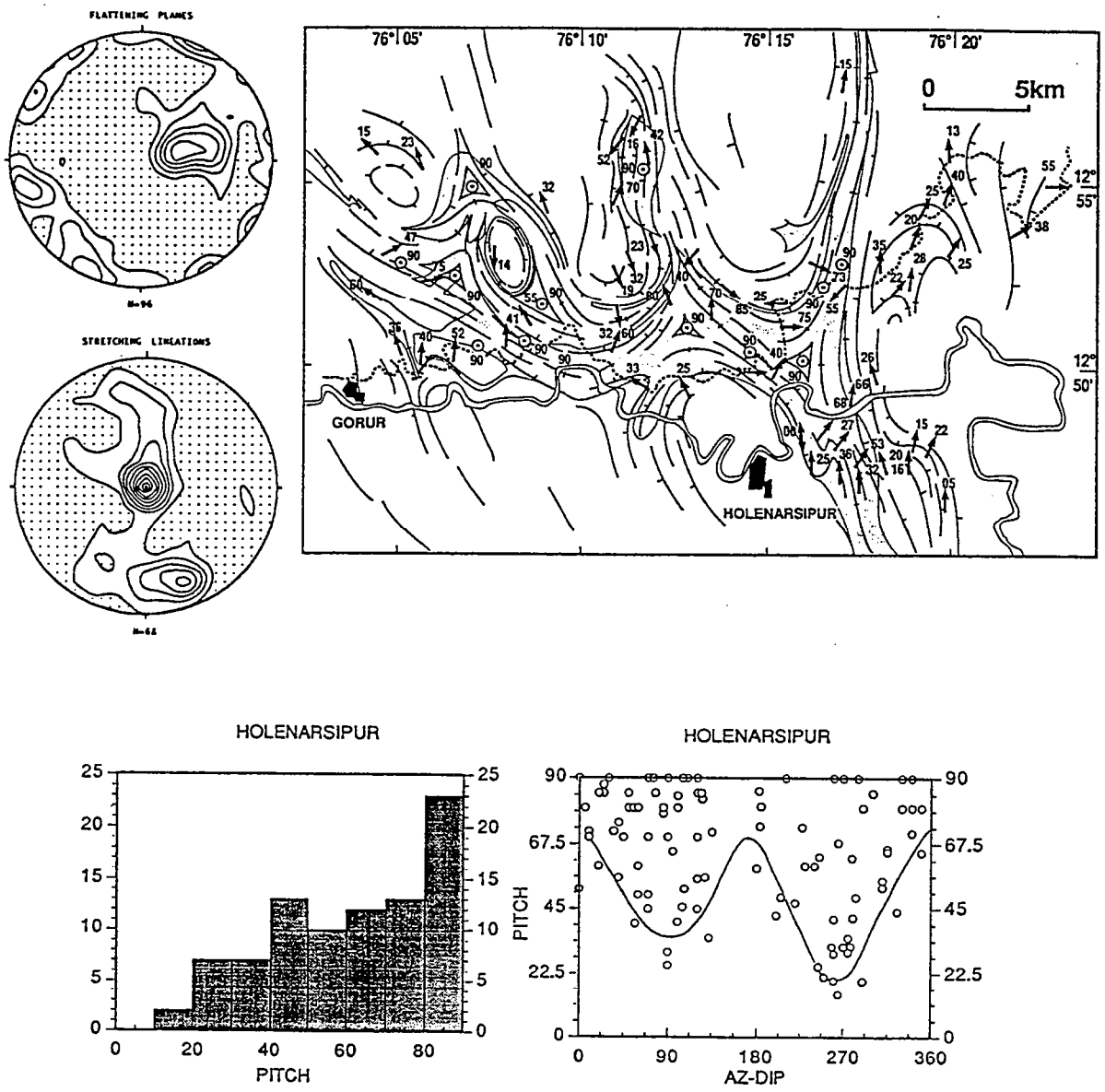

Fig. E. 2. (a) Map of strain trajectories in the Holenasipur area. Greenstones shown in grey ; TTG in white. (b) Stereodiagrams of foliation planes and stretching lineations. (c) Histograms showing the predominance of high pitches of lineation. (d) Pitch vs. orientation of foliation planes (AZ-dip) showing that the lowest pitches of lineations are confined to NS foliation planes associated with strike-slip motions.

Fig. E. 2. (a) Carte des trajectoires de la déformation dans la région d'Holenarsipur. Les "roches vertes" sont représentées en gris ; Les TTG en blanc. (b) Diagrammes stéréo des plans de foliation et des linéations. (c) Histogrammes montrant la prédominance du nombre de linéations associées à un fort pitch. (d) Pitch vs. l'orientation des plans de foliation (AZ-dip) montrant que les pitches des linéations les plus faibles sont systématiquement associés à des mouvements décrochants.

The gneisses have yielded Rb-Sr (Beckinsale et al., 1980, 1982) and Pb-Pb ages (Taylor et al., 1988) between 3.35 Ga and 3.305 Ga. They are intruded by trondhjemitic plutons dated using various methods between 3.2 and 3.0 Ga (Beckinsale et al., 1982; Bhaskar Rao et al., 1983; Monrad, 1983; Stroh et al., 1983; Taylor et al., 1984; Meen et al., 1992; Peucat et al., 1992). The entire area was metamorphosed at amphibolite facies.

The main structural feature of the Holenarsipur area is a regional foliation that affects both supracrustal and infracrustal rocks. This foliation (S1) is characterised by a wide variability in dip and strike (Fig. E. 2 and E. 3). Foliation trajectories (Fig. E. 2) outline a dome-and-basin structure within which supracrustal rocks occupy the synforms and infracrustal rocks the elliptical domal antiforms. At contacts between supracrustal and infracrustal rocks, which are invariably vertical, the foliation is strongly developed and steeply dipping: in the central part of the domal structures, it is less pronounced and has very shallow dips. At these places the intrusive rocks have a relatively isotropic fabric.

Between elliptical domes, a triangular arrangement of the vertical S1 foliation defines triple junctions (Brun, 1983a). These are present in both supracrustal and infracrustal rocks. The triple junctions are preferred sites for trondhjemitic intrusions and quartz-tourmaline veins which indicate major channelised fluid circulation.

The S1 trajectory map also shows a highly foliated linear zone along the eastern boundary of the supracrustal belt. The foliation here is always near vertical and the strike is 170°. This linear part of the belt differs significantly from the dome-and-basin pattern of the surrounding areas.

The attitudes of lineations, like those of the foliations, gradually change from gently plunging in the cores of domes to near vertical at contacts of supra- and infracrustal rocks. In supracrustal rocks, the stretching lineations are generally downdip, except at the linear, easternmost boundary of the supracrustal belt where they are mainly horizontal or plunge gently northward. Within the triple junctions, stretching lineations are well developed and invariably vertical (Fig. E. 2).

The shape of the finite strain ellipsoid (Flinn, 1965) was estimated using four different types of rock fabric (Schwerdtner et al., 1977) (Fig. E. 3), each easily distinguishable in the field. A high variability in the distribution of fabric types throughout the area is demonstrated by the following observations:

- In the central parts of the domes, fabrics are poorly developed .

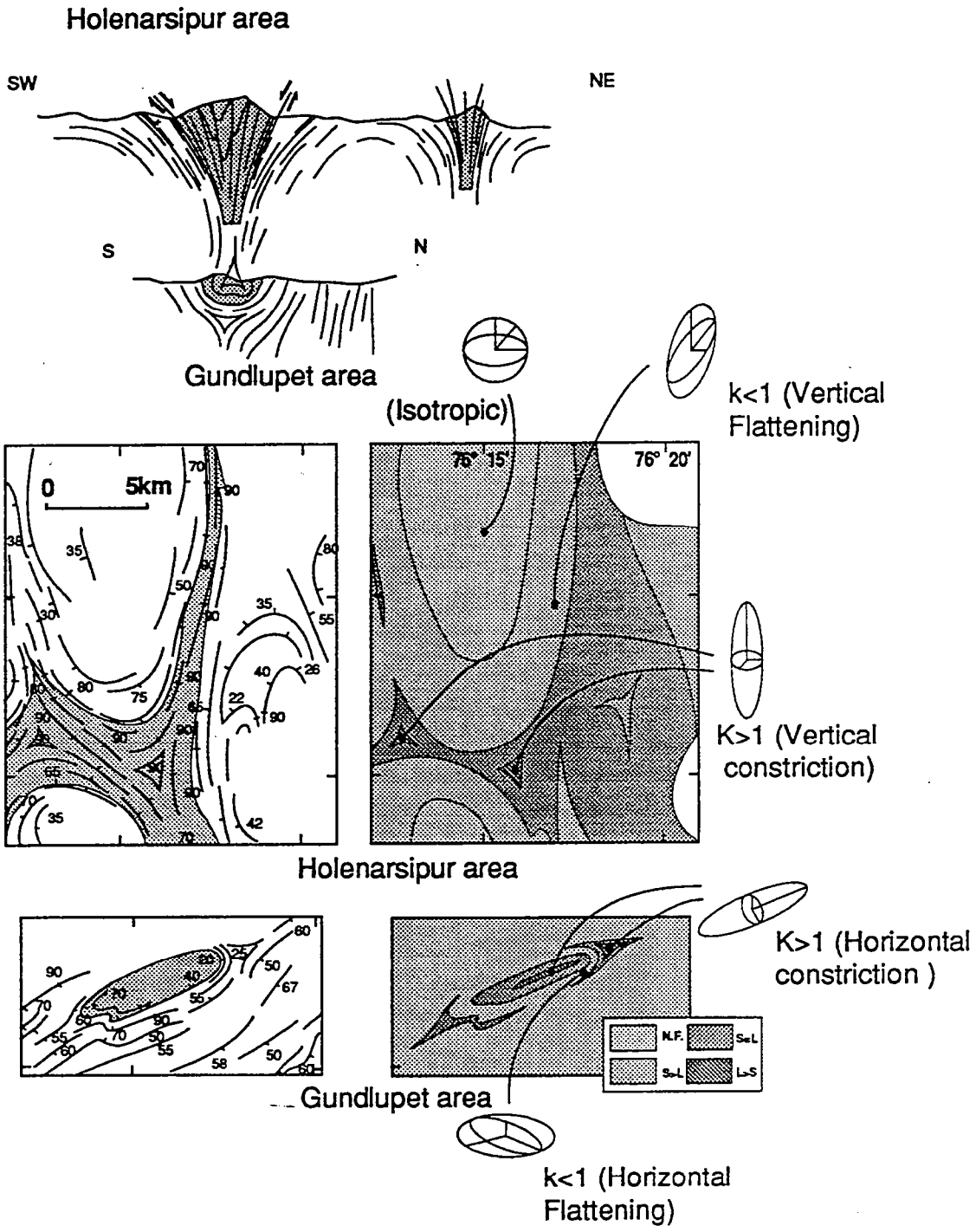

Fig. E. 3. Cross-sections, and maps of foliations and fabrics, of the Holenasipur and Gundlupet areas, Dharwar Craton. For further explanation see text. In the cross-section our interpretation of the structural relationship between the two areas is shown : the Gunlupet area exposes a deeper level than the Holenasipur area.

Fig. E. 3. Coupes et cartes des foliations et fabriques des régions d'Holenarsipur et de Gundlupet, craton de Dharwar. Se reporter au texte pour d'avantage d'explications. On montre sur la coupe notre interprétation des relations structurales entre ces deux régions : la région de Gundlupet présente un niveau structural plus profond que celle d'Holenarsipur.

- Planar fabrics characterise two-thirds of the study area. This fabric is present in areas where the S1 foliation plane exhibits major variations in dip. It dominates in sectors where the foliation is vertical, and is ubiquitous throughout the supracrustal belt, except near its eastern boundary.

- Planar-linear fabric zones are present in two different settings. At margins of triple junctions, planar elements define the triangular arrangement, and lineations are vertical. In the linear zone at the eastern N-S boundary of the belt, lineations dip more gently.

- In the centres of triple junctions the fabric is entirely linear and vertical.

Using kinematic indicators of the type defined by Choukroune et al. (1987), Bouhallier et al. (1992) analysed the sense and direction of shearing and outlined two areas of distinctly contrasting data. The first, which includes the dome-and-basin structures, displays kinematic criteria indicating vertically downward displacements of supracrustal belts relative to the TTG basement (Fig. E. 2). The second, which is restricted to the N-S linear zone at the eastern margin of the belt, is dominated by horizontal sinistral displacements. These trajectories are compatible with those observed by Drury (1983), Chadwick et al. (1989) and Jayananda and Mahabaleswar (1991) in shear zones in surrounding parts of the Dharwar craton (Fig. E. 1).

(2) The Gunlupet area

In the Gunlupet area, ~100 km south of Holenarsipur, supracrustal rocks are highly metamorphosed and limited to small, discontinuous lenses within the gneisses (Fig. E. 1). As in the Holenarsipur belt, a strong and penetrative foliation affects both supracrustal and infracrustal rocks and shows a wide variation of dip and strike. At map scale, foliation trajectories outline domes of infracrustal rocks and basins of supracrustal rocks. However, in the Gundlupet area the basins are elliptical and the domes linear, in contrast to the situation in the Holenarsipur area where both elements are more circular. Another important feature is the local presence of a strong horizontal foliation in the central parts of basins.

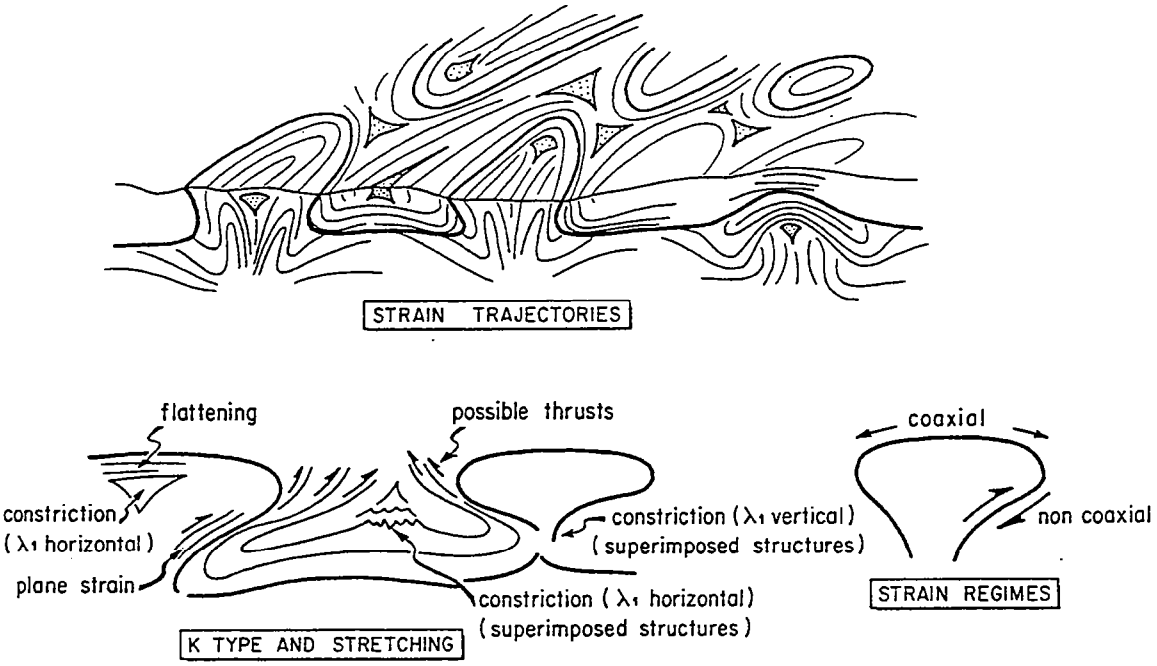

Fig. E. 4. Diagrams of strain trajectories, variations in the type of strain ellipsoid and strain regimes in a medium affected by diapirism. The pattern is inferred from the experimental data of Dixon (1975) and Dixon and Summers (1983), augmented by our field observations.

Fig. E. 4. Diagrammes des trajectoires de la déformation, des variations du type de l'ellipsoïde de la déformation et des régimes de la déformation d'un niveau affecté par le diapirisme. Le modèle est tiré des travaux expérimentaux de Dixon (1975) et de Dixon & Summers, (1983), auxquels nous avons ajouté nos propres observations de terrain.

At contacts between supra- and infracrustal rocks, the foliation is well developed and the strain is very high. At each end of the synformal basins, a triangular arrangement of gently dipping S1 foliations defines a triple junction (Fig. E. 2). The main axes of triple junctions plunge gently and are oriented parallel to: (a) the long axes of the elliptical basins, (b) contacts between supra- and infracrustal units, and (c) the trajectories of stretching lineations, which at a regional scale, plunge gently or are almost horizontal.

The distribution of fabrics throughout the area varies as follows:

- Isotropic zones, and zones of poorly developed fabric, appear absent;
- Planar fabric zones are common in the infracrustal rocks, particularly in regions far from supracrustal rocks.
- Planar-linear fabric zones are developed in the central parts of supracrustal basins, around triple junctions, and at contacts between supra- and infracrustal rocks;
- Linear horizontal fabrics are restricted to the centres of basins, and to triple junctions outside the basins (Fig. E. 2).
- Linear vertical fabrics are absent.
- Apparently superimposed structures occur wherever linear fabrics are mapped. Although some of these were described by Janardhan et al. (1979b) in terms of polyphase deformation, they are simply related to the constrictive nature of the finite strain ellipsoid.
- Evidence of non-coaxial deformation during the main tectonic event is lacking.

Discussion

The dome-and-basin structures affected all rock types - granitoids and greenstones - and the domes appear geometrically unrelated to the intrusion of any of the dominant TTG lithologies. The centres of the domes are not occupied by granitic intrusions. Throughout the granitoids and even in the greenstones, evidence of partial melting in the form of veins and migmatitic patches is observed. Some of the migmatites are strongly deformed by the doming event, others retain their magmatic textures. These observations suggest that the domes formed during the deformation of a pre-existing granite-greenstone sequence during a major period of metamorphism and migmatization.

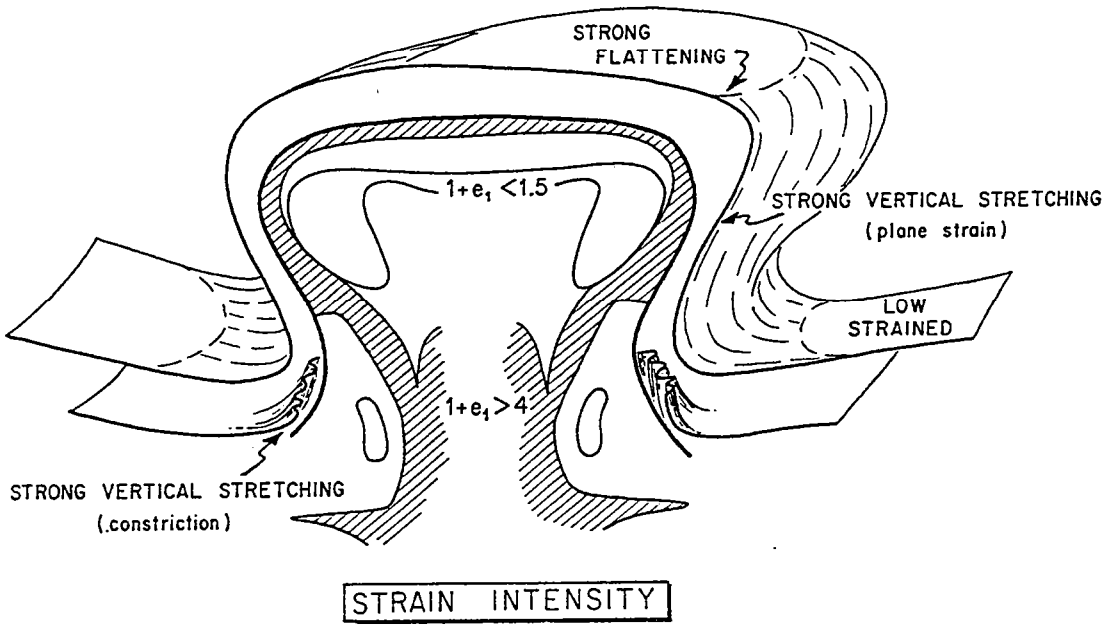

Fig. E. 5 Variations of strain intensity within a diapiric dome (from Dixon, 1975), and in the surrounding area (from Brun, 1983).

Fig. E. 5. Variations de l'intensité de la déformation dans un dôme diapirique (d'après Dixon, 1975), et dans l'encaissant (d'après Brun, 1983).

The style of deformation associated with the dome-and-basin structures is characterized by a number of highly significant features: (a) the locations of superimposed structures coincides with domains in which the deformation ellipsoid is constrictive; (b) the spatial variations of strain intensities and strain ellipsoid type are highly variable, and (c) regions of non-coaxial deformation are restricted to the contacts between supra- and infracrustal series. This combination of features allows only one interpretation, that the deformation resulted from relative vertical displacements between ascending masses of migmatitic gneisses and descending regions of supracrustal rocks (Dixon, 1975; Gorman et al., 1978; Schwerdtner et al., 1978; Bouhallier et al., in press).

In the Holenarsipur area, supracrustal rocks are confined to linear synformal basins that connect with triangular areas where the strain is intense and the fabric strong, linear and vertical. Infracrustal rocks form elliptical domes with poorly developed fabrics in central parts and intense planar fabrics at contacts with supracrustal rocks. The orientation of regional stretching lineations is mainly downdip. Obvious kinematic indicators, where present, indicate non-coaxial deformation during the main tectonic event, and vertically downward displacements of supracrustal rocks relative to the TTG basement.

In the Gundlupet area, supracrustal rocks are confined to elliptical synformal basins whereas infracrustal rocks form linear domes. Vertical linear fabrics are absent, and strong horizontal linear fabrics are restricted to basin centres (Fig. E. 2). The regional stretching lineation is mainly horizontal, the regional deformation is nearly coaxial, and there is no evidence of relative displacement between supra- and infracrustal rocks. Diapirism is again the best explanation for these features. Key observations that support a diapiric origin of structures in the Gundlupet area include the parallelism of foliation trajectories with contacts between supra- and infracrustal rocks, the increase of strain at these contacts, the locations of triple junctions, and the specific organization and distribution of the strain regimes, as illustrated in Fig. E. 4 and Fig. E. 5.

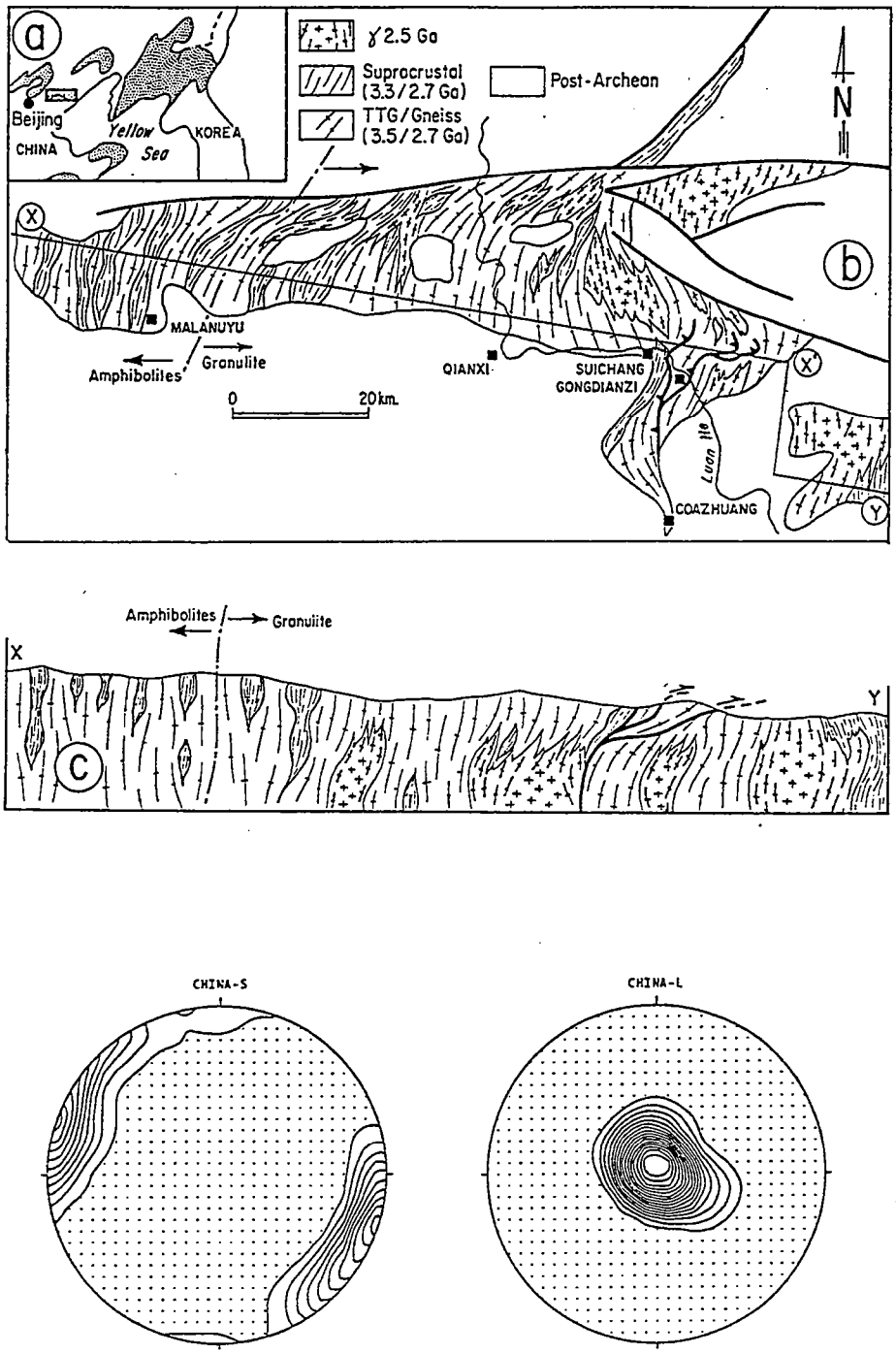

Fig. E. 6. (a) Location in China of the part of the Hebei province treated in this investigation ; (b) map (adapted from an unpublished map of Y. Gang) ; (c) section showing the geology and structure of the region ; (d) stereodiagrams of foliations and lineations (112 measurements). Note the vertical foliation along the entire section, except in the thrust zone which is Proterozoic.

Fig. E. 6 (a) Emplacement géographique de la province chinoise de Hebei présentée dans cette étude ; (b) carte géologique (modifiée d'après une carte non publiée de Y. Gang) ; (c) coupe montrant la géologie et la structure de la région ; (d) diagrammes stéréo des foliations et des linéations (112 mesures). Remarquez la foliation verticale sur la totalité de la coupe, à l'exception de la zone chevauchante qui est d'âge protérozoïque.

From the southward increase of paleopressures (Harris and Jayaram, 1981; Janardhan et al., 1982; Raith et al., 1982), it might be expected that the contrasting structural features of the two areas might be related to their origins at different levels in the crust. The same structures probably are exposed in each area, and differences between them can be attributed to differences in crustal level - deeper for Gundlupet where syntectonic assemblages are granulitic, than for Holenarsipur where assemblages are amphibolitic (Bouhallier, work in progress). For these reasons we propose that the roots of the infracrustal and elliptical domes that outcrop in the Holenarsipur area may be found in the long and linear domes of the Gundlupet area, and the supracrustal elliptical basins of the Gundlupet area may represent deeper levels of inverted diapirs whose upper reaches are exposed as linear connected synforms in the Holenarsipur area (Fig. E. 2).

The principal conclusion is that crust-scale dome-and-basin structures can explain the geometry and kinematics of all the features revealed by the structural analysis of Holenarsipur and Gundlupet areas. These diapiric structures, which are locally affected by zones of horizontal shearing, are the only recognizable structures in the Archaean continental crust of Dharwar craton.

It is useful now to recall the numerous experimental studies that serve as a basis for the interpretation of deformation fields related to gravitational instabilities. These analogue or numerical models allow discussion of the geometry and mechanics of these instabilities (Biot and Ode, 1965; Anketell et al., 1970; Berner et al., 1972; Talbot, 1977; Mareschal and West, 1980; Marsh, 1982; Schmeling et al., 1988), as well as the deformation fields within them (Dixon, 1975; Dixon and Summers, 1983), and the patterns of interference between them (Brun, 1983a,b). Numerous field studies have demonstrated the utility of applying these concepts to natural structures, and the majority of these come from Archean terrains (Schwerdtner, 1984; Schwerdtner et al., 1977,1978, 1980,1983,1985; Brun et al., 1981; Drury, 1977; Collins, 1989; Ramsay, 1989; Delor et al., 1991). Recently Schwertner (1990) reported that certain aspects of the strain field associated with dome-and-basin structures in the Superior Province of Canada, do not conform to that predicted by the diapirism model. Although he was not able to present a convincing explanation for certain features, such as high K-values in triple junctions, he preferred a model of superimposed folding essentially because a lack of tensile bending in the domes, the presence of a synformal granitic sheet and a coherent vergency

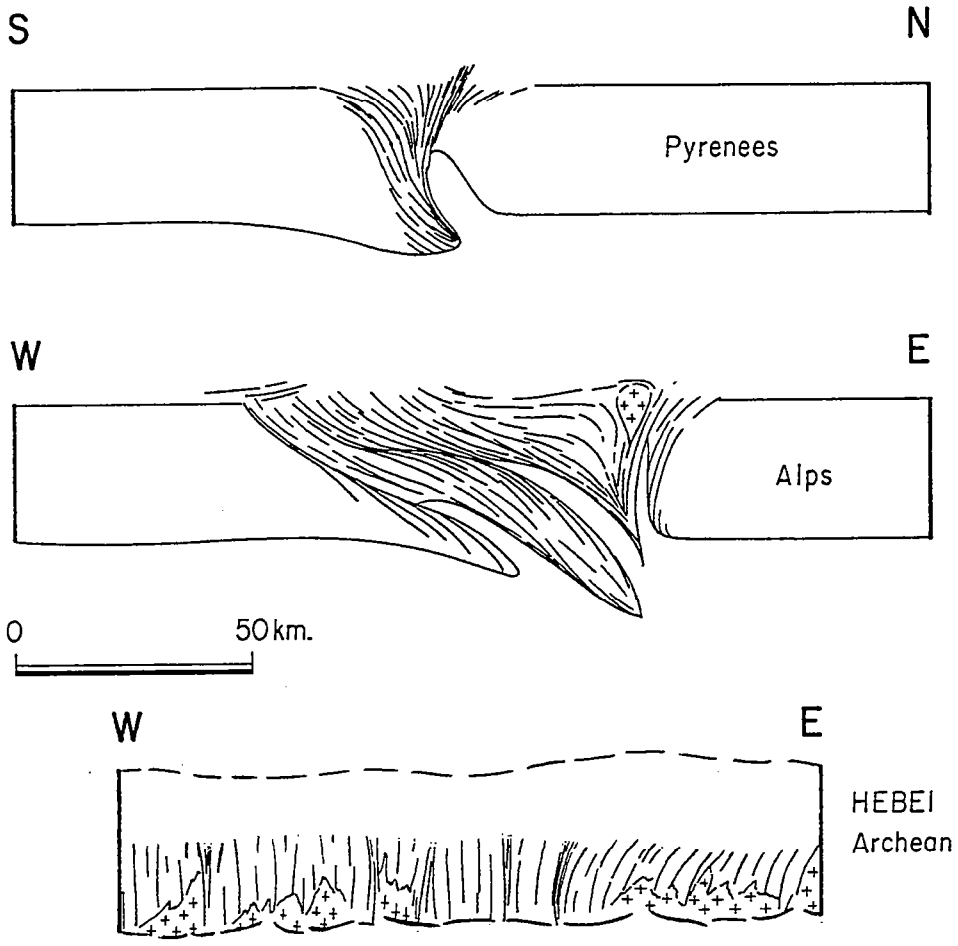

Fig. E. 7. Strain pattern observed in the Hebei region compared with that of two segments of the Alpine chain. The diagrams are drawn at the same scale in order to highlight the great distance over which foliations are consistently vertical in the Hebei region.

Fig. E. 7. Allure du plan d'applatissement de la région de Hebei comparée à celles de deux segments de la chaîne alpine. Les coupes sont présentées à la même échelle afin de montrer la particulièrement longue distance où les foliations sont uniformement verticales dans la région de Hebei.

of folds. Such an interpretation cannot be applied to the examples we studied in India where strain intensity, K values, strain regimes and location of superimposed folding are controlled by the geometry of a given dome, are consistent from one dome to another and from one synformal greenstone unit to another.

It is also important to note that, in the Dharwar craton, there is absolutely no record in the deformation field of crustal thickening by stacking of thrust slices, as may have operated before the initiation of gravitational instabilities. Either such thrusting never happened, or all trace of it has been lost, a circumstance that to us seems highly improbable.

Finally, we note that the deformation field is disturbed by transcurrent shearing which was contemporaneous with the emplacement of the Closepet granite (Jayananda and Mahabaleswar, 1990) and which affected the entire thickness of the Archean crust from greenschist- to granulite-facies regions. We stress that this heterogeneous deformation was related to a thermal episode that affected a vast area of the proto-continent and from near the surface to close to its base.

2. *The Hebei Province, China*

The Hebei province is situated in the northern part of the Sino-Korean craton, an Archean terrane that makes up the entire substratum of northern China (Fig. E. 6). The region has been the object of various geochemical and geochronological investigations, but structural work in the Archean terrains has been limited to several studies of a local and applied nature. In this report we present a 140 km long structural section which is a suitable vehicle to demonstrate that the entire region has been intensely deformed and transformed under catazonal conditions.

Lithologies

In the study area, the distinction between various lithological units and the establishment of a sequence of evolution is not straightforward. Liu et al. (1990) have proposed that, in the west, a single term - the Qianxi complex - should be applied to a complex group of gneissic and supracrustal rocks. However, the same type of material in the eastern Suichang-Coazhuang section has been divided by Sills et al. (1987) and Wang et al. (1990) into two units on the basis of geochemical and geochronological data (Pidgeon, 1980; Jahn et Gang, 1984; Huang et al., 1986; Jahn et al., 1987; Liu et al., 1985; Liu et al., 1992).

The first unit, called the Coazhuang gneissic complex, is older than 3.5 Ga and is made up of supracrustal rocks intruded by felsic, TTG-type gneisses. The supracrustal sequences include mafic to felsic metavolcanics and metasediments such as fuchsite or sillimanite quartzites, marbles, kinzigites and banded ironstones. The second unit, the Suichang gneissic complex, contains equal portions of supracrustal formations and granitoid intrusions with intermediate - monzogranitic and granodioritic - compositions. The depositional age of the supracrustal units is quite well constrained: they are intruded by 2.7 granitoids, and were probably deposited around 3.0 Ga, the age of rhyolites intercalated with the sedimentary rocks (Liu et al., 1990). As in the Coazhuang complex, the supracrustal units contain mafic to felsic metavolcanics and sedimentary rocks with compositions ranging from pelite to greywacke to BIF. The Coazhuang gneissic complex is observed only as disrupted fragments within the Suichang gneisses.

Both sequences, which appear to correspond to two distinct Archean cycles, were intruded 2.7 to 2.45 Ga ago by felsic plutonic rocks with widely variable compositions (gabbro-diorite, monzodiorite, granodiorite, monzogranite). All were affected by a major tectometamorphic event dated around 2.5 Ga (Pidgeon, 1980; Compston et al., 1983; Jahn et al., 1984; Liu et al., 1985; Liu et al., 1990). The youngest magmatic event was the emplacement of pegmatites at about 2.2-2.3 Ga (Liu et al., 1986).

Metamorphism

The entire Qianxi complex is metamorphosed, and in most of the region studied, the grade was granulite facies. Zhang et al. (1981), Zhang and Cong (1982), Sills et al. (1987) and Chen (1990) estimated conditions in the Coating region, in the SE part of our section, as P = 8 kbar and T = 820-840°. In contrast, in the western part of the section, the metamorphism was in the lower amphibolite facies with P = 4.5-6 kbar and T ~600-650° (Sills et al., 1987). Widespread but irregular retrograde metamorphism affected the granulites resulting in the replacement of orthopyroxene, clinopyroxene, and in some areas garnet, by hornblende and biotite. This event probably was post-Archean (Jahn et al., 1984).

Structure (Fig. E 6)

Along the entire 140 km length of our section, all the lithologies described above display a **regional vertical foliation**, the nature of which attests to a pronounced homogeneous **vertical flattening** (Choukroune et

al., 1993). The intensity of finite strain is documented by markers such as pillows in metabasalts from the Shangshuan region, in which the ratio of long to short axes is now 10:1. The only units to have escaped this deformation are the youngest granodioritic plutons, which have essentially undeformed cores surrounded by extremely foliated margins.

The vertical foliation within the ortho- and paragneisses provides evidence of very strong flattening. The direction of major extension is vertical wherever displayed. Furthermore, the deformation seems entirely coaxial: microstructures such as pressure shadows and shear bands are almost always symmetrical, and features such as rotated mineral grains and sygmoidal structures in synkinematic minerals were not found.

On a map scale, the foliation is oriented roughly north-south (020°) in the southern part of the study area, and changes progressively to NE or ENE in the northern part. Local refraction at the margins of competent objects are occasionally observed. The change in regional trend in the north is consistent with a zone of dextral E-W shearing that forms a northern limit to the Archean domain. This phase is clearly younger than the major deformation and is related to an episode of transcurrent movement that affected potassic pegmatites dated at 2.2-2.3 Ga (Liu et al., 1986).

The deformation in mafic rocks is readily correlated with granulite facies metamorphism in the West and amphibolite facies metamorphism in the East. In the gneisses, the same phenomena are generally observed, even though certain charnockites display more static textures which probably result from post-deformation recrystallization. The intimate relationship between deformation and metamorphism receives further convincing support in thin sections which reveal deformation textures of a type that only form at high temperatures, such as the deformation of quartz by a prismatic "C-type" slip mechanism.

To sum up, we interpret the structure of the Archean parts of the Hebei province as the result of deformation that led to a strong, homogeneous vertical flattening and subsequent horizontal shortening. This deformation, which removed all trace of earlier tectonic episodes, was contemporaneous with major metamorphism at 2.5 Ga (Pidgeon, 1980).

The trajectories of the regional foliation appear to be well ordered along most of the section, and are only perturbed in the north by Proterozoic dextral shearing. In the small southeast segment of the cross-section, which follows the valley of the Luan river, the vertical foliation is affected by multiple horizontal shears, along which metre-wide cataclasites

are developed. These cataclasites display E-W lineations and asymmetric microstructures that indicate movement towards the East. The shearing also affects the 2.3 Ga pegmatites and therefore has the same age as the dextral movement evident at the northern margin of the Archean massif. In both cases the Archean material underwent greenschist-facies retrograde metamorphism. The Proterozoic deformation was clearly the last tectonic event to have affected the Hebei province, because the entire sequence is overlain discordantly by a thick tabular sedimentary series of conglomerates, quartzites and carbonates with ages between 1.7 and 0.6 Ga.

Discussion

The Archean of the Hebei province is characterized by a style of deformation that is highly unusual and has never been described in the deep zones of "modern" mountain ranges. In the latter, granulite episodes are related to a late stage in the evolution of the belts, and are manifested by the synmetamorphic development of a horizontal foliation that results from strong **vertical non-coaxial shortening**. Our understanding of the fabric of the present deep continental crust comes mainly from vertical seismic reflection studies. From such studies we know that the entire sub-basement of western Europe between 20 and 30 km depth is made up of a highly reflective domain that is occasionally exposed in Tertiary orogenic zones (Bois et al. 1991). In the Alps and Pyrenees, Brodie et al. (1989) and Bouhallier et al. (1991) have demonstrated that such domains are composed of horizontally foliated Hercynian granulites whose metamorphic evolution is related to tectonism that was locally non-coaxial and corresponded to global vertical shortening. Wherever exposed, such rocks have a generally horizontal foliation, as in the granulitic arc of Finland (Barbey, 1986). In fact we know of no example in the deep zones of recent mountain ranges of granulites subjected to strong horizontal shortening in a coaxial regime. The great intensity, and the peculiar style, of the syngranulitic deformation that accompanied the last Archean magmatic event in the deep crust of the Hebei province, constitutes important evidence of unusual and specific behaviour. In contrast with the situation in the Dharwar craton, where body forces apparently were dominant, boundary forces appear to have played an important role. During this event, the Archean crust behaved differently from that of crust involved in modern orogenic events.

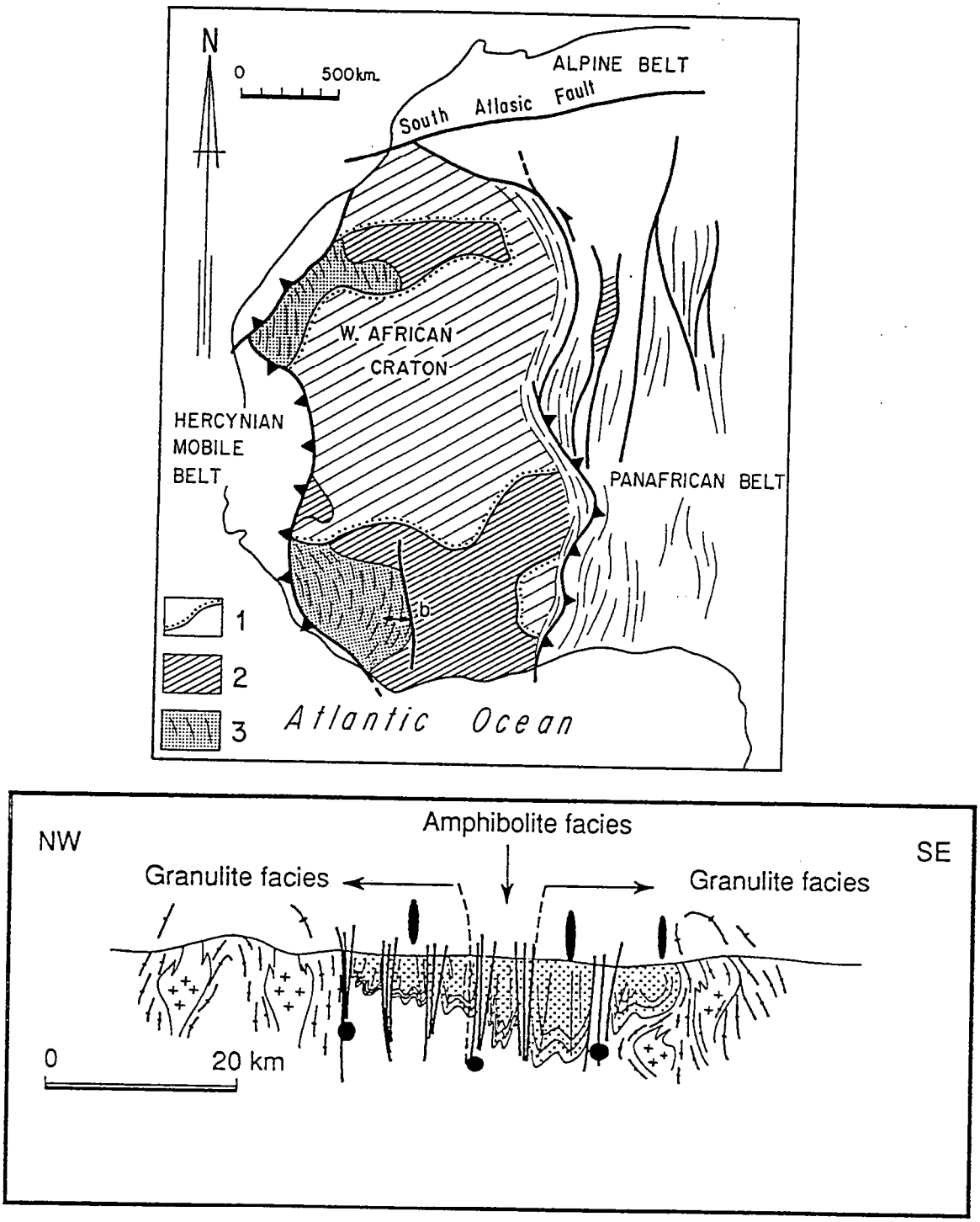

Fig. E. 8 (a) Location of the Man shield within the West African craton. 1 : Archean domains, 2 : Birrimian domains, 3 : Upper Proterozoic to Hercynian basins ; (b) structural cross-section near the city of Man : the supracrustal belt between two granitoid domes is strongly affected by vertical shears, implying horizontal shortening.

Fig. E. 8 (a) Emplacement du bouclier de Man au sein du craton Ouest africain. 1 : terrains archéens, 2 : terrains birrimiens, 3 : bassins d'âge protérozoïque supérieur et hercynien ; (b) coupe structurale près de la ville de Man : la ceinture de roches supracrustales, entre les deux dômes de granitoïdes, est fortement affectée par des zones de cisaillement verticales impliquant un raccourcissement horizontal.

3. *The Man Shield*

The Man shield is an Archean core preserved in largely Eburnean or Birrimian (2 Ga) terranes of the southern part of the West African craton (Fig. E. 7). Most of the shield is in Liberia, but parts extend to Sierra Leone and western Ivory Coast. In the Man region, the subject of the present study, the Archean region is limited to the east by the major Proterozoic Sassandra shear zone (Bessolles, 1977; Caen-Vachette, 1988; Camil et al., 1984).

Lithologies.

The oldest rocks are ~3.2 Ga TTG-type gneisses (Camil, 1984). A supracrustal series containing abundant quartzite (with or without magnetite) and aluminous paragneisses, and lesser mafic metavolcanics, constitutes a greenstone belt that extends 150 km in a NE-SW direction into Liberia. In the study region near the town of Man, the belt is confined between two granitoid domes.

The two classic Archean assemblages are largely migmatised and intruded by charnockites dated at 2.7 Ga and by late pegmatites dated at 2.5 Ga (Rb-Sr ages of Camil et al., 1984) This history is closely comparable to that proposed by Hedge et al. (1975) for similar lithologies in Liberia. There, a formation made up essentially of TTG has been assigned an age around 3.2 on the basis of Rb-Sr dating, and a period of major granitoid intrusion and migmatization has been related to a tectonothermal event during the period 2.7-2.5 Ga. In both regions the age of the supracrustal series is known only to be between 3.2 and 2.7 Ga.

Metamorphism

Almost all the study area has been subjected to high grade, granulite facies metamorphism, and only a small portion of the supracrustal material, in the centre of the greenstone belt, is of lower grade, in the amphibolite facies. Conditions during the major metamorphism associated with the intrusion of charnockites and the widespread migmatization of supracrustal rocks are estimated as P = 5-7 kbar and T = 750-850°C. This metamorphism is part of the tectonothermal event dated at 2.7 Ga. A final stage of retrograde amphibolite facies metamorphism is recognized in zones of late intense deformation (Camil 1984).

Structures

In a cross section of the Man shield (Fig. E. 8), the supracrustal series can be seen to occupy a central region confined between two gneissic domes (Man and Mt. Pekou domes) with vertical to slightly reversed margins. Within the domes, the style of deformation that affects the intrusive charnockites is closely comparable to that of the Dharwar craton, in that vertical lineations are very strongly developed on the flanks of the domes. There are, however, two important differences: the first is that the domes are more linear, and the domains at their summits, where foliations are flat, are elongated. In other words, the ellipticity of the domes is very pronounced. The second difference is in the style of deformation of the supracrustal series where zones of vertical foliation alternate repeatedly with numerous corridors of deformation in which the lineation is horizontal. These corridors are oriented preferentially in two directions; at 010°, the direction of sinistral ductile shearing; and at 060°, the direction of dextral ductile shearing. In the relatively sparse regions between the densely spaced shear zones, the structural characteristics of the migmatized supracrustals are well preserved. A strong syn-migmatitic vertical flattening, with a vertical principal stretching direction, is typical of these regions. Within the corridors, in contrast, the migmatites are retromorphosed and intensely sheared. At margins of gneissic domes the late deformation phase is responsible for the development of mylonitic zones, particularly at borders of charnockitic bodies. Structures indicative of deformation in a viscous state, as well as C/S structures, provide evidence that the late 2.5 Ga pegmatites were sheared during their emplacement.

Discussion

In the Man region it is difficult to constrain the kinematics of the processes responsible for the formation of the gneissic domes and supracrustal basins using field criteria. This is because most early structures were obliterated by the late shearing marked by a dense pattern of retromorphosed ductile-deformed vertical corridors which post-date the doming event. However, what remains of the early strain field is compatible with doming.

III Archean tectonics - a hypothesis:

As a working hypothesis, we propose that the regions described above represent three stages of Archean crustal deformation. We infer that the Archean continents were affected by tectonometamorphic events on a scale approaching or exceeding that of the exposed cratons. In India, a dome-and-basin geometry was developed throughout a region that encompasses all of the presently-exposed Dharwar craton. We have no idea of the original extent of these terranes, but a strong parallel between the geological evolution of the Pilbara in Australia, the Kaapvaal in South Africa, and the Dharwar craton suggests that all three regions may once have been parts of a much larger continent. Certainly the regions we studied provide only a minimum estimate of the area that developed a dome-and-basin structure related to a tectonothermal episode. It is important to add that these processes acted not only over a large area, but also affected the entire thickness of Archean crust. Contrary to the idea of Park (1982) who envisaged a zone of decoupling beneath a diapiric crust, we found evidence of domes at depths from 25-30 km (corresponding to the 8-9 kbar paleopressures in the southern part of the craton) to a few km below the surface.

Such structures are never produced in the same volumes in more recent orogenic belts: gneissic or migmatitic domes certainly exist, but they are restricted to specific domains in which crustal thickening by thrust stacking is important. During the Archean, crustal thickening by this mechanism is neither demonstrable nor necessary: the enormous quantity of juvenile material that accreted to the growing continents was alone sufficient to account for the thickening (Condie, 1990). In the Dharwar craton, the episodes of dome formation are invariably related to the addition of material and to a general migmatisation of pre-existing crustal rocks. Thermal phenomena thus accompanied the tectonic events, and this all happened on a scale very much larger than that represented by migmatitic or high-grade metamorphic domains in modern belts.

Consider again the examples of India and the Man shield. Although body forces and diapirism were responsible for the major structures of these cratons, the regions were also subjected to an additional episode of regional deformation contemporaneous with a large-scale thermal event, which was the result of application of boundary forces. The entire Dharwar craton was affected by transcurrent shearing, the organisation of which

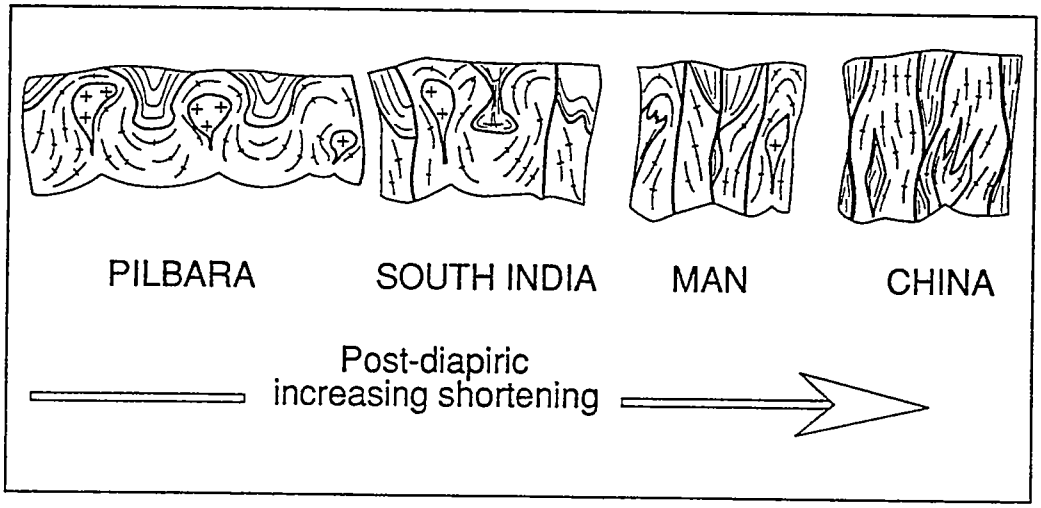

Fig. E. 9. Evolution of Archean crust, interpreted on the basis of our investigations in China, India and Ivory Coast. The intensity of post-diapiric horizontal shortening is minimal in the Pilbara (Delor et al. 1991) and reaches a maximum in the Chinese case.

Fig. E. 9. Schéma évolutif de la croûte archéenne interprété d'après nos investigations en Chine, en Inde et en Cote d'ivoire. L'intensité du raccourcissement horizontal post-diapirique est minimum dans le Pilbara (Delor et al. 1991) et atteint un maximum dans le cas de la Chine.

points to a shortening direction consistent with the ellipticity of the domes. This heterogeneous, globally coaxial, deformation is also contemporaneous with a major thermal event that is manifested in widespread migmatization and the emplacement of the enormous Closepet batholith.

The late Archean deformation is still better developed in the Man shield where zones of deformation related to the doming are cut by ductile shearing that modified the original structure. Here as well, a late magmatic event accompanied the heterogeneous deformation, the causes of which must be sought at the non-observable limits of the Archean craton.

Finally, the Hebei province of the Sino-Korean craton could be considered as the region where the post-dome phase of deformation is the most intense. This vertical, homogeneous and coaxial deformation affected even deep granulite-facies parts of the Archean crust regions during the late Archean thermal event. The deformation also involved a large volume of the crust. We assume that the dome-and-basin geometry is no longer observable in the region because these structures were completely obliterated by the intense deformation at 2.5 Ga.

There are strong analogies between the three regions. Each contains similar rock types, each was subjected to intense and widespread tectonic and metamorphic events, and each was affected by a specific and unusual type of deformation. To account for the differences in structural style illustrated in Fig. E. 9, we call on variations in the intensity of post-diapiric deformation. The explanation is entirely in accord with those advocated by Ermanovics and Davison (1976), Anhaeusser (1984), Hickman (1984), and Padgham (1992) for other Archean regions (though we admit that these authors are in the minority and that for each region there are many others who advocate alternative interpretations). The differences between the three regions discussed earlier could be due solely to variations in the action of boundary forces: the regions are distinguished only by the intensity of the horizontal shortening that followed the development of domes and basins (Fig. E. 9).

IV The Distinctive Character of Archean Deformation

(a) The question of Archean thrusting.

Archean thrusting has been described in all cratons, and, particularly in the past few years, sections through these cratons have been drawn in a style which suggests that the deformation was much the same as in modern orogenic belts (e.g. Drury et al., 1984; Swager et al., 1992; Hammond

and Nisbet, 1992; Treloar et al., 1992, Van Kranendonk and Helmstaedt, 1992). We dispute many of these interpretations and argue: (i) that the prevalence of thrusting has been strongly overemphasized in certain regions, and that certain examples postulated on the basis of field studies are suspect; (ii) that a certain type of thrusting can develop during entirely vertical movements; (iii) and that, even if certain thrusts signify truly tangential tectonics, their presence is not a sufficient criterion to refute a specific, non-modern behaviour of the Archean crust. Of the various examples of thrusting that have been attributed to tangential movements, several categories can be distinguished:

The first concerns thrusting that is apparently restricted to contacts between granite and greenstone, as in the examples described by Stowe (1984), Nutman et al. (1989), Ralser and Park (1992) and Van Kranendonk and Helmstaed (1992). In these examples, the geometry of the domes and the vertical orientation of the supracrustal series are acknowledged, but these characteristics are considered have developed late, following a regime of tangential tectonics which produced the large isoclinal folds responsible for multiple repetition of the series (Bickle et al., 1980; Kusky, 1992). We do not find these examples conclusive because they are not supported by data of the type needed to document the style of deformation. If the situation is indeed as described, it should be readily demonstrated by the superimposition (or interference) of two strain fields: the first, a result of tangential shearing, should be disturbed by a second phase related to the doming. We have seen that such superimposition cannot be demonstrated in India, where the deformation style is entirely compatible with the diapirism model. It is useful to recall that deformation accompanying doming introduces a foliation and may cause isoclinal folding, even at the earliest stage of doming. During continued development of the domes, the axial planes of the folds may be refolded, and segments of the gneissic and supracrustal series may be superimposed (Talbot 1974, 1977). This is the case in the Gunlupet region of the Dharwar craton, where such structures have developed in the complete absence of tangential tectonics. We believe that many of the thrusts described or drawn at gneiss-greenstone contacts are neither necessary nor proven.

The second case concerns thrusting within, and confined to, greenstone belts (Collins, 1989; De Wit, 1991; Corfu et al., 1989, Kidd et al., 1988). This thrusting, which never penetrates the boundaries with gneissic rocks, is readily explained by progressive deformation within portions of greenstone belt descending between rising gneissic domes. Gorman et al.

(1978) noted that the trajectories of such thrusting follow contours within the gneissic domes, and they developed the "sagduction" model to explain structures in the Abitibi belt, Canada. Collins (1989) applied similar reasoning to examples from the Pilbara in Australia. Neither the character, nor the significance of such thrusting can be compared with that associated with the regional-scale tangential tectonics that causes crustal thickening in the interiors of modern, linear orogenic belts.

The third case is that of thrusts at craton margins, such as those recognized between the Kaapvaal and Zimbabwe cratons (Light, 1982; McCourt et Wilson ,1992; Treloar et al., 1992) or in the Pontiac Group in the southern Superior Province in Canada (Camiré and Burg, 1993). The Limpopo belt is probably one of the few belts to have developed during late Archean (2.6 to 2.46 Ga) collision between pre-existing cratons. The extrusion of material from the belt, which had been granulitised in the course of the collision, was achieved by thrusting towards the north onto the Zimbabwe craton, and towards the south onto the Kaapvaal craton. The well-argued account of McCourt and Wilson (1992) contains several interesting points. The first is the age of the thrusting, which is confined to the latest Archean and thus to the latest period of crustal evolution, and not to an earlier stage, as commonly envisaged in other regions (Stowe, 1984, Ralser and Park, 1992, Van Kranendonck and Helmstaed, 1992). Under these circumstances it can readily be accepted that the cratons already had, at the time of their collision, a certain rigidity. The second is the location of the thrusts, which are restricted to a zone between the two cratons. The third is the fact that the collision failed to obliterate earlier deformation related to doming events in the interiors of the cratons. A parallel can thus be drawn with the examples that we discussed earlier in this article, in particular within the Dharwar craton, where the latest Archean deformation might be related to collision between cratons (Drury et al., 1984; Newton, 1990) even if no clear collisional zones can be directly observed.

(b) Important differences between Archean and Modern Thermotectonic Events.

Certain features of the three Archean regions strike us as essential and specific to this type of terrane, and thus crucial to the discussion of the characteristics of Archean crust.

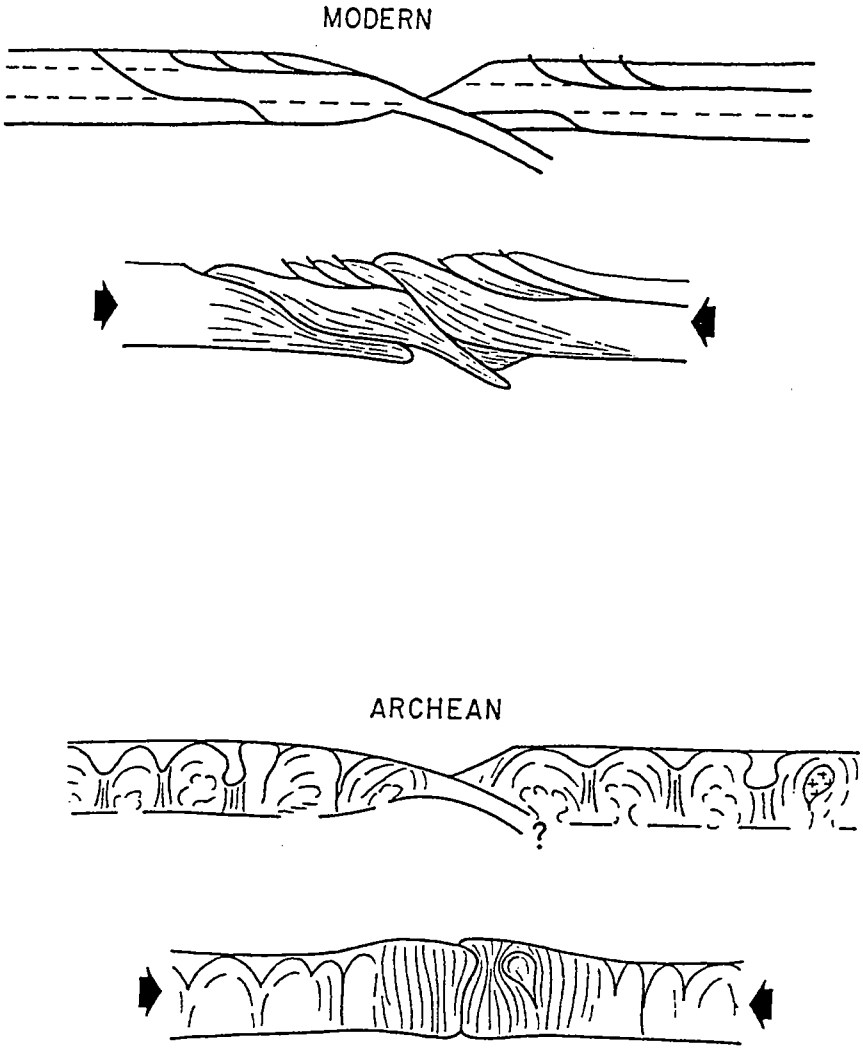

Fig. E. 10. Differences between the internal structures of Archean and modern crust, and the control these features exert when the crust is shortened. The principal difference is the presence in modern crust of roughly horizontal layers with contrasting resistence to deformation.

Fig. E. 10. Différences entre la structuration interne d'une croûte continentale archéenne et celle d'une croûte continentale moderne. Remarquer le contrôle qu'exerce l'héritage structural lorsque la croûte est raccourcie. La différence fondamentale est la présence, dans la croûte moderne, d'anisotropies planaires globalement horizontales

(i) In each region, repeated major thermal and tectonic events involved immense volumes of crust.

(ii) Thermal events in the Indian shield, and probably the Man shield as well, were responsible for triggering large-scale gravitational instabilities that led to the restructuring of the entire protocrust. The planar anisotropy resulting from this restructuring was on average vertical.

(iii) Late tectonometamorphic events had the effect of accentuating the vertical structure through heterogeneous shortening. This ranged from only moderate in the Dharwar and Man shields to intense in the Sino-Korean craton.

(iv) If major thrusting had ever taken place in the interiors of these cratons, all evidence of this process, be it geometric or kinematic, was completely erased by the later events.

We see two ways to explain these features: either the structures resulted from intrinsic properties of the Archean crust; or the thermal or kinematic boundary conditions that reigned during the Archean events were fundamentally different from those during the formation of modern belts. We start with the first explanation. The development of dome and basin structures during the earlier stages of the continental crust, implies **the absence of a zone of horizontal decoupling within this young crust** (Fig. E. 10). Furthermore, the Archean crust has a distinct fabric defined by vertical contacts between domes and supracrustal belts, a predominantly vertical layering within these two units, and vertical orientations of the basic dykes that fed the basalts of the greenstone belts. These features imposed a strong **planar and vertical anisotropy** that is absent from modern crust, which is more heterogeneous and in which the levels of resistance to deformation are horizontally disposed. These are fundamental differences. The Archean protocrust could be shortened essentially by exploiting the pre-existing vertical planes of flattening and/or by transcurrent shearing.

Less can be said about the second explanation, because any discussion of boundary conditions and kinematics in the Archean is inevitably poorly constrained. By contrast, it is relatively easy to discuss the thermal structure. We can state with some certainty that during Archean tectonic events, the entire crust was intensely and totally reheated. This had two major effects. First, the reheating led to the migmatization of enormous

volumes of sialic material, and the resultant decrease in density was the trigger of gravitational instabilities. Second the protocrust was softened, a process that is evident from the absence of contrast in the deformability of the different lithologies and the development of the exceptionally homogeneous character of the deformation, as in Hebei, for example.

We emphasize that the presence of a soft crust and absence of rigid lithosphere was temporary and not the normal situation during the Archean. We accept the evidence for the existence of thick lithosphere beneath the continents for much of the Archean (the existence of Archean diamonds, Richardson et al. 1984; the relatively subdued thermal gradients in Archean metamorphic terrains, Bickle, 1986, Richter, 1985). Nonetheless we propose that the rigid substratum of the continents was temporally destroyed during periodic events that either created or reworked continental crust.

V The Source of Heat and the Nature of Archean Tectonism

From the above descriptions and interpretations, it is evident that Archean continental crust was subjected to tectonothermal events during which new material was added (basalt and TTG) and the entire crust was deformed in a manner unlike that of modern crust. In developing a model to explain these processes we stress certain key points.

(1) During the main events, diapirism on a major scale affected the entire crust and was followed by a later period of large-scale homogeneous shortening: these observations indicate that body forces exceeded the yield strength of the crustal rocks.

(2) To change the strength of material with essentially the same composition as modern crust (granitoids with minor supracrustals), heat must have been added, again on a major scale.

(3) The nature and the scale of homogeneous shortening in the Man and Hebei shields indicates the absence of a rigid substratum during the deformation: i.e. during these events, the crust apparently was not underlain by resistant lithospheric mantle.

(4) The scale of such events - the volumes of crust involved and the quantity of heat added - are so large that only mantle sources can be considered.

(5) Traditional age dating, and studies of detrital zircons in modern river sediments by Goldstein and Arndt (1993) indicate that tectonothermal events were episodic throughout the Precambrian.

Major, sharp events at e.g. 3.1, 2.7 or 2.5 Ga were separated by longer periods of inactivity. This pattern contrasts with the quasi-continuous nature of modern crustal evolution (Arndt, 1992).

(6) The events in India, China and West Africa, whose ages correspond to those of the global events, mainly involved reworking of pre-existing continental crust. In other regions, such as the southern Superior craton at 2.7 Ga, the events started with komatiitic to basaltic volcanism, and climaxed with the production of large volumes of juvenile continental crust.

(7) During the Archean the mantle was hotter. Oceanic crust probably was thick (40-50 km; Sleep and Windley, 1982, Vlaar, 1986), and the lithosphere relatively thin (Bickle, 1986). The thickness of Archean continents is difficult to judge, but cannot have been much more than 40-50 km: a marked contrast between the thicknesses of continental and oceanic crust, as now exists, was not likely in the Archean.

We explain these features with a model involving mantle plumes. The essential features of the model are illustrated in Fig. E. 11. Three stages are shown, each involving interaction between plume and crust. In each stage the plume activity was thought to have been on a major scale, and episodic, triggered by an as yet unexplained mantle processes:

(a) The first case involves the arrival of a plume in a purely oceanic environment. High-degree melting within the plume as it approaches the surface leads to flood volcanism that spreads a thick layer of basaltic to komatiitic rocks on the 40 km thick oceanic crust (Desrochers et al. 1993). The plateaux may accrete in subduction environment leading to calc-alkaline volcanism and plutonism, or heat from the plume may thermally erode and eliminate the lithospheric mantle, leading to partial melting of basaltic crustal rocks and the emplacement of granitoids. The consequence is the formation of juvenile continental crust, as in the 2.7 Ga southern Superior province in Canada (Card, 1990), or the 3.5 Ga Pilbara craton (Bickle et al., 1983).

(b) The second case shows the arrival of a plume beneath pre-existing continental crust of the type that might have formed in the first stage. Here the crust and lithosphere were initially thick and the plume stalled at greater depths. The degree and the amount of mantle melting is therefore less. A significant proportion of the resultant basaltic magma did not penetrate the continental crust but was trapped within it. Volcanism was

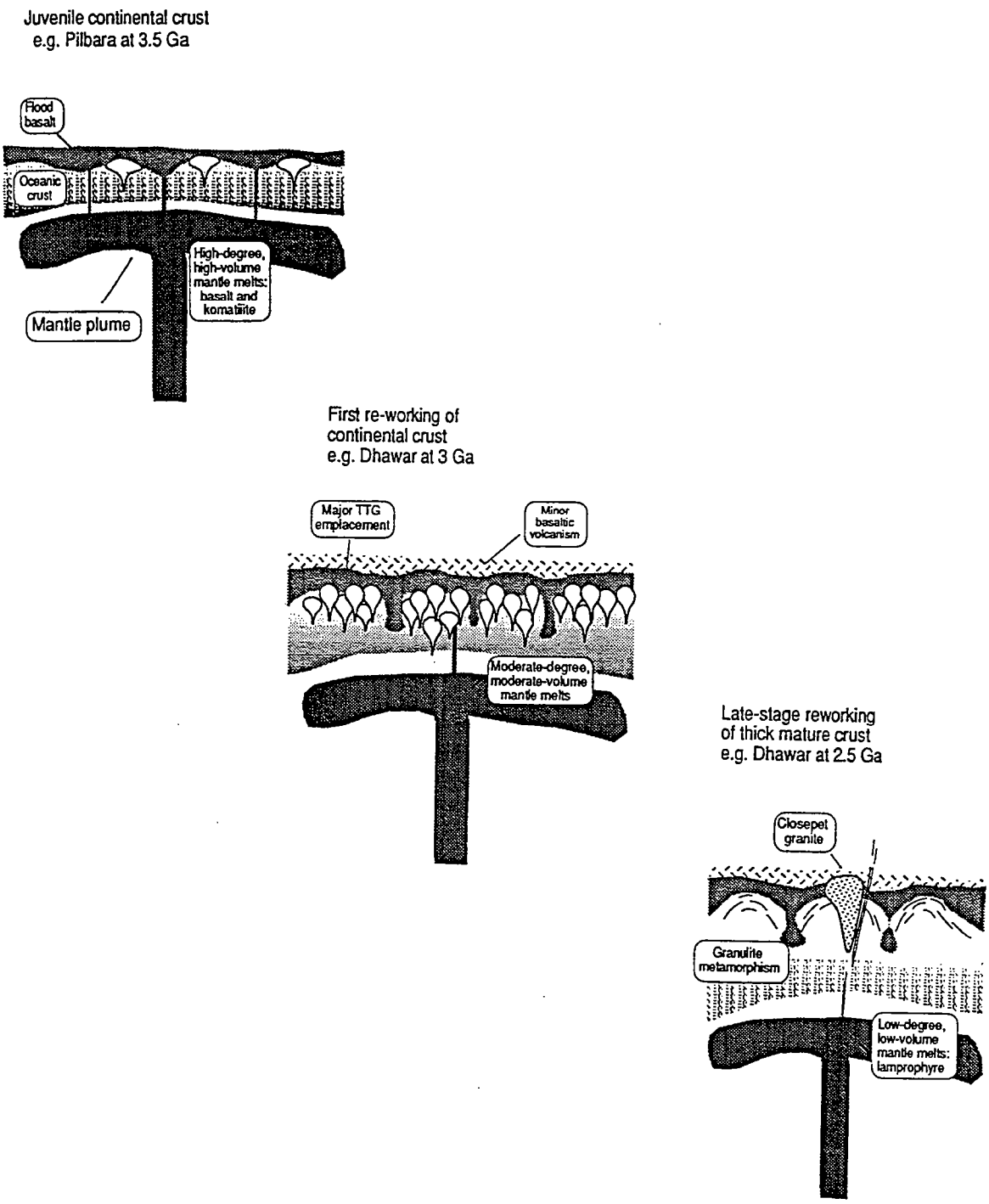

Fig. E. 11. Model of the evolution of Archean crust. For explanation see text.

Fig. E. 11. Modèle évolutif de la croûte archéenne. Voir le texte pour les explications.

subdued. The heat of the plume was nonetheless capable of eroding the lithosphere and causing melting at the base of the crust. The consequences are again the emplacement of granitoids and at a later stage, as heat from the plume migrates to higher levels in the crust, migmatization, metamorphism and diapirism of the type recognized in the Man shield and Indian craton.

(c) The third case shows a plume arriving beneath thick, mature lithosphere. The plume stalled at a greater depth and melting is minor. Only low-degree melts form and these penetrate only to the lower crust. Again the lithosphere is eroded and the lower crust melts, in this case to form intrusions like the Closepet granite of the Dharwar craton. The softened crust is then deformed, probably because of boundary forces whose origin is in the surrounding thick rigid oceanic crust. At this stage, the thick but soft continent was compressed and deformed homogeneously between thick, subduction-resistant oceanic plates, a tectonic set-up far removed from the modern situation.

RÉFÉRENCES BIBLIOGRAPHIQUES

RÉFÉRENCES BIBLIOGRAPHIQUES

Allègre, C.J. 1985. The evolving Earth system. *Terra Cognita*, 5: 5-14.

Anahausser, C.R. 1971. Cyclic volcanicity and sedimentation in the evolutionary development of Archaean greenstone belts of Shield areas. *Geol. Soc. Australia Sp. Publ.*, 3: 57-70.

Anahausser, C.R. 1976. Archaean metallogeny in South Africa. *Econ. Geol.*, 71: 16-43.

Anahausser, C.R. 1984. Structural elements of Archaean granite-greenstone terranes as exemplified by the Barberton Mountain Land, Southern Africa. *In Precambrian Tectonics Illustrated*, Kroner A. & Greiling R. editors, 57-87.

Anketell, J.M., Cegla J. & Dzulinski, S. 1970. On the deformational structures in systems with reversed density gradients. *Ann. Soc. Geol. Poland*, 40:3-29 1970.

Arculus, R.J. & Ruff, L.J. 1990. Genesis of continental crust: evidence from island arcs, granulites, and exospheric processes. In *Granulites and crustal evolution*, D. Vielzeuf and Vidal Ph. (Editors), Kluwer Academic Publishers, Dordrecht, 7-23.

Arndt N. T. & Albarède, F. 1992. Abstract, IGC Kyoto.

Arndt, N.T & Nisbet E.G. 1982. (Editors), *Komatiites*. G. Allen and Unwin, London, 526 p.

Arndt, N.T. 1992. Rate and mechanism of continent growth in the Precambrian. Abstract, *IGC Kyoto.*

Arth, J.G, Barker, F., Peterman, Z. E. & Friedman, I. 1978. Geochemistry of the gabbro-diorite-tonalite-trondhjemite suite of southwest Finland and its implication for the origin of tonalite and trondhjemite magmas. *J. Petrol.*, 19: 289-316.

Arth, J.G. & Hanson, G.N. 1975. Geochemistry and origin of the early precambrian crust of north-estern Minnesota. *Geoch. Cosmochim. Acta*, 39: 325-362

Arth, J.G. 1979. Some trace elements introndhjemites, their implication to magma genesis and palaeotectonic setting. In: F. Barker (Editor), *Trondhjemites, Dacites and Related rocks*, Elsevier, Amsterdam, 123-132.

Barbey, P. 1986. Signification géodynamique des domaines granulitiques: la ceinture des granulites de Laponie (Fennoscandie). *Mem. Doc. CAESS*, Rennes ,7, 324 p.

Barker, F. 1979. Trondhjemites: definition, environement and hypotheses of origin. In: F. Barker (Editor), *Trondhjemites, Dacites and Related rocks*, Elsevier, Amsterdam, 1-12.

Basaltic Volcanism Project. 1981. *Basaltic Volcanism*, Pergamond Press, New York, 1286.

Beckinsale, R.D., Drury, S.A. & Holt, R.W. 1980. 3.360 Myr old gneisses from the south Indian craton. *Nature*, 283: 469-470.

Beckinsale, R.D., Reeves-Smith, G., Gale, N.H., Holt, R.W. & Thompson, B. 1982. Rb-Sr and Pb-Pb isochron ages and REE data for Archaran gneisses and granites, Karnataka state, South India. In: L.D., Ashwal (Editor), Indo-U.S. *Workshop on the Precambrian of south India (abs.). N.G .R I . Hyderabad*, 35-36.

Berner, H., Ramberg, H. & Stephansson, O. 1972. Diapirism theory and experiment. *Tectonophysics*, 15: 197-218.

Berthé, D, Choukroune, P. & Jegouzo, P., 1979. Orthogneiss, mylonite and non-coaxial deformation of granites : The example of the South Armorican Shear Zone. *J. Struct. Geol.*, 1: 31-42.

Bessoles, B. 1977. Géologie de l'Afrique: le craton Ouest Africain.*Mem. BRGM*, Orléans, 403 p.

Bhaskar Rao, Y.J., Sivaraman, T.V., Pantulu, G.V.C., Gopalan, K., & Naqvi, S. M. 1992. Rb-Sr of late-Archaean metavolcanics and granites, Dharwar craton, South India : evidence for early Proterozoic thermotectonic event(s). *Precambrian Research*, 59: 145-170.

Bhaskar Rao, Y.J., Beck, W., Rama Murthy, V., Nirmal Charan, S. & Naqvi, S.M. 1983. Geology, geochemistry, and age of metamorphism of Archaean gray gneisses around Channarayapatna, Hassan district, Karnataka, South India. In S.M. Naqvi & J.J.W., Rogers (Editors),*Precambrian of South India, Geological. Society of India Memoir* , 4: 309-328.

Bibikova, E.V. 1984. The most ancient rocks in the USSR territory by U-Pb data on accessory zircons. In: Kröner et al., (Editors), *Archaean Geochemistry; the origin and evolution of the Archaean continental crust.* Springer, Berlin, 235-250.

Bickle, M.J. 1978. Heat loss from the Earth: A constrain on Archaean tectonics from the relation between geothermal gradients and the rate of plate production, *Earth. Planet. Sci. Lett.*, 40: 301-315.

Bickle, M.J. 1986. Global thermal histories, *Nature.*, 319: 13-14.

Bickle, M.J., Betteney L.F., Boulter C.A, Blake T.S. & Groves, D.I. 1980. Horizontal tectonic interaction of an Archean gneiss belt and greenstones, Pilbara block, Western Australia, *Geology*, 8: 525-529.

Bickle, M.J., Bettenay, L.F., Barley, M.E., Chapman, H.J., Groves, D.I., Campbell, I.H. & de Laeter J.R. 1983. A 3500 Ma plutonic and volcanic calc-alkaline province in the Archaean East Pilbara block. *Contrib. Mineral. Petrol.*, 84: 25-35.

Biot M.A. & Ode H. 1965. Theory of gravity instability with variable overburden and compaction. *Geophysics*, 30: 213-227.

Black, L. P., Williams, I. S. & Compston, W. 1986. Four zircon ages from one rock: the history of a 3930 Ma -old granulite from Mt. Stones, Antartica. *Contrib. Mineral. Petrol.*, 94: 427-437.

Bois, C. & Ecors Scientific Party. 1991. Late and Post-Orogenic Evolution of the Crust studied from ECORS Deep Seismic Profiles. In: Continental Lithosphere Deep Seismic Reflexions, Meissner et al. editors, *A.G.U. geodynamic series* , 22: 53-68.

Bouhallier, H., Choukroune, P. & Ballèvre, M. 1991. Evolution structurale de la croûte Hercynienne profonde: exemple du massif de l'Agly (Pyrénées orientales France), *C. R. Acad. Sci. Paris* , 312: 647-654.

Bouhallier, H., Choukroune, P. & Ballèvre, M. 1993. Diapirism, bulk homogeneous shortening in the Archaean Dharwar craton: the Holenarsipur area, southern India. *Precam Res.*, 63: 43-58.

Bridgwater, D., McGregor, V. R. & Myers, J. S. 1974. A horizontal tectonic regime in the Archaean of Greenland and its implication for early crustal thickening. *Precam. Res.*, 1: 179-197.

Brodie, K.H., Rex D. & Rutter E.H. 1989. On the age of deep extentional faulting in the Ivrea zone, Northern Italy. in Alpine Tectonics.*Geol. Soc. Spec. Pub.*, 45: 203-210.

Bronner, G. 1981. Diapiric structures in the Archaean basement of the south west Reguibat Shield (Mauritanie). *Journal of structural Geology,* Abstract papers, 3: 91.

Brun, J.P. 1983a. Isotropic points and lines in strain fields. *J. Struct. Geol.*, 5: 321-327.

Brun, J.P. 1983b. L'origine des domes gneissiques : modèles et tests. *Bull. Soc. Geol. Fr.*, 25: 219-228

Brun, J. P. & Pons, J. 1981. Patterns of interference between granite diapirism and regional deformation (abstract). In : Coward, M. P. Diapirism and gravity Tectonics : Report of tectonic Studies Group conference held at Leeds University, 25-26 March 1980, J. Struct. Geol. 3: p93.

Brun, J.P., Gapais, D. & Le Theoff, B. 1981a. The mantle gneiss domes of Kuopio (Finland): interfering diapirs, *Tectonophysics*, 74: 283-304.

Buhl, D., Grauert, B., & Raith, M. 1983. U-Pb dating of Archaean rocks from South Indian craton: results from the amphibolite-granulite transition at Kabbal quarry southern Karnataka. *Fortchritte Der Mineralogie*, 61: 43-45.

Burke, K. & Kidd, W.S. F. 1978. Were Archaean continental geothermal gradients much steeper than those of today? *Nature*, 272: 240-241.

Burke, K., Dewey, J.F. & Kidd, W.S.F. 1976. Dominance of horizontal movements, arc and microcontinental collisions during the later permobile regime. In: B. F. Windley (Editor), *The early history of the Earth*, Wiley-Interscience, London, 113-129.

Caen-Vachette, M. 1988. Le craton Ouest africain et le Bouclier Guyannais: un seul craton au Proterozoique inférieur? *J. Afr. Earth Sci*, 7: 479-488.

Camil, J. 1984. Pétrographie, chronologie des ensembles granulitiques archéens et formations associées de la région de Man (Cote d'Ivoire). Abidjan Univ. Thesis, 306 p.

Camil, J., Tempier, P. & Caen-Vachette, M. 1984. Schéma chronologique et structural des formations de la région de Man (Cote-d'Ivoire). in Géologie Africaine, *Mus. R. Afr. Cent.*, Tervuren, 1-10.

Camiré, G.E., & Burg, J.P. 1993. Late Archean thrusting in the Northwestern Pontiac Subprovince, Canadian shield. *Precambrian Research*, 61: 51-66.

Campbell I.H. & Jarvis, G.T. 1984. Mantle convection and early crustal evolution. *Precam Res.*, 26: 15-56.

Campbell, I.H., Griffiths, R.W. & Hill, R.I. 1989. Melting in an Archaean mantle plume: head it's basalts, tail it's komatiites. *Nature*, 339: 697-699.

Card, K.D. 1990. A review of the Superior Province of the Canadian Shield, a product of Archean accretion. *Precambrian Res.*, 48: 99-156.

Chadwick, B., & Nutman, A.P. 1979. Archaean structural evolution in the northwest of the Buksefjorden region, southern West Greenland. *Precambrian Res.*, 9: 199-226.

Chadwick, B., Ramakrishnan & Viswanatha, M.N. 1981. Structural and metamorphic relations between Sargur and Dharwar supracrustal rocks and Peninsular gneisses in central Karnataka. *J. Geol. Soc. India*, 22: 557-569.

Chadwick, B., Ramakrishnan, M. & Viswanatha, M.N. 1981. Structural and metamorphic relations between Sargur and Dharwar supracrustal rocks and Peninsular gneisses in central Karnataka. *Journal of the Geological Society of India*, 22: 557-569.

Chadwick, B., Ramakrishnan, M. & Viswanatha, M.N. 1985a. Bababudan- A late Archaean intracratonic volcanosedimentary basin, Karnataka, Southern India. Part I: Stratigraphy and Basin Development.*Journal of the Geological Society of India*, 26: 769-801.

Chadwick, B., Ramakrishnan, M. & Viswanatha, M.N. 1985 b. Bababudan- A late Archaean intracratonic volcanosedimentary basin, Karnataka, Southern India. Part II: Structure.*Journal of the Geological Society of India*, 26: 802-821.

Chadwick, B., Ramakrishnan, M., Vasudev, V.N. & Viswanatha, M.N. 1989. Facies distributions and structures of a Dharwar volcanosedimentary basin: evidence for late Archaean transpression in Southern India ? *Journal of the Geological Society of London*, 146: 825-834.

Chadwick, B., Ramakrishnan, M., Viswanatha, M.N. & Srinivasa Murthy, V. 1978. Structural studies in the Archaean Sargur and Dharwar supracrustal rocks of the Karnataka craton. *Journal of the Geological Society of India*, 19: 531-549.

Chardon, D. 1993. Approche mécanique des déformations gravitaires de la protocroûte continentale archéenne. DEA, Géologie, Géophysique et Géochimie de la croûte profonde, Géosciences Rennes, 28p.

Chen, M. 1990. Metabasic dyke swarms in a high-grade metamorphic terrane: a case study in the Taipingzhai-Jingchangyu area, Eastern Hebei Province, *Acta Geol. Sin.*, 64: 169-183.

Chinner, G. A. & Sweatman T. R., 1968. A former association of enstatite and kyanite. *Mineralogical Magazine*, 36: 1052-1060.

Choukroune P., Auvray B., Jahn B.M., Chen T., Geng Y. & Liu D. 1993. Coupe structurale de la croute archéenne en Hebei (Craton sino-coréen, Chine du nord), *C. R. Acad. Sci.* Paris, 316: 669-675.

Choukroune, P., Bouhallier, H., Arndt, N. T., Soft Archaean lithosphere during periods of crustal growth or reworking. *Spec. Publ. of Geol. Soc of London*, in press.

Choukroune, P., Gapais, D. & Merle, O. 1987. Shear criteria and structural symmetry. *J. Struct. Geol.*, 9: 525-530.

Clowes, R.M., Cook, F.A, Green, A.G., Keen, C.E., Ludden, J.N., Percival J.A., Quinlan, G.M. & West G.F. 1992. Lithoprobe: new perspectives on crustal evolution. *Can. J. Earth Scii*, 29: 1813-1864.

Cohen, A.S., O'Nions, R.K., Siegenthaler, R. & Griffin, W.L. 1988. Chronology of the pressure-temperature history recorded by a granulite terrane. *Contrib. Mineral. Petrol.*, 98: 303-311.

Collins, W.J. 1989. Polydiapirism of the Archean Mount Edgar Batholith, Pilbara Block, Western Australia. *Precambrian research*, 43: 41-62.

Compston, W., & Kröner, A. 1988. Multiple zircon growth within early Archaean tonalitic gneiss from the ancient gneiss complex, Swaziland. *Earth. Planet. Sci. Lett.*, 87: 13-28.

Compston, W., Zhang, F.P., Foster J.J., Collerson, K.D., Bai, J., & Sun D.Z. 1983. Rubidium-strontium geochronology of Precambrian rocks from the Yenshan Region, North China. *Precamb Res.*, 22: 175-202.

Condie, K.C. 1981. *Archaean greenstone Belts.* Elsevier, Amsterdam, 434 p..

Condie, K.C. 1990. Growth and accretion of continental crust: inferences based on Laurentia, *Chem. Geol.*, 83: 183-194.

Corfu, F., Krogh, T.E., Kwok, Y.Y., Jensen, L.S. 1989. U-Pb zircon geochronology in the southwestern Abitibi greenstone belt, Superior Province, *Can. J. Earth Sci.*, 26: 1747-1763.

Coward, M.P. & Fairhead, J.D. 1980. Gravity and structural evidence for the deep structure of the Limpopo belt, southern Africa. *Tectonophysics*, 68: 31-43.

Cowards, M.P. 1981. Diapirism and gravity tectonics: report of a Tectonic studies Group Conference held at Leeds University, 25-26 mars 1980, *J. Struct. Geol.*, 3: 91.

Coward, M.P. 1983. Thrust tectonics, thin skinned or thichk skinned, and the continuation of thrusts to deep in the crust. *Jour. Struct. Geol.*, 5:113-123.

Coward, M.P., Lintern, B.C. & Wright, L.I. 1976. The pre-cleavagedeformation of the sediments and gneisses of the northern part of the Limpopo belt. In: B. F. Windley (Editor), *The early history of the earth,* Wiley- Interscience, London, 323-330.

Crawford, A.R. 1969. Reconnaissance Rb-Sr dating of the Precambrian rocks of Southern Peninsula India. *Journal of the Geological Society of India*, 10: 117-166.

De Wit M.J. Armstrong R., Hart, R.J., & Wilson, A.H. 1987a. Felsic igneous rocks within the 3.3 to 3.5 Ga Barberton greenstone belt: high crustal level equivalents of the surrounding tonalite-trondhjemite terrain, emplaced during thrusting. *Tectonics*, 6: 529-549.

De Wit, M.J. 1982. Gliding and overthrust Nappe tectonics, in the Barberton greenstone belt. *J. Struct. Geology*, 4: 117-136.

De Wit, M.J., 1991. Archean greenstone belt tectonism and basin development:some insights from the Barberton and Pieterburg greenstone belts, Kaapvaal craton, South Africa, *J. Af. Earth Sci.*, 13: 45-63.

De Wit, M.J., Hart, R.A. & Hart, R.J. 1987b. The Jamestown ophiolite complex, Barberton mountain belt: a section through 3.5 Ga oceanic crust. *J. Afr. Earth Sci..*, 6: 681-730.

De Wit, M.J., Roering, C., Hart, R.J., Armstrong, R.A., de Ronde, C.E.J., Green, R.W.E., Tredoux, M., Peberdy, E., & Hart, R.A. 1992. Formation of an Archaean continent. *Nature*, 357: 553-562.

Delor, C. Burg, J P. & Clarke, G. 1991. Relations diapirisme-metamophisme dans la province du Pilbara (Australie Occidentale): implications pour les régimes thermiques et tectoniques à l'Archéen. *Comptes rendus à l'Académie des sciences de Paris*, 312: 257-263.

Desrochers, J.-P., Hubert, C., Ludden, J.N., & Pilote, P. 1993. Accretion of Archaean oceanic plateau fragments in the Malartic Composite Block, Abitibi Greenstone Belt, Canada. *Geology*, 451-454.

Dewey, J.F. 1988. Extensional collapse of orogens. *Tectonics*, 7: 1123-1139.

Dewey, J.F. & Horsfield, B. 1970. Plate tectonics, orogeny and continental growth. *Nature*, 225: 521-525.

Dewey, J.F. & Windley B.F. 1981. Growth and differenciation of the continental crust. *Philos. Trans. R. Soc. Lond.*, 301: 189-206.

Dixon J.M. & Summers, J.M. 1983. Patterns of total and incremental strain in subsiding troughs: experimental centrifuged models of inter-diapiric synclines. *Can. J .Earth Sci.* , 20: 1843-1861.

Dixon J.M. 1974. A new methode of determining finite strain in models of geological structures. *Tectonophysics*, 24: 99-114.

Dixon, J.M.1975. Finite strain and progressive deformation models of diapiric structures, *Tectonophysics*, 28: 89-104.

Drury, SA. & Holt, R.W. 1980. The tectonic framework of the south India craton: a reconnaissance involving LANDSAT imagery. *Tectonophysics*, 65: 111-115.

Drury, S.A. 1977. Structures induced by granite diapirs in the Archaean greenstone belt at Yellowknife, Canada: implications for Archaean geotectonics. *Journal of Geolgy*, 85: 345-358.

Drury, S.A. 1983a. A regional tectonic study of the Archaean Chitradurga greenstone belt, Karnataka based on Landsat interpretation. *J. Geol. Soc. India*, 24: 167-184.

Drury, S.A. 1983b. The petrogenesis and setting of Archaean metavolcanics from Karnataka state, South India. *Geochim. Cosmochim. Acta*, 47: 317-329.

Drury, S.A., Harris, N.B.W., Holt, R.W., Reeves-Smith, G.J. & Wightman, R.T. 1984. Precambrian tectonics and crustal evolution in south India. *Journal of Geology*, 92: 3-20.

Drury, S.A., Holt, R.W., Van Clasteren, P.C. & Beckinsale, R.D. 1983c. Sm-Nd and Rb-Sr ages for Archaean rocks in Western Karnataka. *South India Journal of the Geological Society of India*, 24: 454-459.

Drury, S.A. 1977. Structures induced by granite diapirs in the Archaean greenstone belt at Yellowknife, Canada: implications for Archaean geotectonics,*Journal of Geology*, 85, 345-358.

Drury, S.A., Van Calsteren, P.C. & Reeves-Smith, G.J. 1986. Sm-Nd isotopic data from Archean metavolcanic rocks at Holenarsipur, south India. *Journal of Geology*, 95: 837-843.

England, P. & Bickle, M. 1984. Continental thermal and tectonic regimes during the Archean. *Journal of Geology*, 92: 353-367.

Ermanovics , I.F., & Davison W.L. 1976. The Pikwitonei Granulites in relation to the North-western Superior province of the Canadian shield. In: B. F. Windley, *The early history of the Earth. John Wiley & Sons, London*, 331-347.

Ernst, W.G. 1972. Occurence and mineralogic evolution of blueschist belts with time. *Amer. J. Sci.*, 272: 657-668.

Eskola, P.E. 1949. The problem of mantled gneiss domes. *Quart. Jour. Geol. Geol. Soc. London*, 104: 461-476.

Evans, O.C. & Hanson, G.H. 1992. Most late Archaean tonalites, trondhjemites and granodiorites (TTG) in the SW Superior Province wree derived from mantle melts, not by melting of basalts. *AGU Abstract* V22D-3: 330

Ferry, J.M. & Spear, F.S. 1978. Experimental calibrationof the partitioning of Fe and Mg between biotite and garnet. *Contributions to Mineralogy and Petrology*, 66: 113-117.

Fletcher R.C. 1972. Application of a mathemetical model to the emplacement of mantled gneiss domes. *Amer. J. Sc*, 272, 3: 197-216.

Flinn, D. 1965. On the symmetry principle and the deformation ellipsoid. *Geol. Mag.*, 102: 36-45.

Friend, C.R.L. & Nutman. 1991. Shrimp U-Pb geochronology of the Closepet granite and Peninsular gneisses, Karnataka, South of India. *Journal of the Geological Society of India*, 38: 357-368.

Friend, C.R.L. 1981. Charnockite and granite formation and influx of CO2 at Kabbaldurga. *Nature*, 294: 550-552.

Friend, C.R.L. 1983. The link between charnockite formation and granite production: Evidence from Kabbaldurga, Karnataka, South India. In: M.P., Atherton and C.D., Cribble (Editors), *Migmatites, melting, metamorphism, Shiva, Nantwich*, 264-276.

Fryer, B.J., Fyfe, W.S., & Kerrich, R. 1979. Archaean volcanogenic oceans. *Chem. Geol.*, 24: 25-35.

Fyfe,W.S. 1978. Evolution of the earth crust: modern plate tectonics to ancient hot spot tectonics? *Chem. Geol.*, 23-89.

Fyfe,W.S. 1974. Archaean tectonics. *Nature*, 24: 338.

Fyson, W. K., 1984. Fold and cleavage patterns in Archaean metasediments of the Yellowknife supracrustal domain, Slave Province, Canada. In A., Kröner & R., Greiling (Editors), *Precambrian Tectonics Illustrated*, I.U.G.S.,281-293.

Gautier, P., Brun, J.P. & Jolivet, L. 1993. Structure and Kinematics of upper cenozoic extensional detachment on Naxox and Paros (Cyclades islands, Greece). *Tectonics*, 12: 1180-1194.

Ghent, E.D., Stout, M.Z., Black, P.M. & Brothers R.N. 1987. Chloritoid-bearing rocks associated with blueschists and eclogites, northern New Caledonia. *Journal of metamorphic Geology*, 5: 239-254.

Glikson, A.Y. 1979. Early Precambrian tonalite-trondhjemites nuclei. *Earth. Sci. Rev.*, 15: 1-73.

Goldstein, S.L. & N.T. Arndt. The history of a continent in a sample of river sand: the age components of an Orinoco River sediment. *Earth Planet. Sci. Lett.* in press.

Goodwin, A.M. 1981. Archaean plates and greenstone belts. In: *Precambrian plate tectonics*, Kröner (Editor), Elsevier, 4: 108-109.

Goodwin, A. M, 1991. Precambrian Geology, Academic Press, 666p.

Gopalakrishna, D., Hansen, E.C. Janardhan, A.S. & Newton, R.C. 1986. The southern high-grade margin of the Dharwar craton. *J. Geol.* 94: 247-260.

Gorman, B. E., Pearce, T.H. & Birkett, T.C. 1978. On the structure of Archaean greenstone belts. *Precambrian research*, 6: 23-41.

Grambling, J.A. 1990. Internally-consistent geothermometry and H_2O barometry in metamorphic rocks: the example garnet-chlorite-quartz. *Contribution to Mineralogy and Petrology*, 105: 617-628.

Green, D.H. 1972. Archaean greenstone belts may include terrestrial equivalents of lunar maria. *Earth Planetary Sci. Letters*, 15: 263-270.

Grew, E.S. & Manton, W.I. 1984. Age of allanite from Kabbaldurga quarry Karnataka. *J. Geol. Soc. India*, 25: 193-195.

Gruau, G., Tourpin, S., Fourcade, S. & Blais, S. 1992. Loss of isotopic (Nd, O) and chemical (REE) memory during metamorphism of komatiites: new evidence from eastern Finland. *Contrib. Mineral. Petrol.*, 112: 66-82.

Gupta, J.N., Pandey, B.K., Prasad, R.N., Yadav, G.S. , Ramesh Kumar, K., & Rao, S.S. 1988. Rb-Sr geochronology of some granitic rocks around Arbail and age of uraniferous arenite and quartz-pebble conglomerates of Western Karnataka. *Memoir of the Geological Society of India*, 9: 101-108.

Hammond, E.C., & Nisbet B.W. 1992. Towards a structural and tectonic framework for the central Norseman-Wiluna greenstone belt, Western Australia. In: J.E. Glover & S.E. Ho (Ed.), *The Archaean: Terrains, Processes and Metallogeny*, Perth: The Geology Key Centre & University extension, the University of Western Australia, 39-50.

Hansen, E.C., Janardhan, A.S., Newton, R.C., Prame, K.B.M., & Ravindra Kumar G.R.1987. Arrested charnockite formation in Southern India and Sri Lanka. *Contrib. Mineral. Petrol.*, 96: 225-244.

Hansen, E.C., Newton, R.C. & Janardhan, A.S. 1984. Pressures, temperatures, and metamorphic fluids across an unbroken amphibolite-facies to granulite-facies transition in Southern Karnataka, India. In Kröner, A., Goodwin, A.M. & Hanson, G. N., eds., *Archaean geochemistry*, Berlin, Springer-Verlag, 161-181.

Hargraves, R.B. 1984. Precambrian tectonic style: a liberal uniformitarian interpretation. In: *Precambrian Plate Tectonics*, Kröner, A. (Editor), Elsevier, 4: 21-56.

Hargraves, R.B. 1986. Faster spreading or greater ridge lenght in the Archaean? *Geology*, 14: 750-752

Harris, N.B.W. & Jayaram, S. 1981. Metamorphism of cordierite gneisses from the Bangalore region of the Indian Archaean. *Lithos*, 15: 89-98.

Hedge, C.E., & Marvin, R.F. 1975. Naesser, Age provinces in the basement rocks of Liberia.*J. Res. US Geol. Survey*, 3: 425-429.

Helmstaedt, H., Padgham, W.A. & Brophy, J.A. 1986. Multiple dykes in the lower Kam Group, Yellowknife Greenstone Belt: evidence for Archean sea floor spreading? *Geology*, 14: 562-566.

Hickman, A.H. 1984. Archaean diapirism in the Pilbara Block, Western Australia in A., Kröner & R., Greiling (Editors), *Precambrian Tectonics Illustrated*, I.U.G.S.,113-127.

Hodges, K.V. & Spear, F.S. 1982. Geothermometry, geobarometry and the Al2SiO5 triple point at Mt. Moosilauke, New Hampshire. *American Mineralogist*, 67: 1118-1134.

Hoffman, P.F. 1989. Precambrian geology and tectonic history of North America. In: Bally, A. W. & Palmer, A. R. (Editors). *The geology of North America*, vol. A. Geological society of America, 447-512.

Holland, T.J.B. & Powell, R. 1990. An enlarged and updated internally consistent thermodynamic dataset with uncertainities and correlations: the system K_2O - Na_2O - CaO - MgO - MnO - FeO - Fe_2O_3 - Al_2O_3 - TiO_2 - SiO_2 - C - H_2 - O_2. *Journal of Metamorphic Geology*, 8: 89-124.

Holder, M.T. 1979. An emplacement mechanism for post-tectonic granites and its implications for their geochemical features. In: *Origin of granite batholits - geochemical evidence*, Atherton, M. P. & Tarney, J. (Editors). Shiva publishing limited, Orpington, U. K., 116-128.

Holmes, A. 1928. Radioactivity and earth movements. *Trans. Geol. Soc. Glasgow*, 18: 559-606.

Huang, W.Z. & De Paolo, D.J. 1986. Sm-Nd isotope study of early Archean rocks, Qianan, Hebei province, China,. *Geochim. Cosmochim. Acta*, 50: 625-631.

Hurley, P.M. & Rand, J.R. 1969. Pre-drift continental nuclei. *Science*, 164, 1229.

Hurley, P.M. 1968. Absoluta abondance and distribution of Rb, K and Sr in the earth. *GCA*, 32: 273.

Hussain, S.M. & Naqvi, S.M. 1983. Geological, geophysical and geochemical studies over the Holenarsipur schist belt, Dharwar craton, India. In S.M., Naqvi & J.J.W., Rogers (Editors), *Precambrian of South India, Geological. Society of India,Memoir*, 4: 73-95.

Iyengar, B.R.C. 1971. Precambrian rocks of Holenarsipur, Hassan district, Mysore State, South India. *Journal of indian Geosciences association*, 131: 31-44.

Jackson, M.P.A., Erikson, K. A. & Harris, C. W. 1987. Early Archaean foredeep sedimentation related to crustal shortening: a reinterpretation of the Barberton Sequence, Southern Africa. *Tectonophysics*, 136: 197-221.

Jackson , M.P. & Talbot, C.J. 1989. Anatomy of mushroom shaped diapirs. *J. Struct. Geol.*, 11: 211-230.

Jagoutz, E. 1988. Nd and Sr systematics in an eclogite xenolith from Tanzania: evidence for frozen mineral equilibria in the continental lithosphere. *Geochim. Cosmochim. Acta*, 52: 1285-1293.

Jahn, B.M., Glikson, A.Y., Peucat, J.J., & Hickan, A.H. 1981. REE geochemistry and isotopic data of Archaean silicic volcanics and granitoïds from the Pilbara Block, western Australia: implications for the early crustal evolution. *Geochim. Cosmochim. Acta*, 45: 1633-1652.

Jahn, B.M. & Zhang Z.Q. 1984. Archean granulite gneisses from Eastern Hebei Province,China: rare earth geochemistry and tectonic implications, *Contrib. Mineral. Petrol.*, 85: 224-243.

Jahn, B.M., Auvray, B., Cornichet, J., Bai, Y.L., Shen Q.H., & Liu D.Y. 1987. 3.5 Ga old amphibolites from Eastern Hebei Province, China: field occurrence petrography, Sm-Nd isochron age and REE geochemistry. *Precamb. Res.*, 34: 311-346.

Janardhan, A.S., Srikantapa, C. & Ramachandra, H.M. 1978. The Sargur schist complex- an Archaean high-grade terrain in southern India. In: Windley, B.F., & Naqvi, S. M., (editors). *The Origin and evolution of Archaean continental crust: Amsterdam,* Elsevier, 127-149.

Janardhan, A.S., Ramachandra, H.M., & Ravindra Kumar, G.R. 1979. Structural history of Sargur supra crustals and associated gneisses, Southwest of Mysore, Karnataka. *Geol. Soc. India* , 20: 61-72.

Janardhan, A.S., Newton, R.C. & Hansen, E.C. 1982. The transformation of amphibolite facies gneiss to charnockite in Southern Karnataka and northern Tamil Nadu, India. *Contribution to Mineralogy and Petrology* , 79: 130-149.

Janardhan, A.S., Newton, R.C. & Smith, J.V. 1979. Ancient crustal metamorphism at low pH2O: charnockite formation at Kabbaldurga, south India. *Nature*, 278: 511-514.

Jayananda, M. & Mahabaleswar, B. 1990. Relationship between shear zones and igneous activity: the Closepet Granite of southern India, Proc. Indian Acad.Sci. (Earth Planet.Sci.) ,100: 31-36.

Jayananda M., Martin H., & Mahabaleshwar, B. . 1992. The mechanism of recycling of the Archaean continental crust:example from the Closepet granite,southern India, In: *The Archaean: Terrains,Processes and Metallogeny*, J.E. Glover and S.E. Ho editors, The Geology Key Centre & University extension & the University of Western Australia,Perth, 213-222.

Jayananda, M., Martin, H., Peucat, J.J. & Mahabaleswar, B.S. 1994. Late Archaen crust-mantle interaction: the Closepet granite, South India. Evidence from Sm-Nd isotopes, major and trace elements geochemistery. *Contrib. mineral. Petrol.*, in press.

Jayaram, B., 1899. Notes on geological work in the Hassan district. *Rec. Mysore Geol. Dept.*, 2: 131-138.

Jayaram, B. 1910. Note on the work done during the field season of 1909-10. *Rec. Mtsore Geol. Dept.*, 11: 175-184.

Jelsma, H.A., Van Der Berk, P.A., & Vinyu, M.L. 1993. Tectonic evolution of the Bindura-Shamva greenstone belt (northern Zimbabwe) : progressive deformation around diapiric batholiths. *Journal of structural Geology*, 15: 163-176.

Kaila, K.L. & Tewari, H.C. 1982. Structure and tectonics of the Cuddapah basin in the light of DSS studies. In: Bhattacharji, S. & Balakrishna, S., eds., *Evolution of the intracratonic Cuddapah basin*. Hyderhabad, Inst. Indian Peninsular Geol., p. 53-62.

Kidd, W.S.F., Kusky, T., & Bradley, D.C. 1988. Late Archean greenstone tectonics: evidence for thermal and thrust loading, lithospheric susidence from stratigraphic sections in the Slave Province, Canada, in *Workshop on the deep crust of Southern India*, L.D. Ashwald editor, Lunar and Planet.Instit., Houston, 79-80.

Kinny, P.D. 1986. 3920 zircons from a tonalitic Amitsoq gneiss in the Godthab district of southern West Greenland. *Earth Planet. Sci. Lett.*, 79: 337-347.

Kramers, J.D. 1988. An open-system fractional crystallisation model for very early continental crust formation. *Precambrian Res.*, 38: 281-295

Kranck, E.H., On folding-movements in the zone of the basement. *Geol. Rundsch.* 47: 261-282 1957.

Krogstad, E. ., Balakrishnan, S., Mukhopadyay, D.K., Rajamani, V. & Hanson, G.N. 1989. 'Plate tectonics 2.5 billion years ago: Evidence at Kolar, South India. *Science*, 243: 1337-1340.

Kröner, A. & Layer, P.W. 1992. Crust formation and plate motion in the early Archaean. *Science*, 256: 1405-1411.

Kröner, A. 1981a. Precambrian crustal evolution and continental drift. *Geol. Rund.*, 70: 412-428.

Kröner, A. 1981b. Precambrian plate tectonics. In A. Kröner (Editor). *Precambrian plates tectonics*. Elsevier, Amsterdam, 57-90.

Kröner, A. 1985. Evolution of the Archaean continental crust. *Ann. Rev. Earth Planet. Sci.*, 13: 49-74.

Kröner, A. 1991. Tectonic evolution in the Archaean and Proterozoic. *Tectonophysics*. 187: 393-410.

Kusky, T.M. 1992. Relative timing of deformation and metamorphism at mid- to upper crustal levels in the Point Lake Orogen, Slave Province, Canada. In J.E. Glover, & S.E. Ho editors., *The Archaean: Terrains, Processes and Metallogeny*, The Geology Key Centre & University extension, University of Western Australia, 59-72..

Kusky, T. M. 1993. Collapse of Archean orogens and the generation of late- to postkinematic granitoids, Geology, 21: 925-928.

Lambert R.J. 1976. Archaean thermal regimes, Crustal and Upper Mantle Temperatures, and a progressive evolutionary model for the Earth. In Windley B. F. (Editor), *The early history of the Earth*, 363-373.

Lambert R.J. 1981. Earth tectonics and thermal history: review and a hot-spot model for the Archaean. In: *Precambrian plate tectonics*, Kröner (Editor), Elsevier, 4: 453-467.

Light, M.P.R. 1982. The Limpopo mobile belt: a result of continental collision. *Tectonics*, 4: 325-342.

Liou, J.G., Maruyama, S., Wang, X., Graham, S., Xiao, S., Feng, Y., Liang, Y., Zho, M., & Tang., Y. 1988. Geological evidence for a major Proterozoic coherent blueschist terrane in Aksu, Xinjiang, China. Eos, *Trans. Am. Geophys. Union*, 69: 1513.

Liu D.Y, Q.H. Shen, Z.Q. Zhang, B.M. Jahn & B. Auvray. 1990. Archean crustal evulution in China:U-Pb geochronology of the Qianxi complex. *Precamb Res.*, 48: 223-244.

Liu, D.Y., Nutman, A.P., Compston, W., Wu, J.S., & Shen, Q.H. 1992. Remnants of >3800 Ma crust in the Chinese part of the Sino-Korean Craton. *Geology*, 20: 339-342.

Liu, D.Y., Shen, Q.H., Jahn, B.M., Zhang, Z.Q., Auvray, B., Zhang, Q.Z. & Ye X.J. 1986. U-Pb geochronology of granitoids from the archean metamorphic terranes of eastern Hebei Province, China, *ICOG VI , Cambridge* (extended abstract).

Liu, D.Y., Page, R.W., Compston, W. & Wu, J.S. 1985. U-Pb Zircon geochrology of late Archean metamorphic rocks in the Taihangshan-Wutaishan area, North China. *Precamb Res.*, 27: 85-109.

Ludden, J., Hubbert, C. & Gariepy, C. 1986. The tectonic evolution of the Abitibi greenstone belt of Canada. *Geological Magazine*, 123: 153-166.

Malloe, S. 1982. Petrogenesis of Archaean tonalites. *Geol. Rundsch.*, 71: 328-346.

Mareschal, J.C. & West, G.F. 1980. A model for tectonism. Part 2. Numerical models of vertical tectonism in greenstones belts. *Can. J. Earth Sci.*, 17: 60-71.

Marsh B.D. 1982. On the mechanism of igneous diapirism, stoping and zone melting, *Am. J. Sci.*, 282, 808-855.

Martin H. 1986. Effect of steeper Archaean geothermal gradient on geochemistry of subduction-zone magmas. *Geology*, 14: 753-756.

Martin H. 1993. The mechanisms of petrogenesis of the Archaean continental crust-Comparison with modern processes. *Lithos*, 30: 373-388.

Martin, H., Peucat, J.J., Auvray, B. & Jayananda, M. 1993. The Archaean "sanukitoid" magmatism: example of the Closepet granite (South India). *Terra nova*, 5: 38.

McCourt, S. & Wilson, J.F. 1992. Late Archaean and early Proterozoic tectonics of the Limpopo and Zimbawe Provinces,Southern Africa. In: *The Archaean Terranes, Processes and Metallogeny*, J. O. Glover and S. E. Ho editors, The Geology Key Centre & University extension, University of Western Australia, Perth, 237-245.

McCourt, S. & Vearncombe, J.R. 1992. Shear zones of the Limpopo Belt and adjacent granitoid-greenstone terranes: implications for late Archean collision tectonics in southern Africa, *Precamb Res.*, 55: 539-552.

McGregor, A.M. 1951. Some milestones in the Precambrian of Southern Rhodesia. *Trans. Geol. Soc. S. Afr.*, 54: 27-70.

McKenzie, D.P., & Weiss, N. 1975. Speculations on the thermal and tectonic history of the earth. *Geophys. J. R. Astron. Soc.*, 42: 131-174.

McLennan, S.M. & Taylor, S.R. 1982. Geochemical constraints on the growth of the continental crust. *J. Geol.*, 90: 342-361.

Meen, J.K., Rogers, J.J. & Fullagar, P.D. 1992. Lead isotopic composition of the Western Dharwar craton, southern India: Evidence for distinct Middle Archean terranes in a Late Archean Craton. *Geochimica et Cosmochimica Acta*, 56: 2455-2470.

Mezger, K., Essene, E.J. & A.N. Halliday, A.N. 1992. Closure temperature of the Sm-Nd system in metamorphic garnets. *Earth Planet. Sci. Lett.*, 113:3 97-409.

Monrad, J.R. 1983. Evolution of sialic terrains in the vicinity of the Holenarsipur belt, Hassan District, Karnataka, India. In S.M., Naqvi & J.J.W., Rogers (Editors), *Precambrian of South India, Geological. Society of India Memoir*, 4: 343-364.

Moorbath, S. 1975. Evolution of Precambrian crust from strontium isotopic evidence. *Nature*, 254: 395-398.

Moorbath, S. 1979. Les plus anciennes roches terrestres et la croissance des continents. P. L.S: *La dérive des continents*, 187-200.

Mukhopadhyay, D. 1986. Structural pattern in the Dharwar craton. *J. Geol.*, 94: 167-186.

Myers, J. S., 1976. The early Precambrian Gneiss Complex of Greenland. In: The early History of the Earth, B. F. Windley (Editor),165-211.

Myers, J. S., 1984. Archaean tectonics of the Fiskenaesset region of southwest Greenland. In: *Pecambrian tectonics illustrated*, A. Kröner and R. Greiling (eds), 95-112.

Myers, J. S. & Watkins K. P., 1985. Origin of granite-greenstone patterns, Yilgarn Block, Western Australia. *Geology* 13: 778-780.

Naha, K., Srinivasan, R. & Jayaram, S. 1990. Structural evolution of the peninsular Gneiss - an early Precambrian migmatitic complex from South India. *Geol. Rundschau*, 79: 99-109.

Naha, K., Srinivasan, R. & Jayaram, S. 1991. Sedimentational, structural history of the Archaean Dharwar tectonic province, southern India. *Proc. Indian Acad. Sci.*, 100: 413-433.

Naqvi, S.M., Divakara Rao , V., Hussain, S.M., Narayana, B.L., Nirmal Charan, S., Govil, P.K., Bhaskar Rao, Y.J., Jafri, S. H., Rama Rao, P., Balram, V., Masood, A., Pantulu, K.P., Gnaneswar Rao, T. & Subba Rao, D.V. 1983b. Geochemistry of gneisses from Hassan district and adjoining areas,

Karnataka, India in S.M., Naqvi and J.J.W., Rogers (Editors), *Precambrian of South India, Geol. Soc. India Mem.*, 4: 401-416.

Naqvi, S.M. & Rodgers, J.J.W., (editors). 1983. *Precambrian of South India, Geological. Society of India Memoir* , 4: 556.

Naqvi, S.M., Allen, P., Subra Rao, M.V., Gnaneshwar Rao, T. 1983 a. Geochemistry of coexisting staurolite and kyanite from an early Archaean greenstone belt of Dharwar craton, India in S.M., Naqvi, and J.J.W., Rogers (Editors), *Precambrian of South India, Geol. Soc. India Mem.*, 4: 267-274.

Naqvi, S.M., ViswanathanI, S. & ViswanathaI, M.N. 1978. Geology and geochemistry of the Holenarsipur schist belt and its place in the evolutionary history of the Indian Peninsula in B.F., Windley and S.M., Naqvi (Editors), *Archaean Geochemistry*, Elsevier, Amsterdam, 109-126.

Nelson, B.K. & de Paolo D.G. 1985. Rapid production of continental crust 1.7-1.9 b.y. ago: Nd and Sr isotopic evidence from the basement of the North American midcontinent. *Geol. Soc. Am. Bull* ., 96: 746-754.

Nesbitt R.W., Jahn B.M. & Purvis A.C. 1982. Komatiites: an early Precambrian phenomenon. *J. Volc. Geother. Res.*, 14: 31-45.

Newton R.C. 1990a. The late Archean high-grade terrain of South India and the deep structure of the Dharwar craton. In: M.H. Salisbury, & D.M. Fountain, editors, *Exposed Cross-Sections of the Continental Crust*, Amsterdam, Kluwer Academic Publishers, 305-326.

Newton R.C., & Haselton H.T. 1981. Thermodynamics of the plagioclase - Al2SiO5 - quartz geobarometer. in R.C. Newton, A. Navrotsky, and B.J. Wood, eds. *Thermodynamics of minerals and melts*, Springer Verlag, New-York, 131-148

Newton R.C. 1990b. Fluids and melting in the Archaean deep crust of southern India in J.R., Ashworth and M., Brown (Editors), *High-temperature Metamorphism and Crustal Anatexis*, Unwin Hynman, 149-179.

Nisbet, E.G. 1982. The tectonic setting and petrogenesis of komatiites. In: N. T. Arndt and Nisbet E. G. (Editors), *Komatiites*. G. Allen and Unwin, London, 501-520.

Nisbet, E.G., Cheadle, M.J., Arndt, N.T. & Bickle M.J. 1993. Constraining the potential temperature of the Archaean mantle: A rewiew of the evidence from komatiites. *Lithos*, 30: 291-307.

Nutman, A.P., C. R. L. Friend, C. R. L., Baadsgaard, H., & McGregor, V.R. 1989. Evolution and assembly of Archean gneiss terranes, In: the Godthabsfjord region, southern West Greenland: structural, metamorphic and isotopic evidence, *Tectonics*, 3: 573-589.

Nutman, A.P., Chadwick, B., Ramakrishnan, M. & Viswanatha, M.N. 1992. SHRIMP U-Pb ages of detrital zircon in Sargur supracrustal rocks in Western Karnataka, Southern India. *Journal of the Geaological Society of India*, 39: 367-374.

Oxburgh, E.E. & Turcotte, D.L. 1970. Thermal structure of island arcs. *Geol. Soc. Am. Bull.*, 81: 1665-1688.

Padgham W.A. 1992. Mineral deposits in the Archean Slave Structural Province; lithological and tectonic setting. *Precamb Res.*, 58: 1-24.

Park, R.G. 1982. Archaean Tectonics. *Geolog. Rundschau*, 71: 22-37.

Parrish, R.R. 1990. U-Pb dating of monazite and its application to geological problems. *Can. J. Earth Sci.*, 27:1431-1450.

Pekeris, C.L. 1935. Thermal convection in the interior of the Earth. Mon. Not. R. Astron. *Soc. Geophys. Suppl.*, 3:343-367.

Perchuk, L.L. & Lavrent'eva, I.V. 1983. Experimental investigations of exange equilibria in the system cordierite- garnet-biotite. In Saxena S. K. (Ed.). *Kinetics and equilibrium in mineral* reactions, Springer Berlin, Heidelberg, New-York, 199-239.

Peucat, J.J., Gruau, G., Martin, H., Auvray, B., Fourcade, S., Choukroune, P., Bouhallier, H. & Jayananda, M. 1993b. A 2.5 Ga mega-plume in South India?*Terra nova*, 5: 321.

Peucat, J.J., Vidal, P., Bernard-Griffiths, J. & Condie, K.C. 1989. Sr, Nd and Pb isotopic systematics in Archean low- to high-grade transition zone of Southern India: syn-accretion vs. post-accretion granulites. *Journal of Geology*, 97: 537-550.

Peucat, J.J, Jayananda, M. & Mahabaleswar, B. S.,1993a, Age of younger tonalitic magmatism and granulitic metamorphism in the South Indian transition zone (Krishnagiri), comparaison with older Peninsular gneisses from the Gorur-Hassan area. *Journal of Metamorphic Geology*, 11: 879-888.

Pichamuthu, C.S. 1961. "Tectonic of Mysore State", *Proc. Indian Acad. Sci.*, 53: 135-139.

Pichamuthu, C.S. 1962. Some observations on the structures, metamorphism, and geological evolution of Peninsular India. *Journal of the Geological Society of India*, 13: 106-118.

Pichamuthu, C.S. 1967. The Precambrian of India. In Rankama K. (Editors), *The Precambrian*, Interscience, New York, 3: 1-96.

Pidgeon R.T. 1980. 2480 Ma old zircons from granulites facies rocks from East Hebei Province, North China, *Geol. Rev.*, 26: 198-207.

Platt, J.P. 1980. Archean greenstone belts: a structural test of tectonic hypotheses. *Tectonophysics*, 65: 127-150.

Potrel, A. 1994. Evolution tectono-métamorphique d'un segment de croûte continentale archéenne. Exemple de l'Amsaga (craton Ouest Africain ; Mauritanie), thèse d'Université.

Powell, R. & Holland T.J.B. 1988. An internally consistent dataset with uncertainities and correlations: 3. Applications to geobarometry, worked examples and a computer program. *Journal of Metamorphic Geology*, 6: 173-204.

Raase, P., Raith, M., Ackermand, D. & Lal, R.K. 1986. Progessive metamorphism of mafic rocks from greenschist to granulite facies in the Dharwar craton of south India. *Journal of Geology*, 94: 261-282.

Radhakrishna, B.P. & Ramakrishnan, M. (Editors). 1990. Archaean greenstone belts of South India. *Geological Society of India* , 19:497.

Radhakrishna, B.P. & Naqvi, S.M. 1986. Precambrian continental crust of India and its evolution. *J. Geol.*, 94:145-166.

Raith, M., Raase, P., Ackermand, D., & Lal, R.K. 1982. The Archaean craton of Southern India: metamorphic evolution and P-T conditions. *Geologische Rundschau*, 71: 280-290.

Raith, M., Raase, P., Ackermand, D., & Lal, R.K. 1983. Regional geothermobarometry in the granulite facies terrane of South India. *Royal Society (Edimburgh) Earth Sciences Transactions*, 73: 221-244.

Ralser, S. & Park, A.F. 1992. Tectonic evolution of the Archaean rocks of the Tavani Area, Keewatin, N.W.T.,Canada. In: J.E. Glover, & S.E. Ho editors, *The Archaean: Terrains, Processes and Metallogeny*, Perth: The Geology Key Centre & University extension, University of Western Australia, 99-106.

Ramakrishnan, M. & Viswanatha, M.N. 1981. Holenarsipur belt in J., Swami Nath & M., Ramakrishnan (Editors). Early Precambrian supracrustals of Southern Karnataka. *Memoir of the Geological Survey of India*, 112: 115-141.

Rama Rao. 1936. Recent investigations on the Archaean complex of Mysore. *Proc. Indian Sci. Cong.*, 215-244.

Ramberg, H. 1967. *Gravity, deformation and the Earth's crust.* Academic press, London, 214 p.

Ramberg, H. 1971. Model studies in relation to intrusion of plutonic bodies. In: Newall G. & Rast N. (Editors), *Mechanism of Igneous intrusion*, Geol. Jour., Spec. Issue, 2: 261-286.

Ramberg, H. 1973. Model studies of gravity-controlled tectonics by the centrifuge technique. In: de Jong K. A. and Scholten R. (Editors), *Gravity and Tectonics*, John Wiley, New York, N. Y., 49-66.

Ramsay, J.G. 1967. *Folding and Fracturing of rocks*. New York, Mc Graw-Hill.

Ramsay, J.G. 1975. Ann. Rep. Research Institute of African Geology, Univ. Leeds, abstract.

Ramsay, J.G. 1989. Emplacement kinematics of a granite diapir: the Chindamora batholith, Zimbabwe. *Journal of structural Geology*, 11: 191-209.

Rapp, R.P., Watson, E.B., & Miller, C.F.. 1991. Partial melting of amphibolite/eclogite and the origine of Archaean trondhjemeites and tonalites. *Precambrian Res.*, 51: 1-25.

Rayleigh, L. 1893. Investigation of the character of the equilibrium of an incompressible heavy fluid of variable density. *Proc. Lond. Math. Soc.*, 14: 170-177.

Reymer, A. P. S. & Schubert, G., *Am. Geophys. Union Geodyn.* Ser. A301, 189

Richardson, S.H., Gurney, J. J., Erlank, A. J., & Harris, J. W. 1984. Origin of diamonds in old enriched mantle, *Nature*, 310: 198-203.

Richter, F.M. 1984. Regionalised models for the thermal evolution of the Earth. *Earth and Planet. Sc. Letters*, 68: 471-484.

Richter, F.M. 1988. A major change in the thermal state of the Earth at Archaean-Proterozoic Boundary: Consequences for the nature and preservation of continental lithosphere. Journal of Petrology, *Special Lithosphere Issue*. 39-52

Richter, F.M., Models for the Archean thermal regime, *Earth Planet. Sci. Let.*, 73: 350-360 1985.

Ringwood, A.E. 1974. The petrological evolution of island arc systems. *J. Geol. Soc. Lond.*, 130: 183-204.

Roering, C., Van Reenen, D.D., Smit, C.A., Barton, J.M., de Beer, J.H., de Wit, M.J., Stettler, E.H., van Schalkwyk, J.F., Stevens, G & Pretorius, S. 1992. Tectonic model for the evolution of the Limpopo Belt. *Precamb. Res.*, 55: 539-552.

Rogers, J.J.W., Callahan, E.J., Dennen, K.O., Fullagar, P.D., Stroh, P.T. and Wood, L.F. 1986. Chemical evolution of peninsular gneiss in the western Dharwar craton, Southern India. *J. Geol.*, 94: 233-246.

Rogers, J.J.W. 1986. The Dharwar craton and the assembly of Peninsular India. *J Geol.*, 94: 129-143.

Saggerson, E.P. & Owen, L.M. 1971. Metamorphism as a guide to depth of the top of the mantle in southern Africa. *Geol. Soc. S. Africa Sp. Publ.*, 2: 335-349.

Saggerson, E.P. & Turner, L.M. 1972. Some evidence for the evolution of regional metamorphism in Africa. *Proc. 24th Intl. Geol. Congr. Montreal*, 1: 153-161.

Schmeling H., Cruden, A.R., & Marquart, G. 1988. Finite deformation in and around a fluid sphere moving through a viscous medium: implications for diapiric ascent. *Tectonophysics*, 149: 17-34.

Schubert, G. 1988. In Workshop of the growth of continental crust, L. D. Ashwall, Ed. (Lunar and Planetary Institut, Houston) pp 131-132

Schwerdtner, W.M. & Lumbers, S.B. 1980. Major diapiric structures in the Superior and Greenville Structurale provinces of the Canadian shield of Ontario. In strangway, D. W., editors, The continental crust and its mineral deposits. *Geological association of Canada, special paper* , 20: 149-180.

Schwerdtner, W.M. 1984. Archaean gneiss domes in the Wabigoon Subprovince of the Canadian Shield, northwestern Ontario. In A., Kröner and R., Greiling (Editors), *Precambrian Tectonics Illustrated*, I.U.G.S., 129-134.

Schwerdtner, W.M., Bennet, P.J. & Janes, T.W. 1977. Application of L-S fabric scheme to structural mapping and paleostrain analysis. *Can. J. Earth Sci.*, 14: 1021-1032.

Schwerdtner, W.M., Stone, D., Osadetz, K., Morgan, J. & Stott, G.M. 1979. Granitoid complexes and the Archean tectonic record in the southern part of northwestern Ontario, *Can. J. Earth Sci.*, 16: 1965-1977.

Schwerdtner, W.M., Stott, G.M., & Sutcliffe, R.H. 1983. Strain patterns of crescentic granitoid plutons in the Archean greenstone terrain of Ontario, *J. Struct. Geol.* 5: 419-430.

Schwerdtner, W.M., Morgan, J., & Stott, G.M. 1985. Contacts between greenstone belts and gneiss complexes within the Wabigon subprovince,Ontario, In: L.D. Ayres, P.C. Thurston, K.D. Card, & W. Weber editors, *Evolution of Archean supracrustal sequences*, Geol. Ass. Can., 117-124.

Schwerdtner, W.M., Sutcliffe, R.H., & Troeng, B. 1978. Patterns of total strain within the crestal region of immature diapirs, *Can. J. Earth* Sci., 15: 1437-1447.

Shackelton, RM. 1976. Shallow and deep level exposures of Archaean crust India and Africa in B.F., Windley (Editor), *The Early History of the Earth*, London and New York, Wiley, 317-321.

Shackleton, R.M. 1981. Structure of Southern Tibet, report on a traverse from Lhasa to Khatmandu organized by Academia Sinica. *Jour. Struct. Geol.*, 3: 97-105.

Shackleton, R.M. 1986. Precambrian collision tectonics in Africa. In Coward M. P. and Ries, A. C. (Editors) Collision Tectonics, *Geol. Soc. Soc. Spec. Publ.*, 19: 329-349.

Sills, J.D., Wang, K.Y., Yan, Y.H., & Windley, B.F. 1987. The Archean granulite-gneiss terrain in E. Hebei Province, N.E. China: geological framework and metamorphic conditions. *Geol. Soc. London, Spec. Publ.*, 27: 297-305.

Sleep, N.H., & Windley, B.F. 1982. Archean plate tectonics: constraints and inferences. *J. Geol.*, 90: 363-379.

Snowden, P. A., 1984. Non-diapiric batholiths in the North of Zimbabwe Shield. In: A. Kröner and Greiling (eds). *Precambrian Tectonics illustrated.* Nägele und Obermiller, Stuttgart, 135-145.

Snowden and Bickle, 1976. The Cinamora batholith: diapiric intrusion or interference fold ? *J. Geol. Soc. London 132; p131-137.*

Spray, J. G. 1985. Dynamothermal transition zone between Archaean greestone and granitoid gneiss at Lake Dundas, western Australia. *Journal of Structural Geology*, 7: 187-203.

Spry, A. 1969. *Metamorphic textures.* Pergamon Press, New-York, 350 p.

Sreenivas, B.L. & Srinivasan, R. 1968. Dharwar conglomerates restudy. *J. Geol. Soc. India*, 9: 197-205.

Srinivasan, R. & Ojakangas, R.W. 1986. Sedimentology of quartz-pebble conglomerates and quartzites of the Archaean Bababudan group, Dharwar craton, South India: evidence for early crustal stability. *J. Geol.*, 94: 199-214.

Srinivasan, R. 1988. Present status of the Sargur group of the Archean Dharwar craton, South India. *J. Geol. Soc. India*, 60: 57-72.

Stähle, H.J., Raith, M., Hoernes, S. & Delfs, A. 1987. Element mobility during incipient granulite formation at Kabbaldurga, southern India. *Journal of Petrology*, 28: 803-834.

Stephansson, O. 1977. Granite diapirism in Archaean rocks. *Journal of the Geological Society of London*, 133: 357-361.

Stowe, C.W. 1984. The early Archean Selukwe nappe,Zimbabwe, In: A. Kroner, and R. Greiling editors, *Precambrian Tectonics Illustrated*, Stuttgart: Schweitzerbart, 41-56.

Stroh, P.T., Monrad, J.R., Fullagar, P.D., Naqvi, S.M., Hussein, S.M. & Rogers, J.J.W. 1983. 3000-m.y.-old Halecote trondjhemite: a record of stabilisation of the Dharwar craton. In S.M., Naqvi & J.J.W., Rogers (Editors), *Precambrian of South India, Geological. Society of India , Memoir*, 4: 365-376.

Subba Raju, M., Sreenivasa Rao, T., Setti, D.N. &Reddi, B.S.R. 1978. Recent advance in our knowledge of the Pakhal Super- Group, with a special reference to the central part of the Godavari valley. *Geol. Soc. India Records*, 110: 39-59.

Swager, C.P., Witt, W.K., Griffin, T.J., Ahmat, A.L., Hunter, W.M., McGoldrick, P.J., & Wyche, S. 1992. Late-Archaean granite-greenstones of the Kalgoorlie Terrane, Yilgarn Craton, Western Australia, In: J.E. Glover and S.E. Ho editors, *The Archaean: Terrains, Processes and Metallogeny*, Perth, The Geology Key Centre & University extension, University of Western Australia, 107-122.

Swami Nath, J. & Ramakrishnan, M. (Editors). 1981. Early Precambrian supracrustals of Southern Karnataka. *Memoir of the Geological Survey of India*, 112, 350 p.

Swami Nath, J. & Ramakrishnan, M. (Editors). 1981. Early Precambrian supracrustals of Southern Karnataka. *Geol. Surv. India Mem.*, 112, 350 p.

Swami Nath, J., Ramakrishnan, M. & Viswanatha, M.N. 1976. Dharwar stratigraphic model and Karnataka craton evolution. *Rec. Geol. Surv. India*, 107: 149-175.

Taira, A., Pickering, K.T., Windley, B.F. & Soh, W. 1992. Accretion of Japanese island arcs and implications for the origin of Archaean greenstone belts. *Tectonics*, 11: 1224-1244.

Talbot, C.J. 1973. A plate tectonic model for the Archaean crust. *Phil. Trans. R. Soc. Lond.* A. 273: 413-427.

Talbot, C.J. 1987. Strains and vorcity beneath a tabular batholith in the Zambesi belt, northeast Zimbabwe. *Tectonophysics*, 138: 121-158.

Talbot, C.J. 1974. Fold nappes as asymmetric mantled gneiss domes and ensialic orogeny, *Tectonophysics*, 24: 259-276.

Talbot, C.J. 1977. Inclined and asymmetric upward-moving gravity structures. *Tectonophysics*, 42: 159-181.

Talbot, C.J., Ronnlund, P., Schmeling, H., Koyi, H., & Jackson, M.P.A. 1991. Diapiric spoke patterns, *Tectonophysics*, 188: 187-201.

Tarney, J. & Windley, B.F. 1981. Marginal basins through geological time. *Phil. Trans. R. Soc. Lond.*, A300: 263-285.

Taylor, P.N., Chadwick, B., Moorbath, S., Ramakrishnan, M. & ViswanathaI, M.N. 1984. Petrography, chemistry and isotopic ages of Peninsular gneiss, Dharwar acid volcanic rocks and the Chitradurga granite with special reference to the late Archaean evolution of the Karnataka craton, Southern India. *Precambrian Research*, 23: 349-375.

Taylor, P.N., Chadwick, S., Friend, C.R.L., Ramakrishnan, M. & Viswanatha, M.N. 1988. New age data on the geological evolution of Southern India. In L.D., Ashwal (Editor), *Indo -US Workshop on the deep continental crust of south India*, N. G. R. I. Hyderabad, 181-183.

Taylor, S.R., & McLennan S.M., 1985. *The Continental Crust: its Composition and Evolution*, Blackwell, Oxford, 312 p.

Tourpin, S., 1991. Perte des mémoires isotopiques (Nd, Sr, O) et géochimiques (REE) primaires des komatiites au cours du métamorphisme: exemple de la Finlande Orientale, Mémoires du CAESS, 47: 185p.

Treloar, P.J., Coward, M.P., & Harris, N.B.W. 1992. Himalayan-Tibetan analogies for the evolution of the Zimbabwe craton and Limpopo Belt, *Precamb Res.*, 55: 571-587.

Van den Driessche, J. & Brun, J.P. 1991. Tectonic evolution of the Montage Noire (french Massif Central): a model of extensional gneiss dome. *Geodinamica Acta*, 5: 85-91.

Van den Driessche, J, Brun, J. P., Sokoutis, D. & Mulugeta, D., 1993. Extensional gneiss domes: laboratory models. In Seranne, M. and Malavieille J. (Eds), Late orogenic extension in mountain belts. Doc. B. R. G. M., France, 219: 200-201

Van Kranendonk, M.J. & Helmstaedt, H.1992. Late Archaean sructural history of allochtonous Upernarvik supracrustal rocks in the high-grade Nain Province, Labrador: evidence of a link between the tectonic evolution of gneiss terrains and greenstone belts. In: J.E. Glover, & S.E. Ho editors, *The*

Archaean: Terrains, Processes and Metallogeny, Perth: The Geology Key Centre & University extension, University of Western Australia, 137-150 .

Van Reenen, Roering, C., Ashwal L.D. & De Wit M.J. 1992. The Arcaean Limpopo granulite belt: tectonics and deep crustal processes. *Precambrian Res.,* 55: 587 p.

Veizer, J. & Jansen, S.L. 1979. Basement and sedimentary recycling and continental evolution. *J. Geol.,* 87: 341

Venkata Dasu, S.P., Ramakrishnan, M. & Mahabaleswar, B. 1991. Sargur-Dharwar relationship around the komatiite-rich Jayachamarajapura greenstone belt in Karnataka. *J. Geol. Soc. India,* 38: 577-592.

Venkatasubramanian, V.S. & Narayanaswamy, R. 1974a. Rb-Sr whole rock isochron studies on granitic rocks from Chitradurga and North Mysore. *J. Geol. Soc. In dia,* 15: 77-81.

Venkatasubramanian, V.S. & Narayanaswamy, R. 1974b. Studies in Rb-Sr geochronology and trace element geochemistry in granitoids of Mysore craton, *India. J. Indian Inst. Sci.,* 56: 19-42.

Venkatasubramanian, V.S. & Narayanaswamy, R. 1974c. The age of some gneissic pebbles in Kaldurga conglomerate, Karnataka, South India. *J. Geol. Soc. India,* 15:318-319.

Venkatasubramanian, V.S. 1975. Studies in the geochronology of the Mysore craton. *Geophys. Res. Bull. NGRI,* 13: 239-246.

Viljoen, R.P. & Viljoen R.P. 1969. Evidence for the existence of a mobile extrusive peridotite magma from the Komati Formation of the Overwacht Group. In the upper mantle project, *Geol. Soc. S. Afr. Spec. Publ.,* 2: 87-112

Viswanatha, M.N. & Ramakrishnan, M. 1975. The pre-Dharwar supracrustal rocks of the Sargur schist complex in Southern Karnataka and their tectono-metamorphic significance. *Ind. Mineral.,* 16: 48-65.

Viswanatha, M.N., Ramakrishnan, M. & Swami N.J. 1982. Angular uncomformity between Sargur and Dharwar supracrustals in Shigegudda, Karnataka craton, South India. *J. Geol. Soc. India,* 23: 85-89.

Vlaar, N.J., Archean global dynamics. *Geolog. Mijnb.,* 65: 91-101 1986.

Wang, K., Windley, B.F., Sills, J.D. & Yan, Y. 1990. The Archean gneiss complex in E. Hebei Province, North China, *Precamb Res.,* 48: 245-265.

Wasserburg, G.J., Mac Donald G.L.F., Hoyle, F. & Flower, W.A. 1964. Relative contributions of uranium, thorium and potassium to heat production in the earth. Science, 143: 465-467.

Wegman, C.E. 1935. Zur deutung der Migmatite. Geol. Rundsch., 26: 306-350.
West, G.F. and Mareschal, J.C. 1979. A model for Archean tectonism. Part 1. The thermal conditions. *Can. J. Earth Sci.*, 16: 1942-1950.

West G.F et Marechal J.C. 1979: A model for Archean tectonism. Part 1: The thermal conditions. *Can. J. Earth. Sci. 16, p. 1942-1950.*

Wilks M.E. 1988. The Himalayas - a modern analogue for Archaean crustal evolution. *Earth Plan. Sc. Let.*, 87: 127-136.

Williams, M.L., & Grambling, J.A. 1990. Manganese, ferric iron, and the equilibrium between garnet and biotite. *American Mineralogist,* 75: 886-908.

Windley, B.F. & Bridgewater, D. 1971. The evolution of Archaean low- and high-grade terrains. *Geol. Soc. Austr. Sp. Publ.*, 3: 33-46.

Windley, B.F. 1973. Crustal development in the Precambrian. *Phil. Trans. Roy. Soc. Lond.*, A273: 315-581.

Windley, B.F. 1984. *The evolving Continents (2nd edition),* Wioley, London, 399 p.

Windley, B.F. 1993. Uniformitarism today: plate tectonics is thekey to the past. *J. Geol. Soc. London,* 150: 7-19.

Winther, T.K. & Newton, R.C. 1991. Experimental melting of an hydrous low-K tholeiite: evidence of the origin of Archaean cratons. *Bull. Geol. Soc. Den.*, 39: 213-228.

Woidt, W.D. 1978. Finite element calculations applied to salt dome analysis. *Tectonophysics,* 50: 369-386.

York, D. 1969. Least square fitting of a striaght line with correlated errors. *Earth Planet. Sci. Lett.*, 70:27-39.

Zhang, R.Y & Cong, B.L. 1982. Mineralogy and P-T conditions of cristallisation of early Archean granulites from Qianxi County, NE China. *Scientia Sinica,* 25: 96-112.

Zhang, R.Y., Cong, B.L., Ying, Y.P., & Li, J.L. 1981. Ferrifayalite-bearing eulysite from Archaean granulites in Qianan county, Hebei, North China, *Tschermaks, Min. Petrol. Mitt.*, 28: 167-187.

ANNEXES

Photo (a) : Intrusions de veines trondhjémitiques leucocrates dans les gneiss péninsulaires (près du village de Gorur, secteur d'Holenarsipur).

Photo (b) : Métapélite à phénocristaux de disthène et de staurotide (sur le bord du canal, près du village de Karali, dans la ceinture de roches vertes d'Holenarsipur).

Photo (c) : Détails des veines trondhjémitiques leucocrates intrusives et déformées dans les gneiss péninsulaires (près du village de secteur d'Holenarsipur).

Photo (d) : Amphibolites d'un des points triples de la foliation de la ceinture de roches vertes d'Holenarsipur (près du village d'Huvinahalli). Le plan de foliation est vertical et de direction très variable. La linéation d'étirement est verticale, et la déformation de nature constrictive. Toutes les pierres volantes leucocrates sont des quartzites à tourmaline injectés et déformés dans les amphibolites.

N

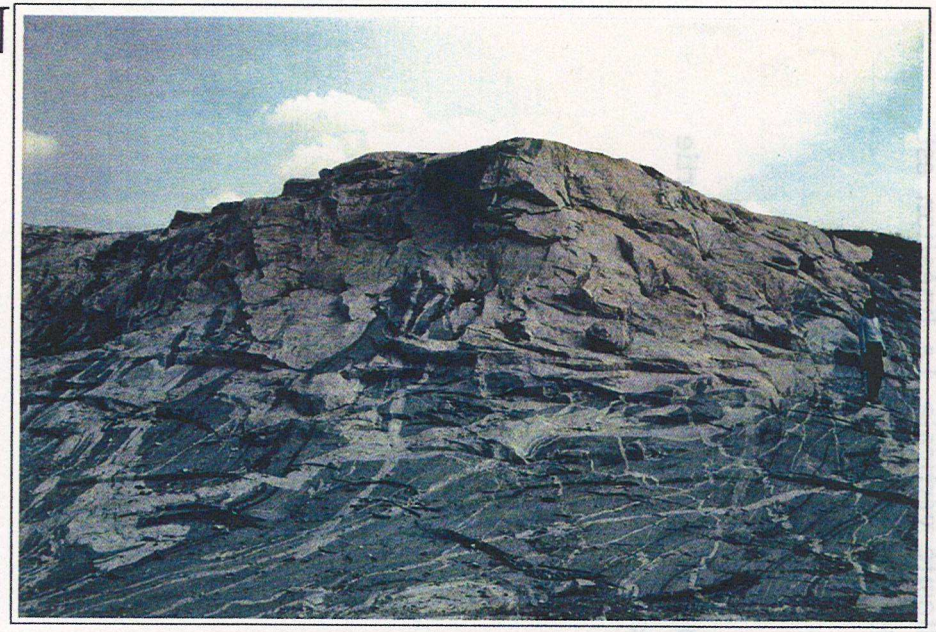

S

a

N

S

c

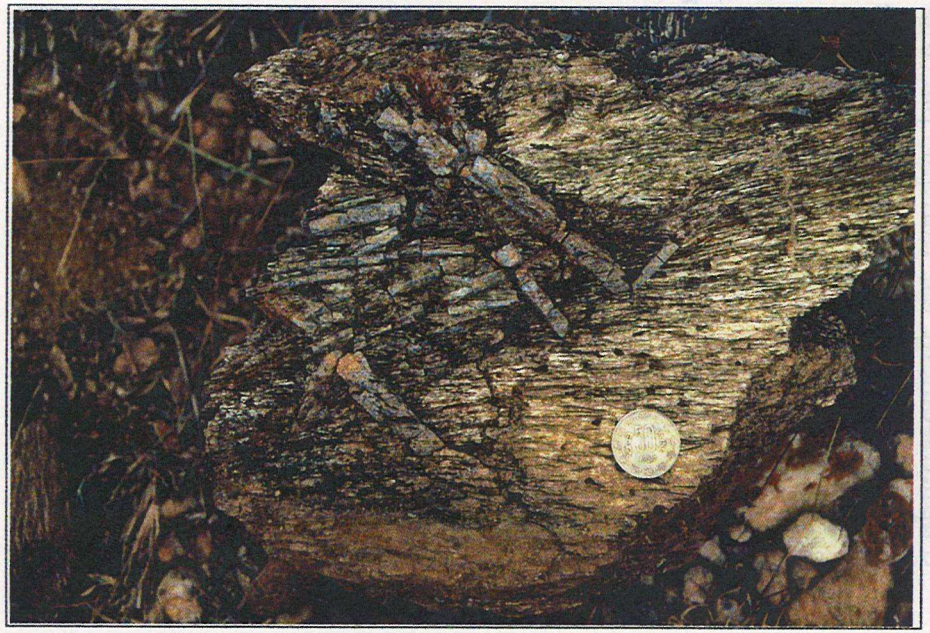

b

W

E

d

Photo (e) : Porphyroblastes de grenat dans les gneiss du secteur de Gundlupet (près du village de Chikka Baganahalli)

Photo (f) : Gneiss péninsulaires au Sud du bassin de roches supracrustales de Terakanambi. On remarque, sur la photo, la présence de critères cinématiques en faille normale (Nord du village de Kodasage).

Photo (g) : Roches basiques intensément crénulées. Le dernier plan d'aplatissement est marqué par une schistosité verticale. La linéation est horizontale (ceinture de roches vertes au Nord de Gundlupet).

Photo (h) : Roches basiques intensément foliées présentes dans la partie centrale du bassin de roches vertes de Terakanambi (Est de Gundlupet).

W

e

EW

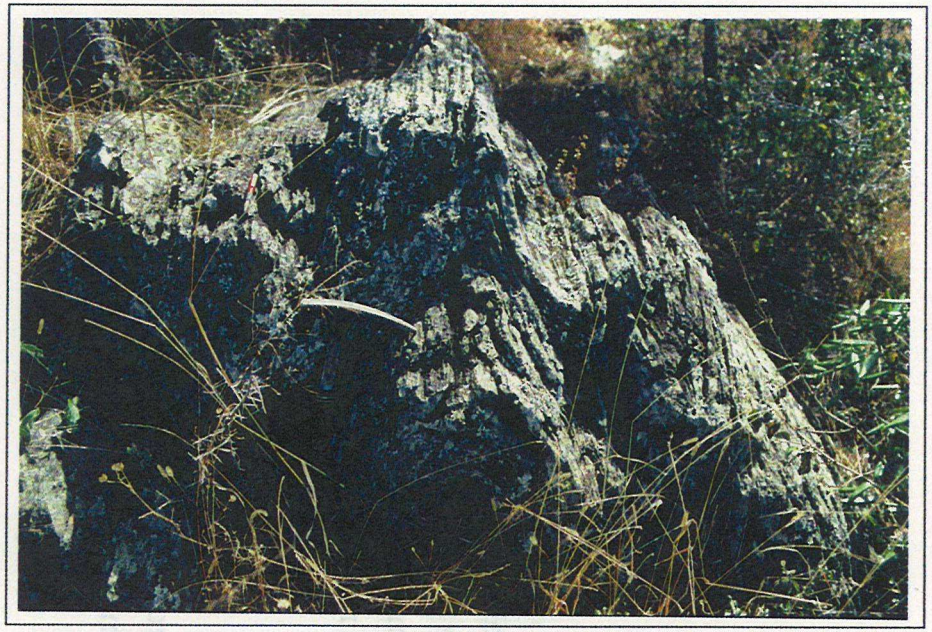

E

g

N

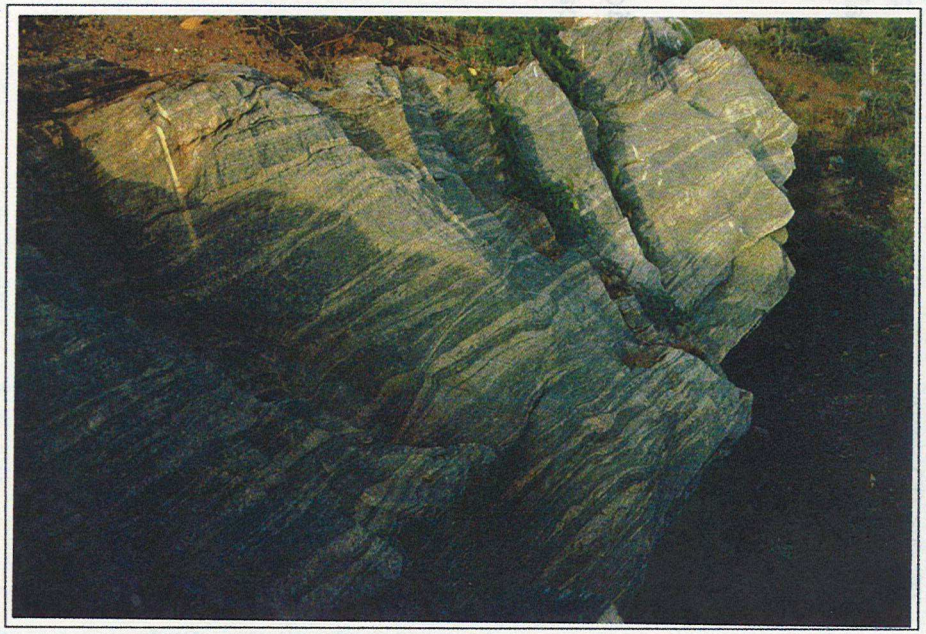

f

S

S

N

h

Photo (i) : Quartzite plissé à texture fortement linéaire. Les plis ont un axe pratiquement vertical et présentent une forte dispersion de leur plan axial. Ce type d'observations est restreint aux zones confinées à l'intérieur des points triples de la foliation de la ceinture de roches vertes d'Holenarsipur.

Photo (j) : Roche basique à texture fortement linéaire. La linéation d'étirement est horizontale, parallèle au manche du marteau (ceinture de roches vertes de Gundlupet).

Photo (k) : Filons basiques intrusifs et plissés dans les gneiss péninsulaires de la région de Gundlupet. Le plan axial des plis est vertical et parallèle à la foliation gneissique.

Photo (l) : Alternance de roches basiques et de roches calco-silicatées crénulées de la partie centrale du bassin de roches supracrustales de Terakanambi (secteur de Gundlupet).

W E

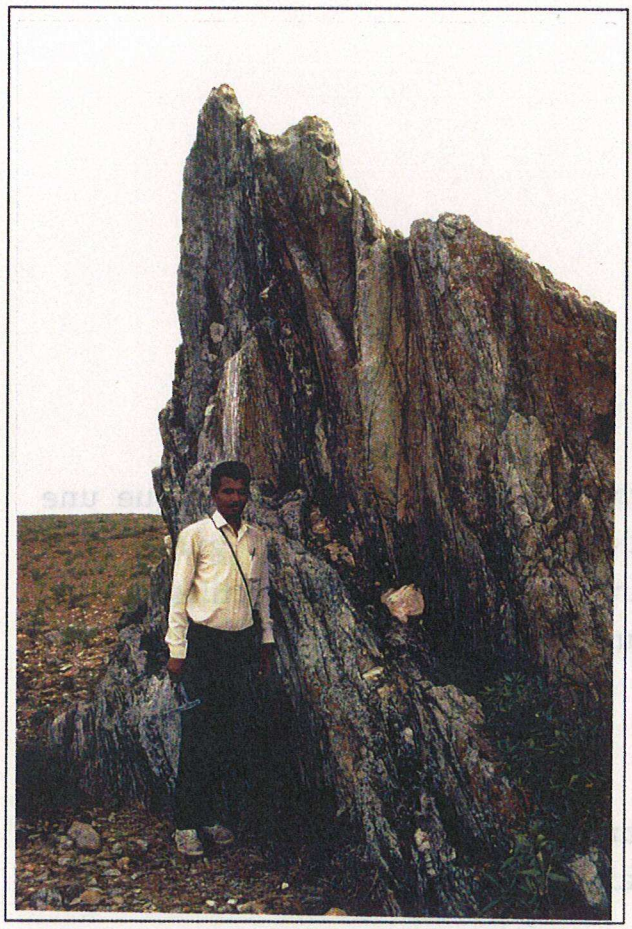

i

S N

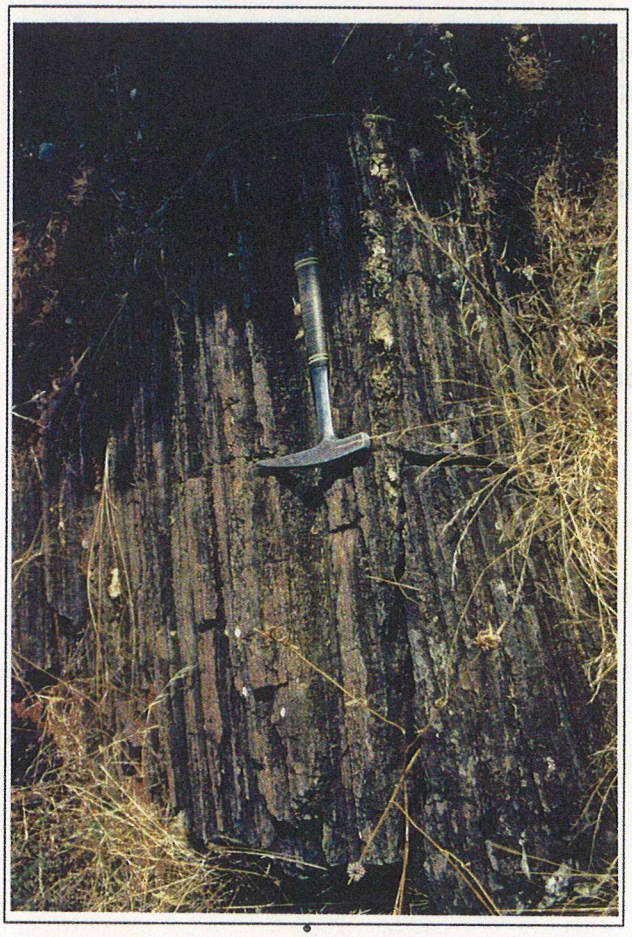

j

S N

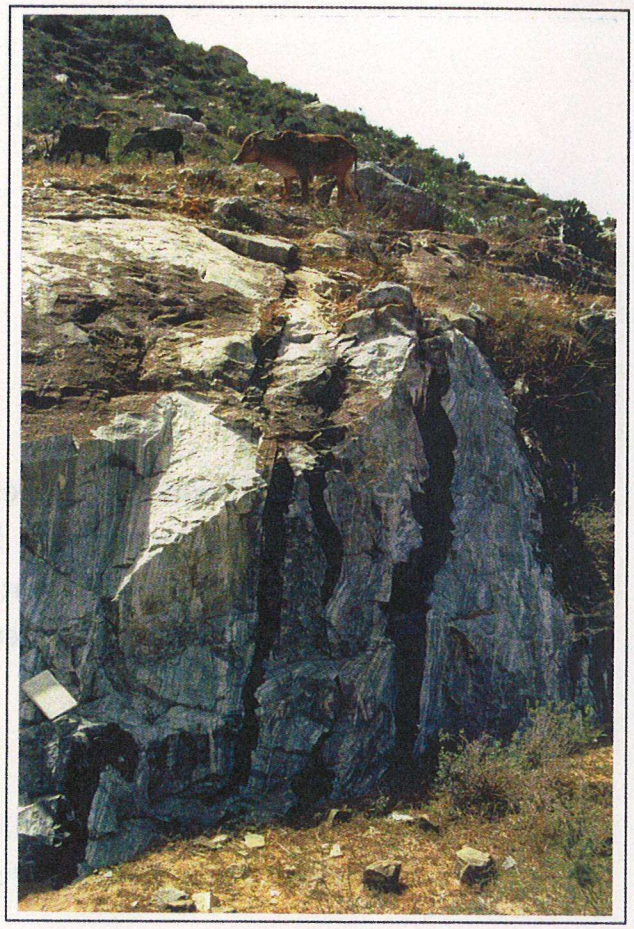

k

S N

l

Photo (m) : Réseau de fentes en échellon dont l'ouverture indique une composante non-coaxiale dextre de la déformation. Les gneiss sont migmatitiques et présentent des bandes de cisaillement ductiles dextres (dôme migmatitique du secteur de Gundlupet).

Photo (n) : Gneiss péninsulaires fortement déformés, présentant une foliation verticale et une texture planaire (secteur de Gundlupet).

Photo (o) : Gneiss péninsulaires migmatitiques, présentant des figures d'interférence issues d'un double raccourcissement (l'un verticale, l'autre horizontale). Ce type d'interférence a uniquement été observé dans les parties centrales de certains dômes gneissiques (secteur de Gundlupet).

Photo (p) : Détails d'une des fente de la photo (m). Les leucosomes des gneiss migmatitiques remplissent les fentes.

W E

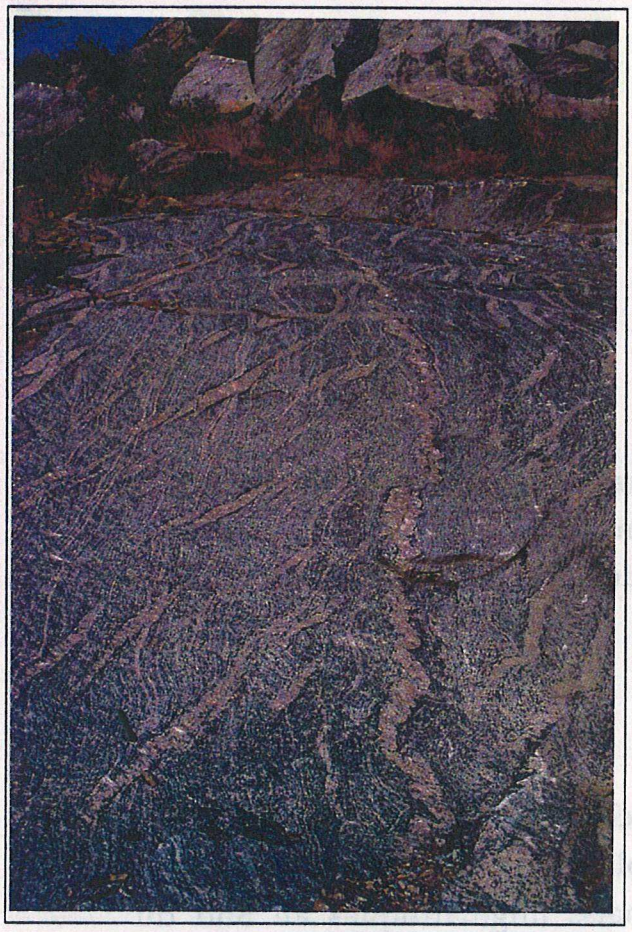

m

W E

o

N S

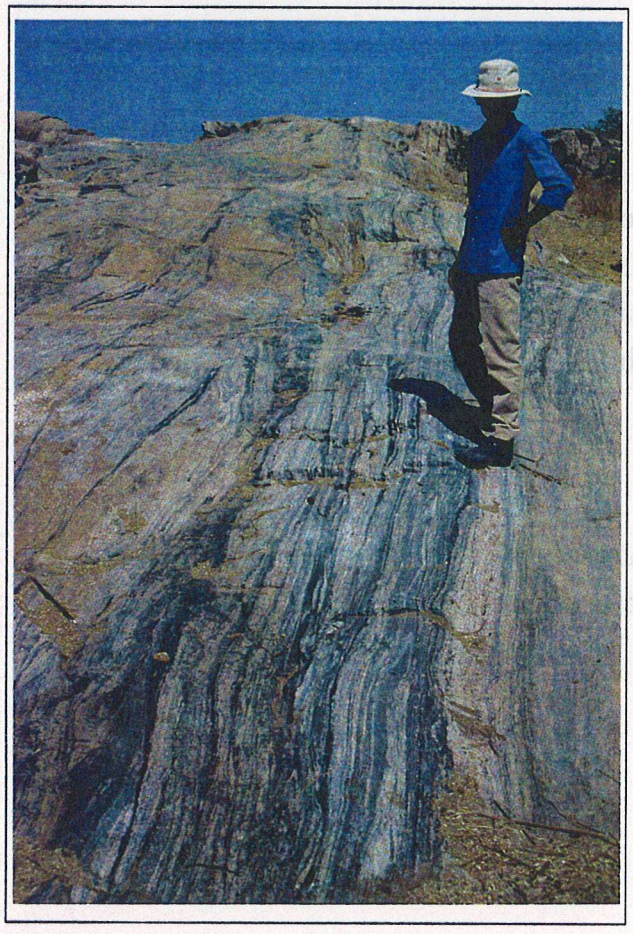

n

p

Photo (q) : Bandes de cisaillements décrochantes dextres, d'orientation N20. Les plans de cisaillement et la foliation migmatitique sont sub-verticaux. Ces structures affectent les gneiss migmatitiques encaissants au batholite du Closepet.

Photo (r) : Bandes de cisaillements décrochantes senestres, d'orientation N160. Les plans de cisaillement et la foliation migmatitique sont sub-verticaux. Ces structures affectent les gneiss migmatitiques au Sud du batholite de Closepet dans la région de Kabbaldurga. Les "patches" granulitiques (plus foncés) soulignent très nettement les bandes de cisaillement.

Photo (s) : Bandes de cisaillements décrochantes senestres, d'orientation N160. Les plans de cisaillement et la foliation migmatitique sont sub-verticaux. Ces structures, comme celles de la photo (q), sont caractéristiques des gneiss migmatitiques encaissants au batholite du Closepet.

Photo (t) : Bande de cisaillement décrochante dextre, d'orientation N20. La bande de cisaillement localisée à l'extrémité du crayon (plus foncée) est marquée par une concentration d'Opx plus importante que celle des gneiss (secteur de Kabbaldurga).

N

q

SW E

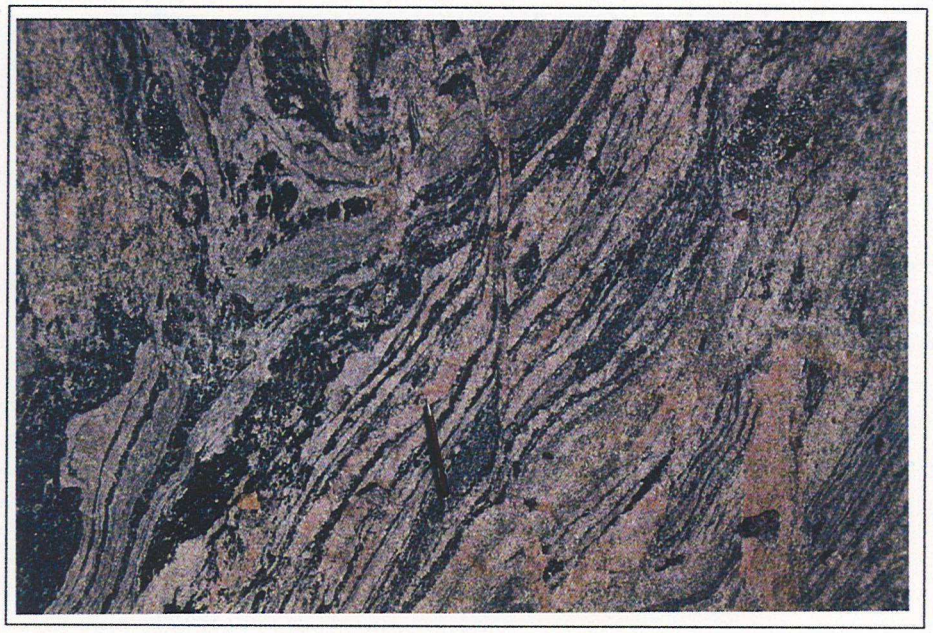

s

N S

r

N S

t

Appendix A

Rock name : DOM (for x(H2O) = 1.0)
Calculations with high celadonitic content in muscovite

	alm	py	phl	ann	east	mst	fst	mu
a	0.273	0.00210	0.0730	0.0330	0.0600	0.00170	0.344	0.730
sd(a)/a	0.15000	0.68425	0.31958	0.41524	0.34206	0.76215	0.20000	0.10000

	cel	clin	daph	ames	q	ky	H2O
a	0.0263	0.0488	0.00910	0.0248	1.00	1.00	1.00
sd(a)/a	0.42117	0.36419	0.56343	0.42600	0	0	

reactions
1) alm + daph + 16ky = 2fst + 7q
2) 55alm + 36ames + 27q = 40py + 6mst + 33daph
3) 8alm + 7py + 36ames + 27q = 6fst + 33clin
4) 32alm + py + 63ames + 108ky = 24fst + 51clin
5) 64alm + 125ames + 218ky = 48fst + 100clin + 4H2O
6) east + cel = phl + mu
7) 8ann + 2fst + 15q = 9alm + 8mu + daph
8) 3east + 6q = py + phl + 2mu
9) 21phl + 3daph + 90ky = 5alm + 13py + 6mst + 21mu

Rock : average PT(for x(H2O) = 1.0)

Single end-member diagnostic information
For 95% confidence, fit (= sd(fit)) should be less than 1.39
however a larger value may be OK - look at the diagnostics!

	avP	sd	avT	sd	cor	fit
lsq	8.6	1.6	599	12	-0.186	0.98

	P	sd(P)	T	sd(T)	cor	fit	e*	hat
alm	8.84	1.75	600	13	-0.034	0.97	-0.29	0.23
py	8.72	1.61	603	13	-0.155	0.90	-1.15	0.12
phl	8.63	1.61	597	13	-0.197	0.97	0.42	0.12
ann	8.97	1.68	598	12	-0.213	0.94	0.82	0.10
east	8.31	1.76	600	13	-0.277	0.97	-0.32	0.18
mst	8.50	1.61	596	12	-0.179	0.79	1.61	0.03
fst	8.42	1.70	598	12	-0.132	0.98	-0.26	0.11
mu	8.70	1.63	597	13	-0.219	0.96	-0.34	0.05
cel	8.23	1.79	599	12	-0.173	0.97	0.42	0.22
clin	8.84	1.68	596	13	-0.277	0.96	-0.43	0.16
daph	8.46	1.62	602	14	-0.220	0.96	0.58	0.20
ames	8.56	1.66	599	13	-0.117	0.98	-0.06	0.14
q	8.58	1.61	599	12	-0.186	0.98	0	0
ky	8.58	1.61	599	12	-0.186	0.98	0	0
H2O	8.58	1.61	599	12	-0.186	0.98	0	0

T = 599°C, sd = 12,
P = 8.6 kbars, sd = 1.6, cor = -0.186, f = 0.98
****

Appendix A

Rock name : DOM (for x(H2O) = 1.0)
Calculations with high celadonitic content in muscovite

	alm	py	phl	ann	east	mst	fst	mu
a	0.2273	0.09210	0.07230	0.03390	0.00000	0.00170	0.3444	0.7290
sd(a)/a	0.13000	0.68425	0.31958	0.41524	0.34206	0.72615	0.29000	0.10000

	cel	clin	daph	ames	q	ky	H2O
a	0.0293	0.0458	0.00910	0.0248	1.00	1.00	1.00
sd(a)/a	0.42117	0.36419	0.55413	0.42000	0	0	

reactions

1) alm + daph + 10ky = 2fst + 7q
2) 55alm + 3eames + 27q = 49py + 6mst + 33daph
3) 8alm + 7py + 3ames + 27q = 6fst + 23clin
4) 32alm + py + 63ames + 108ky = 24fst + 51clin
5) 64alm + 125ames + 218ky = 49fst + 106clin + 4H2O
6) east + cel = phl + mu
7) 8ann + 2fst + 15q = 5alm + 8mu + daph
8) 3east + 6q = py + phl + 2mu
9) 21phl + 3daph + 80ky = 5alm + 13py + 6mst + 21mu

Rock : average PT(for x(H2O) = 1.0)

Single end-member diagnostic information
For 95% confidence, fit (= sd(Fit)) should be less than 1.39
However a larger value may be OK - look at the diagnostics!

	avp	sd	avT	sd	cor	fit
1eq	8.6	1.6	599	12	-0.185	0.98

	P	sd(P)	T	sd(T)	cor	fit	e*	Nat
alm	8.84	1.75	600	13	-0.094	0.97	-0.29	0.23
py	8.72	1.61	603	13	-0.155	0.90	-1.15	0.12
phl	8.63	1.61	597	13	-0.197	0.97	0.42	0.12
ann	8.97	1.65	598	12	-0.219	0.94	0.82	0.10
east	8.31	1.76	600	13	-0.277	0.97	-0.32	0.18
mst	8.50	1.61	596	12	-0.179	0.79	1.61	0.03
fst	8.42	1.70	595	12	-0.132	0.98	-0.26	0.11
mu	8.70	1.63	597	13	-0.219	0.96	-0.34	0.05
cel	8.23	1.70	599	12	-0.173	0.97	0.42	0.22
clin	8.84	1.68	596	13	-0.277	0.96	-0.43	0.16
daph	8.46	1.62	602	14	-0.220	0.96	0.58	0.20
ames	8.56	1.66	599	13	-0.117	0.58	-0.66	0.14
q	8.58	1.61	599	12	-0.186	0.98	0	0
ky	8.58	1.61	599	12	-0.186	0.98	0	0
H2O	8.58	1.61	599	12	-0.186	0.98	0	0

T = 599°C, sd = 12,
P = 8.6 kbars, sd = 1.6, cor = -0.186, f = 0.98
****

Rock name :DOM (for x(H2O) = 1.0)
Calculations with low celadonitic content in muscovite

	alm	py	phl	ann	east	mst	fst	mu
a	0.273	0.00210	0.0730	0.0330	0.0600	0.00170	0.344	0.692
sd(a)/a	0.15000	0.68425	0.31958	0.41524	0.34206	0.76215	0.20000	0.10000

	cel	clin	daph	ames	q	ky	H2O
a	0.00432	0.0488	0.00910	0.0248	1.00	1.00	1.00
sd(a)/a	0.52372	0.36419	0.56343	0.42600	0	0	

reactions
1) alm + daph + 16ky = 2fst + 7q
2) 55alm + 36ames + 27q = 40py + 6mst + 33daph
3) 8alm + 7py + 36ames + 27q = 6fst + 33clin
4) 32alm + py + 63ames + 108ky = 24fst + 51clin
5) 64alm + 125ames + 218ky = 48fst + 100clin + 4H2O
6) 3east + 6q = py + phl + 2mu
7) 8ann + 2fst + 15q = 9alm + 8mu + daph
8) 21phl + 3daph + 90ky = 5alm + 13py + 6mst + 21mu
9) 2py + 3ann + clin + 18ky = 3alm + 2mst + 3cel

Rock : average PT(for x(H2O) = 1.0)

Single end-member diagnostic information
For 95% confidence, fit (= sd(fit)) should be less than 1.39
however a larger value may be OK - look at the diagnostics!

	avP	sd	avT	sd	cor	fit
lsq	5.7	2.2	597	15	0.191	1.28

	P	sd(P)	T	sd(T)	cor	fit	e*	hat
alm	5.48	2.32	595	17	0.324	1.28	0.30	0.22
py	5.90	2.13	600	16	0.220	1.25	-0.87	0.14
phl	5.84	2.14	594	16	0.150	1.25	0.69	0.12
ann	5.98	2.28	597	15	0.180	1.27	0.46	0.12
east	4.97	2.32	598	15	0.124	1.24	-0.78	0.19
mst	5.47	1.89	594	13	0.201	1.11	1.77	0.03
fst	5.31	2.18	594	15	0.247	1.24	-0.76	0.09
mu	5.58	2.22	598	16	0.130	1.28	0.24	0.06
cel	7.08	2.03	600	13	0.237	1.09	-1.77	0.20
clin	5.69	2.29	597	16	0.092	1.28	0.05	0.16
daph	5.59	2.15	600	16	0.132	1.26	0.68	0.20
ames	5.48	2.23	595	16	0.258	1.27	-0.50	0.15
q	5.72	2.18	597	15	0.191	1.28	0	0
ky	5.72	2.18	597	15	0.191	1.28	0	0
H2O	5.72	2.18	597	15	0.191	1.28	0	0

T = 597°C, sd = 15,
P = 5.7 kbars, sd = 2.2, cor = 0.191, f = 1.28
****

Rock name :DOM (for x(H2O) = 1.0)
Calculations with low celadonitic content in muscovite

	alm	py	phl	onn	east	mst	fst	mu
a	0.2273	0.00210	0.0790	0.0330	0.0000	0.00170	0.2425	0.692
sd(a)/a	0.15000	0.68425	0.31958	0.41524	0.34296	0.76215	0.20000	0.10000

	cel	clin	doph	omes	q	ky	H2O
a	0.00432	0.0488	0.00010	0.0248	1.00	1.00	1.00
sd(a)/a	0.52372	0.36419	0.56343	0.42600	0	0	

reactions

1) alm + doph + 15ky = 2fst + 7q
2) 55alm + 36omes + 27q = 49py + 6mst + 33doph
3) 8alm + 7py + 3domes + 27q = 6fst + 33clin
4) 32alm + py + 63omes + 130ky = 24fst + 51clin
5) 64alm + 125omes + 218ky = 48fst + 100clin + 4H2O
6) 3east + 6q = py + phl + 2mu
7) 8onn + 2fst + 15q = 9alm + 8mu + doph
8) 2lphl + 3doph + 99ky = 5alm + 13py + 6mst + 21mu
9) 2py + 3onn + clin + 18ky = 3alm + 2mst + 3cel

Rock : average PT(for x(H2O) = 1.0)

Single end-member diagnostic information
For 95% confidence, fit (= sd(fit)) should be less than 1.39
However a larger value may be OK - look at the diagnostics!

	avP	sd	avT	sd	cor	fit
lsq	5.7	2.2	597	15	0.191	1.28

	P	sd(P)	T	sd(T)	cor	fit	e*	bat
alm	5.48	2.32	595	17	0.324	1.28	0.30	0.22
py	5.90	2.13	600	16	0.220	1.25	-0.87	0.14
phl	5.84	2.14	594	16	0.150	1.25	0.69	0.12
onn	5.98	2.28	597	15	0.180	1.27	0.46	0.12
east	4.97	2.32	598	15	0.124	1.24	-0.78	0.19
mst	5.47	1.89	594	13	0.201	1.11	1.77	0.03
fst	5.31	2.18	594	15	0.247	1.24	-0.76	0.09
mu	5.58	2.22	598	16	0.130	1.25	0.24	0.06
cel	7.08	2.03	600	13	0.237	1.09	-1.77	0.20
clin	5.69	2.29	597	16	0.092	1.28	0.05	0.16
doph	5.59	2.15	600	16	0.132	1.26	0.68	0.20
omes	5.48	2.23	595	16	0.258	1.27	-0.50	0.15
q	5.72	2.18	597	15	0.191	1.28	0	0
ky	5.72	2.18	597	15	0.191	1.28	0	0
H2O	5.72	2.18	597	15	0.191	1.28	0	0

T = 597°C, sd = 15,
P = 5.7 kbars, sd = 2.2, cor = 0.191, f = 1.28
****

Rock name : CEN (for x(H2O) = 1.0)

	phl	ann	east	mu	cel	mst	fst	clin
a	0.0830	0.0156	0.0788	0.677	0.0214	0.00184	0.342	0.0773
sd(a)/a	0.30408	0.50643	0.31042	0.10000	0.43730	0.75441	0.20000	0.31278

	daph	ames	ky	q	H2O
a	0.00274	0.0432	1.00	1.00	1.00
sd(a)/a	0.66575	0.37655	0	0	

reactions
1) 5fst + 3ames + 11q = 3mst + 4daph + 20ky
2) east + cel = phl + mu
3) 27east + clin + 39q = 17phl + 10mu + 2mst
4) 26east + ames + 39q = 16phl + 10mu + 2mst
5) 3east + 5q = 2phl + mu + 2ky
6) 5phl + 3daph = 5ann + 3clin
7) 62phl + 39mu + 6fst = 8ann + 93east + 138q + 12H2O

Rock : average PT(for x(H2O) = 1.0)

Single end-member diagnostic information
For 95% confidence, fit (= sd(fit)) should be less than 1.45
however a larger value may be OK - look at the diagnostics!

	avP	sd	avT	sd	cor	fit
lsq	8.4	1.9	614	16	0.210	0.70

	P	sd(P)	T	sd(T)	cor	fit	e*	hat
phl	8.43	1.96	617	18	0.231	0.68	-0.27	0.26
ann	8.27	1.97	615	16	0.190	0.68	-0.35	0.05
east	8.03	2.15	616	16	0.103	0.68	-0.30	0.21
mu	8.37	1.95	617	17	0.193	0.67	0.26	0.09
cel	8.39	2.32	614	16	0.300	0.70	-0.02	0.35
mst	8.11	1.96	610	16	0.236	0.55	0.98	0.08
fst	8.36	1.95	614	16	0.210	0.67	0.27	0.01
clin	8.68	2.05	612	16	0.103	0.66	-0.39	0.16
daph	8.46	1.96	612	16	0.166	0.67	-0.44	0.13
ames	8.96	2.18	619	17	0.354	0.64	0.53	0.28
ky	8.37	1.95	614	16	0.210	0.70	0	0
q	8.37	1.95	614	16	0.210	0.70	0	0
H2O	8.37	1.95	614	16	0.210	0.70	0	0

T = 614°C, sd = 16,
P = 8.4 kbars, sd = 1.9, cor = 0.210, f = 0.70
****

Rock name : CEN (for x(H2O) = 1.0)

	phl	ann	east	bi	cel	mst	fst	clin
a	0.0830	0.8156	0.0758	0.977	0.0214	0.00184	0.342	0.0773
sd(a)/a	0.3048	0.3864	0.3104	2	0.4230	0.7544	0.2666	0.3128

	dqph	anes	ky	q	H2O
a	0.0274	0.0432	1.00	1.00	1.00
sd(a)/a	0.6825	0.3755	0	0	

reactions

1) 5fst + 2anes + 11d = 3mst + 4dqph + 20ky
2) east + cel = phl + mu
3) 22east + clin + 39q = 17phl + 10mu + 2mst
4) 26east + anes + 39q = 16phl + 10mu + 2mst
5) 3east + 5q = 2phl + mu + 2ky
6) 5phl + 3dqph = 5ann + 3clin
7) 62phl + 33mu + 6fst = 8ann + 93east + 128q + 12H2O

Rock : average PT(for x(H2O) = 1.0)

Single end-member diagnostic information
For 95% confidence, fit (= sd(fit)) should be less than 1.45
However a larger value may be OK - look at the diagnostics!

	avP	sd	avT	sd	cor	fit
isq	8.4	1.9	614	16	0.210	0.70

	P	sd(P)	T	sd(T)	cor	fit	w*	hat
phl	8.43	1.96	617	18	0.231	0.65	-0.27	0.26
ann	8.27	1.97	615	16	0.130	0.58	-0.35	0.05
east	8.83	2.15	616	16	0.109	0.65	-0.30	0.21
mu	8.37	1.95	617	17	0.133	0.67	0.26	0.09
cel	8.39	2.32	614	16	0.300	0.70	-0.02	0.35
mst	8.11	1.96	616	16	0.236	0.55	0.98	0.05
fst	8.36	1.95	614	16	0.210	0.67	0.27	0.01
clin	8.66	2.05	612	16	0.109	0.66	-0.39	0.16
dqph	8.46	1.96	612	16	0.166	0.67	-0.44	0.13
anes	8.96	2.18	619	17	0.354	0.64	0.53	0.26
ky	8.37	1.95	614	16	0.210	0.70	0	0
q	8.37	1.95	614	16	0.210	0.70	0	0
H2O	8.37	1.95	614	16	0.210	0.70	0	0

T = 614°C, sd = 16,
P = 8.4 kbars, sd = 1.9, cor = 0.210, F = 0.70
****

Appendix B

Rock name : OEA (for x(H2O) = 1.0)

non-unit activities :

name	a
epi	0.550

<===>

phases : st, g, chl epi (bi, mu, q, fluid)

P(kbar)	T(°C)	Xalm	Xgro
4.0	574	0.732	0.162
5.0	588	0.697	0.166
6.0	600	0.660	0.170
7.0	612	0.621	0.174
8.0	622	0.580	0.178
9.0	631	0.537	0.181
10.0	639	0.493	0.185
11.0	647	0.447	0.189
12.0	654	0.399	0.193

Appendix B

Rock name : OEA (for x(H2O) = 1.0)

num-unit activities :
name a
cpx 0.550

phases : st, g, cld cpx (bi, mu, q, fluid)

P(kbar)	T(°C)	Xalm	Xpro
4.0	574	0.732	0.162
5.0	588	0.697	0.166
6.0	600	0.669	0.170
7.0	612	0.621	0.174
8.0	622	0.589	0.178
9.0	631	0.537	0.181
10.0	639	0.495	0.185
11.0	647	0.447	0.189
12.0	654	0.399	0.193

MEMOIRES DE GEOSCIENCES-RENNES
Universite de Rennes I - Campus de Beaulieu
35042 - RENNES Cedex tel : 99.28.60.80

Dans la même collection :

N°1 - H. MARTIN - Nature, origine et évolution d'un segment de croûte continentale archéenne : contraintes chimiques et isotopiques. Exemple de la Finlande orientale. **392 p., 183 fig., 51 tabl., 4 pl. (1985).** **Epuisé**

N°2 - G. QUERRE - Palingénèse de la croûte continentale à l'archéen les granitoïdes tardifs (2,5-2,4 Ga) de Finlande Orientale. Pétrologie et géochimie. **226 p., 74 fig., 41 tabl., 3 pl. (1985).** **Epuisé**

N°3 - J. DURAND - Le Grès Armoricain. Sedimentologie. Traces fossiles. Milieux de depôt. **150 p., 76 fig., 9 tabl., 19 pl. (1985).** **Epuisé**

N°4 - D. PRIOUR - Genèse des zones de cisaillement : Application de la méthode des éléments finis à la simulation numérique de la déformation des roches. **157 p., 106 fig., 7 tabl., (1985).** **55F.**

N°5 - V. NGAKO - Evolution métamorphique et structurale de la bordure sud-ouest de la "série de Poli". Segment camerounais de la chaîne panafricaine. **185 p., 76 fig., 16 tabl., 12 pl. (1986).** **Epuisé**

N°6 - J. DE POULPIQUET - Etude géophysique d'un marqueur magnétique situé sur la marge continentale sud-armoricaine. **159 p., 121 fig., 5 tabl. (1986).** **55F.**

N°7 - P. BARBEY - Signification géodynamique des domaines granulitiques. La ceinture des granulites de Laponie : une suture de collision continentale d'âge Protérozoique inférieur (1.9-2.4 Ga). **324 p., 89 fig., 46 tabl., 11 pl. (1986).** **Epuisé**

N°8 - Ph. DAVY - Modélisation thermo-mécanique de la collision continentale. **233 p., 72 fig., 2 tabl. (1986).** **Epuisé**

N°9 - Y. GEORGET - Nature et origine des granites peralumineux a cordiérite et des roches associées. Exemples des granitoides du Massif Armoricain (France) : Pétrologie et géochimie. **250 p., 140 fig., 67 tabl., (1986).** **Epuisé**

N°10 - D. MARQUER - Transfert de matière et déformation progressive des granitoides. Exemple des massifs de l'Aar et du Gothard (Alpes centrales Suisses). **287 p., 134 fig., 52 tabl., 5 cartes hors-texte (1987).** **120 F.**

N°11 - **J.S. SALIS** -Variation séculaire du champ magnétique terrestre. Direction et Paléointensité sur la période 7.000 70.000 BP dans la chaîne des Puys. **190 p., 73 fig., 28 tabl., I carte hors-texte (1987).** **90F.**

N°12 - **Y. GERARD** - Etude expérimentale des interactions entre déformation et transformation de phase. Exemple de la transition calcite-aragonite. **126 p., 42 fig., 3 tabl., 10 pl. (1987).** **75F.**

N°13 - **H. TATTEVIN** - Déformation et transformation de phases induites par ondes de choc dans les silicates. Caractérisation par la microscopie électronique en transmission. **150 p., 50 fig., I tabl., 13 pl. (1987).** **95F.**

N°14 - **J.L. PAQUETTE** - Comportement des systèmes isotopiques U-Pb et Sm-Nd dans le métamorphisme éclogitique. Chaîne Hercynienne et chaîne Alpine. **190 p., 88 fig., 39 tab., 2 pl. (1987).** **95F.**

N°15 - **B. VENDEVILLE** - Champs de failles et tectonique en extension modélisation experimentale. **392 p., 181 fig., I tabl.,82 pl. (1987).** **Epuisé**

N°16 - **E. TAILLEBOIS** - Cadre géologique des indices sulfures a Zn, Pb, Cu, Fe du secteur de Gouézec-St-Thois : Dévono-Carbonifère du flanc Sud du Bassin de Châteaulin (Finistere). **195 p., 64 fig., 41 tabl., 8 pl. photo., 8 pl. h.texte. (1987).** **110F**

N°17 - **J.P. COGNE** - Contribution a l'étude paléomagnétique des roches déformées. **204 p., 86 fig., 17 tabl., (1987).** **90F.**

N°18 - **E. DENIS** - Les sédiments briovériens (Protérozoïque supérieur) de Bretagne septentrionale et occidentale : Nature, mise en place et évolution. **263 p., 148 fig., 26 tab., 8 pl. (1988).** **140F.**

N°19 - **M. BALLEVRE** - Collision continentale et chemins P-T : l'unité pennique du Grand Paradis (Alpes Occidentales). **340 p., 146 fig., 10 tabl., (1988).** **Epuisé**

N°20 - **J.P. GRATIER** - L'équilibrage des coupes géologiques. Buts, méthodes et applications. Atelier du Groupe d'Etudes Tectoniques le 8 Avril 1987 à Rennes. **165 p., 82 fig., 2 tabl. (1988).** **85F.**

N°21 - **R.P. MENOT** - Magmatismes paléozoïques et structuration carbonifère du Massif de Belledonne (Alpes Francaises). Contraintes nouvelles pour les schémas d'évolution de la chaine varisque ouest-européenne. **465 p., 101 fig., 31 tab., 6 pl., (1988).** **200F**

N°22 - **S. BLAIS** - Les ceintures de roches vertes archéennes de Finlande Orientale : Géologie, pétrologie, géochimie et évolution géodynamique. **312 p., 107 fig., 98 tab., 11pl. photo, I pl. h.texte, (1989).** **160F**

N°23 - **A. CHAUVIN** - Intensité du champ magnétique terrestre en période stable de transition, enregistrée par des séquences de coulées volcaniques du quaternaire. **217 p., 100 fig., 13 tab. (1989).** **100F.**

N°24 - **J.P. VUICHARD** - La marge austroalpine durant la collision alpine évolution tectonométamorphique de la zone de Sesia-Lanzo. **307 p., 143 fig., 26 tab., 6 pl. hors-texte. (1989).** **170F.**

N°25 - **C. GUERROT** - Archéen et Protérozoïque dans la chaîne hercynienne ouest-européenne : géochimie isotopique (Sr-Nd-Pb) et géochronologie U-Pb sur zircons. **180 p., 68 fig., 29 tab., I pl. (1989)** **90F.**

N°26 - **J.L. LAGARDE** - Granites tardi carbonifères et déformation crustale. L'exemple de la Méseta marocaine. **353 p., 244 fig., 15pl. (1989)** **210F.**

N°27 - **Ph. BARDY** - L'orogène cadomien dans le Nord-Est du Massif Armoricain et en Manche Occidentale. Etude tectonométamorphique et géophysique. **395 p., 142 fig., 7 tab., I pl. hors-texte. (1989).** **175F.**

N°28 - **D. GAPAIS** - Les Orthogneiss : Structures, mécanismes de déformation et analyse cinématique. **377 p., 184 fig., 3 tab., (1989).** **275F.**

N°29 - **E. LE GOFF** - Conditions pression-température de la déformation dans les orthogneiss : Modèle thermodynamique et exemples naturels. **321 p., 146 fig., 42 tab. (1989).** **150F.**

N°30 - **D. KHATTACH** - Paléomagnétisme de formations paléozoiques du Maroc. **220 p., 97 fig., 35 tab., (1989).** **100F.**

N°31 - **A. HAIDER** - Géologie de la formation ferrifère précambrienne et du complexe granulitique encaissant de Buur (Sud de la Somalie). Implications sur l'évolution crustale du socle de Buur. **215 p., 18 fig., 42 tab., 7 pl. (1989).** **130 F.**

N°32 - **T. DANIEL** - Traitement numérique d'image appliqué a l'analyse texturale de roches déformées. **186 p., 121 fig., 4 tab., (1989).** **210 F.**

N°33 - **C. LECUYER** - Hydrothermalisme fossile dans une paléocroûte océanique associée a un centre d'expansion lent : Le complexe ophiolitique de Trinity (N. Californie, U.S.A). **342 p., 109 fig., 73 tab., (1989).** **200 F.**

N°34 - **P. RICHARD** - Champs de failles au dessus d'un décrochement de socle: modélisation expérimentale. **382 p., 137 fig., (1989). 400 F.**

N°35 - **J. de BREMOND d'ARS** - Estimation des propriétés rhéologiques des magmas par l'étude des instabilités gravitaires. Pétrologie du complexe plutonique lité de Guernesey. **370 p., 128 fig., 64 tabl., (1989). 180 F.**

N°36 - **A. LE CLEAC'H** - Contribution a l'étude des propriétés physiques des mineraux à haute pression : Spectroscopie et calcul des grandeurs thermodynamiques de la lawsonite, des épidotes et des polymorphes de SiO_2. **190 p., 72 fig., 37 tabl., (1989). 100 F.**

N°37 - **0. MERLE** - Cinématique des nappes superficielles et profondes dans une chaîne de collision. **280 p., 165 fig., 3 tabl., (1990). 160F.**

N°38 - **P. ALLEMAND** - Approche expérimentale de la mécanique du rifting continental. **205 p., 106 fig., 13 tabl., (1990). 160F.**

N°39 - **Ch. BASILE** - Analyse structurale et modélisation analogique d'une marge transformante : l'exemple de la marge de Côte-d'Ivoire - Ghana. **230 p., 161 fig., 7 tabl., (1990) . 130F .**

N°40 - **M. AUDIBERT** - Déformation discontinue et rotations de blocs. Méthodes numériques de restauration. Application à la Galilée. **250 p., 80 fig., 5 tabl., (1991). 150F.**

N°41 - **G. RUFFET** - Paléomagnétisme et 40Ar/39Ar : étude combinée sur des intrusions Précambriennes et Paléozoïques du Trégor. (Massif Armoricain) . **261 p., 80 fig., 19 tabl., (1991). 120F.**

N°42 - **P. SUZANNE** - Extrusion latérale de l'Anatolie : Géometrie et mécanisme de la fracturation. **262 p., 100 fig., 12 pl., 5 tabl., (1991). 210F.**

N°43 - **G. FIQUET** - Propriétés thermodynamiques de minéraux du manteau superieur. Calorimétrie à haute tempéerature et spectroscopie Raman à haute pression et haute témperature. **274 p., 101 fig., 53 tabl., (1991). 130F.**

N°44 - **J. MARTINOD** - Instabilités périodiques de la lithosphère (Flambage, Boudinage en compression et en extension). **283 p., 117 fig., 3 tabl., 2 pl. couleur., (1991). 170F.**

N°45 - **M.O. BESLIER** - Formation des marges passives et remontée du manteau: Modélisation expérimentale et exemple de la marge de la Galice. **257 p., 86 fig., 5 tab., 2 pl. noir/blanc, 2 Pl. couleur., (1991). 180F.**

N°46 - **J.B.L. FRANCOLIN** - Analyse structurale du Bassin du Rio Do Peixe. (Brésil), **250 p., 83 fig., 3 tab., 9 pl. couleur, (1992).** **300F.**

N° 47 - **5. TOURPIN** - Perte des mémoires isotopiques (Nd, Sr, O) et géochimiques (REE) primaires des komatiites au cours du métamorphisme : exemple de la Finlande Orientale **185 p., 53 fig., 23 tabl., (1992).** **100F.**

N° 48 - **J.A. BARRAT** - Genèse des magmas associés à l'ouverture d'un domaine océanique : Géochimie des laves du Nord-Est de l'Afrique (Mer Rouge - Afar) et d'Arabie. **175 p., 47 fig., 23 tab., (1992).** **100F.**

N° 49 - **E. HALLOT** - Injection dans les réservoirs magmatiques Contraintes pétrologiques (Massifs de Fort La Latte et de Saint Brieuc, Bretagne Nord) et modélisation analogique. **331 p., 101 fig., 30 tabl., (1993).** **180F.**

N°50 - **T. SOURIOT** - Cinématique de l'extension post-pliocène en Afar. Imagerie SPOT et modélisation analogique. **225 p., 2 pl. coul., I tabl., 91 fig., 16 pl. photo., I carte H.Texte, (1993).** **I90F.**

N° 51 - **T. EUZEN** - Pétrogenèse des granites de collision post- épaississement. Le cas des granites crustaux et mantelliques du Complexe de Pontivy Rostrenen (Massif Armoricain, France). **350 p., 2 pl. coul., 34 tabl. en annexe, (1993).** **I90F.**

N° 52 - **J. LE GALL** - Reconstitution des dynamismes éruptifs d'une province paléovolcanique : l'exemple du graben cambrien du Maine (Est du Massif Armoricain). Pétrogenèse des magmas andésitiques et ignimbritiques et leur signification dans l'évolution géodynamique cadomienne. **370 p., 30pl. photo., I pl. coul. (1993).** **350 F.**

N° 53 - **J. C. THOMAS** - Cinématique tertiaire et rotations de blocs dans l'ouest de l'Asie Centrale (Tien Shan Kirghiz et dépression Tadjik). Etude structurale et paléomagnétique. **330 p., 107 fig., 2 pl. coul., 18 tabl., 1 carte, annexes. (1993).** **220 F.**

N°54 - **F. LAFONT** - Influences relatives de la subsidence et de l'eustatisme sur la localisation et la géométrie des réservoirs d'un système deltaïque. Exemple de l'Ecoène du bassin de Jaca, Pyrénées Orientales., **270 p., 115 fig., dont 17 pl. couleur. (1994).** **150 F.**

N° 55 - **C. BIELLMANN** - Stabilité et réactivité des carbonates à très hautes pression et température. Implications pour le stockage du carbone dans le manteau terrestre., **230 p., 74 fig., 11 tabl., 1 pl. couleur (1993).** **175 F.**

N°56 - **A. POTREL** - Evolution tectono-métamorphique d'un segment de croûte continentale archéenne. Exemple de l'Amsaga (R.I. Mauritanie). Dorsale Réguibat (Craton Ouest Africain). **400 p., (dont annexes) 125 fig., 21 tabl., 1 pl. couleur, 43 Pl. photo (1994).** **270 F.**

N° 57 - **M. KUNTZ** - Approche expérimentale de la déformation dans les systèmes préfracturés : contribution à l'étude de l'inversion tectonique des bassins sédimentaires. **220 p., 19 pl., 87 fig., 3 tabl. (1994).** **155 F.**

N° 58 - **D. ROUBY** - Restauration en carte des domaines faillés en extension. Méthode et applications. **266 p., 98 fig. dont annexes (1994).** **180 F.**

N° 59 - **J.J. TONDJI-BIYO** - Chevauchements et bassins compressifs. influence de l'érosion et de la sédimentation. Modélisation analogique et exemples naturels. **426 p., 141 fig., 4 pl. couleur, 21 tableaux, dont annexes (1995).** **270 F.**

N° 60 - **H. BOUHALLIER** - Evolution structurale et métamorphique de la croûte continentale archéenne (Craton de Dharwar, Inde du Sud). **277 p., 90 fig., 5 pl. couleurs, 7 tabl., (1995).** **150 F.**

BON DE COMMANDE

à retourner à : Mme FALAISE

Mémoires de Géosciences - RENNES
Université de Rennes I - Campus de Beaulieu
35042 - RENNES Cédex (France)
Tél : 99.28.60.80 Fax : 99.28.67.80

NOM .....

ORGANISME .....

ADRESSE .....

Veuillez me faire parvenir les ouvrages suivants :

N°	Auteur	Nb exemplaires	P.U.	Total

Frais d'envoi : 20,00F par volume	Total	
par volume supplémentaire : 5,00 F	Frais d'envoi	
	Montant total	

Veuillez établir votre chèque au nom de Monsieur l'Agent Comptable de l'Université de Rennes I et le joindre à votre bon de commande.

BON DE COMMANDE

à retourner à : Mme FALAISE

Mémoires de Géosciences - RENNES
Université de Rennes I - Campus de Beaulieu
35042 - RENNES Cédex (France)
Tél : 99.28.60.80 Fax : 99.28.67.80

NOM .....

ORGANISME .....

ADRESSE .....

Veuillez me faire parvenir les ouvrages suivants :

N°	Auteur	Nb exemplaires	P.U.	Total

Frais d'envoi : 20,00F pour volume — Total

par volume supplémentaire : 5,00 F — Frais d'envoi

Montant total

Veuillez établir votre chèque au nom de Monsieur l'Agent Comptable de l'Université de Rennes I et le joindre à votre bon de commande.

Résumé

Le but de cette thèse est de caractériser l'évolution tectono-métamorphique d'un segment de croûte continentale archéenne (> 2.5 Ga). L'objet étudié est le craton de Dharwar (Inde du Sud) qui présente, du Nord vers le Sud, une transition continue de niveaux structuraux de plus en plus profonds. Cette région n'est affectée par aucune déformation post-archéenne.

Nous montrons que les champs de déformation mis en évidence résultent de l'interférence entre le développement d'instabilités gravitaires diapiriques et un raccourcissement régional. Toutes les structures d'échelle crustale résultantes (diapirs et décrochements) sont générées au cours d'un seul et même événement que nous avons daté aux environs de 2.5 Ga. Elles sont contemporaines (i) d'un épisode de formation de croûte continentale juvénile (batholite du Closepet), (ii) d'un métamorphisme régional parfois intense (migmatisation, granulitisation). La cartographie des champs de déformation nous permet d'infirmer la présence de structures chevauchantes ou d'un empilement caractéristique des zones de collision continentale modernes.

L'étude pétrographique révèle que seules certaines zones diapiriques dont la subsidence a été la plus rapide ont enregistré une évolution prograde avec une augmentation de pression de 3 à 7-8 kbar. De plus, ces régions montrent une hétérogénéité dans la composition de la phase fluide qui semble être associée à une différence de perméabilité induite par la nature et l'orientation des textures des roches métamorphiques.

En conclusion, la croûte continentale archéenne du craton de Dharwar ne montre pas de structure tectonique susceptible d'avoir généré un épaississement crustal important. Sa déformation est due principalement à des forces de volume (diapirisme) et, dans une moindre mesure, à des forces de surface (décrochements). Le développement d'instabilités gravitaires diapiriques, parce qu'il affecte des volumes de croûte considérables et qu'il ne peut être rapporté à aucune évidence structurale d'épaississement crustal, constitue une particularité de la tectonique de l'Archéen.

Mots clés :

Archéen, tectonique, champs de déformation, diapirisme, circulation de fluides, Inde du sud.

Editions de GEOSCIENCES RENNES
Université de Rennes I
F - 35042 - RENNES Cédex